JSCSEN 79(12)1461–1597(2014)

ISSN 1820-7421(Online)

Journal of the Serbian Chemical Society

Electronic Version

VOLUME 79

No 12

BELGRADE 2014

Available on line at

www.shd.org.rs/JSCS/

Journal of the Serbian Chemical Society
JSCS-info@shd.org.rs • www.shd.org.rs/JSCS

J. Serb. Chem. Soc. Vol. 79, No. 12 (2014)

CONTENTS

Published by the Serbian Chemical Society
Karnegijeva 4/III, 11000 Belgrade, Serbia
Printed by the Faculty of Technology and Metallurgy
Karnegijeva 4, P.O. Box 35-03, 11120 Belgrade, Serbia

Journal of the Serbian Chemical Society
JSCS-info@shd.org.rs • www.shd.org.rs/JSCS
J. Serb. Chem. Soc. *79* (12) 1461–1467 (2014)
JSCS–4679
UDC 547.53.024+547.861.3+544.723.232+539.196:547.233–304.2
Original scientific paper

Investigation of key interactions between the second extracellular loop of the dopamine D2 receptor and several hydroxy-*N*-{[2-(4-phenylpiperazin-1-yl)ethyl]phenyl}-nicotinamides

VLADIMIR ŠUKALOVIĆ[1]*, VUKIĆ ŠOŠKIĆ[2], DJURDJICA IGNJATOVIĆ[3], DEANA ANDRIĆ[4], JELENA PENJIŠEVIĆ[1] and SLADJANA KOSTIĆ-RAJAČIĆ[1]

[1]*ICTM – Department of Chemistry, University of Belgrade, Njegoševa 12, 11000 Belgrade, Serbia,* [2]*ORGENTEC Diagnostika GmbH, Carl-Zeiss-Str. 49, 55129 Mainz, Germany,* [3]*Institute for Biological Research "Siniša Stanković", University of Belgrade, Bulevar despota Stefana 142, 11060 Belgrade, Serbia and* [4]*Faculty of Chemistry, University of Belgrade, Studentski trg 12–16, 11000 Belgrade, Serbia*

(Received 23 April, revised 2 July, accepted 6 July 2014)

Abstract: The dopaminergic receptor system has been the focus for the development of new pharmacotherapeutic agents targeting a number of central nervous system related disorders, such as drug addiction, schizophrenia, depression, and Parkinson's disease, to name just a few. To date, the crystal structure for the human D2 receptor is not known, despite its vital function and importance as a therapeutic target. Herein, a recent advancement in the determination of key receptor–ligand interactions for the available arylpiperazine-like ligands, using a D2 receptor model based on the crystal structure of the D3 receptor is presented. To determine key interactions responsible for high dopaminergic activity, computer-docking analysis was used together with experimental data. A total of 4 dopaminergic ligands showing moderate to high affinity were tested and the obtained results rationalized using ligand structures docked into the proposed D2 receptor model.

Keywords: arylpiperazine; G protein-coupled receptors; docking; molecular modeling.

INTRODUCTION

The second extracellular loop (ECL) of dopamine D2 (D2DA) receptors is a part of the ligand-binding site. The exact 3D structure of this receptor domain is so far unknown.[1] The crystal structure for the ECL receptor area of G protein-coupled receptors (GPCRs) is not available because of the high flexibility of that

* Corresponding author. E-mail: vladimir.sukalovic@abc-servis.com
doi: 10.2298/JSC140423070S

receptor domain. Still ECLs plays a significant role in ligand–receptor interactions and therefore it is important to learn more about the molecular processes involved in the ligand binding. A study of the structural and functional roles of extracellular loops may help in the understanding of certain aspects of ligand binding affinity that cannot be fully explained by interactions with the canonical binding site located in the transmembrane part of the receptor.

Several attempts were made to establish key receptor–ligand interactions in the ECL area[1,2] by using the methods of molecular modeling. In this paper, results are published that were obtained through an investigation of receptor––ligand interactions in the ECL area of D2DAR, and a set of already available four hydroxy-*N*-{[2-(4-phenylpiperazin-1-yl)ethyl]phenyl]nicotinamides[3] (Table I). For the sake of clarity, the ligand molecule was considered as a tail part (phenylpiperazine), a linker part (*meta*- and *para*-amino-phenylethyl) and a head part (heteroaryl group). The tail part was kept constant, while the linker and head parts were varied as described below:

– Ligand **1** is a long linear molecule able to protrude and to bind into the ECL receptor area. It contains polar groups in the head area to allow hydrogen

TABLE I. Structures of the tested hydroxy-*N*-{[2-(4-phenylpiperazin-1-yl)ethyl]phenyl]nicotinamides, *i.e.*, 6-hydroxy-*N*-{4-[2-(4-phenylpiperazin-1-yl)ethyl]phenyl}nicotinamide (**1**), 2--hydroxy-*N*-{4-[2-(4-phenylpiperazin-1-yl)ethyl]phenyl}nicotinamide (**2**), 6-hydroxy-*N*-{3--[2-(4-phenylpiperazin-1-yl)ethyl]phenyl}nicotinamide (**3**), 2-hydroxy-*N*-{3-[2-(4-phenylpiperazin-1-yl)ethyl]phenyl}nicotinamide (**4**), for binding to the D2DA receptors and the determined K_i values that are the mean of three independent experiments performed in triplicate at 7 competing ligand concentrations

No.	R	K_i / nM
	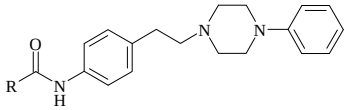	
1	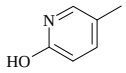	19.5
2	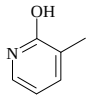	154.3
	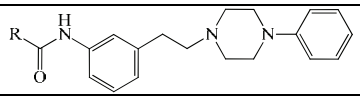	
3	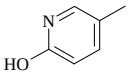	95.9
4	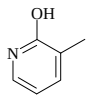	120.1

bonding with D2DAR.

– Ligand **2** is the same as ligand **1** but with an altered polar group arrangement in the head part.

– Ligand **3** is a *meta*-regioisomer of ligand **1**, which makes it shorter and therefore suboptimal for binding into the ECL D2DAR area.

– Ligand **4** is the same as ligand **3** but with an altered polar group arrangement in the head part.

In this way, it was assumed that only the hydrogen bond interaction between the ligand and receptor ECL area could be studied, while keeping all other interactions constant.

EXPERIMENTAL

Biological assays

Radioligand [^{3}H]spiperone was purchased from Amersham Biosciences (Amersham, UK). CHO-hD2S cells stably expressing the native human D2DA receptor were obtained from Professor Phillip G. Strange (University of Reading, UK). The cell lines maintain the isolation of membranes with the D2DA receptor. Competition binding assays at the D2 DA receptor were performed using [^{3}H]spiperone (0.4 nM) by the protocol provided in previous publications.[4] Competition binding studies were performed with seven varied concentrations of the test compounds run in triplicate tubes, and isotherms from three assays were calculated by computerized nonlinear regression analysis to yield K_i values.

Docking analysis

A D2DR homology model, used in the docking analysis, was built using the crystal structure of D3DR as the template. The receptor binding site was defined to include all key amino acid residues, as described previously.[2,5]

The 3D structures of the ligand were generated using the Discovery Studio program.[6] Assuming physiological conditions, the basic aliphatic nitrogen atom of piperazine was protonated. The geometry was optimized using the CHARMM force field applying the conjugate gradient method until the energy difference between successive cycles was below 0.0042 kJ mol^{-1}.[7]

Docking of the selected ligands as presented in Table 1 was realized by simulated annealing using the LIBDOCK module from Discovery Studio, employing the CHARMM force field. The initial position of the ligand in the binding site was arbitrary, while the protonated nitrogen on the ligand part was kept in close proximity to Asp 114 of the receptor. No further ligand constraints were applied. Up to 100 structures were produced in every run and each finally optimized in order to remove steric interaction with a gradient limit of 0.0042 kJ mol^{-1} or 4000 optimization steps. A structure was selected based on the following criteria: lowest total energy of the complex, shortest salt bridge formed between Asp 114 of the D2DR and protonated piperazine nitrogen, chair conformation of the arylpiperazine ring and the aryl part of the molecule positioned in the rear of the hydrophobic pocket of the receptor Phe 386, Trp 390 and Tyr 420.[8] After these initial criteria were satisfied, a second step was performed to examine other interactions that could be formed between the receptor and ligand (hydrogen bonds, aromatic–aromatic interactions, *etc*.). In this way, the best possible docking structures were selected. The structures were visualized using DS Visualise, v. 2.5.1[6], and the obtained images were rendered using PovRay Raytracer, v. 3.6.[9]

Electronic surface potential (ESP) calculation

The geometry of the ligands was further optimized in Gaussian 03W software[10] using the DFT B3LYP method with a 6-31g* basis set. The geometry obtained in this way was used for calculation of the ESP. Only the head and linker part of the ligand were subjected to calculation, since the tail segment cannot influence the ESP distribution. The obtained results were visualized in gOpenMol.[11]

RESULTS AND DISCUSSION

The experimental results showed that all ligands bind to D2DR with moderate to high affinity (Table I). The D2DAR receptor cavity is defined by two binding sites, *i.e.*, the orthosteric binding site (OBS) located in the receptor interior and the second binding pocket (SBP).[5] The OBS consists of the following amino acid residues: Asp 114, Ser 194, Ser 197, Ser 167, Trp 386, Phe 390 and Tyr 420. During ligand binding, the role of residue Asp 114 is to anchor *via* a salt bridge with the charged nitrogen atom. Residues Trp 386, Phe 390 and Tyr 420 form a hydrophobic pocket inside the OBS. The hydrophobic tail segment of the ligand forms multiple edge-to-face (ETF) interactions with the pocket amino acid residues, resulting in correct orientation of the ligand inside the OBS. Ser 194/197 and Ser 167 form additional hydrogen bonds that result in a high affinity complex.[5,8]

The head segment of ligands **1**–**4** can interact with amino acid residues located in the SBP, including the ECL area (Ile 166, Leu 170, Leu 171, Ile 184, Phe 189, Val 190, His 397 and Ile 398). Amino acid residues Ile 166, Leu 170, Leu 171, Ile 184, Val 190 and Ile 398 can form hydrophobic interactions. Phe 189 and His 397 are oriented in a way that allows edge-to-face interactions to occur. Ligand **1** can establish an additional hydrogen bond with Asn 186 (Fig. 1).

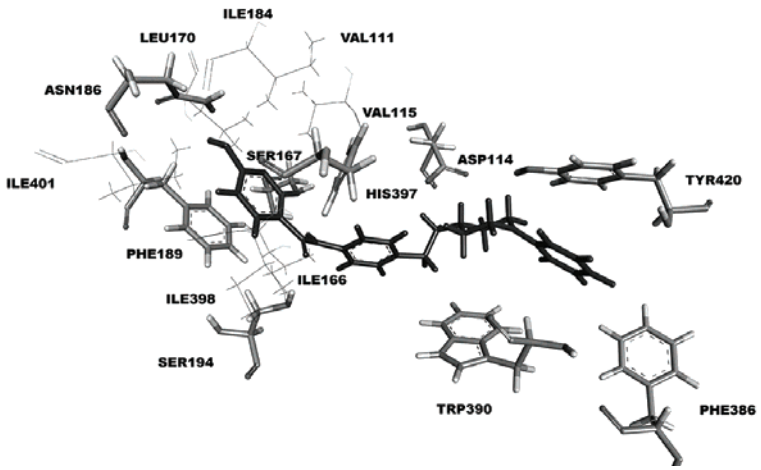

Fig. 1. Docking results – 3D model of D2DR with the position of ligand **1** (black) inside the binding site. Only key amino acid residues are displayed for clarity.

The individual differences in the affinity of ligands could be explained by the obtained docking results.

Ligand **1** was optimally positioned inside the binding site of the receptor, leading to a high affinity complex. Key interactions include a short salt bridge with Asp 114, the ligand tail part oriented between Trp 386, Phe 390 and Tyr 420, forming several edge-to-face interaction, hydrogen bonds with Ser 194 and Ser 167, the ligand head part correctly oriented between Phe 189 and His 397, and a hydrogen bond between the ligand head part and Asn 186 (Fig. 2).

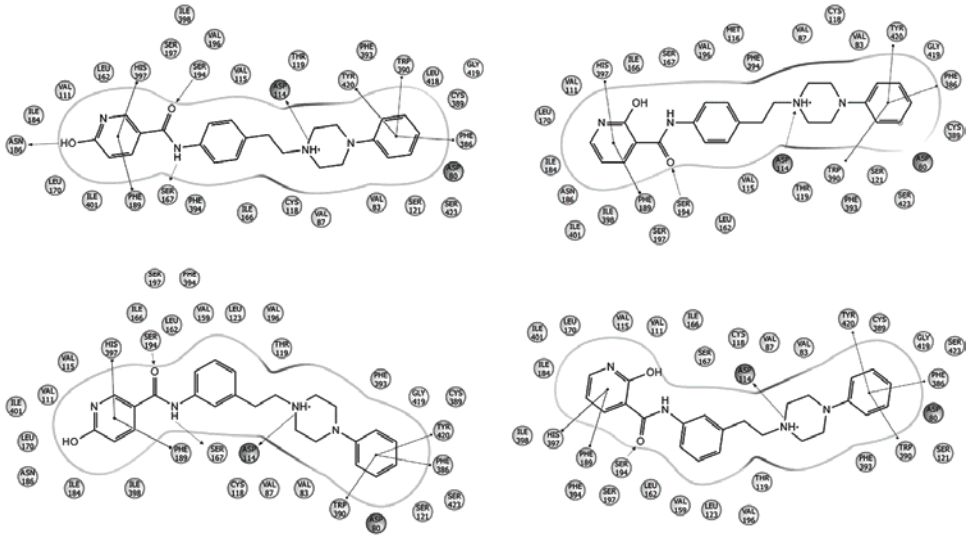

Fig. 2. Schematic representation of the key interaction between D2DR and ligand **1** (top left), ligand **2** (top right), ligand **3** (bottom left) and ligand **4** (bottom right). The aromatic interactions are shown as solid lines, while hydrogen bonds and the salt bridge are denoted by dashed lines.

Ligand **2** occupied the same space inside the D2DR but its head part could not form a hydrogen bond with Asn 186 due to the formation of an intramolecular hydrogen bond with the carbonyl oxygen. This led to reduced affinity for D2DR.

Ligand **3**, being shorter than ligand **1**, could not benefit from the interaction with Asn 186, but retained some interactions in the ECL area. The docking results showed aromatic interactions with Phe 189 and His 397 but simultaneously, the positioning of the hydroxyl group of the head part of the ligand inside the mainly hydrophobic pocket diminished the formation of aromatic interaction with the surrounding hydrophobic groups.

Ligand **4**, is a *meta*-isomer of ligand **2** and docks in a similar manner. Again the intramolecular hydrogen bond leads to a reduced number of interactions with D2DR, resulting in a receptor affinity in the same range as with ligand **2**.

The ligand affinity depended on the aromatic interactions within the OBS and SBP. These interactions were of the edge-to-face type and depended on the correct ESP distribution. The negative ESP in the aromatic part of the ligand tail segment, which forms the edge for ETF interactions with Trp 386 and Tyr 420 (OBS), was preferred, which led to high ligand affinity.[8]

The SBP amino acid residues Phe 189 and His 397 can establish ETF interactions, contributing to ligand affinity. The ESP distribution in the head segment of the ligands **1**–**4** show that aromatic interactions with Phe 189 and His 397 were possible *via* hydrogen atoms in the nicotinamide part of the molecule and the negative ESP on Phe 189 (the ligand is the edge and Phe 189 is face), and *via* the partially positively charged proton on His 397 and the negative ESP on the nicotinamide nitrogen in the ligand head part (Fig. 3).

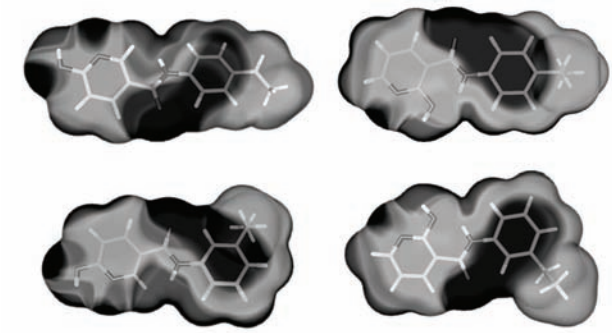

Fig. 3. ESP distribution in ligand **1** (top left), ligand **2** (top right), ligand **3** (bottom left) and ligand **4** (bottom right). Only the head and linker parts are shown for clarity. The negative ESP is shown in dark gray, while the positive ESP is shown in light gray.

CONCLUSION

In previous studies, a 3D model of D2DR was proposed; special focus was on molecular modeling of key receptor–ligand interactions in the ECL area.[2,5] In this publication, the role of Phe 189, His 397 and Asn 186 in ligand binding was stressed. Phe 189 and His 397 provided aromatic type interactions while Asn 186, which is located in the middle of ECL2, provided hydrogen bonding interaction with 6-hydroxy-*N*-{4-[2-(4-phenylpiperazin-1-yl)ethyl]phenyl}nicotinamide.

The obtained results showed that the ECL receptor area plays an important role in the binding of long linear-shaped ligands that cannot entirely fit into the canonical D2DR bind site. The ECL domain is a part of the receptor-binding site, and provides several key receptor–ligand interactions, leading to high affinity complexes.

Acknowledgement. This research was part of the Project No. 172032 funded by the Ministry for Education, Science and Technological Development of the Republic of Serbia.

И З В О Д

ИСПИТИВАЊЕ КЉУЧНИХ ИНТЕРАКЦИЈА ИЗМЕЂУ ДРУГЕ ЕКСТРАЦЕЛУЛАРНЕ ПЕТЉЕ ДОПАМИНСКОГ D2 РЕЦЕПТОРА И РАЗЛИЧИТИХ ХИДРОКСИ-*N*-{[2-(4--ФЕНИЛПИПЕРАЗИН-1-ИЛ)ЕТИЛ]ФЕНИЛ}-НИКОТИНАМИДА

ВЛАДИМИР ШУКАЛОВИЋ[1], ВУКИЋ ШОШКИЋ[2], ЂУРЂИЦА ИГЊАТОВИЋ[3], ДЕАНА АНДРИЋ[4], ЈЕЛЕНА ПЕЊИШЕВИЋ[1] и СЛАЂАНА КОСТИЋ-РАЈАЧИЋ[1]

[1]ИХТМ – Центар за хемију, Универзитет у Београду, Његошева 12, 11000 Београд, [2]ORGENTEC Diagnostika GmbH, Carl-Zeiss-Str. 49, 55129 Mainz, Germany, [3]Институт за биолошка истраживања „Синиша Станковић“, Универзитет у Београду, Булевар деспота Стефана 142, 11060 Београд и [4]Хемијски факултет, Универзитет у Београду, Студентски трг 12–16, 11000 Београд

Допаминергички систем се већ дуже време налази у фокусу истраживања усмерених ка развоју нових фармакотерапијских супстанци, намењених лечењу обољења централног нервног система (ЦНС), као што су: наркоманија, шизофренија, депресија и Паркинсонова болест. До данас, кристална стуктура допаминског D2 рецептора није позната, упркос његовој битној функцији и важности у циљаној терапији обољења ЦНС. У овом раду, представљамо напредак у одређивању кључних рецептор–лиганд интеракција, између арилпиперазину сличних лиганада и модела D2 рецептора добијеног на основу кристалне струкуре D3 рецептора. Употребом докинг анализе, упоредо са експерименталним резултатима, одређене су кључне интеракције које доприносе високој допаминергичкој активности. Укупно 4 лиганда арилпиперазинске структуре су тестирана, показала су умерени до високи афинитет везивања, а добијени резултати су објашњени путем доковања лиганада у предложени модел D2 рецептора.

(Примљено 23. априла, ревидирано 2. јула, прихваћено 6. јула 2014)

REFERENCES

1. C. De Graaf, N. Foata, O. Engkvist, D. Rognan, *Proteins* **71** (2008) 599
2. V. Sukalovic, D. Ignjatovic, G. Tovilovic, D. Andric, K. Shakib, S. Kostic-Rajacic, V. Soskic, *Bioorg. Med. Chem. Lett.* **22** (2012) 3967
3. G. Tovilovic, N. Zogovic, L. Harhaji-Trajkovic, M. Misirkic-Marjanovic, K. Janjetovic, L. Vucicevic, S. Kostic-Rajacic, A. Schrattenholz, A. Isakovic, V. Soskic, V. Trajkovic, *ChemMedChem* **7** (2012) 495
4. D. J. Roberts, H. Lin, P. G. Strange, *Mol. Pharmacol*. **66** (2004) 1573
5. V. Sukalovic, V. Soskic, M. Sencanski, D. Andric, S. Kostic-Rajacic, *J. Mol. Model.* **19** (2013) 1751
6. Discovery Studio Modeling Environment, Release 2.5, Accelrys Software Inc., San Diego, CA, 2009
7. B. R. Brooks, R. E. Bruccoleri, B. D. Olafson, D. J. States, S. Swaminathan, M. Karplus, *J. Comput. Chem*. **4** (1983) 187
8. V. Sukalovic, M. Zlatovic, D. Andric, G. Roglic, S. Kostic-Rajacic, V. Soskic, *Arzneim. Forsch*. **55** (2005) 145
9. Pov-Ray, *The Persistence of Vision Ray-Tracer*, Version 3.6 2003–2011, http://www.povray.org/ (Accessed Feb, 2014)
10. Gaussian 03, Revision C.02, Gaussian, Inc., Wallingford, CT, 2004
11. D. L. Bergman, L. Laaksonen, A. Laaksonen, *J. Mol. Graphics Modell*. **15** (1997) 301.

Journal of the Serbian Chemical Society
JSCS-info@shd.org.rs • www.shd.org.rs/JSCS
J. Serb. Chem. Soc. *79* (12) 1469–1475 (2014)
JSCS–4680
UDC 547.53.024+547.721+547.73+547.77+542.913:615.27–188
Original scientific paper

Synthesis and antioxidant activity study of pyrazoline carrying an arylfuran/arylthiophene moiety

VIDYASHREE H. S. JOIS[1], BALAKRISHNA KALLURAYA[1]* and KOTATHATTU S. GIRISHA[2]

[1]*Department of Studies in Chemistry, Mangalore University, Mangalagangothri, Konaje – 574 199, India and* [2]*Solid State and Structural Chemistry Unit (SSCU), Indian Institute of Science, Bangalore – 560 012, India*

(Received 9 January, revised 4 September, accepted 8 September 2014)

Abstract: A novel series of *N*-acetyl-3-aryl-5-(5-(*p*/*o*-nitrophenyl)-2-furyl/ /thienyl)-substituted pyrazolines (**3a**–**o**) were synthesized by the reaction of 1-aryl-3-(5-(*p*/*o*-nitrophenyl)-2-furyl/thienyl)-2-propene-1-ones with hydrazine hydrate in acetic acid medium. The structures of the newly synthesized compounds were established by IR, ^{1}H-NMR, mass spectra and a single-crystal X-ray study. The antioxidant activities of the synthesized compounds were determined using the DPPH scavenging assay. The compounds **3a**, **3f**, **3h** and **3o** showed moderate activity.

Keywords: *N*-acetyl-3,5-disubstituted pyrazoline; antioxidant activity; arylfuran; arylthiophene.

INTRODUCTION

Pyrazoline is an important five member heterocyclic compound containing nitrogen as the hetero atom. Several pyrazoline derivatives possess important pharmacological activities. Pyrazoline and their derivatives were found to possess a broad spectrum of biological activities, such as antitumor[1] and anti-inflammatory activities,[2] MAO-B inhibition[3] and antioxidant[4] activity. The derivatives of pyrazoline are used in applications such as dyestuffs, analytical reagents and as agrochemicals.[5] Similarly, substituted furan/thiophene derivatives also exhibit significant biological activities, such as antibacterial, HIV-1 fusion inhibitions, antitumor, anti-inflammatory and antioxidant properties, *etc*.[6–10] Prompted by these observations and in continuation of an ongoing search for biologically active heterocycles,[11–14] the synthesis of a novel series of *N*-acetyl pyrazoline carrying an arylfuran/arylthiophene moiety is reported herein. These synthesized compounds were evaluated for their antioxidant activity. A few of the tested

* Corresponding author. E-mail: bkalluraya@gmail.com
doi: 10.2298/JSC140109090J

compounds showed significant antioxidant activity, when compared with the standard butylated hydroxytoluene (BHT).

EXPERIMENTAL

Materials, methods and instrumentation

All the employed chemicals were of analytical reagent (AR) grade and were obtained from Spectrochem and CDH. The formation of pyrazoline was confirmed by analytical IR, ^{1}H-NMR and mass spectra and single crystal X-ray data. IR spectra of the compounds were recorded on Thermo Nicolet Avatar 330-FTIR spectrophotometer. The melting points of the newly synthesized compounds were determined in open capillary tubes and are uncorrected. The ^{1}H-NMR spectra were recorded on a Bruker Avance-II 400 MHz NMR spectrometer using $CDCl_3$ as solvent and tetramethylsilane (TMS) as internal standard. All the chemical shift values are expressed on the δ scale downfield from TMS. The mass spectra were recorded on a Water-Micromass Q-Tof Micro LC mass spectrometer. Elemental analyses were realized on a Vario-El Elementar-III model analyzer. The X-ray crystallographic study of compound **3h** was performed on a Bruker X8 Proteum CCD diffractometer. The homogeneity of the compounds was controlled by thin layer chromatography using silica gel plates (Merck) using petroleum ether: ethyl acetate (9:1) as the mobile phase.

*General procedure for the preparation of 1-aryl-3-(5-(*p/o-*nitrophenyl)-2-furyl/thienyl)-2-propene-1-ones (**2a**–**o**)*

To a mixture of substituted acetophenone (0.01 mol) and substituted 5-arylfurfural/5-aryl thiophene-2-carboxaldehyde (0.01 mol) in ethanol (25 mL), 30% sodium hydroxide (5 mL) was added drop by drop under ice bath and the mixture was agitated for 4 h. The solid separated was filtered, washed thoroughly with water and recrystallized from ethanol–DMF solvent. The structures of the propenones are given in Table I.

General procedure for the preparation of N-*acetyl-3-aryl-5-(5-(*p/o-*nitrophenyl)-2-furyl/ /thienyl) substituted pyrazolines (**3a**–**o**)*

A mixture of chalcone (0.01 mol), hydrazine hydrate (0.05 mol) and glacial acetic acid (40 mL) was refluxed for 4 h. The resulting mixture was poured into ice cold water (100 mL) and allowed to settle. The solid that separated was collected by filtration, washed with cold water and then recrystallized from DMF–ethanol mixture. The structures of the newly synthesized pyrazolines are given in Table I.

Biological evaluation

The 2,2-diphenyl-1-picrylhydrazyl (DPPH) radical scavenging activity was determined following the method of Mensor *et al.*[15] using ethanol with DPPH as the control. The percentage radical scavenging activity, *RSA*, was determined using the following equation:

$$RSA = \frac{(A_c - A_s)}{A_c} \times 100$$

where A_c is the absorbance of the control and A_s is the absorbance of the sample. All the experiments were performed in triplicate; the results are expressed as mean ± standard deviation (*SD*).

Antioxidant activity

All synthesized compounds were screened for their antioxidant activity against the DPPH radical. A pre-screening of the various substituted pyrazolines **3a**–**o** was performed as a

preliminary evaluation. The compounds **3a**, **3d**, **3e**, **3f**, **3h**, **3n** and **3o** were taken for further screening. The compounds were dissolved in DMSO to obtain a solution of 0.001 mg mL^{-1} concentration. From this stock solution, 0.2 mL was pipetted out and diluted to 2.5 mL with ethanol. Ethanol with DPPH was used as the control. The absorbance of these compounds was recorded at 518 nm. BHT was used as the standard for the antioxidant activity screening.

TABLE I. Structures of the synthesized 1-aryl-3-(5-(*p*/o-nitrophenyl)-2-furyl/thienyl)-2-propene-1-ones (**2a**–**o)** and *N*-acetyl-3-(substituted aryl)-5-(5-aryl-2-furyl/thienyl)pyrazolines (**3a**–**o**)

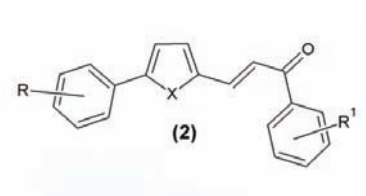

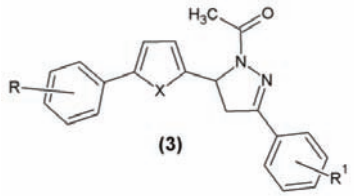

Compd.	R	R^1	X
2a, **3a**	*p*-NO_2	*p*-CH_3	O
2b, **3b**	*p*-NO_2	*p*-OCH_3	O
2c, **3c**	*p*-NO_2	*p*-Cl	O
2d, **3d**	*p*-NO_2	*o*,*p*-Cl	O
2e, **3e**	*p*-NO_2	*p*-OH	O
2f, **3f**	*p*-NO_2	*p*-NO_2	O
2g, **3g**	*p*-NO_2	*p*-NH_2	O
2h, **3h**	*o*-NO_2	*p*-CH_3	O
2i, **3i**	*p*-NO_2	*p*-CH_3	S
2j, **3j**	*p*-NO_2	*p*-OCH_3	S
2k, **3k**	*p*-NO_2	*p*-Cl	S
2l, **3l**	*p*-NO_2	*o*,*p*-Cl	S
2m, **3m**	*p*-NO_2	*p*-OH	S
2n, **3n**	*p*-NO_2	*p*-NO_2	S
2o, **3o**	*p*-NO_2	*m*-NO_2	S

RESULTS AND DISCUSSION

Chemistry

The 5-(*p*/*o*-nitrophenyl)furfural/2-thiophenecarboxaldehydes were obtained by the coupling of *p*/*o*-nitrobenzene-1-diazonium salt with furfural/2-thiophenecarboxaldehyde as per the reported procedure.[16] 5-Arylfurfural/aryl-2-thiophenecarboxaldehyde **1** was condensed with various substituted acetophenone in the presence of sodium hydroxide to obtain a series of chalcones **2**. The obtained chalcones were treated with hydrazine hydrate in presence of glacial acetic acid medium to obtain the 3,5-disubstituted-*N*-acetylpyrazoline**s 3**.

The synthetic route for the compounds is outlined in Scheme 1. The analytical and spectral data of the prepared compounds are given in the Supplementary material to this paper.

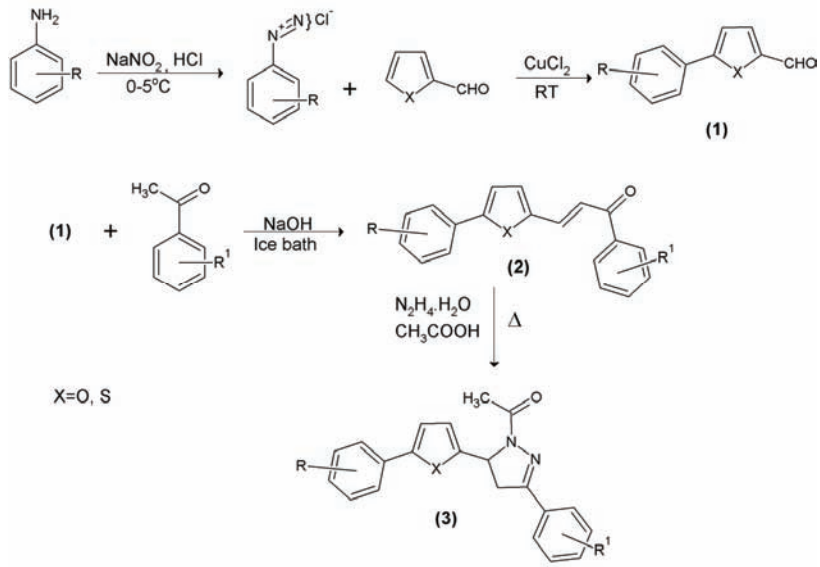

Scheme 1. The schematic route for the synthesis of the *N*-acetyl-3-aryl-5-(substituted aryl-2--furyl/thienyl) pyrazolines.

The IR spectrum of compound **3b** showed an absorption band at 1646 cm^{-1} due to the *N*-acetyl carbonyl group. In the ^{1}H-NMR spectrum of compound **3b**, the three *N*-acetyl protons resonated at δ 2.4 ppm as a singlet. The methoxy protons appeared as a singlet at δ 3.8 ppm. The proton on the stereogenic carbon of the pyrazoline ring appeared as a doublet of doublet centred at δ 5.7 ppm (J = = 5.2 and 12.0 Hz) integrating for one proton. The prochiral CH_2 protons of pyrazoline ring appeared as two distinct doublets of doublet centred at δ 3.4 ppm (J = 5.2 and 17.6 Hz) and at δ 3.6 ppm with coupling constants of 12.0 and 17.6 Hz. The C-3 and C-4 protons of the furan ring appeared as a doublet at δ 6.4 and 6.7 ppm in the ^{1}H-NMR spectrum of compound **3b**. The signal at δ 165.24 ppm was assigned to the carbonyl carbon. The C=N carbon appeared at δ 156.36 ppm. The C-5 carbon and the C-4 carbon of pyrazoline appeared at δ 75.2 and 68.3 ppm, respectively. The CH_3 carbon appeared at δ 12.5 ppm. The aromatic carbons resonated between δ 154.6–122.4 ppm. The mass spectrum of this compound showed the molecular ion peak (M^++1) at m/z 406.2 consistent with its molecular formula $C_{22}H_{19}N_3O_5$. Moreover, in a typical example, the single crystal XRD of pyrazoline **3h** was recorded and it was in conformation with the proposed structure.[17] The structure of compound **3h** determined from single crystal XRD data is given in Fig. 1 and the crystallographic results for the compound are summarized in Table II.

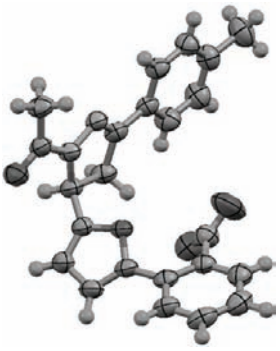

Fig. 1. The structure of compound **3h** determined from single crystal XRD data.

TABLE II. Summary of crystallographic results for the compound **3h**

Parameter	Value
Empirical formula	$C_{22}H_{19}N_3O_4$
Formula weight	389.4
Description and colour	Block, brown
Temperature, K	298(2)
Wavelength, Å	0.71073
Crystal system, space group	Triclinic, P1
Unit cell parameters	a = 7.6235(3) Å, b = 10.5652(4) Å, c = 13.1177(4) Å, α = 103.344(2)˚, β = 95.025(2)°, γ = 108.221(2)°
Volume, Å^3	961.78(6)
Z, calculated density	2
Absorption coefficient, mm^{-1}	0.094
Crystal size, mm	0.23×0.22×0.21

Antioxidant activity

All the synthesized compounds were screened for their antioxidant activity against the DPPH radical. The pre-screening of the various substituted pyrazolines **3a**–**o** was realized at different concentration level as a preliminary evaluation. The compounds **3a**, **3d**, **3e**, **3f**, **3h**, **3n** and **3o** were taken for further screening and tested at 0.2 mg. The percentage radical scavenging activities of the compounds were compared with that of the standard BHT at the same concentration.

The tested compounds showed antioxidant activity ranging from 26.82––63.68 %, whereas the standard BHT showed 97.60 % inhibition. Compounds **3a** and **3h** with a methyl substituent at the *para* position of the phenyl ring showed good activity compared to that of the standard. Similarly, compounds **3f** and **3o** with a nitro substituent at the *para* and *meta* positions, respectively, exhibited moderate activity. The title compound bearing a furan moiety showed significant activity, whereas the compound bearing a thiophene moiety exhibited the lowest inhibition towards the DPPH radical. A graphical representation of the results is given in Fig. 2.

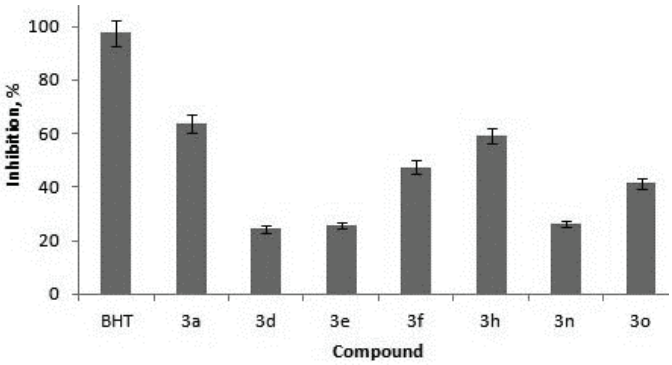

Fig. 2. The antioxidant activity of some of the synthesized pyrazolines. The error bars show the mean ± *SD*.

CONCLUSIONS

A novel series of pyrazoline derivatives containing a arylfuran/thiophene moiety were reported. The results of the antioxidant screening by the DPPH radical scavenging assay revealed that among the fifteen synthesized compounds, only pyrazoline **3a**, **3f**, **3h** and **3o** showed moderate antioxidant activity.

SUPPLEMENTARY MATERIAL

Analytical and spectral data of the prepared compounds are available electronically from http://www.shd.org.rs/JSCS/, or from the corresponding author on request.

Acknowledgements. The authors are grateful to the NMR centre IISc, Bangalore, and SAIF Punjab University, India, for recording the IR, NMR and mass spectra.

ИЗВОД

СИНТЕЗА И АНТИОКСИДАТИВНА АКТИВНОСТ АРИЛФУРИЛ/ТИЕНИЛ СУПСТИТУИСАНИХ ДЕРИВАТА ПИРАЗОЛИНА

VIDYASHREE H. S. JOIS[1], BALAKRISHNA KALLURAYA[1] и KOTATHATTU S. GIRISHA[2]

[1]*Department of Studies in Chemistry, Mangalore University, Mangalagangothri, Konaje – 574 199 и* [2]*Solid State and Structural Chemistry Unit (SSCU), Indian Institute of Science, Bangalore – 560 012, India*

Синтетисана је серија *N*-ацетил-3-арил-5-(5-(*p*/*o*-нитрофенил)-2-фурил/тиенил) супституисаних деривата пиразолина (**3a**–**o**), реакцијом између 1-арил-3-(5-(*p*/*o*-нитрофенил)-2-фурил/тиенил)-2-пропен-1-она са хидразин-хидратом у присуству сирћетне киселине. Структуре нових деривата су одређене помоћу IC и NMR спектроскопије и масене спектрометрије и рендгенске структурне анализе монокристала. Испитане су антиоксидативне активности добијених једињења DPPH тестом. Деривати **3a**, **3f**, **3h** и **3o** показују умерену активност.

(Примљено 9. јануара, ревидирано 4. септембра, прихваћено 8. септембра 2014)

REFERENCES

1. C. Congiu, V. Onnis, L. Vescil, M. Castorina, C. Pisano, *Bioorg. Med. Chem.* **18** (2010) 6238

2. E. Bansal, V. K. Srivastava, A. Kumar, *Eur. J. Med. Chem.* **36** (2001) 81
3. N. Gokhan-Kelekci, S. Yabanoglu, E. Kupeli, U. Salgin, O. Ozgen, G. Ucar, E. Yesilada, E. Kendi, A. Yesilade, A. Bilgin, *Bioorg. Med. Chem.* **15** (2007) 5775
4. T. S. Jeong, K. S. Kim, J. R. Kim, K. H. Cho, S. Lee, W. S. Lee, *Bioorg. Med. Chem. Lett.* **14** (2004) 2719
5. R. Mulder, K. Wellinga, J. J. Van Daalen, *Naturwissenschaften* **62** (1975) 531
6. Z.-P. Xiao, H. Ouyang, X.-D. Wang, P.-C. Lv, Z.-J. Haang, S.-R. Yu, T.-F. Yi, Y.-L. Yang, H.-L. Zhu, *Bioorg. Med. Chem.* **19** (2011) 3884
7. S. Jiang, S. R. Tala, H. Lu, P. Zou, I. Avan, T. S. Ibrahim, N. E. Abo-Dya, A. Abdel--Majeid, A. K. Debnath, A. R. Katritzky, *Bioorg. Med. Chem. Lett.* **21** (2011) 6895
8. A. A. Fadda, E. Abdel-Latif, R. E. El-Mekawy, *Pharmacol. Pharm.* **3** (2012) 148
9. H. A. Stefani, G. V. Botteselle, J. Zukerman-Schpector, I. Caracelli, D. da Silva Corrêa, S. H. P. Farsky, I. D. Machado, J. R. Santin, C. B. Hebeda, *Eur. J. Med. Chem.* **47** (2012) 52
10. J. J. Harnett, M. Auguet, I. Viossat, C. Dolo, D. Bigg, P.-E Chabrier, *Bioorg. Med. Chem. Lett.* **12** (2002) 1439
11. Nithinchandra, B. Kalluraya, S. Aamir, A. R. Shabaraya, *Eur. J. Med. Chem*. **54** (2012) 597
12. K. V. Sujith, B. Kalluraya, A. Adhikari, K. Vijayanarayana, *Med. Chem. Res*. **21** (2012) 543
13. K. S. Girisha, B. Kallurya, *Synth. Commun.* **42** (2012) 3097
14. K. S. Girisha, B. Kallurya, J. H. S. Vidyahsree, *Indian J. Chem., B* **51** (2013) 1767
15. L. I. Mensor, F. S. Menezes, G. G. Leitao, A. S. Reis, T. Don Santos, C. S. Coube, S. Leitao, *Phytother. Res.* **15** (2001)127
16. B. S. Holla, B. Kalluraya, S. N. Shetty, *Indian J. Heterocycl. Chem.* **2** (1992) 61
17. N. Vinutha, M. S. Kumar, V. H. S. Jois, K. Balakrishna, N. K. Lokanath, D. Revannasiddaiah, *Acta Crystallogr., E* **69** (2013) o1528.

Journal of the Serbian Chemical Society
JSCS@tmf.bg.ac.rs • www.shd.org.rs/JSCS
J. Serb. Chem. Soc. 79 (12) S166–S172 (2014) *Supplementary material*

SUPPLEMENTARY MATERIAL TO

Synthesis and antioxidant activity study of pyrazoline carrying an arylfuran/arylthiophene moiety

VIDYASHREE H. S. JOIS[1], BALAKRISHNA KALLURAYA[1]* and KOTATHATTU S. GIRISHA[2]

[1]Department of Studies in Chemistry, Mangalore University, Mangalagangothri, Konaje – 574 199, India and [2]Solid State and Structural Chemistry Unit (SSCU), Indian Institute of Science, Bangalore – 560 012, India

J. Serb. Chem. Soc. 79 (12) (2014) 1469–1475

ANALYTICAL AND SPECTRAL DATA OF THE SYNTHESIZED COMPOUNDS

1-(4-Methylphenyl)-3-[5-(4-nitrophenyl)furan-2-yl]prop-2-en-1-one ***(2a)***. Mol. Form.: $C_{20}H_{15}NO_4$ (*FW*: 333.3); *m.p.*: 149–150 °C (Lit. 148–150 °C[1]); ^{1}H-NMR (400 MHz, $CDCl_3$, δ / ppm): 6.56 (1H, *d*, *J* = 15.3 Hz, H-3), 6.83 (1H, *d*, *J* = 15.3 Hz, H-2), 7.0–8.2 (8H, *m*, Ar-H), 6.2 (1H, *d*, *J* = 3.6 Hz, furan H-3), 6.8 (1H, *d*, *J* = 3.6 Hz, furan H-4), 2.4 (3H, *s*, CH_3).

1-(4-Methoxyphenyl)-3-[5-(4-nitrophenyl)furan-2-yl]prop-2-en-1-one ***(2b)***. Mol. Form.: $C_{20}H_{15}NO_5$ (*FW*: 349.3); *m.p.*: 163–165 °C (Lit. 165–166[1]); ^{1}H-NMR (400 MHz, $CDCl_3$, δ / ppm): 6.63 (1H, *d*, *J* = 15.3 Hz, H-3), 6.71 (1H, *d*, *J* = 15.3 Hz, H-2), 6.9–8.1 (8H, *m*, Ar-H), 6.3 (1H, *d*, *J* = 3.6 Hz, furan H-3), 6.8 (1H, *d*, *J* = 3.6 Hz, furan H-4) 3.8 (3H, *s*, OCH_3).

1-(4-Chlorophenyl)-3-[5-(4-nitrophenyl)furan-2-yl]prop-2-en-1-one ***(2c)***. Mol. Form.: $C_{19}H_{12}ClNO_4$; (*FW*: 353.7); *m.p.*: 155 °C (Lit. 156–157 °C[1]); ^{1}H-NMR (400 MHz, $CDCl_3$, δ / ppm): 6.68 (1H, *d*, *J* = 15.4 Hz, H-3), 6.93 (1H, *d*, *J* = 15.4 Hz, H-2), 7.3–8.2 (8H, *m*, Ar-H), 6.4 (1H, *d*, *J* = 3.6Hz, furan H-3), 6.8 (1H, *d*, *J* = 3.6 Hz, furan H-4).

1-(2,4-Dichlorophenyl)-3-[5-(4-nitrophenyl)furan-2-yl]prop-2-en-1-one ***(2d)***. Mol. Form.: $C_{19}H_{11}Cl_2NO_4$ (*FW*: 388.2); *m.p.*: 157 °C (Lit. 157–158 °C[1]); ^{1}H-NMR (400 MHz, $CDCl_3$, δ / ppm): 6.71 (1H, *d*, *J* = 15.5 Hz, H-3), 7.02 (1H, *d*, *J* = 15.5 Hz, H-2), 7.3–8.0 (7H, *m*, Ar-H), 6.2 (1H, *d*, *J* = 3.6Hz, furan H-3), 6.7 (1H, *d*, *J* = 3.6 Hz, furan H-4).

1-(4-Hydroxyphenyl)-3-[5-(4-nitrophenyl)furan-2-yl]prop-2-en-1-one ***(2e)***. Mol. Form.: $C_{19}H_{13}NO_5$ (*FW*: 335.3); *m.p.*: 152–153 °C (Lit. 152–154 °C[2]); ^{1}H-

* Corresponding author. E-mail: bkalluraya@gmail.com

NMR (400 MHz, $CDCl_3$, δ / ppm): 6.64 (1H, *d*, *J* = 15.5 Hz, H-3), 7.12 (1H, *d*, *J* = 15.5 Hz, H-2), 7.3–8.0 (8H, *m*, Ar-H), 5.8 (1H, *s*, OH), 6.3 (1H, *d*, *J* = 3.6 Hz, furan H-3), 6.8 (1H, *d*, *J* = 3.6 Hz, furan H-4).

1-(4-Nitrophenyl)-3-[5-(4-nitrophenyl)furan-2-yl]prop-2-en-1-one (***2f***). Mol. Form.: $C_{19}H_{12}N_2O_6$ (*FW*: 364.3); *m.p.*: 205 °C (Lit. 205–206 °C[1]); ^{1}H-NMR (400 MHz, $CDCl_3$, δ / ppm): 6.71 (1H, *d*, *J* = 15.3 Hz, H-3), 7.12 (1H, *d*, *J* = 15.3 Hz, H-2), 7.1–8.2 (8H, *m*, Ar-H), 6.6 (1H, *d*, *J* = 3.6 Hz, furan H-3), 6.8 (1H, *d*, *J* = 3.6 Hz furan H-4).

1-(4-Aminophenyl)-3-[5-(4-nitrophenyl)furan-2-yl]prop-2-en-1-one (***2g***). Mol. Form.: $C_{19}H_{12}N_2O_4$ (*FW*: 334.3); *m.p.*: 234–236 °C (Lit. 235–236 °C[1]); ^{1}H-NMR (400 MHz, $CDCl_3$, δ / ppm): 6.89 (1H, *d*, *J* = 15.2 Hz, H-3), 7.10 (1H, *d*, *J* = 15.2 Hz, H-2), 7.3–8.0 (8H, *m*, Ar-H), 6.4 (1H, *d*, *J* = 3.6 Hz, furan H-3), 6.8 (1H, *d*, *J* = 3.6 Hz, furan H-4), 9.1 (2H, *s*, NH_2).

1-(4-Methylphenyl)-3-[5-(2-nitrophenyl)furan-2-yl]prop-2-en-1-one (***2h***). Mol. Form.: $C_{20}H_{15}NO_4$ (*FW*: 333.3); *m.p.*: 133 °C (Lit. 134 °C[1]); ^{1}H-NMR (400 MHz, DMSO-d_6, δ / ppm): 6.71(1H, *d*, *J* = 15.2 Hz, H-3), 7.05 (1H, *d*, *J* = = 15.2 Hz, H-2), 7.3–7.6 (8H, *m*, Ar-H), 6.4 (1H, *d*, *J* = 3.2 Hz, furan H-3), 6.6 (1H, *d*, *J* = 3.2 Hz, furan H-4), 2.2 (3H, *s*, CH_3).

1-(4-Methylphenyl)-3-[5-(4-nitrophenyl)-2-thienyl]prop-2-en-1-one (***2i***). Mol. Form.: $C_{20}H_{15}NO_3S$ (*FW*: 349.4); *m.p.*: 159 °C (Lit. 158–160 °C[2]); ^{1}H--NMR (400 MHz, $CDCl_3$, δ / ppm): 6.78 (1H, *d*, *J* = 15.3 Hz, H-3), 7.15 (1H, *d*, *J* = 15.3 Hz, H-2), 7.2–8.2 (8H, *m*, Ar-H), 7.0 (1H, *d*, *J* = 3.2 Hz, thiophene H-3), 6.8 (1H, *d*, *J* = 3.2 Hz, thiophene H-4), 2.13 (3H, *s*, CH_3).

1-(4-Methoxyphenyl)-3-[5-(4-nitrophenyl)-2-thienyl]prop-2-en-1-one (***2j***). Mol. Form.: $C_{20}H_{15}NO_4S$ (*FW*: 365.4); *m.p.*: 152–153 °C (Lit. 151–153 °C[2]); ^{1}H-NMR (400 MHz, $CDCl_3$, δ / ppm): 6.68 (1H, *d*, *J* = 15.3 Hz, H-3), 7.15 (1H, *d*, *J* = 15.3 Hz, H-2), 7.2–8.0 (8H, *m*, Ar-H), 6.4 (1H, *d*, *J* =3.6Hz, thiophene H-3), 6.6 (1H, *d*, *J* = 3.6 Hz, thiophene H-4), 3.89 (3H, *s*, CH_3).

1-(4-Chlorophenyl)-3-[5-(4-nitrophenyl)-2-thienyl]prop-2-en-1-one (***2k***). Mol. Form.: $C_{19}H_{12}ClNO_3S$ (*FW*: 369.8); *m.p.*: 108–109 °C (Lit. 109–110 °C[2]); ^{1}H NMR (400 MHz, $CDCl_3$, δ / ppm): 6.73 (1H, *d*, *J* = 15.5 Hz, H-3), 7.02 (1H, *d*, *J* = 15.5 Hz, H-2), 7.3–8.0 (7H, *m*, Ar-H), 6.2 (1H, *d*, *J* = 3.6Hz, thiophene H-3), 6.6 (1H, *d*, *J* = 3.6 Hz, thiophene H-4).

1-(2,4-Dichlorophenyl)-3-[5-(4-nitrophenyl)-2-thienyl]prop-2-en-1-one (***2l***). Mol. Form.: $C_{19}H_{11}Cl_2NO_3S$ (*FW*: 404.2); *m.p.*: 102 °C (Lit. 103 °C[2]); ^{1}H--NMR (400 MHz, $CDCl_3$, δ / ppm): 6.64 (1H, *d*, *J* = 15.3 Hz, H-3), 6.93 (1H, *d*, *J* = 15.3 Hz, H-2), 7.0–7.8 (7H, *m*, Ar-H), 6.4 (1H, *d*, *J* = 3.6 Hz, thiophene H-3), 6.7 (1H, *d*, *J* =3.6 Hz, thiophene H-4).

1-(4-Hydroxyphenyl)-3-[5-(4-nitrophenyl)-2-thienyl]prop-2-en-1-one (***2m***). Mol. Form.: $C_{19}H_{13}NO_4S$ (*FW*: 351.3); *m.p.*: 134–135 °C (Lit. 135 °C[2]); ^{1}H--NMR (400 MHz, $CDCl_3$, δ / ppm): 6.58 (1H, *d*, *J* = 15.3 Hz, H-3), 6.98 (1H, *d*,

J = 15.3 Hz, H-2), 7.1–8.2 (8H, *m*, Ar-H), 6.4 (1H, *d*, *J* = 3.6 Hz, thiophene H-3), 6.8 (1H, *d*, *J* = 3.6 Hz, thiophene H-4).

*1-(4-Nitrophenyl)-3-[5-(4-nitrophenyl)-2-thienyl]prop-2-en-1-one (**2n**)*: Mol. Form.: $C_{19}H_{12}N_2O_5S$ (*FW*: 380.3); *m.p.*: 175–176 °C (Lit. 176–177 °C[2]); ^{1}H-NMR (400 MHz, $CDCl_3$, δ / ppm): 6.81 (1H, *d*, *J* = 15.3 Hz, H-3), 7.14 (1H, *d*, *J* = 15.3 Hz, H-2), 7.1–7.9 (8H, *m*, Ar-H), 6.4 (1H, *d*, *J* = 3.6 Hz, thiophene H-3), 6.8 (1H, *d*, *J* = 3.6 Hz, thiophene H-4).

*1-(3-Nitrophenyl)-3-[5-(4-nitrophenyl)-2-thienyl]prop-2-en-1-one (**2o**)*. Mol. Form.: $C_{19}H_{12}N_2O_5S$ (*FW*: 380.3); *m.p.*: 119–120 °C (Lit. 118–220 °C[2]) ^{1}H--NMR (400 MHz, DMSO-d_6, δ / ppm): 6.83 (1H, *d*, *J* = 15.3 Hz, H-3), 7.2 (1H, *d*, *J* = 15.3 Hz, H-2), 7.1–7.9 (8H, *m*, Ar-H), 6.4 (1H, *d*, *J* = 3.6 Hz, thiophene H-3), 6.7 (1H, *d*, *J* = 3.6 Hz, thiophene H-4).

*1-{3-(4-Methylphenyl)-5-[5-(4-nitrophenyl)furan-2-yl]-4,5-dihydro-1*H*-pyrazol-1-yl}ethanone (**3a**)*. Yield: 78 %; *m.p.*: 143 °C; Anal. Calcd. for $C_{22}H_{19}N_3O_4$ (*FW*: 389.4): C, 67.86; H, 4.92; N, 10.79 %. Found: C, 67.83; H, 4.87; N, 10.74 %; IR (cm^{-1}): 1661 (C=O stretching of –N–$COCH_3$ group), 3238 (Ar–H); ^{1}H-NMR (400 MHz, $CDCl_3$, δ / ppm): 2.3 (3H, *s*, $COCH_3$), 2.4 (3H, *s*, CH_3), 5.5 (1H, *dd*, *J* = 5.2 Hz, *J* = 12 Hz, pyrazoline H-5), 3.4 (H, *dd*, *J* = 5.2 Hz, *J* = 17.5 Hz, pyrazoline H-4), 3.7 (1H, *dd*, *J* = 12 Hz, *J* = 17.5 Hz, pyrazoline H-4 *trans*), 6.2 (1H, *d*, *J* = 3.6 Hz, furan H-3), 6.8 (1H, *d*, *J* = 3.6 Hz, furan H-4), 7.0––8.2 (8H, *m*, Ar-H); MS (*m*/*z*): 390.23 (M^++1).

*1-{3-(4-Methoxyphenyl)-5-[5-(4-nitrophenyl)furan-2-yl]-4,5-dihydro-1*H*-pyrazol-1-yl}ethanone (**3b**)*. Yield: 81 %; *m.p.*: 152–153 °C; Anal. Calcd. for $C_{22}H_{19}N_3O_5$ (*FW*: 405.4): C, 65.18; H, 4.72; N, 10.36 %. Found: C, 65.11; H, 4.68; N, 10.29 %; IR (cm^{-1}): 1646 (C=O stretching of –N–$COCH_3$ group), 3103 (Ar–H); ^{1}H-NMR (400 MHz, $CDCl_3$, δ / ppm): 2.4 (3H, *s*, $COCH_3$), 3.8 (3H, *s*, OCH_3) 5.7 (1H, *dd*, *J* = 5.2 Hz, *J* = 12 Hz, pyrazoline H-5), 3.4 (H, *dd*, *J* = 5.2 Hz, *J* = 17.6 Hz, pyrazoline H-4), 3.6 (1H, *dd*, *J* = 12 Hz, *J* = 17.6 Hz, pyrazoline H-4 *trans*), 6.4 (1H, *d*, *J* = 3.6 Hz, furan H-3), 6.7 (1H, *d*, *J* = 3.6 Hz furan H-4), 6.9–8.1 (8H, *m*, Ar-H). ^{13}C-NMR (100 MHz, $CDCl_3$, δ / ppm): 165.24 (C=O), 156.36 (C=N), 154.6, 151.9, 148.3, 145.7, 142.8, 134.2, 132.2, 130.2, 128.4, 127.3, 125.5, 122.4 (Ar-C), 75.2 (C-5 of pyrazoline), 68.3 (C-4 of pyrazoline), 21.21 (CO–**C**H_3), 12.5 (CH_3). MS (*m*/*z*): 406.53 (M^++1).

*1-{3-(4-Chlorophenyl)-5-[5-(4-nitrophenyl)furan-2-yl]-4,5-dihydro-1*H*-pyrazol-1-yl}ethanone (**3c**)*. Yield: 73 %; *m.p.*: 136 °C; Anal. Calcd. for $C_{21}H_{16}ClN_3O_4$ (*FW*: 409.8): C, 61.54; H, 3.94; N, 10.25 %. Found: C, 61.50; H, 3.88; N, 10.21 %; IR (cm^{-1}): 1665 (C=O stretching of –N–$COCH_3$ group), 3246 (Ar–H): ^{1}H-NMR (400 MHz, $CDCl_3$, δ / ppm): 2.4 (3H, *s*, $COCH_3$), 5.7 (1H, *dd*, *J* =5.2 Hz, *J* = 12 Hz, pyrazoline H-5), 3.4 (1H, *dd*, *J* = 5.2 Hz, *J* = 17.6 Hz, pyrazoline H-4), 3.6 (1H, *dd*, *J* = 12 Hz, *J* = 17.6 Hz, pyrazoline H-4 *trans*), 6.4 (1H, *d*, *J* = 3.6 Hz, furan H-3), 6.8 (1H, *d*, *J* = 3.6 Hz, furan H-4) 7.4–8.2 (8H, *m*,

Ar-H); ^{13}C-NMR (100 MHz, $CDCl_3$, δ / ppm): 165.52 (C=O), 156.77 (C=N), 154.3, 151.5, 148.7, 145.7, 142.8, 134.8, 132.6, 130.9, 128.1, 127.3, 125.9, 121.9 (Ar-C), 75.9 (C-5 of pyrazoline), 67.6 (C-4 of pyrazoline), 21.9 (CO–**C**H_3). MS (*m*/*z*): 410.14 (M^++1), 412.11 (M^++3).

*1-{3-(2,4-Dichlorophenyl)-5-[5-(4-nitrophenyl)furan-2-yl]-4,5-dihydro-1*H-*pyrazol-1-yl}ethanone* (***3d***). Yield: 63 %; *m.p.*: 150–151 °C; Anal. Calcd. for $C_{21}H_{15}Cl_2N_3O_4$ (*FW*: 444.2): C, 56.77; H, 3.40; N, 9.46 %. Found: C, 56.73; H, 3.37; N, 9.40 %; IR (cm^{-1}): 1669 (C=O stretching of –N–$COCH_3$ group): ^{1}H-NMR (400 MHz, $CDCl_3$, δ / ppm): 2.3 (3H, *s*, $COCH_3$), 5.6 (1H, *dd*, *J* = 5.2 Hz, *J* = 11.8 Hz, pyrazoline H-5), 3.4 (1H, *dd*, *J* = 5.2 Hz, *J* = 17.6 Hz, pyrazoline H-4), 3.6 (1H, *dd*, *J* = 11.8 Hz, *J* = 17.6 Hz, pyrazoline H-4 *trans*), 6.2 (1H, *d*, *J* = 3.6 Hz, furan H-3), 6.7 (1H, *d*, *J* = 3.6 Hz, furan H-4), 7.3–8.0 (7H, *m*, Ar-H); MS (*m*/*z*): 445.7 (M^++1).

*1-{3-(4-Hydroxyphenyl)-5-[5-(4-nitrophenyl)furan-2-yl]-4,5-dihydro-1*H-*pyrazol-1-yl}ethanone* (***3e***). Yield: 69 %; *m.p.*: 225–226 °C; Anal. Calcd. for $C_{21}H_{17}N_3O_5$ (*FW*: 391.3): C, 64.45; H, 4.38; N, 10.74 %. Found: C, 64.40; H, 4.37; N, 10.71 %; IR (cm^{-1}): 1665 (C=O stretching of –N–$COCH_3$), 3198 (Ar-H); ^{1}H-NMR (400 MHz, $CDCl_3$, δ / ppm): 2.4 (3H, *s*, $COCH_3$), 5.5 (1H, *dd*, *J* = 5.2 Hz, *J* = 11.2 Hz, pyrazoline H-5), 3.2 (H, *dd*, *J* =5.2 Hz, *J* =17.4 Hz, pyrazoline H-4), 3.4 (1H, *dd*, *J* = 11.2 Hz, *J* = 17.4 Hz, pyrazoline H-4 *trans*), 5.8 (1H, *s*, OH), 6.3 (1H, *d*, *J* = 3.6 Hz, furan H-3), 6.8 (1H, *d*, *J* = 3.6 Hz, furan H-4) 7.3–8.0 (8H, *m*, Ar-H); MS (*m*/*z*): 392.09 (M^++1).

*1-{3-(4-Nitrophenyl)-5-[5-(4-nitrophenyl)furan-2-yl]-4,5-dihydro-1*H-*pyrazol-1-yl}ethanone* (***3f***). Yield: 56 %; *m.p.*: 125–126 °C; Anal. Calcd. for $C_{21}H_{16}N_4O_6$ (*FW*: 420.3): C, 60.00; H, 3.84; N, 13.33 %. Found: C, 59.96; H, 3.85; N, 13.29 %; IR (cm^{-1}): 1666 (C=O stretching of –N–$COCH_3$ group), 3229 (Ar–H): ^{1}H-NMR (400 MHz, $CDCl_3$, δ / ppm): 2.4 (3H, *s*, $COCH_3$), 5.6 (1H, *dd*, *J* = 5.2 Hz, *J* = 11.8 Hz, pyrazoline H-5), 3.4 (H, *dd*, *J* = 5.2 Hz, *J* = 17.6 Hz, pyrazoline H-4), 3.5 (1H, *dd*, *J* = 11.8 Hz, *J* = 17.6 Hz, pyrazoline H-4 *trans*), 6.6 (1H, *d*, *J* = 3.6 Hz, furan H-3), 6.8 (1H, *d*, *J* = 3.6 Hz furan H-4), 7.1–8.2 (8H, *m*, Ar-H); MS (*m*/*z*): 421.45 (M^++1).

*1-{3-(4-Aminophenyl)-5-[5-(4-nitrophenyl)furan-2-yl]-4,5-dihydro-1*H-*pyrazol-1-yl}ethanone* (***3g***). Yield: 53 %; *m.p.*: 247–248 °C; Anal. Calcd. for $C_{21}H_{18}N_4O_4$ (*FW*: 390.3): C, 64.61; H, 4.65; N, 14.35 %. Found: C, 64.58; H, 4.59; N, 14.31%; IR (cm^{-1}): 1652 (C=O stretching of –N–$COCH_3$ group), 3248 (Ar–H); ^{1}H-NMR (400 MHz, $CDCl_3$, δ / ppm): 2.3 (3H, *s*, $COCH_3$), 5.7 (1H, *dd*, *J* = 5.0 Hz, *J* = 12.0 Hz, pyrazoline H-5), 3.1 (1H, *dd*, *J* = 5.0 Hz, *J* = 17.8 Hz, pyrazoline H-4), 3.3 (1H, *dd*, *J* = 12.0 Hz, *J* = 17.8 Hz, pyrazoline H-4 *trans*), 6.4 (1H, *d*, *J* = 3.6 Hz, furan H-3), 6.8 (1H, *d*, *J* = 3.6 Hz, furan H-4), 9.1 (2H, *s*, NH_2), 7.3–8.0 (8H, *m*, Ar-H); ^{13}C-NMR (100 MHz, $CDCl_3$, δ / ppm): 166.3 (C=O), 157.0 (C=N), 155.3, 152.5, 148.9, 145.2, 144.8, 134.1, 132.5, 130.3,

128.9, 126.3, 125.1, 122.8 (Ar-C), 74.7 (C-5 of pyrazoline), 69.6 (C-4 of pyrazoline), 21.1 (CO–**C**H_3). MS (*m*/*z*): 391.23 (M^++1).

*1-{3-(4-Methylphenyl)-5-[5-(2-nitrophenyl)furan-2-yl]-4,5-dihydro-1*H*-pyrazol-1-yl}ethanone (**3h**)*. Yield: 85 %; *m.p.*: 149 °C; Anal. Calcd. for $C_{22}H_{19}N_3O_4$ (*FW*: 389.4): C, 67.86; H, 4.92; N, 10.79 %. Found: C, 67.80; H, 4.88; N, 10.75 %; IR (cm^{-1}): 1647 (C=O stretching of –N–$COCH_3$ group), ^{1}H-NMR (400 MHz, DMSO-d_6, δ / ppm): 2.4 (3H, *s*, $COCH_3$), 2.1 (3H, *s*, CH_3), 5.6 (1H, *dd*, *J* = 4.8 Hz, *J* = 11.4 Hz, pyrazoline H-5), 3.3 (H, *dd*, *J* = 4.8 Hz, *J* = = 17.6 Hz, pyrazoline H-4), 3.5 (1H, *dd*, *J* = 11.4 Hz, *J* = 17.6 Hz, pyrazoline H-4 *trans*), 6.4 (1H, *d*, *J* = 3.2 Hz, furan H-3), 6.6 (1H, *d*, *J* = 3.2 Hz, furan H-4), 7.3–7.6 (8H, *m*, Ar-H). ^{13}C-NMR (100 MHz, $CDCl_3$, δ / ppm):166.54 (C=O), 155.56 (C=N), 153.6, 151.9, 149.3, 145.2, 143.8, 134.5, 133.9, 131.4, 128.9, 127.7, 124.5, 123.4 (Ar-C), 77.2 (C-5 of pyrazoline), 68.9 (C-4 of pyrazoline), 21.3 (CO–**C**H_3), 13.6 (CH_3). MS (*m*/*z*): 390.18 (M^++1).

*1-{3-(4-Methylphenyl)-5-[5-(4-nitrophenyl)-2-thienyl]-4,5-dihydro-1*H*-pyrazol-1-yl}ethanone (**3i**)*. Yield: 79 %; *m.p.*: 89–90 °C; Anal. Calcd. for $C_{22}H_{19}N_3O_3S$ (FW: 405.4): C, 65.17; H, 4.72; N, 10.36 %. Found: C, 65.18; H, 4.68; N, 10.31 %; IR (cm^{-1}): 1658 (C=O stretching of –N–$COCH_3$ group), ^{1}H-NMR (400 MHz, $CDCl_3$, δ / ppm): 2.4 (3H, *s*, $COCH_3$), 1.9 (3H, *s*, CH_3), 5.8 (1H, *dd*, *J* = 4.4 Hz, *J* = 11.6 Hz, pyrazoline H-5), 3.3 (1H, *dd*, *J* = 4.4 Hz, *J* = = 17.6 Hz, pyrazoline H-4), 3.7 (1H, *dd*, *J* = 11.6 Hz, *J* = 17.6 Hz, pyrazoline H-4 *trans*), 7.0 (1H, *d*, *J* = 3.2 Hz, thiophene H-3), 7.0 (1H, *d*, *J* = 3.2 Hz, thiophene H-4), 7.2–8.2 (8H, *m*, Ar-H). ^{13}C-NMR (100 MHz, $CDCl_3$, δ / ppm): 165.24 (C=O), 156.36 (C=N), 154.6, 151.9, 148.3, 145.7, 142.8, 134.2, 132.2, 130.2, 128.4, 127.3, 125.5, 122.4 (Ar-C), 75.2 (C-5 of pyrazoline), 68.3 (C-4 of pyrazoline), 21.21 (CO–**C**H_3), 12.5 (CH_3); MS (*m*/*z*): 306.16 (M^++1).

*1-{3-(4-Methoxyphenyl)-5-[5-(4-nitrophenyl)-2-thienyl]-4,5-dihydro-1*H*-pyrazol-1-yl}ethanone (**3j**)*: Yield: 81 %; *m.p.*: 89 °C; Anal. Calcd. for $C_{22}H_{19}N_3O_4S$ (*FW*: 421.4): C, 62.69; H, 4.54; N, 9.97 %. Found: C, 62.63; H, 4.51; N, 9.88 %; IR (cm^{-1}): 1656 (C=O stretching of –N–$COCH_3$ group); ^{1}H-NMR (400 MHz, $CDCl_3$, δ / ppm): 2.4 (3H, *s*, $COCH_3$), 3.7 (3H, *s*, CH_3), 5.9 (1H, *dd*, *J* = 4.4 Hz, *J* = 11.6 Hz, pyrazoline H-5), 3.3 (H, *dd*, *J* = 4.4 Hz, *J* = = 17.6 Hz, pyrazoline H-4), 3.7 (1H, *dd*, *J* = 11.6 Hz, *J* = 17.6 Hz, pyrazoline H-4 *trans*), 6.4 (1H, *d*, *J* =3.6 Hz, thiophene H-3), 6.6 (1H, *d*, *J* = 3.6 Hz, thiophene H-4), 7.2–8.0 (8H, *m*, Ar-H); MS (*m*/*z*): 422.18 (M^++1).

*1-{3-(4-Chlorophenyl)-5-[5-(4-nitrophenyl)-2-thienyl]-4,5-dihydro-1*H*-pyrazol-1-yl}ethanone (**3k**)*. Yield: 61 %; *m.p.*: 69–70 °C; Anal. Calcd. for $C_{21}H_{16}ClN_3O_3S$ (*FW*: 425.8): C, 59.22; H, 3.79; N, 9.87 %. Found: C, 59.17; H, 3.75; N, 9.84 %; IR (cm^{-1}): 1661 (C=O stretching of –N–$COCH_3$ group); ^{1}H-NMR (400 MHz, $CDCl_3$, δ / ppm): 2.2 (3H, *s*, $COCH_3$), 5.5 (1H, *dd*, *J* =5.2 Hz, *J* = 11.8 Hz, pyrazoline H-5), 3.4 (H, *dd*, *J* = 5.2 Hz, *J* = 17.6 Hz, pyrazoline

H-4), 3.6 (1H, *dd*, *J* = 11.8 Hz, *J* = 17.6 Hz, pyrazoline H-4 *trans*), 6.2 (1H, *d*, *J* = 3.6 Hz, furan H-3), 6.5 (1H, *d*, *J* = 3.6 Hz, furan H-4) 7.2–8.0 (7H, *m*, Ar-H); MS (*m*/*z*): 426.7 (M^++1).

*1-{3-(2,4-Dichlorophenyl)-5-[5-(4-nitrophenyl)-2-thienyl]-4,5-dihydro--1*H*-pyrazol-1-yl}ethanone (**3l**)*. Yield: 63 %; *m.p.*: 94 °C; Anal. Calcd. for $C_{21}H_{15}Cl_2N_3O_3S$ (*FW*: 460.3): C, 54.79; H, 3.28; N, 9.13 %. Found: C, 54.75; H, 3.21; N, 9.09 %; IR (cm^{-1}): 1667 (C=O stretching of –N–$COCH_3$ group), 3255 (Ar–H); ^{1}H-NMR (400 MHz, $CDCl_3$, δ / ppm): 2.4 (3H, *s*, $COCH_3$), 5.7 (1H, *dd*, *J* = 5.0 Hz, *J* = 11.8 Hz, pyrazoline H-5), 3.4 (H, *dd*, *J* = 5.0 Hz, *J* = = 17.4 Hz, pyrazoline H-4), 3.5 (1H, *dd*, *J* = 11.8 Hz, *J* = 17.4 Hz, pyrazoline H-4 *trans*), 6.4 (1H, *d*, *J* = 3.6 Hz, thiophene H-3), 6.7 (1H, *d*, *J* =3.6 Hz, thiophene H-4), 7.0–7.8 (7H, *m*, Ar-H); MS (*m*/*z*): 461.63 (M^++1).

*1-{3-(4-Hydroxyphenyl)-5-[5-(4-nitrophenyl)-2-thienyl]-4,5-dihydro-1*H*--pyrazol-1-yl}ethanone (**3m**)*. Yield: 69 %; *m.p.*: 205–206 °C; Anal. Calcd. for $C_{21}H_{17}N_3O_4S$ (*FW*: 407.4): C, 61.90; H, 4.21; N, 10.31 %. Found: C, 61.86; H, 4.19; N, 10.28 %; IR (cm^{-1}): 1667 (C=O stretching of –N–$COCH_3$ group), 3242 (Ar–H); ^{1}H-NMR (400 MHz, $CDCl_3$, δ / ppm): 2.2 (3H, *s*, $COCH_3$), 5.2 (1H, *dd*, *J* = 5.2 Hz, *J* = 11.8 Hz, pyrazoline H-5), 3.3 (H, *dd*, *J* = 5.2 Hz, *J* = 17.6 Hz, pyrazoline H-4), 3.5 (1H, *dd*, *J* = 11.8 Hz, *J* = 17.6 Hz, pyrazoline H-4 *trans*), 6.4 (1H, *d*, *J* = 3.6 Hz, thiophene H-3), 6.8 (1H, *d*, *J* = 3.6 Hz, thiophene H-4), 7.1– –8.2 (8H, *m*, Ar-H), 5.8 (1H, *s*, OH); MS (*m*/*z*): 408.14 (M^++1).

*1-{3-(4-Nitrophenyl)-5-[5-(4-nitrophenyl)-2-thienyl]-4,5-dihydro-1*H*-pyrazol--1-yl}ethanone* (***3n***). Yield: 61 %; *m.p.*: 137–138 °C; Anal. Calcd. for $C_{21}H_{16}N_4O_5S$ (*FW*: 436.4): C, 57.79; H, 3.70; N, 12.84 %. Found: C, 12.84; H, 3.67; N, 12.80 %; IR (cm^{-1}): 1663 (C=O stretching of –N–$COCH_3$ group), 3232 (Ar–H); ^{1}H-NMR (400 MHz, $CDCl_3$, δ / ppm): 2.3 (3H, *s*, $COCH_3$), 5.6 (1H, *dd*, *J* = 5.0 Hz, *J* = 12.0 Hz, pyrazoline H-5), 3.4 (H, *dd*, *J* = 5.0 Hz, *J* = 17.6 Hz, pyrazoline H-4), 3.5 (1H, *dd*, *J* = 12.0 Hz, *J* = 17.6 Hz, pyrazoline H-4 *trans*), 6.4 (1H, *d*, *J* = 3.6 Hz, thiophene H-3), 6.8 (1H, *d*, *J* = 3.6 Hz, thiophene H-4), 7.1– –7.9 (8H, *m*, Ar-H); MS (*m*/*z*): 437.26 (M^++1).

*1-{3-(3-nitrophenyl)-5-[5-(4-nitrophenyl)-2-thienyl]-4,5-dihydro-1*H*-pyrazol-1-yl}ethanone (**3o**)*. Yield: 52 %; *m.p.*: 117–118 °C; Anal. Calcd. for $C_{21}H_{16}N_4O_5S$ (*FW*: 436.4): C, 57.79; H, 3.70; N, 12.84 %. Found: C, 57.76; H, 3.65; N, 12.81 %; IR (cm^{-1}): 1669 (C=O stretching of –N–$COCH_3$ group), ^{1}H--NMR (400 MHz, DMSO-d_6, δ / ppm): 2.4 (3H, *s*, $COCH_3$), 5.7 (1H, *dd*, *J* = 5.2 Hz, *J* = 12.0 Hz, pyrazoline H-5), 3.3 (H, *dd*, *J* = 5.2 Hz, *J* = 17.4 Hz, pyrazoline H-4), 3.6 (1H, *dd*, *J* = 12.0 Hz, *J* = 17.4 Hz, pyrazoline H-4 *trans*), 6.4 (1H, *d*, *J* = 3.6 Hz, thiophene H-3), 6.7 (1H, *d*, *J* = 3.6 Hz, thiophene H-4), 7.1–7.9 (8H, *m*, Ar-H); MS (*m*/*z*): 437.59 (M^++1).

REFERENCES

1. A. D'Souza, *PhD Thesis*, Mangalore University, Phajeer, 1994, p. 254
2. S. N. Shetty, *PhD Thesis*, Mangalore University, Phajeer, 1997, p. 135.

Journal of the Serbian Chemical Society
JSCS-info@shd.org.rs • www.shd.org.rs/JSCS
J. Serb. Chem. Soc. 79 (12) 1477–1490 (2014)
JSCS–4681
UDC **Trichinella spiralis*+543:616–008.92
Original scientific paper

Detection of a *Trichinella*-specific IgE in human trichinellosis – the creation of a new test

MARIJA DEVIĆ, ALISA GRUDEN-MOVSESIJAN
and LJILJANA SOFRONIĆ-MILOSAVLJEVIĆ*

Institute for the Application of Nuclear Energy – INEP, University of Belgrade, Banatska 31b, 11080 Belgrade, Serbia

(Received 2 April, revised 23 June 2014, accepted 24 June 2014)

Abstract: Trichinellosis is a parasitic disease of humans caused by nematodes from the genus *Trichinella*, predominantly *Trichinella spiralis*. If *Trichinella* infection is suspected based on an epidemiological link and clinical criteria within defined period of time, then finding of *Trichinella*-specific antibodies in the examined sera provides definitive proof of the establishment of infection. Detection of a *Trichinella*-specific IgE that could precede, coincide or follow IgG seroconversion not only confirms the existence of infection, but could narrow the time frame in which the infection occurred to a year or even less. Since there are no commercially available tests for monitoring the presence of a *Trichinella*-specific IgE during the course of the disease, the present work was aimed at establishing this kind of ELISA test. The specificity and sensitivity of hitherto described *Trichinella*-specific IgE ELISAs are not sufficiently satisfactory; the two major problems are poor discrimination between positive and negative results and cross reactivity with sera of patients with different parasitic diseases. In this study, a *Trichinella*-specific IgE capture ELISA was developed that overcomes the problems of specificity and sensitivity and enables the determination of *Trichinella*-specific IgE.

Keywords: *Trichinella spiralis*; *Trichinella*-specific IgE; capture ELISA.

INTRODUCTION

Trichinellosis is a parasitic disease of humans caused by nematodes from the genus *Trichinella*, predominantly *Trichinella spiralis*.[1] Humans become infected through consumption of raw or undercooked infected meat. Host defense is activated upon the parasitic invasion and could be monitored through changes in blood parameters, such as eosinophilia (short lasting phenomenon, *i.e.*, duration measurable in days) and the presence of anti-*Trichinella* antibodies (long lasting, *i.e.*, detectible over months or years, as the presence of specific IgG antibodies).

* Corresponding author. E-mail: sofronic@inep.co.rs
doi: 10.2298/JSC140402065D

However, the finding of *Trichinella*-specific IgG in human sera might not be proof of *Trichinella* infection *per se*,[2] as it indicates that infection with this parasite had occurred sometime in the past (antibodies can be detectable from 12 to 60 days post infection and may persist for more than 30 years after infection),[3] regardless of whether it was asymptomatic or with visible clinical signs of illness, and that live parasites are still present in the host organism. In the case of mild or asymptomatic trichinellosis, it is hard to distinguish between recently acquired and chronic *Trichinella* infection. The presence of *Trichinella*-specific IgE could help in narrowing the period in which the infection had occurred. Namely, specific IgE appears early, within the first 2 weeks from infection, and could be found in the sera of *Trichinella*-infected persons one year after infection.[4,5]

Although best known for its role in allergy, IgE has also been studied in parasitic diseases (helminth infections) that are accompanied with symptoms resembling allergy, as is the case with trichinellosis. It is known that *T. spiralis* infection induces the synthesis of a specific IgE, and its connection with eosinophilia and direct involvement in allergic manifestation was suggested.[6] Animal models of *Trichinella* infection revealed a protective role to the host of a specific IgE.[7] However, such a role, with the present knowledge, could not be ascribed to a specific IgE in humans, although there are epidemiological studies for other helminths that confirm protection from re-infection.[8,9] Infection with *Trichinella*, as with other helminths, also results in temporary elevation of the total IgE during the course of the disease, which may not exceed the normal range. The role of unspecific IgE is not as clear,[6,10–12] but there are findings that connect high concentrations of unspecific IgE with beneficial effects to the parasite.[13]

Numerous attempts have been made to detect the presence of a *Trichinella*-specific IgE, but the detection rates reported in the literature varied from 7–100 %, due to the differences in the type of the assay used, the reliability of the test used for this purpose, and the acuteness of the infection.[6] Problems in the detection of *Trichinella*-specific IgE antibodies by a classical indirect enzyme-linked immunosorbent assay (ELISA) arise from its unfavorable competition with IgG antibodies for binding to antigen coated wells. This is a consequence of the naturally low concentration of IgE in sera, compared to the many times higher values for IgG. This does not mean that *Trichinella*-specific IgE antibodies in the sera could not be detected, but the probability for their detection with classical ELISA is very low, due to reduced sensitivity of the technique, which causes false negative (FN) results.

The goal of this study was to develop a sensitive ELISA test for determination of *Trichinella*-specific IgE in human serum samples, since there is no such test on the market. Two types of ELISAs for *Trichinella*-specific IgE detection were formulated and their analytical validation and comparison with

classical indirect ELISA that uses untreated serum samples were performed. The most commonly employed method for overcoming the problem of the excess IgG concentration and maximizing IgE detection is pretreatment of the examined sera with various commercially available absorbents with the aim of removing IgG prior to specific-IgE determination.[14,15] Thus, one type of test was classical indirect ELISA using sera treated with an in-house designed IgG absorbent. The other, capture ELISA for *Trichinella*-specific IgE detection (capture *Trichinella* IgE ELISA), solved the problem of competition between the two specific antibody isotypes – IgE and IgG, by employing a specific approach, which paired two monoclonal antibodies, one that allowed the separation of IgE antibodies from all other classes of antibodies in human sera (anti-human IgE monoclonal antibody) and the other that recognized an epitope on *Trichinella* spp. muscle larvae excretory–secretory antigens (detection 7C2C5 monoclonal antibody).

EXPERIMENTAL

Antigen preparation

T. spiralis muscle larvae (L1 larvae) were recovered from Wistar rats (infected with 7000 *T. spiralis* L1 per rat, ISSN 161, sacrificed three months post infection) by digesting the carcasses in pre-warmed gastric juice (1 % pepsin in 1 % HCl, pH 1.6–1.8).[16] For the production of muscle larvae excretory–secretory antigens (ES L1), the larvae were kept under controlled conditions (37 °C, 5 % CO_2) in complete Dulbecco's modified Eagle's medium (Sigma–Aldrich, Germany) supplemented with 10 mM HEPES, 2 mM L-glutamine, 1 mM sodium pyruvate (all from Sigma–Aldrich, Germany) and 50 U mL^{-1} Pen/Strep (Galenika, Serbia) for 18 h. Culture supernatants containing ES L1 products of the muscle larvae were dialyzed, concentrated and stored at –20 °C until use.[17]

Preparation of HRP conjugates

Monoclonal antibody (mAb) 7C2C5 has been maintained by the Serbian National Reference Laboratory for Trichinellosis (SrNRLT) since 1986, due to a joint project and with agreement of Dr. Gamble HR, USA. This mAb is specific for the epitope unique for the muscle larvae of the whole genus *Trichinella*, which is present on 45, 49 and 53 kDa protein components of *T. spiralis* ES L1 antigens.[18,19] 7C2C5 mAb does not exhibit any cross-reactivity with antigens from other parasites.[18] MAbs, 7C2C5 and mouse anti-human IgE (Medix Biochemica, Finland), were labeled with horseradish peroxidase (HRP) according to the procedure described elsewhere.[20] In brief, activation of the reactive groups on antibodies and of the enzyme was performed by incubation with carbonate buffer and buffer with $NaIO_4$, respectively. After the incubation and blocking of the remaining reactive sites on the antibodies, separation of labeled from un-labeled fractions was performed on a Sephacryl S-200 column. The quality of 7C2C5-HRP conjugate was assessed by an in-house *Trichinella*-ELISA test, while the quality of the anti-human IgE–HRP product was assessed by an in-house ELISA for the quantitative determination of the total serum IgE.

Pre-treatment of serum samples with IgG absorbent

Purified sheep polyclonal antibodies to human IgG (γ-chain specific, INEP, Serbia) were used as the IgG absorbent. The key step in serum stripping was the determination of the optimal volume of polyclonal antibodies for efficient removal of IgG antibodies from human

sera. The optimal ratio between serum and IgG absorbent was determined by absorbing fixed volumes of sera with different volumes of IgG absorbent. Finally, 50 µL of sera were mixed and incubated with 100 µL of IgG-absorbent for 1 h at room temperature. The immune complexes were removed by centrifugation at 6500 g for 10 min. The remaining supernatants were transferred to new tubes and tested for the presence of IgG by radioimmunodiffusion plates (RID IgG INEP, Serbia) and assayed for *Trichinella*-specific IgE.

Serum samples

This study included 28 serum samples collected from patients with confirmed diagnosis of trichinellosis. All serum samples were from the bank of SrNRLT, INEP, and were declared positive for the presence of anti-*Trichinella* antibodies (true positive, TP). The positivity was confirmed by two methods, ELISA (in-house *Trichinella*-ELISA test, INEP, Serbia) and indirect immunofluorescence assay (FITC *T. spiralis* Antibody Detection Kit; INEP, Serbia), both designed and validated for detection of parasite specific antibodies in serum samples. An ELISA based on excretory–secretory antigens (ES L1) could yield false positive results (FP) due to potential cross-reactivity with sera of patients with other parasitic or allergic diseases. This study included a total of 70 *T. spiralis* non-infected persons, covering 40 serum samples from healthy blood donors used as negative controls, sera from 20 patients with toxoplasmosis and echinococcosis and 10 patients with allergic diseases, which were involved in the estimation of the analytical specificity, diagnostic sensitivity and diagnostic specificity. Analytical specificity refers to the ability of an assay to measure a particular substance, rather than others, in a sample (in the present case *T. spiralis* specific IgE); diagnostic sensitivity is the percentage of persons who have confirmed infection (trichinellosis) and are identified by the assay as positive for a given substance (specific IgE) – true positive; diagnostic specificity is the percentage of persons who do not have the indicated infection and who are identified as negative for a given substance (specific IgE) in the assay – true negative (TN).[21]

All sera samples were split into aliquots and stored at –20 °C until testing.

ELISA procedure

Classical indirect ELISA. To detect *Trichinella*-specific IgE antibodies, the standard test configuration with a 3-step procedure was used. Briefly, 96-well polystyrene microtiter plates (Immulon Microtiter 96-well plates and strips, Thermo Scientific) were coated with 100 µL per well of ES L1 antigens (5 µg mL^{-1} in 0.1 M carbonate buffer, pH 9.6) and incubated overnight at 4 °C. The plates were washed with washing solution (0.05 % Tween 20 in phosphate buffer (PBS), pH 7.2), and the remaining binding sites were blocked with 1 % BSA in PBS pH 7.2 for 1 h at room temperature. After the washing step, 100 µL per well of each 1/3 diluted serum sample was added in duplicate and incubated for 18 h at 4 °C. After extensive washing, 100 µL per well of anti-human IgE mAb–HRP was added to each well and incubated for 3 h at room temperature. After a final wash, 100 µL per well of chromogenic solution (3,3′,5,5′-tetramethylbenzidine hydrogen peroxide–TMB substrate) was added and the plates were incubated at room temperature for 10 min. After stopping the reaction with 2 M H_2SO_4, the optical densities (*OD*) were measured at 450 nm using a Diamedix (Miami, FL, USA) microassay BP-12 ELISA reader.

To reduce the IgG concentration in the sample and mitigate the IgG/IgE antibody competition, the serum samples were pretreated with IgG absorbent, as previously explained. After removal of the immune complexes, the remaining supernatants were transferred to new tubes and used for the detection of specific IgE in a classical indirect ELISA.

Capture Trichinella *IgE ELISA*. The test configuration was achieved through a 4-step procedure. The 96-well plates were coated with 100 µL of mouse anti-human IgE mAb (2 µg mL^{-1} in 0.1 M carbonate buffer, pH 9.6), and incubated overnight at 4 °C. The plates were washed with washing solution (0.05 % Tween 20 in PBS, pH 7.2) and the remaining binding sites were blocked with 1 % BSA in PBS, pH 7.2, 200 µL per well, for 1 h at room temperature. After washing, the serum samples, diluted 1:3 in PBS, were added in duplicate and incubated for 2 h at 37 °C. The plates were again washed and ES L1 antigens (2 µg mL^{-1}, 100 µL per well) were added for 2 h at room temperature, with mixing. After removal of unbound ES L1 antigens with washing, 100 µL of HRP labeled 7C2C5 mAb (1:500 dilution) was added to each well for 1 h at room temperature. The optimal concentrations of the reagents (anti human-IgE mAb, serum dilution and ES L1 antigens) had previously been determined. After a final wash, 100 µL per well of chromogenic solution (3,3′,5,5′-tetramethylbenzidine hydrogen peroxide–TMB substrate) was added and the plates were incubated at room temperature for 10 min. After stopping the reaction with 2 M H_2SO_4, the *OD* was measured at 450 nm using a Diamedix (Miami, FL, USA) microassay BP-12 ELISA reader.

Statistics

Receiver operating characteristic (ROC) analyses[22] were performed using MedCalc software, version 13.1 (MedCalc Software, Ostend, Belgium). Other results were analyzed using GraphPad Prism software, version 6 (GraphPad Software Inc., La Jolla, CA, USA).

Accreditation

The INEP Laboratory (that includes SrNRLT) has accredited services for human laboratory medicine according to UNI CEI EN ISO/IEC 17025:2005.

RESULTS

Classical indirect ELISA for the detection of Trichinella*-specific IgE using untreated and treated serum samples*

The results for the determination of the presence of anti-*Trichinella* IgE in untreated sera by classical indirect ELISA are given in Fig. 1A. The obtained absorbance (*A*) values were low (between 0.04 and 0.1). The ranges of *A* values for the positive and negative samples were very similar and, consequently, discrimination between them and interpretation of such results could not be performed.

Using serum samples treated with IgG absorbent, this kind of ELISA was able to detect *Trichinella*-specific IgE in 93 % (26 out of 28) in *Trichinella* antibody positive sera. The obtained absorbance values for the positive sera were higher than those obtained in the Classical Indirect ELISA using unprocessed sera, but still the range of the measured absorbance remained low (with a highest *OD* value of 0.340). The results are shown in Fig. 1B. An ROC curve was built with data from the positive reference population (28 samples from patients with a confirmed diagnosis of trichinellosis) and the negative reference population (40 samples from blood donors) (Fig. 1C). According to the ROC analysis, the best cut-off *OD* value was 0.078; based on this cut-off value, the sensitivity and specificity of the test were 92.9 and 100 %, respectively. The area under the ROC

curve (*AUC*), which indicates accuracy, determined for the best cut-off *OD* value was equal to 0.98.

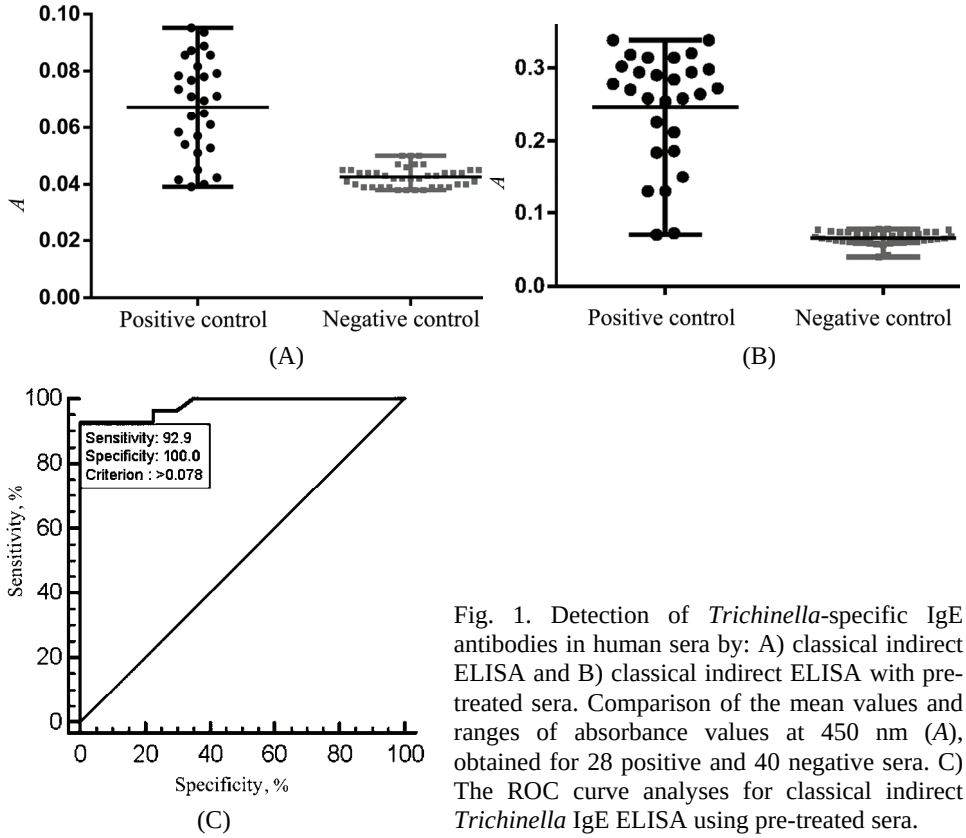

Fig. 1. Detection of *Trichinella*-specific IgE antibodies in human sera by: A) classical indirect ELISA and B) classical indirect ELISA with pre-treated sera. Comparison of the mean values and ranges of absorbance values at 450 nm (*A*), obtained for 28 positive and 40 negative sera. C) The ROC curve analyses for classical indirect *Trichinella* IgE ELISA using pre-treated sera.

Preliminary estimation of repeatability was determined using five positive and five negative sera from the mentioned panel of sera. The intra- and inter--assay variability statistics are given in Table I. Results are shown as mean values of standard deviations and coefficients of variation obtained in five times performed intra- and inter-assays (*CV* / % = *SD*/mean values of samples absorbance). Coefficients of variation with values less than 20 % indicate adequate

TABLE I. Intra- and inter-assay repeatability for classical indirect *Trichinella* IgE ELISA using pre-treated sera; times run: 5

Assay	Serum	*SD*	*CV* / %
Intra	Negative	0.0025	8.2
	Positive	0.00258	2.93
Inter	Negative	0.0061	18.23
	Positive	0.005	6.0

repeatability at this stage of the assay development (validation).[23] All of the obtained results were within the acceptable range of error.

Analytical specificity was assessed by use of panel of sera collected from people suffering from parasitic (toxoplasmosis or echinococcosis) or other (allergic) diseases where the presence of parasite-specific IgE or increased total IgE, respectively, may influence the detection of *Trichinella*-specific IgE. Three out of ten sera of patients with toxoplasmosis gave positive results in the test, and it is already well known that there is some degree of cross-reactivity between specific antibodies to *Toxoplasma gondii* and the ES L1 antigen of *T. spiralis*.[24,25] None of the sera of patients with echinococcosis were reactive in this type of ELISA. The analytical specificity of the indirect *Trichinella* IgE ELISA was 90 %.

Diagnostic sensitivity and specificity were estimated from the results of the testing of 28 serum samples of patients with confirmed diagnosis of trichinellosis (TP), 40 sera samples from healthy blood donors – as the negative control (TN), and 30 sera from patients with other known infection or allergy (having potential to cross-react with the ES L1 antigen of *T. spiralis*). The results obtained by testing the sera by indirect *Trichinella* IgE ELISA are summarized in Table II. The diagnostic specificity was 95 %, calculated as $TN/(TN+FP)$, and the sensitivity was 89 %, calculated as $TP/(TP+FN)$. The positive predictive value was 93 %, calculated as $TP/(TP+FP)$, and the negative predictive value was 95 %, calculated as $TN/(TN+FN)$, where *TP* is the number of true positives, *FN* the number of false negatives, *TN* the number of true negatives and *FP* the number of false positives.

TABLE II. Data for the determination of the diagnostic specificity and sensitivity for classical indirect *Trichinella* IgE ELISA using pre-treated sera

ELISA result	Serum	Number of infected subjects	Serum	Number of *Trichinella* non-infected subjects
Positive	True positive	26	False positive	3
Negative	False negative	2	True negative	67
Total		28		70

Capture Trichinella *IgE ELISA*

Capture ELISA solved the problem of the competition between the excess amounts of IgG and the low concentration IgE for the same binding site on ES L1. By using monoclonal antibodies against human IgE bound to the solid phase, this test, in the first step, ensures separation of IgE antibodies in the serum from all other classes of antibodies before determination of *Trichinella*-specific IgE antibodies. *Trichinella*-specific IgE could then be detected using ES L1 antigens as specific ligands. ES L1 antigens bound to specific IgE could be revealed by the interaction with HRP-labeled 7C2C5 mAb. Capture ELISA produced higher *OD* signals than the indirect ELISA, providing significantly better discrimination

between samples from patients with trichinellosis and healthy persons (Fig. 2A). ROC curve analysis was performed with the same panel of sera as in the previously described ELISA. According to the ROC analysis (Fig. 2B), the best cut-off for the *OD* values was 0.115; based on this cut-off value, the sensitivity and specificity were both 100 %. The *AUC*, which indicates accuracy, was determined for the *OD* values and was equal to 1.

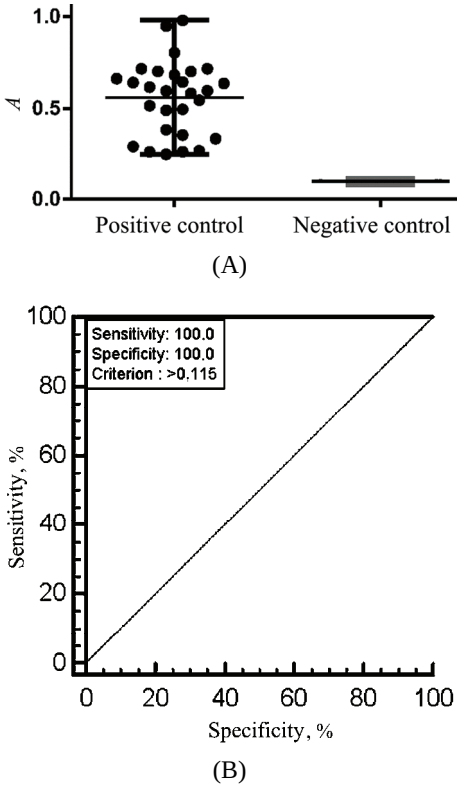

Fig. 2. Detection of *Trichinella*-specific IgE antibodies in human sera by capture ELISA. A) Comparison of the mean values and ranges of absorbance values at 450 nm (*A*), obtained for 28 positive and 40 negative sera. B) The ROC curve analyses for capture *Trichinella* IgE ELISA.

Preliminary estimation of repeatability was again determined according to the results of intra- and inter-assay testing of five positive and five negative sera. The intra- and inter-assay variability statistics are presented in Table III. Since differences between the absorbance values of the serum duplicates did not exceed *CV* values of 2 % for the positives and 6 % for the negatives in the intra assay, and 4% for the positives and 8 % for the negatives in inter assay testing, it is clear that constructed capture *Trichinella* IgE ELISA test possessed great reproducibility.

The analytical specificity was also assessed by the use of the same panel of sera as in previously described ELISA (patients with toxoplasmosis, echinococcosis and sera of patients with allergic diseases). This type of ELISA technique

shows no cross-reactivity with any of the tested serum, with an analytical specificity of 100 %.

TABLE III. Intra- and inter-assay repeatability for capture *Trichinella* IgE ELISA; times run: 5

Assay	Serum	*SD*	*CV* / %
Intra	Negative	0.0025	5.5
	Positive	0.0006	1.28
Inter	Negative	0.0044	7.71
	Positive	0.017	3.5

Diagnostic specificity and sensitivity were derived from testing samples with known infection status – 28 serum samples with confirmed diagnosis of trichinellosis, 40 samples from blood donors as negative controls, and 30 sera with potential cross-reactivity with the ES L1 antigen of *T. spiralis* (total of 70 *T. spiralis* non-infected persons). The results obtained by testing the above-mentioned sera with the capture *Trichinella* IgE ELISA are summarized in Table IV. The diagnostic specificity was 100 %, the diagnostic sensitivity was 100 %, the positive predictive value was 100 % and the negative predictive value was 100 %.

TABLE IV. Data for the determination of the diagnostic specificity and sensitivity for capture *Trichinella* IgE ELISA

ELISA result	Serum	Number of infected subjects	Serum	Number of *Trichinella* non-infected subjects
Positive	True positive	28	False positive	–
Negative	False negative	–	True negative	70
Total		28		70

Since the level of non-specific IgE also increases during helminth infection and because this test utilizes anti-human IgE mAb for capturing IgE from human sera, the effect of non-specific IgE on the result of the assay for *Trichinella*-specific IgE was estimated. No obvious decrease in the absorbance values for *Trichinella*-specific IgE was observed after addition of non-specific IgE-containing serum in range 0–180 kIU L^{-1} (Table V).

To summarize all the data from three previously described ELISAs, their characteristics were compared. The results for the absorbance ranges and the mean values, presented in Fig. 3, clearly show that the range of the obtained absorbance values in the capture *Trichinella* IgE ELISA (0.260–0.960) was much broader than in the classical indirect ELISA using treated sera (0.074–0.340) and untreated sera (0.04–0.10), which enables better interpretation of the results and increases the sensitivity of the test. Data obtained for the classical indirect ELISA using treated sera and the capture ELISA are compared in Table VI and it is obvious that the capture ELISA test for *Trichinella*-specific IgE exhibited very good performances.

TABLE V. The effect of non-specific IgE on the *Trichinella*-specific IgE determination by capture *Trichinella* IgE ELISA

Concentration of added nonspecific IgE in serum sample, kIU L^{-1}	$A_{450\ nm}$
0	0.377
3	0.357
7	0.378
10	0.368
30	0.377
60	0.369
120	0.366
180	0.369

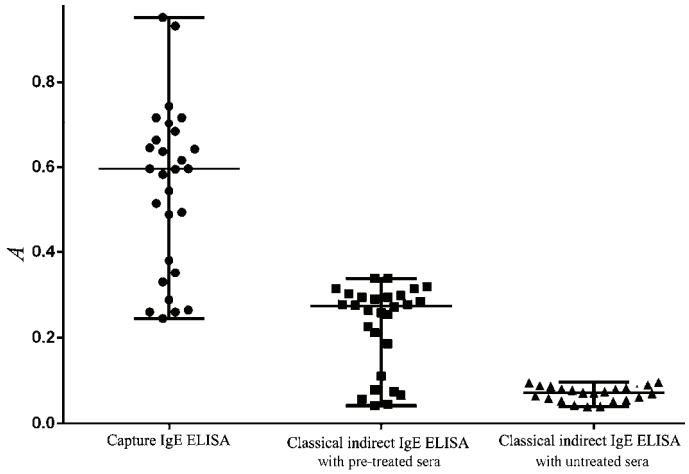

Fig. 3. Comparison of the mean values and ranges for the absorbance results obtained in ELISAs for the detection of *Trichinella*-specific IgE: capture *Trichinella* IgE ELISA, classical indirect *Trichinella* IgE ELISA with pre-treated sera and classical indirect ELISA with untreated sera.

TABLE VI. Comparison of the characteristics of classical indirect *Trichinella* IgE ELISA with pre-treated sera and capture *Trichinella* IgE ELISA for the detection of *Trichinella*-specific IgE antibodies in human sera

Characteristic	Classical indirect *Trichinella* IgE ELISA with pre-treated sera	Capture *Trichinella* IgE ELISA
$A_{450\ nm}$ range	0.074–0.340	0.260–0.960
Intra-assay repeatability for positive samples, %	2.93	1.28
Inter-assay repeatability for positive samples, %	6	3.5
Analytical specificity, %	90	100
Diagnostic specificity, %	95	100
Diagnostic sensitivity, %	89	100

DISCUSSION

The herein presented investigation was focused on creating ELISA tests that could give reliable results concerning the presence of *T. spiralis* specific IgE in the examined sera. One approach was to utilize the formerly established classical indirect ELISA but with serum samples treated with an IgG absorbent to increase the sensitivity of the test, and the other was to develop a new test, *i.e.*, a capture ELISA with performances adequate for the discrimination between specific IgE positive and negative samples. The classical indirect ELISA using untreated serum samples proved to be inadequate for the detection of *Trichinella*-specific IgE antibodies, giving false negative results because of the large quantities of specific IgG that masked the presence of a low-level of specific IgE.

Other authors using the same type of ELISA were able to detect *Trichinella*--specific IgE in a small number of patients (7 %) or in percentages ranging from 13 to 46 %.[4,6] Bruschi *et al.*[26] amplified the indirect ELISA and reported detection rates of 80 % after two months and 20 % after one year for specific IgE determination. Although the amplified method was more sensitive than the classical indirect test, this kind of ELISA does not solve the problem of competition, which was the reason for the contradictory results presented in the literature.[6,27,28] The present attempts to eliminate competition included pre-treatment of serum samples with IgG absorbent, with the aim of removing excess IgG. Many studies, however, showed that commercially available absorbents were not sufficient to improve IgE detection,[29] and the technique with protein A and G agarose beads did not give consistent results in the assay.[30,31] It was observed that these processing techniques resulted in a loss of certain amounts of IgE (data not shown), which may cause variations between tests. In addition, commercial IgG absorbents were not suitable due to the dilution effect. To avoid these problems, our own IgG absorbent was created and used in the Classical Indirect ELISA. Range of absorbance values achieved by this test was higher than obtained by classical indirect ELISA. However, the measured absorbance values remained relatively low and the problem of discrimination between positive and negative results still existed. According to the ROC analyses, the test expressed good sensitivity (92 %) and specificity (100 %), which is better than results obtained with Amplified ELISA.[26] As in other ELISA procedures, the problem of cross-reactivity remained (analytical specificity 90 %). Cross reactivity is in fact the major obstacle in serological diagnosis of various parasites and pathogens because of the shared epitopes among them. The presence of shared antigens of *Trichinella* spp. has been widely documented for other parasites and pathogens.[22,25] Hitherto, different laboratories have dealt with this problem, but they all had a common approach and that was to use different antigens or their isolated components in attempts to increase specificity. With tyvelose (carbohydrate epitope specific for

Trichinella spp) coated plates, Gamble *et al.*[32] obtained good specificity, however, the sensitivity of the test was not satisfactory.

Here, a completely new approach to solve the problems concerning the determination of *Trichinella*-specific IgE is offered. First obstacle was to remove the high levels of *Trichinella*-specific IgG that cause false negative results for specific IgE, and second to eliminate cross-reactivity. This challenge resulted in the development of a capture *Trichinella* IgE ELISA that ensured the capturing of the IgE antibodies by immobilized anti-human IgE mAb, and detection of *Trichinella*-specific IgE among them by introducing ES L1 antigens and HRP labeled 7C2C5 mAb. 7C2C5 mAb recognizes the immunodominant epitopes on ES L1 antigens bound to specific IgE. Using HRP labeled 7C2C5 mAb, the signal was successfully amplified, thus solving the problem of low absorbance values and ranges that were found in the application of previously described ELISA tests. More importantly, the obtained specificity of the capture *Trichinella* IgE ELISA test was 100 % and false positive results were eliminated.

CONCLUSIONS

The herein presented results indicate the very good performances of the capture ELISA test for *Trichinella*-specific IgE detection that, once validated, could contribute to a better understanding of the diagnostic significance of specific IgE detection in patients with trichinellosis. Extended studies with this kind of test could confirm whether specific IgE is suitable as a marker for the early phase of infection with *Trichinella* or, at least, whether it could provide additional data for estimating the time when the infection occurred, and as such, whether it could be used as a tool for differentiating between newly acquired and chronic infection.

Acknowledgment. This research was supported by the Ministry of Education, Science and Technological Development of the Republic of Serbia, Grant No. 173047.

ИЗВОД

ОТКРИВАЊЕ СПЕЦИФИЧНИХ IgE АНТИТЕЛА У ТРИХИНЕЛОЗИ КОД ЉУДИ – СТВАРАЊЕ НОВОГ ТЕСТА

МАРИЈА ДЕВИЋ, АЛИСА ГРУДЕН-МОВСЕСИЈАН и ЉИЉАНА СОФРОНИЋ-МИЛОСАВЉЕВИЋ

Институт за примену нуклеарне енергије – ИНЕП, Универзитет у Београду, Банатска 31б, 11080 Београд

Трихинелоза је паразитско обољење људи које изазива нематода из рода *Trichinella*, најчешће *Trichinella spiralis*. Налаз *Trichinella*-специфичних антитела у серуму је дефинитивни доказ постојања инфекције овом нематодом у случају када је инфекција суспектна на основу клиничке слике и постојећих лабораторијских и епидемиолошких података. Присуство IgE антитела специфичних за *Trichinella* у серуму пацијената може бити знак недавне инфекције или пак последица инфекције која се десила у неком тренутку у прошлости. Позитиван налаз *Trichinella*-специфичних IgE антитела би, с друге стране, могао да укаже на време које је протекло од инфекције, с обзиром на то да се

присуство IgE антитела може пратити у ограниченом временском интервалу, највише до годину дана након инфекције. Постоји, међутим, проблем у детектовању специфичних IgE антитела, који се јавља услед незадовољавајуће сензитивности и специфичности постојећих тестова од којих ниједан није комерцијално доступан. Наиме, до сада описани тестови су слабо разграничавали позитивне од негативних серума и нису решавали појаву лажно позитивних резултата услед унакрсне реактивности са другим паразитским болестима. Ова студија је била посвећена стварању новог теста сендвич ELISA за детекцију специфичних IgE антитела који превазилази проблеме у вези са специфичношћу и сензитивношћу и омогућава поуздано откривање *Trichinella*-специфичних IgE антитела.

(Примљено 2. априла, ревидирано 23. јуна, прихваћено 24. јуна 2014)

REFERENCES

1. E. Pozio, E. Hoberg, G. la Rosa, D. S. Zarlenga, *Infect. Genet. Evol.* **9** (2009) 606
2. J. Dupouy-Camet, F. Bruschi, in *FAO/WHO/OIE guidelines for the surveillance, management, prevention and control of trichinellosis*, 1st ed. FAO/WHO/OIE, Paris, 2007, p. 37
3. W. Fröscher, F. Gullott, M. Saathoff, W. Tackmann, *Eur. Neurol.* **28** (1988) 221
4. K. D. Murrell, F. Bruschi, *Prog. Clin. Parasitol.* **4** (1994) 117
5. F. Bruschi. L. Chiumiento, *Endocr., Metab. Immune Disord.: Drug Targets* **12** (2012) 4
6. N. Watanabe, F. Bruschi, M. Korenaga, *Trends Parasitol.* **21** (2005) 175
7. M. F. Gurish, P. J. Bryce, H. Tao, A. B. Kisselgof, E. M. Thornton, H. R. Miller, D. S. Friend, H. C. Oettgen, *J. Immunol.* **172** (2004) 1139
8. D. W. Dunne, A. E. Butterworth, A. J. C. Fulford, H. C. Kariuki, J. G. Langley, J. H. Ouma, A. Capron, R. J. Pierce, R. F. Sturrock, *Eur. J. Immunol.* **22** (1992) 1483
9. P. Rihet, C. E. Demeure, A. Bourgois, A. Prata, A. J. Dessein, *Eur. J. Immunol.* **21** (1991) 2679
10. D. Negrão-Corrêa, *Rev. Inst. Med. Trop. Sao Paulo* **43** (2001) 291
11. N. Watanabe, in *Progress of Medical Parasitology in Japan*, Vol. 7, M. Otsuru, S. Kamegai, S. Hayashi, Eds., Meguro Parasitological Museum, Tokyo, 1999, p. 321
12. *Principles of validation of diagnostic assays for infectious diseases*, in *Manual of diagnostic tests and vaccines for terrestrial animals*, World Organisation for Animal Health, Paris, 2008, p. 34
13. N. Watanabe, *Parasitol. Int*. **63** (2014) 332
14. A. M. Atta, A. D'Oliveira Júnior, J. Correa, M. L. B. Atta, R. P. Almeida, E. M. Carvalho, *Am. J. Trop. Med. Hyg.* **59** (1998) 426
15. W. G. Jaoko, M. Lund, E. Michael, P. E. Simonsen, *Acta Trop.* **80** (2001) 51
16. H. R. Gamble, A. S. Bessonov, K. Cuperlovic, A. A. Gajadhar, F. van Knapen, K. Noeckler, H. Schenone, X. Zhu, *Vet. Parasitol.* **93** (2000) 393
17. I. Radovic, A. Gruden-Movsesijan, N. Ilic, M. Mostarica-Stojkovic, Lj. Sofronic-Milosavljevic, *Mem. Inst. Oswaldo Cruz* **107** (2012) 503
18. R. Gamble (Holder), United States Patent, Number 4,670,384 (1987)
19. M. G. Ortega-Pierres, L. Yepez-Mulia, W. Homan, H. R. Gamble, P. L. Lim, D. I. Wassom, J. A. Appleton, *Parasite Immunol.* **18** (1996) 273
20. P. Tijssen, *Techniques in biochemistry and molecular biology*, Elsevier, Amsterdam, 1985, p. 171
21. R. H. Jacobson, *Rev. Sci. Tech.* **17** (1998) 469
22. M. H. Zweig, G. Campbell, *Clin. Chem.* **39** (1993) 561

23. A. Pryseley, K. Mintiens, K. Knapen, Y. Van der Stede, G. Molenberghs. *J. Appl. Stat*. **37** (2010) 1729
24. M. A. Gomez-Morales, A. Ludovisi, M. Amati, S. Cherchi, P. Pezzotti, E. Pozio, *Clin. Vaccine Immunol*. **15** (2008) 1723
25. J. L. De la Rosa, P. Alcantara, D. Correa, *Clin. Diagn. Lab. Immunol*. **2** (1995) 122
26. F. Bruschi, C. Tass, E. Pozio, *Am. J. Trop. Med. Hyg*. **43** (1990) 186
27. F. Van Knapen, J. H. Franchimont, A. R. Verdonk, J. Stumpf, K. Undeutsch, *Am. J. Trop. Med. Hyg*. **31** (1982) 973
28. I. Ljungstrom, L. Hammarstrom, W. Kocieck, C. I. E. Smith, *Clin. Exp. Immunol*. **74** (1988) 230
29. R. L. Mamoni, C. L. Rossi, Z. P. Camargo, M. H. S. L. Blotta, *Am. J. Trop. Med. Hyg*. **65** (2001) 237
30. Y. Kadooka, T. Idota, H. Gunji, M. Shimatani, H. Kawakami, S. Dosako, T. Samori, *Int. Arch. Allergy Immunol*. **122** (2000) 264
31. M. L. Souza-Atta, M. I. Araújo, A. D'Oliveira Júnior, A. Ribeiro-de-Jesus, R. P. Almeida, A. M. Atta, E. M. Carvalho, *Braz. J. Med. Biol. Res*. **32** (1999) 1101
32. H. R. Gamble, E. Pozio, F. Bruschi, K. Nocler, C. M. O. Kapel, A. A. Gajdhar, *Parasite* **11** (2004) 3.

Journal of the Serbian Chemical Society
JSCS-info@shd.org.rs • www.shd.org.rs/JSCS
J. Serb. Chem. Soc. 79 (12) 1491–1503 (2014)
JSCS–4682
UDC 547.455.623'292:54.05+
577.15:616.379–008.64
Original scientific paper

How the sialylation level of serum *N*-acetyl-*β*-D-glucosaminidase A form in Type 1 diabetes mellitus influences their activity?

VESNA B. JOVANOVIĆ[1#], JELENA M. AĆIMOVIĆ[1#], VESNA S. DIMITRIJEVIĆ SREĆKOVIĆ[2] and LJUBA M. MANDIĆ[1*#]

[1]*Faculty of Chemistry, Chair of Biochemistry, University of Belgrade, Studentski trg 12–16, Belgrade 11158, Serbia and* [2]*Institute of Endocrinology, Diabetes and Metabolic Diseases, Clinical Center of Serbia, Belgrade 11000, Dr Subotića 13, Serbia*

(Received 30 April, revised 9 July, accepted 17 July 2014)

Abstract: It was verified that the serum *N*-acetyl-*β*-D-glucosaminidase (NAG) activity is elevated in diabetes, but there are no reports about changes in the sialic acid (SA) content in the carbohydrate parts of the NAG A form and its influence on the total changes in NAG activity in type 1 diabetes mellitus patients with and without secondary complications. The NAG A form was isolated from the serum of 81 insulin-dependent diabetes mellitus (IDDM) patients with and without secondary complications (retinopathy, polyneuropathy and nephropathy) and 25 healthy persons, and purified and characterised. The content of *α*-2,6-bound SA, the isoenzyme patterns of the purified A form, and the total NAG and A form activities were determined. In all diabetic groups, the sialylation levels of the A form were 2–3.5 times lower compared to control, while their acidities (fractions with p*I* 4.25–5.1) increased, particularly with progression of secondary complications. Total serum NAG activities and percentages of A form were significantly higher ($P < 0.001$) in all diabetic groups and negatively correlated with the *α*-2,6-bound SA content of the A form. In addition, they decreased as secondary diabetic complications became more complex. The observed changes could be the consequence of structural changes in the A form due to significant increases in its acidity, *i.e.*, negative charge, which originated from groups other than SA.

Keywords: *N*-acetyl-*β*-D-glucosaminidase; A isoenzyme isolation and characterization; sialylation level, diabetes mellitus type 1; secondary complications.

INTRODUCTION

The serum *N*-acetyl-*β*-D-glucosaminidase (NAG, EC 3.2.1.52) activity and sialic acid (SA) are elevated in individuals diagnosed with diabetes mellitus[1–3]

* Corresponding author. E-mail: ljmandic@chem.bg.ac.rs
# Serbian Chemical Society member.
doi: 10.2298/JSC140430076J

and diabetic complications.[4–6] NAG is a lysosomal enzyme that is involved in the degradation of the oligosaccharide chains of glycoproteins, glycolipids and glycosaminoglycans. All serum NAG isoenzymes are glycoproteins that can be separated into two major isoenzymes, A and B, and several minor isoenzymes (I, P and S). They derive from different combinations of two polypeptide chains, α- and β-subunits, with additional heterogeneity conferred by posttranslational modifications. Among them carbohydrate part of NAG A contains the highest level of SA, which significantly contributes to the overall negative charge of its molecules. Therefore, NAG A has the lowest isoelectric point (its p*I* is close to 5).[7] In addition, SA may contribute to the stability and survival of glycoproteins (*e.g.*, NAG) in blood circulation.[8] Many reasons for the increase in serum NAG activity in diabetics have been proposed, such as poor glycemic control;[9] the glycomaterial deposits on blood vessels; long-term disruption of metabolic equilibrium in diabetics with an alleviated release of lysosomal enzymes, especially the A form,[10] into the extracellular liquid, which interferes with the mechanisms controlling the half-life of enzymes.[11] However, none of these explanations have been fully elucidated.

Increased NAG exocytosis, *i.e.*, the redistribution of the percentage of secreted enzyme compared to the percentage transported to lysosome, as well as changes in the activity and half-life of serum NAG could result from posttranslational modifications of enzymes (changes in the SA content in their carbohydrate components) in patients with hyperglycaemia. To the best of our knowledge, there are no reports that examine the changes in the carbohydrate components of NAG isoenzymes in diabetic patients with various secondary complications. To gain insight into these changes, the NAG A form from the serum of patients with insulin-dependent diabetes mellitus (IDDM) with and without various secondary complications was isolated and characterized, and the SA in the carbohydrate components of the A forms was analyzed and their correlation with changes in the total NAG activity examined. In this study, for the first time, the reduced sialylation levels of the A form from patients with IDDM is reported. However, the acidity of the A form (negative charge) increased as the diabetic complications progressed. These findings provide a deeper understanding of the changes in NAG activity in diabetics compared to healthy individuals and between groups of patients with IDDM.

EXPERIMENTAL

Subjects

Eighty-one patients with IDDM were grouped according to the following secondary complications:[10] without complications (W.Compl., n = 24); with retinopathy (R, n = 19); with retinopathy and polyneuropathy (R+P, n = 18); and with retinopathy, polyneuropathy and nephropathy (R+P+N, n = 20). The characteristics of these patients are listed in Table I. The

control group consisted of 25 healthy volunteers of appropriate ages and sex. This study was approved by the institutional ethics committee on human research.

TABLE I. Clinical and biochemical characteristics of the control group and groups of patients with IDDM; W.Compl. – without complications, R – with retinopathy, R+P – with retinopathy and polyneuropathy, R+P+N – with retinopathy, polyneuropathy and nephropathy. The values are expressed as the mean ± standard deviation (*SD*). [a]$P < 0.001$, [b]$P < 0.01$, [c]$P < 0.05$ compared with the control group. [d]$P < 0.001$, [e]$P < 0.05$ compared with W.Compl. [f]$P < 0.001$, [g]$P < 0.01$, [h]$P < 0.05$ compared with R. [i]$P < 0.001$, [j]$P < 0.01$, [k]$P < 0.05$ compared with R+P. *SBP*, systolic blood pressure; *DBP*, diastolic blood pressure

Characteristic	Control group	W.Compl.	R	R+P	R+P+N
n (M/F)	25 (11/14)	24 (12/12)	19 (7/12)	18 (11/7)	20 (9/11)
Age, y	30.2±8.7	24.6±7.4	26.2±2.2	33.8±14.8	31.2±10.1
Diabetes duration, y	–	6.6±5.5	14.8±5.5[d]	15.1±11[d]	18.3±9.4[d]
SBP / mmHg	109±9	115±8[c]	119±5[a,e]	122±7[b,e]	132±9[a,d,g]
DBP / mmHg	83±6	77±6	83±5	80±7	88±6
Glucose concentration, mmol L^{-1}	4.8±0.5	11.5±2.9[a]	14.3±2.6[a,e,j]	9.0±2.9[a]	12.9±3.1[a,k]
HbA_{1c}, %	4.9±0.5	9.3±0.8[a]	11.1±0.9[a]	10.1±1.4[a]	10.1±0.5[a]
Albuminuria, mg per 24 h	13.34±6.1	18.12±5.40	15.32±7.2	10.25±3.5	192.5±99.5[a,d,f,i]
Proteinuria, g L^{-1}	–	–	–	–	1.09±0.73
NAG activity, IU L^{-1}	3.19±0.5[a]	4.54±1.15[a]	5.72±1.06[a,e]	5.44±0.92[a]	5.08±2.05[a]
A form, %	69.38±4.98	83.82±5.82[a]	84.48±5.2[a]	81.9±5.24[a]	76.22±7.42[a,e,k]

Chemicals and instrumentation

All chemicals that were used were of analytical grade and were purchased from Merck (Darmstadt, Germany) and Sigma–Aldrich (Steinheim, Germany). Con A-Sepharose 4B and Sephadex G-100 were obtained from GE Healthcare (Uppsala, Sweden). SNA-HRPO was purchased from MyBioSource (San Diego, CA, USA). Spectrophotometric measurements were performed using a Beckman DU-50 spectrophotometer (Fullerton, USA) and an LKB 5060-066 microplate reader (Uppsala, Sweden).

Serum samples

Blood samples were collected after the patients had fasted overnight between 07:00 pm and 07:30 am.

Biochemical methods

Using 2-methoxy-4-(2-nitrovinyl)phenyl-2-(acetylamine)-2-deoxy-*β*-D-glucopyranoside, the activity of NAG was determined as previously described.[10] A unit of enzymatic activity (IU) was defined as the amount of enzyme used to hydrolyse 1 μmol of substrate in one minute at 37 °C (IU L^{-1} = μmol min^{-1} L^{-1}). The intra- and inter-assay variations of the measurements of total NAG activity were 1.8 and 3.2 %, respectively.

The fasting serum glucose, glycated haemoglobin (HbA_{1c}) and microalbuminuria were determined with a Hitachi 912 autoanalyser using commercial kits (Randox, Crumlin, UK). The content of proteins was determined by the Bradford method.[12]

Isoelectrofocusing and native polyacrylamide gel electrophoresis (PAGE) were performed according to the manufacturers' recommendations using a Multiphor® II electropho-

resis system (Pharmacia BioTech Ltd., Little Chalfont, Buckinghamshire, UK) and a Hoefer® SE 260 electrophoretic unit (San Francisco, CA, USA), respectively. The enzyme activity was determined by dividing the polyacrylamide gels into sections (3 mm×5 mm) and incubating each section with substrate at 37 °C for 24 h.

Isolation and purification of the serum NAG A isoenzyme

Ion-exchange chromatography on DEAE cellulose column was used to separate the NAG isoenzyme forms from fresh serum (4–6 mL) of each person from the control and the IDDM groups. Prior to the chromatography, the serum was dialysed overnight against 0.01 mol L^{-1} of phosphate buffer, pH 7.0, at 4 °C. The B form was eluted with 0.01 mol L^{-1} phosphate buffer, pH 7.0. The A form was isolated using a linear concentration gradient (0–0.3 mol L^{-1}) of sodium chloride in the same buffer. Fractions containing 90 % of the total A isoenzyme activity were pooled according to the groups, concentrated by ultrafiltration (PM-30; Amicon) and stored at –20ºC.

Gel chromatography. All pooled solutions of the isolated A isoenzyme were dialysed overnight at 4 °C against 0.05 mol L^{-1} phosphate buffer containing 0.15 mol L^{-1} sodium chloride, pH 7.0 and applied to a Sephadex G-100 column. The enzyme was eluted with the same buffer. Fractions containing 35–50 % of the total eluted A isoenzyme activity were pooled, concentrated by ultrafiltration and dialysed overnight at 4 °C against 20 mmol L^{-1} of 2-amino-2-(hydroxymethyl)propane-1,3-diol (Tris) buffer, pH 7.0, containing 1 mmol L^{-1} manganese(II) chloride, 1 mmol L^{-1} calcium chloride and 0.5 mmol L^{-1} sodium chloride (wash buffer).

Affinity chromatography. The dialysed solution was then applied to a Concanavalin A-Sepharose 4B column equilibrated with wash buffer. The enzyme was eluted with 0.5 mol L^{-1} α-methyl-D-mannoside dissolved in wash buffer. The two fractions with the highest enzyme activity were pooled and stored at –20 °C for electrophoresis, isoelectrofocusing and enzyme-linked lectin binding assays.

Enzyme-linked lectin binding assays (ELBAs)

The ELBAs were performed in 96-well microtitre plates (Nunc, Roskilde, Denmark) coated overnight at 4 °C with 200 µL of fetuin (0.01 mg mL^{-1}) or BSA (0.01 mg mL^{-1}) solution in 0.025 mmol L^{-1} phosphate buffer, pH 7.4, containing 0.15 mol L^{-1} sodium chloride (PBS) per well. The plates were then washed once with 200 µL of PBS/0.05 % (*V*/*V*) Tween 20 buffer (PBS-T) and blocked with 200 µL of 1 % BSA dissolved in PBS-T buffer at room temperature for 1 h. After blocking, the wells were washed twice with 200 µL of PBS-T buffer and then 75 µL of the purified A isoenzyme of serum NAG (starting protein concentration of 1 mg mL^{-1} that was serially diluted in PBS-T) of the control and IDDM patients and 75 µL of SNA conjugated with HRPO (diluted 1:5000 in assay buffer) were added. After incubation in the dark at room temperature for 2 h, the wells were washed twice with 200 µL of PBS-T buffer.

The spectrophotometric determination of the binding HRPO activity per well was performed by mixing 100 µL of urea–hydrogen peroxide (1.8 mg mL^{-1}) and 100 µL of TMB (1.4 mg mL^{-1}). After 10 min at room temperature, 50 µL of sulphuric acid (2 mol L^{-1}) was added, and the absorbance at 450 nm was measured. All sample dilutions were analysed in triplicate in two repeated experiments.

The reactivity of the A form of serum NAG with SNA lectin (binding SA) in the ELBA system was expressed as the concentration of the A form of NAG (in µg mL^{-1}), which led to 50 % inhibition of SNA linking to immobilised fetuin.

The procedures and experiments were in accordance with the ethical standards of the responsible committee on human experimentation (institutional and national) and with the Helsinki Declaration of 1975, as revised in 2000.

Statistical analysis

The Student's *t*-test, linear regression analysis and Pearson's correlation coefficient were used to analyse the data. Only values in which $P < 0.05$ were considered to be significant.

RESULTS

In all IDDM groups (W.Compl., R, R+P and R+P+N), the mean values of total NAG activity and percentage of the dominant A form (Table I) in serum were significantly higher ($P < 0.001$) compared to those of the control group (3.19±0.5 IU L^{-1} and 69.38±4.98 %, respectively). Significant positive correlations were obtained (0.945, 0.943, 0.940 and 0.963, respectively; $P < 0.001$) by comparing these two parameters as well as the activity of the A form of NAG and glycaemia (0.511, 0.537, 0.609 and 0.568, respectively; $P < 0.05$).

During the separation of the NAG isoenzymes from the serum of the control and IDDM groups by ion-exchange chromatography, a difference in the bonding strength between the A form and DEAE-cellulose was observed (Fig. 1). Additionally, the A isoenzyme of patients with R+P+N was eluted with a slightly higher concentration ((6.95±0.89)×10^{-2} mol L^{-1}) of sodium chloride compared to those of the other three diabetic groups. However, the mean values of the sodium chloride concentration used to elute 50 % of the serum A isoenzyme activity of the control and diabetic groups did not differ statistically (Table II).

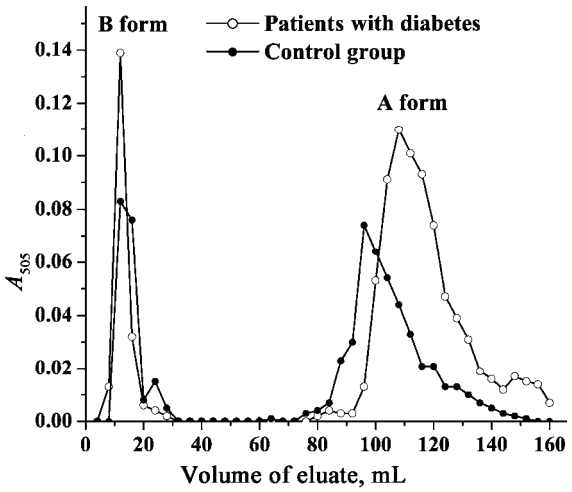

Fig. 1. NAG isoenzyme profiles of the control and IDDM groups obtained by ion-exchange chromatography on DEAE cellulose. The sodium chloride gradient from 0 to 0.3 mol L^{-1} was introduced after 54 mL of eluate.

To determine the origin of the increased negative charge of NAG A in diabetics, the isoenzymes of NAG A were isolated and purified from the serum of the control and all diabetic groups. In all groups, the A form was purified 180- to

TABLE II. Mean values of NaCl concentration (in 0.01 M of phosphate buffer, pH 7.0) used to elute 50 % of the NAG A isoenzyme from the DEAE-cellulose column from the serum of the control and IDDM groups; W.Compl. – without complications; R – with retinopathy; R+P – with retinopathy and polyneuropathy; R+P+N – with retinopathy, polyneuropathy and nephropathy

Group	c_{NaCl} / 10^{-2} mol L^{-1}
Control	6.37±0.37
W.Compl.	6.35±0.62
R	6.35±0.72
R+P	6.40±0.51
R+P+N	6.95±0.89

200-fold, yielding 10.8–16 % of enzyme (Table III). The purity of the isolated A forms was analysed by native PAGE electrophoresis (Fig. 2), whereby one dominant band was observed. This band was derived from the A form of NAG (molecular mass of 120 kDa),13 which was confirmed by determination of enzyme activity in the gel slice. The relative electrophoretic mobility (*REM*) of the A form gradually increased with progression of diabetic complications (Table III), indicating a slight increase in the acidity of the A form.

TABLE III. Purification – fold, yield, % and relative electrophoretic mobilities (*REM*) obtained by native PAGE of the A form isolated and purified from the serum of the control and IDDM groups; W.Compl. – without complications; R – with retinopathy; R+P – with retinopathy and polyneuropathy; R+P+N – with retinopathy, polyneuropathy and nephropathy

Line	Group	Purification – fold	Yield, %	*REM*
1	Control	200	11	0.560±0.018
2	W.Compl.	195	16	0.582±0.020
3	R	180	10.8	0.619±0.024
4	R+P	190	12	0.629±0.022
5	R+P+N	185	13	0.639±0.027

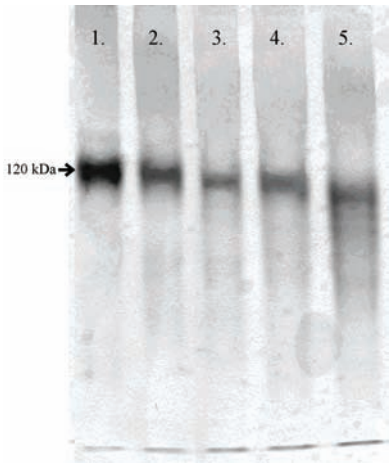

Fig. 2. Native PAGE of purified serum NAG A form from control (lane 1) and IDDM groups (lane 2, W.Compl.; lane 3, R; lane 4, R+P; lane 5, R+P+N) showing the changes in mobility of the A form. The electrophoresis was performed on 9 % polyacrylamide gels and the protein bands were visualised by Coomassie Brilliant Blue (CBB).

Significant differences in the distribution of the A form fraction between the control group and IDDM patients with secondary complications were observed by isoelectrofocusing (Fig. 3A). In the IDDM group, apart from the dominant A isoenzyme fraction (p*I* value approximately 5.6; p*I* range 5.1–6.0), more acidic fractions were observed (p*I* values in the range 4.25–5.10, Fig. 3B). Using densitometry, the percentage of these fractions (p*I* 4.25–5.10) was found to increase with the progression of secondary complications, so that they were 2–4 times higher compared to that of the control group (Table IV). In the R+P+N group, the percentage of this fraction was reached 51.5±1.8 %.

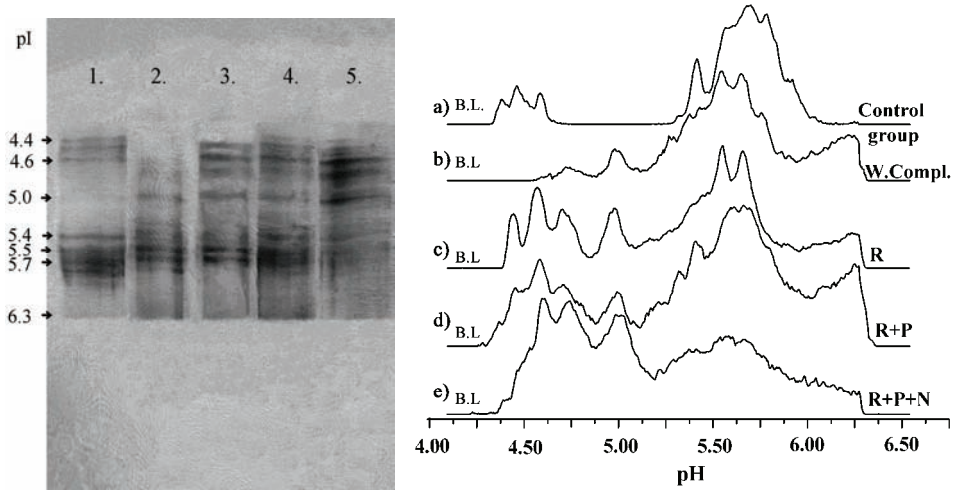

(A) (B)

Fig. 3. A) IEF (linear gel of pH 3–10) of purified A form from the serum of the control (lane 1) and IDDM groups (lane 2, W.Compl; lane 3, R; lane 4, R+P; lane 5, R+P+N). B) Densitometry of NAG A forms from the serum of the control a) and IDDM groups: b), c), d) and e). B.L., base line in the determination of the abundance of the more acidic fractions of the A form.

TABLE IV. Percentage of the more acidic fractions (p*I* in the range 4.25–5.1) of the A form in the control group and the groups of patients with IDDM; The data presented are mean values from three experiments ± *SD*; W.Compl. – without complications; R – with retinopathy; R+P – with retinopathy and polyneuropathy; R+P+N – with retinopathy, polyneuropathy and nephropathy

Group	More acidic fractions of A form, %
Control	12.8±0.2
W.Compl	10.1±0.7
R	35.1±2.2
R+P	28.8±1.8
R+P+N	51.5±1.8

The SA content in the carbohydrate parts of isolated A isoenzymes from the serum of control and IDDM groups (Table V) was analysed using ELBA, which is based on the competitive binding of NAG and fetuin (an immobilised glycoprotein ligand) to SNA lectin (specific for terminally α-2,6-bound SA) conjugated with HRPO. The A form from the serum of the control group exhibited the highest inhibitory effect on SNA binding to fetuin (*i.e.*, the highest α-2,6--bound SA content). In the case of the A isoenzyme from the serum of all IDDM groups, to achieve 50 % inhibition of SNA binding to fetuin, 2–3.5 times higher concentrations of the A form were required compared to that of the control group. Thus, the A forms in diabetic groups were less sialylated compared to those of the control group. Furthermore, comparisons between diabetic groups showed that the lowest and highest sialylation levels of the A form were observed in the R and R+P+N groups, respectively.

TABLE V. Content of α-2,6-bound SA in the isolated and purified A isoenzymes from the serum of the control group and patients with IDDM, which was estimated based on the concentration, μg mL^{-1}, of the serum A form leading to 50 % inhibition of SNA binding to fetuin. All measurements were performed in triplicate, in two repeated experiments, and are presented as mean ± *SD*; W.Compl. – without complications; R – with retinopathy; R+P – with retinopathy and polyneuropathy; R+P+N – with retinopathy, polyneuropathy and nephropathy

Group	$c_{(A\ form)}$ / μg mL^{-1}, leading to 50 % inhibition
Control	18.99±0.84
W.Compl.	54.54±1.52
R	62.52±1.70
R+P	42.20±1.84
R+P+N	32.13±0.91

An overview of the changes in the total serum NAG activity, the contribution of the A isoenzyme activity in the total NAG activity and the NAG A isoenzyme α-2,6-bound SA content is presented in Fig. 4.

DISCUSSION

In all IDDM groups, the total NAG activity and percentage of the A form were significantly higher compared to those of the control group, which is in agreement with previously reported data.[3,4] Changes in total NAG activity correlated with changes in the activity of the A form as diabetic complications become more complex (from W.Compl. to R+P+N), which was confirmed by the high correlation coefficients (from 0.940 to 0.963) determined between these two parameters. Due to the significant positive correlation observed between the activity of the serum NAG A form and glycaemia, it was concluded that the total NAG activity increased in IDDM patients mainly as a result of the increased exocytosis (release into circulation) of the A form in hyperglycaemic pat-

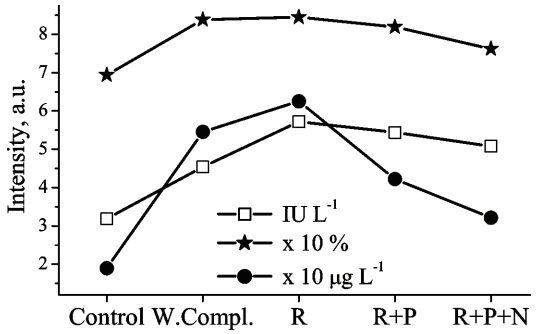

Fig. 4. Summary of the changes in the total serum NAG activity (□), contribution of the A isoenzyme activity to the total NAG activity (★), and NAG A isoenzyme *α*-2,6-bound SA content (●) in the control and IDDM groups, which correspond to the concentration, μg mL^{-1}, of the A form leading to 50 % inhibition of SNA binding to fetuin. W.Compl. – without complications; R – with retinopathy; R+P – with retinopathy and polyneuropathy; R+P+N – with retinopathy, polyneuropathy and nephropathy.

ients.[10] In hyperglycaemics, extracellular glucose passes through the metabolic ways independent of insulin, leading to an increase in the flux of *N*-acetyl-glucosamine (GlcNAc).[14,15] Disturbed glycosaminoglycane metabolism (substance deposition in the blood vessels of diabetics with complications) and excess posttranslational *O*-glycosylation of proteins with GlcNAc (*via O*-GlcNAc transferase) could be involved in the pathogenesis of diabetes and the development of secondary complications.[16,17] Thus, the increase in *O*-GlcNAc could result in the activation and release of NAG for its removal.[18] However, because no statistically significant differences were found between the NAG activities from the serum of diabetic groups with various complications, it was concluded that the deposition of glycomaterial was not the main reason for the changes in NAG activity.[10]

Increases in the flux of GlcNAc in diabetics could also cause increased intracellular posttranslational protein modifications,[14,15] leading to changes in NAG carbohydrate components and NAG distribution inside and outside cells.[19] In assays of NAG posttranslational modifications in fibroblast cultures, structural differences between the NAG carbohydrate components from lysosomes and NAG secreted into the medium were established.[20]

During ion-exchange chromatography and native PAGE of the serum NAG isoenzymes, it was observed that the negative charge of the A form was higher in the IDDM groups than in the control group. In the IDDM groups, apart from the dominant A isoenzyme fraction (p*I* value approximately 5.6), more acidic fractions were observed (p*I* values in the range 4.25–5.1). The percentage of these fractions increased 2–4 times with the progression of secondary complications compared to that of the control group. In the R+P+N group, the percentage of fractions attained 51.5±1.8 %. Considering that NAG *α*-subunits (only present in

the A form) contain oligosaccharide chains with SA as terminal residues[21] and that changes in the SA content could affect an increase in the acidity of the A form, experiments were performed to determine whether there were increases in the sialylation levels of NAG in the IDDM groups.

The obtained results demonstrated that the degree of α-2,6 sialylation of the A form in all diabetic groups was lower compared to that in the control group. Comparing the diabetic groups, the lowest sialylation level of the A form was observed in the R group, whereas the highest was observed in the R+P+N group. The reduced intensity of NAG sialylation in diabetics could be a consequence of a reduced activity of sialyltransferases or an increased activity of sialidases. In the endothelial cells of diabetic rats with hyperglycaemia, the sialidase activity was reported to be increased by 78 %, whereas the sialyltransferase activity was decreased by 15 %.[22,23] On the other hand, an increase in serum neuraminidase[6] and unchanged sialyltransferase activity[24] were observed in diabetics. Thus, it is assumed that the activation/inhibition ratio of these enzymes in diabetics determine the sialylation levels of glycoproteins, resulting in the occurrence of various sialoforms as well as NAG. The molecular mechanisms of these effects, the physiological consequences of the structural and functional changes in molecules with modified glycosylation and how these changes are reflected in the development of diabetic complications are unknown. Only the effects of modified glycosylation patterns could be observed. The present results showed a reduced content of α-2,6 bound SA in the IDDM groups. These results also indicated that the increased acidity of the A form in the IDDM groups compared to control group had another cause.

In addition to SA, the total negative charge of NAG could also be attributed to other negatively charged groups (*e.g.*, phosphate or sulphate). Newly synthesised lysosomal enzymes lack or exhibit reduced levels of mannose-6-phosphate residues in their oligosaccharide chains, leading to hypersecretion and intracellular deficiency of multiple lysosomal enzymes.[25] Thus, NAG, which is secreted in higher levels in diabetes, may have a reduced number of phosphate groups. A sulphate cap could be added to the end of complex-type carbohydrate chains[26] or Tyr residues of secretory proteins.[27] The sequence within the β-subunit of the A form of serum NAG could be a site for Tyr sulphation.[27] Negative charges derived from sulphation may contribute to the changes in the structure and activity of the A form. Additional studies are required to understand better these changes in NAG A.

How do the changes in the acidity of the NAG A isoenzyme correlate with the increased activity of serum NAG in diabetics? Increased serum NAG activity in patients with hyperglycaemia could result from an increased rate of exocytosis and/or reduced clearance of enzymes. Hyperglycaemia could lead to an increase in the exocytosis of lysosomal enzymes through several mechanisms[28–36] with

NAG packed in secretory vesicles with other secretory products. The clearance of lysosomal enzymes from the serum proceeds through the asialoglycoprotein (ASGR), mannose and cation-independent mannose 6-phosphate receptors (CI-MPR).[31–33] The sialylation of the carbohydrate chains of protein masks the residues of D-galactose and *N*-acetyl-D-galactosamine, which are specifically recognized by ASGR. The asialo A form of NAG was reported to be rapidly eliminated after injection from the circulation of rats.[34] The decreased sialylation of the A form in all IDDM groups compared to that of the control group should lead to the rapid removal of the isoenzyme from the circulation. However, increases in the A form and total NAG activities were observed in all diabetic groups (Fig. 4). Thus, it could be concluded that the rate of NAG exocytosis in patients with hyperglycaemia is higher than that of its clearance. The results obtained in the present study could be explained by the number of ASGR in diabetics, which drastically decreases on the cell surface.[35] The expression of ASGR requires a balance between the intracellular concentrations of *c*-GMP and *c*-AMP. In diabetics, an intracellular increase in *c*-AMP leads to a decrease in the number of ASGRs on the cell surface.[36] The decreased number of ASGRs leads to slower NAG removal from circulation (*i.e.*, to prolongation of the enzyme half-life), increasing the NAG activity in serum if the asialo derivative is active. In accord with the present data, Miller *et al.*[20] showed that sialidase action (removal of SA) does not alter the activity of the NAG A form.

Lastly, the changes in total serum NAG activity and A isoenzyme profiles in IDDM patients with various secondary complications negatively correlated with changes in the SA content (Fig. 4) and negative charges (acidity, in general) of the most abundant NAG A form. Due to the presence of a larger number of negatively charged groups (compared to those of SA) on the surface of more than 50 % of the A form isolated from the R+P+N group, the activity of the A form is reduced, leading to a significantly lower contribution to the total NAG activity compared to those of the W.Compl ($P < 0.01$) and R ($P < 0.05$) groups. Thus, in the diabetic groups, the decrease in total serum NAG activity with the progression of secondary complications could result from structural changes in the A form due to significant increases in the negative charge (acidity, in general). Based on the presented results, additional insight into these changes could be obtained by investigating the contribution of sulphate and phosphate residues to NAG, as well as changes in the activity of other lysosomal enzymes.

CONCLUSIONS

The total serum NAG and A isoenzyme activities in IDDM patients were negatively correlated with the *α*-2,6-bound SA content of the NAG A form. In this study, for the first time, it was found that patients with IDDM have reduced sialylation levels of the A form. However, the acidity of the A form increased in IDDM compared to control group. These results indicate that the increase in aci-

dity of the A form in the IDDM groups has another cause (*e.g.*, the negative charge could originate from groups other than SA).

Abbreviations. NAG, *N*-acetyl-*β*-D-glucosaminidase; IDDM, insulin-dependent diabetes mellitus; R, retinopathy; P, polyneuropathy; N, nephropathy; BSA, bovine serum albumin; TMB, 3,3′5,5′-tetramethylbenzidine; SNA, *Sambucus nigra* lectin; HRPO, horseradish peroxidase; ELBA, enzyme-linked lectin binding assay; *SD*, standard deviation.

Acknowledgement. This work was supported by the Ministry of Education, Science and Technological Development of the Republic of Serbia (Grant No. 172049).

ИЗВОД

КАКО САДРЖАЈ СИЈАЛИНСКЕ КИСЕЛИНЕ У А-ОБЛИКУ СЕРУМСКЕ *N*-АЦЕТИЛ-*β*-D-ГЛУКОЗАМИНИДАЗЕ УТИЧЕ НА ЊЕГОВУ АКТИВНОСТ У ДИЈАБЕТЕС МЕЛИТУСУ ТИПА 1?

ВЕСНА Б. ЈОВАНОВИЋ[1], ЈЕЛЕНА М. АЋИМОВИЋ[1], ВЕСНА С. ДИМИТРИЈЕВИЋ СРЕЋКОВИЋ[2] и ЉУБА М. МАНДИЋ[1]

[1]Хемијски факултет Универзитета у Београду, Катедра за биохемију, Студентски трг 12–16, 11158 Београд и [2]Институт за ендокринологију, дијабетес и болести метаболизма, Клинички центар, Др Суботића 13, Београд

До сада је показано да је активност серумске *N*-ацетил-*β*-D-глукозаминидазе (NAG) повећана у дијабетесу, али промена садржаја сијалинске киселине (SA) у глико-компоненти А облика NAG и њен утицај на промене у укупној активности NAG код пацијената оболелих од дијабетеса типа 1 (IDDM, са секундарним компликацијама и без њих), нису разматрани. Стога је А изоензимски облик NAG изолован и пречишћен из серума 81 IDDM пацијента, са секундарним компликацијама (ретинопатија, полинеуропатија и нефропатија) и без њих, и из серума 25 здравих особа, а потом окарактерисан. Одређена је укупна активност NAG и активност А облика, садржај *α*-2,6 везане SA у пречишћеном А облику и профил овог изоензима. Заступљеност *α*-2,6 везане SA у А облику свих група дијабетичара била је 2–3,5 пута мања у поређењу са контролом, док је његова киселост (фракције са p*I* од 4,25 до 5,1) расла, посебно са напредовањем секундарних компликација. Укупне активности серумског NAG и процентни удели А облика у укупној активности били су значајно повишени ($P < 0,001$) код свих група дијабетичара, и у негативној корелацији са садржајем *α*-2,6 везане SA у А облику. Поред тога, оне су опадале са усложњавањем секундарних компликација. Утврђене промене могу бити последица промене структуре А облика услед значајног повећања његове киселости, односно негативне шарже која потиче од група које нису остаци SA.

(Примљено 30. априла, ревидирано 9. јула, прихваћено 17. јула 2014)

REFERENCES

1. M. A. Crook, K. Earle, A. Morocutti, J. Yip, G. Viberti, J. C. Pickup, *Diabetes Care* **17** (1994) 305
2. J. Skrha, J. Hilgertova, *Clin. Chim. Acta* **282** (1999) 167
3. L. Mandic, D. Filipovic, *Biochem. Mol. Biol. Int.* **45** (1998) 545
4. M. Mysliwiec, K. Zorena, A. Balcerska, J. Mysliwska, P. Lipowski, K. Raczynska, *Clin. Biochem.* **39** (2006) 851
5. J. K. Powrie, G. F. Watts, M. A. Crook, J. N. Ingham, N. A. Taub, K. M. Shaw, *Diabetic Med.* **13** (1996) 238

6. J. Roozbeh, A. Merat, F. Bodagkhan, R. Afshariani, H. Yarmohammadi, *Int. Urol. Nephrol.* **43** (2011) 1143
7. M. Borzym-Kluczyk, E. Olszewska, I. Radziejewska, A. Lewszuk, K. Zwierz, *Clin. Chem. Lab. Med*. **46** (2008) 131
8. J. Du, M. A. Meledeo, Z. Wang, H. S. Khanna, V. D. Paruchuri, K. J. Yarema, *Glycobiology* **19** (2009) 1382
9. P. H. Hsiao, W. S. Tsai, W. Y. Tsai, J. S. Lee, Y. K. Tsau, C. H. Chen, *Am. J. Nephrol*. **16** (1996) 300
10. V. B. Jovanovic, V. S. Dimitrijevic-Sreckovic, L. M. Mandic, *J. Clin. Lab. Anal*. **22** (2008) 307
11. J. A. Summerfield, J. Vergalla, E. A. Jones, *J. Clin. Invest*. **69** (1982) 1337
12. M. M. Bradford, *Anal. Biochem*. **72** (1976) 248
13. J. A. Verpoorte, *Biochemistry* **13** (1974) 793
14. K. Liu, A. J. Paterson, E. Chin, J. E. Kudlow, *Proc. Natl. Acad. Sci. USA* **97** (2000) 2820
15. R. J. Clark, P. M. McDonough, E. Swanson, S. U. Trost, M. Suzuki, M. Fukuda, W. H. Dillmann, *J. Biol. Chem.* **278** (2003) 44230
16. K. Komosinska-Vassev, K. Olczyk, E. M. Kozma, P. Olczyk, G. Wisowski, K. Winsz-Szczotka, *Clin. Chem. Lab. Med*. **43** (2005) 924
17. D. M. Lehman, D. J. Fu, A. B. Freeman, K. J. Hunt, R. J. Leach, T. Johnson-Pais, J. Hamlington, T. D. Dyer, R. Arya, H. Abboud, H. H. Goring, R. Duggirala, J. Blangero, R. J. Konrad, M. P. Stern, *Diabetes* **54** (2005) 1214
18. O. Kordonouri, R. Hartmann, C. Muller, T. Danne, B. Weber, *Horm. Res.* **50 Suppl 1** (1998) 23
19. R. Barone, H. Carchon, E. Jansen, L. Pavone, A. Fiumara, N. U. Bosshard, R. Gitzelmann, J. Jaeken, *J. Inherit. Metab. Dis.* **21** (1998) 167
20. A. L. Miller, B. C. Kress, R. Stein, C. Kinnon, H. Kern, J. A. Schneider, E. Harms, *J. Biol. Chem.* **256** (1981) 9352
21. B. Overdijk, E. P. Beem, G. J. van Steijn, L. A. Trippelvitz, J. J. Lisman, J. Paz Parente, P. Cardon, Y. Leroy, B. Fournet, H. van Halbeek, *Biochem. J*. **232** (1985) 637
22. N. Rellier, D. Ruggiero-Lopez, M. Lecomte, M. Lagarde, N. Wiernsperger, *Life Sci*. **64** (1999) 1571
23. L. Cohen-Forterre, J. Andre, G. Mozere, J. Peyroux, M. Sternberg, *Biochem. Pharmacol*. **40** (1990) 507
24. G. Ronquist, O. Walinder, *Diabetes Metab*. **9** (1983) 212
25. S. Tiede, M. Cantz, J. Spranger, T. Braulke, *Hum. Mutat*. **27** (2006) 830
26. Y. Kato, R. G. Spiro, *J. Biol. Chem*. **264** (1989) 3364
27. A. Hille, T. Braulke, K. von Figura, W. B. Huttner, *Eur. J. Biochem*. **188** (1990) 577
28. F. Wang, Y. Wang, M. S. Kim, P. Puthanveetil, S. Ghosh, D. S. Luciani, J. D. Johnson, A. Abrahani, B. Rodrigues, *Cardiovasc. Res*. **87** (2010) 127
29. S. H. Ayo, R. Radnik, J. A. Garoni, D. A. Troyer, J. I. Kreisberg, *Am. J. Physiol*. **261** (1991) F571
30. R. R. Hodges, I. Raddassi, D. Zoukhri, A. Toker, A. Kazlauskas, D. A. Dartt, *Invest. Ophthalmol. Vis. Sci*. **45** (2004) 3974
31. A. Hasilik, K. von Figura, *Eur. J. Biochem*. **121** (1981) 125
32. A. Koster, K. von Figura, R. Pohlmann, *Eur. J. Biochem*. **224** (1994) 685
33. M. Spiess, *Biochemistry* **29** (1990) 10009
34. T. Bearpark, J. L. Stirling, *Biochem. J*. **168** (1977) 435
35. P. Scarmato, C. Cherqui-Eisenberg, G. Durand, J. Feger, *Experientia* **45** (1989) 480
36. R. J. Stockert, *J. Biol. Chem*. **268** (1993) 19540.

Journal of the Serbian Chemical Society
JSCS-info@shd.org.rs • www.shd.org.rs/JSCS

J. Serb. Chem. Soc. *79* (12) 1505–1513 (2014)
JSCS–4683

UDC 546.472'482+547.856:542.9+
547.571+547.551:615.281–188
Original scientific paper

Synthesis, characterization and antibacterial activities of Zn(II) and Cd(II) complexes of a 3-amino-2-phenylquinazolin-4(3*H*)--one Schiff base

DHIRAJ BRAHMAN and BISWAJIT SINHA*

Department of Chemistry, University of North Bengal, Darjeeling-734013, India

(Received 30 January, revised 18 June, accepted 11 September 2014)

Abstract: Zn(II) and Cd(II) complexes of a Schiff base derived from 3-amino-2-phenylquinazolin-4(3*H*)-one and 2-(2-formylphenoxy) acetic acid were prepared and characterized by elemental and different spectroscopic (IR, UV–Vis and NMR) analyses. The elemental analysis indicated the formation of the complexes: $[ML(AcO)]\cdot H_2O$, where M stands for Zn(II) or Cd(II) and L stands for the Schiff base. The molar conductivities of the prepared complexes revealed their non-electrolytic nature. The complexes were also investigated for their antimicrobial activities using the turbidimetric assay method.

Keywords: Zn(II); Cd(II); quinazolin-4(3*H*)-one Schiff base; 2-(2-formylphenoxy) acetic acid; antibacterial activities.

INTRODUCTION

Schiff bases derived from an amine and aldehydes are an important class of ligands that co-ordinate to metal ions through the azomethine nitrogen.[1–3] Among the wide variety of nitrogen-containing heterocycles explored for the development of pharmaceutically important molecules, quinazoline is an important compound in medicinal chemistry and subsequently have emerged as an important pharmacophore.[4] The quinazoline moiety has O and N donor atoms and can act, therefore, as a good chelating agent. Quinazolin-4(3*H*)-one and its derivatives are versatile nitrogen-containing heterocyclic compounds that have long been known as a promising class of biologically active compounds.[5] Compounds containing 4(3*H*)-quinazolinone ring system were reported to possess varied biological activities, such as antibacterial, antifungal, antitubercular, antiviral, anticancer and anticonvulsant activities, depending on the substituents in the ring system.[6–9]

* Corresponding author. E-mail: biswachem@gmail.com
doi: 10.2298/JSC140130093B

The aldehydic precursor 2-(2-formylphenoxy) acetic acid plays an important role in reducing the toxicity of the parent drug and acts as a part of a pro-drug called aconiazide.[10,11] A survey of the literature[12–19] revealed that the reaction of quinazoline hydrazide **2** and 2-(2-formylphenoxy) acetic acid has hitherto remained unattended. Therefore, it was thought worthwhile to synthesize a novel quinazoline Schiff base and its complexes with transition metals. Hence, in this work, the synthesis and characterization of the Schiff base ligand derived from quinazolin-4-(3*H*)-one and 2-(2-formylphenoxy) acetic acid and its mononuclear complexes with Zn(II) and Cd(II) ions are reported.

EXPERIMENTAL

Materials and measurements

Pyridine, benzoyl chloride, anthranilic acid, hydrazine hydrate, salicylaldehyde, monochloroacetic acid, cadmium acetate dihydrate and zinc acetate dihydrate were procured from S. D. Fine Chemicals, India. Except monochloroacetic acid (purity 98 %) and hydrazine hydrate (purity 80 %), all the chemicals were of 99 % purity. The spectroscopic grade solvents were also purchased from S. D. Fine Chemicals, India and used without further purification. 2-(2-Formylphenoxy) acetic acid and quinazolin-4(3*H*)-one were prepared by following reported procedures.[20,21]

The FT-IR spectra of the ligand and metal complexes were recorded in KBr discs in the range 400–4000 cm^{-1} using a Shimadzu FTIR 8300 spectrophotometer. ^{1}H- and ^{13}C-NMR spectra were recorded on an FT-NMR Bruker Advance II 400 MHz spectrometer with TMS as the internal standard. Mass spectrum of the ligand was recorded employing a ZQMAA225 mass spectrometer using acetonitrile as a solvent. Due to the poor solubility of the synthesized metal complexes in common solvents, their masses were not recorded. The UV–Vis spectra were measured in DMF with a JascoV-530 spectrophotometer. Elemental microanalyses were realized using a CHNOS elemental analyzer (Model 550 Carlo-Erba). The molar conductances of the complexes (1×10^{-3} mol dm^{-3}) were measured in DMF with a Systronic-308 conductivity bridge at 25 °C under atmospheric pressure. The melting points of the ligand and the complexes were determined using the open capillary method.

Synthesis of the ligand

The syntheses of 3-amino-2-phenylquinazolin-4(3*H*)-one was reported earlier.[21] The synthesis of 3-amino-2-phenylquinazolin-4(3*H*)-one is shown in Scheme 1. A mixture of 2-phenyl-4*H*-3,1-benzoxazin-4-one (2.23 g, 0.01 mol), **1,** and hydrazine hydrate (0.5 mL, 0.01 mol) in ethanol was refluxed for 8 h. The excess of solvent was then evaporated and the

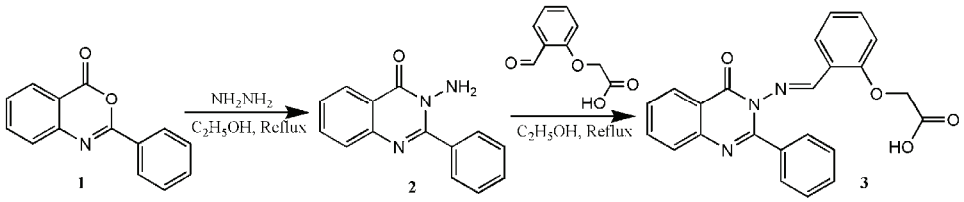

Scheme 1. The synthesis of the ligand (LH): **1**, 2-phenyl-4*H*-3,1-benzoxazin-4-one; **2**, 3-amino-2-phenylquinazolin-4(3*H*)-one; **3**, the ligand (LH).

resulting solid 3-amino-2-phenylquinazolin-4(3*H*)-one **2** was filtered off, dried under vacuum and recrystallized from ethanol. Its melting point was 142 °C and its yield was 72 %.

Next, a mixture of 3-amino-2-phenylquinazolin-4(3*H*)-one and 2-(2-formylphenoxy) acetic acid in equimolar amount (5 mmol each: 1.18 and 0.90 g, respectively) in absolute ethanol was refluxed for about 5 h. The solution was then cooled and poured into ice-cold water. The resulting white product, 2-{2-[((4-oxo-2-phenyl-3(4*H*)-quinazolinyl)imino)-methyl]phenoxy}acetic acid **3** was filtered off, washed with dried ethanol and recrystallized from ethanol.

Synthesis of complexes

A solution of 0.5 mmol of metal acetate dihydrate [Zn(II) and Cd(II)]: 0.109 and 0.134 g, respectively) in 15 mL ethanol was added to 0.5 mmol, 0.200 g of the ligand dissolved in 20 mL absolute ethanol. The solution was heated under reflux for about 2 h. The resulting precipitate was filtered off washed with cold dried ethanol and dried under vacuum over fused $CaCl_2$.

Antibacterial activity

The antibacterial activities of the ligand and its complexes were assayed against the Gram-negative bacteria *Escherichia coli* (K12MTCC302) by the turbidimetric method. The test compounds were dissolved in DMSO (SRL, Extra-pure, India) to prepare stock solutions, which were aseptically filtered through a bacterial membrane. The required volumes of filtrate were transferred to tubes containing a defined volume of nutrient broth to achieve the desired concentration of the compounds. The concentrations of the tested compounds were 25, 50, 100, 200, 300, 400, 600, 800 and 1000 μg mL^{-1} and the standard drug for comparison was ampicillin. A loop full of bacteria from a 24 h-old slant culture were transferred to 10 mL of nutrient broth (Himedia M 502) and incubated at 37 °C for 6 h. The tubes in duplicate containing 5 mL nutrient broth were incubated with 0.1 mL of a 6-h liquid culture. The tubes containing the nutrient broth were incubated at 37 °C for 18 h and the relative growths in the tubes were determined turbidimetrically by spectrophotometry.

RESULTS AND DISCUSSION

All the isolated compounds were found to be air-stable and were characterized based on elemental and different spectroscopic analyses, the results of which are given in the Supplementary material to this paper. The metal complexes were insoluble in common organic solvents except in DMF and DMSO.

Molar conductivity

The molar conductivity (Λ_M) of the synthesized complexes were measured at 25 °C and under atmospheric pressure in DMF. The molar conductivities of the complexes (1×10^{-3} mol dm^{-3}) indicated that the complexes behave as non-electrolytes in DMF, which suggests that no anion was present outside the coordination sphere as a counter anion of the central metal ion.

Infrared spectra of the Schiff base ligand and its complexes

The comparative IR spectral study of ligand and its complexes revealed the coordination mode of the synthesized ligand during the complex formations. The

weak broad bands at 3084 cm^{-1} and 3230–3294 cm^{-1} in the spectrum of the free ligand may be attributed to the –NH stretching and the hydrogen bonded –OH of the carboxylic moiety, respectively. In the complexes the disappearance of these bands followed by a shift of acid carbonyl from 1734.6 to 1684–1690 cm^{-1} implied deprotonation and subsequent coordination of the oxygen of carbonyl (C=O) group to the metal ions (M^{2+}). In the spectra of the free ligand and the complexes, the band at 1653.8–1654.8 cm^{-1} was due to the amide C=O and this band did not change, supporting the fact that the carbonyl oxygen of the amide did not participate in the metallation. The azomethine band at 1602.7 cm^{-1} in the spectrum of the free ligand shifted towards lower frequency range 1590–1597.9 cm^{-1}, which indicated coordination of the N-atom of the azomethine group to M^{2+}. This fact was further supported by concomitant increase in the $\nu_{N–N}$ stretching frequency from 930 cm^{-1} towards the range 963–960 cm^{-1} for free ligand and the complexes, respectively.[22,23] In addition, the coordination of the ethereal oxygen (>C–O–C<) to M^{2+} was confirmed by the observed frequency increase of the 1215.1 cm^{-1} band towards the range 1232–1256 cm^{-1} on complexation. The medium intensity broad bands at 3435 and 3420 cm^{-1} for the Zn(II) and Cd(II) complexes, respectively, are due to the presence of water molecules in the coordinating sphere.[24] Assignment of the proposed coordination sites was further supported by the appearance of medium bands at 592.1 and 594.1 cm^{-1} attributed to $\nu_{M–N}$ for the Zn(II) and Cd(II) complexes, respectively.[25,26]

^{1}H- and ^{13}C-NMR spectra

The ^{1}H- and ^{13}C-NMR spectra of the ligand and the Cd(II) complex were recorded in DMSO-d_6. The 2D-NMR spectrum for the ligand was also recorded in order to distinguish the different protons on the phenyl ring of the quinazoline moiety. The ^{1}H-NMR spectrum of the ligand showed the following signals (δ / / ppm): 4.79 (*s*), 6.99–8.56 (*m*), 8.87 (*s*) and 11.99–12.24 (*s*); these signals may be assigned to the protons in –O–CH_2–, the aromatic moiety, the azomethine (HC=N) group, –OH (carboxylic proton hydrogen bonded with –N= group) and the free –OH (carboxylic) group, respectively. Since the ^{1}H-NMR spectrum of the synthesized ligand showed close signals in the δ range 6.99–8.87 ppm, its 2D spectra were recorded. In the 2D spectrum of the ligand, three sets of correlations: the quinazoline protons (H_5–H_8), the arylidene protons (H_3''–H_6'') and the phenyl protons of the 2-phenyl group (H_2'–H_4'), were observed. In the total correlated spectroscopy (TOCSY) spectrum, a distinct set of four cross-peaks was observed, indicating four consecutive protons with δ values of 8.56, 7.95, 7.62 and 6.99 ppm. The atom numbering of the ligand is shown in Fig. 1A. An analysis of the cross-peaks of ^{1}H–^{1}H correlation spectroscopy (COSY) spectra (Fig. 1B) revealed the nearest member of each proton. Since the proton at the ortho--position to the amidic group was assumed to be most deshielded (marked as H_5),

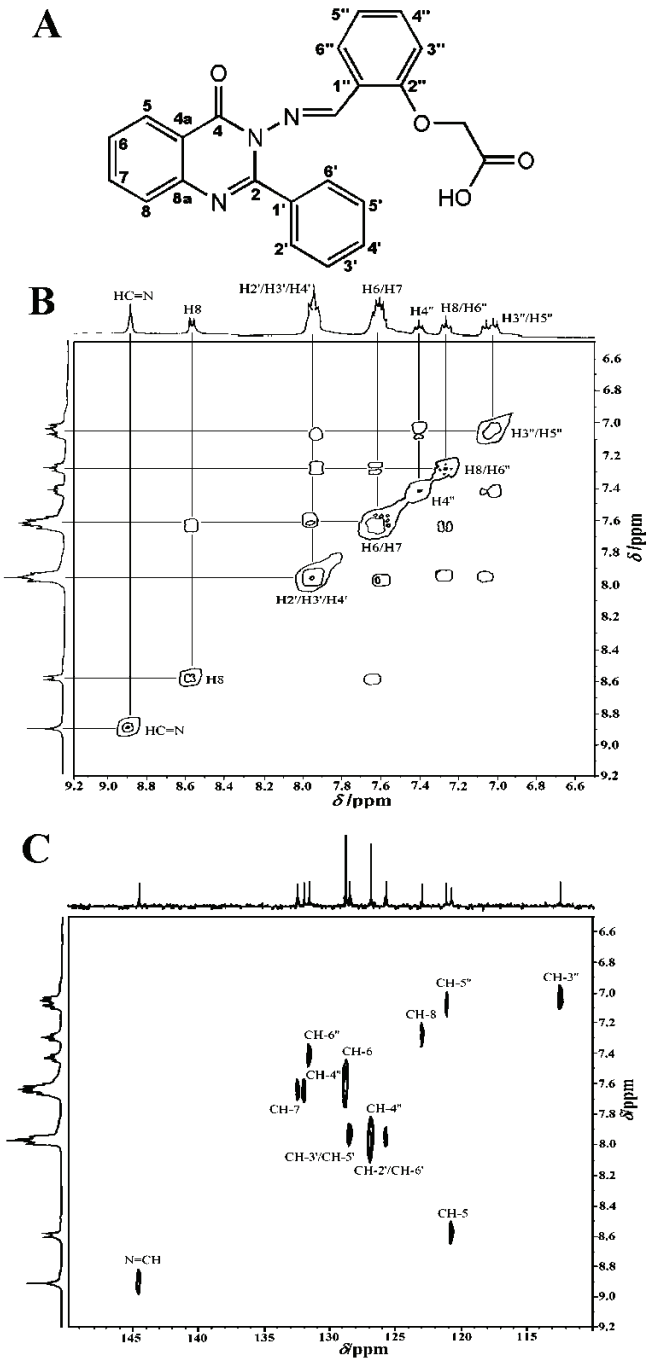

Fig. 1. A) Atom numbering of the ligand structure; B) ^{1}H–^{1}H COSY spectra of the ligand; C) ^{1}H–^{13}C COSY spectra of the ligand.

all other protons were assigned with respect to this proton (H_5). The sequential assignments were thus at δ values: 8.56 (H_5), 7.61 (H_6), 7.65 (H_7) and 7.27 ppm (H_8). The arylidene protons (H_3''–H_6'') and the 2-phenyl protons (H_2'–H_4') were also assigned in similar fashions. The arylidene protons were assigned the following δ values: 7.04 (H_3''), 7.56 (H_4''), 6.99 (H_5'') and 7.40 ppm (H_6''), and 2-phenyl protons were assigned the δ values: 7.95 (H_2'), 7.91 (H_3') and 7.93 ppm (H_4'). After the assignment of the entire ^{1}H-spectrum of the ligand, the ^{1}H–^{13}C COSY spectrum was further analyzed to assign the eleven ^{1}H–^{13}C peaks (Fig. 1C).

In the ^{1}H-NMR spectrum of the Cd(II) complex the signal due to carboxylic proton had disappeared, which confirmed the involvement of the carboxylic group in the coordination. The shifts in the signal assigned to the azomethine proton and the methylene proton at 8.73 and 4.53 ppm in the complex were indications of the coordination of the nitrogen of the azomethine linkage and ethereal oxygen of the –O–CH_2– linkage to the metal ion. A signal at around 2.45–2.50 ppm was also observed and assigned to methyl protons of the acetate group coordinated to the metal ion. This fact clearly indicated that during complex formation, one proton (carboxylic) of the free ligand was deprotonated and it behaved as a monobasic tridentate ligand. Unfortunately, it was not possible to perform NMR studies on the Zn(II) complex due to its poor solubility in DMSO-d_6.

Electronic spectra

The electronic spectra of the ligand and its Zn(II) and Cd(II) complexes, recorded in DMF, are shown in Fig. 2. In the electronic spectra, the n→π* transition associated with the azomethine group of the ligand was found at 332 nm but was shifted to longer wavelengths for Cd(II) and Zn(II) complexes. These results indicated that the nitrogen atom of azomethine group remained coordinated to the metal ions in the complexes. From the electronic and other spectral data, it could

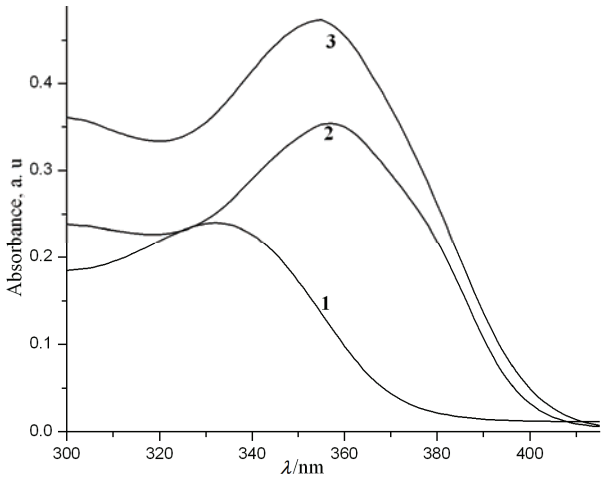

Fig. 2. UV–Vis spectra of the ligand and its Zn(II) and Cd(II) complexes. 1, LH; 2, Cd(II) complex; 3, Zn(II) complex.

thus be concluded that both the complexes had tetrahedral geometry. The probable structure of the metal complexes is shown in Fig. 3.

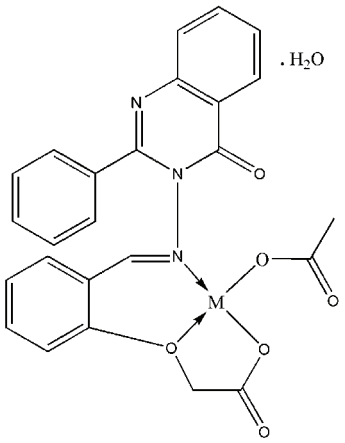

Fig. 3. Probable structure of the synthesized metal complexes (M = Cd(II) or Zn(II)).

Antibacterial activities

The ligand and its Zn(II) complex did not show any antibacterial activity against *E. coli* up to 1000 μg mL^{-1}, whereas the Cd(II) complex showed antibacterial activity at 100 μg mL^{-1}. Thus, it could be concluded that the incorporation of the 2-(2-formylphenoxy) acetic acid group in the quinazoline molecule quenched the antibacterial activity of the parent quinazoline molecule.

CONCLUSIONS

In this paper, the syntheses and physicochemical characterization of a 3-amino-2-phenylquinazolin-4(3*H*)-one Schiff base ligand and its Zn(II) and Cd(II) complexes are described. The antibacterial activities of the synthesized compounds are also described. The results of elemental analysis confirmed a 1:1 ratio of ligand to metal binding. Based on the physical and spectral analyses (IR, UV–Vis and NMR), tetrahedral geometry was proposed for the complexes of quinazolin-4-(3*H*)-one Schiff base. In the complexes, the azomethine nitrogen, ethereal oxygen and phenoxy oxygen occupied the three coordination sites. The fourth coordination site was occupied by an acetate group and one water molecule of crystallization was present in the complex, as confirmed by elemental analysis. The Zn(II) complex did not show any antibacterial activity, whereas the Cd(II) complex showed marked antibacterial activity. Again, it was found that the incorporation of the 2-(2-formylphenoxy) acetic acid group in the quinazoline molecule quenched the antibacterial activity of the parent quinazoline molecule.

SUPPLEMENTARY MATERIAL

Physical, analytical and spectral data for the ligand and its Zn and Cd complexes are available electronically from http://www.shd.org.rs/JSCS/, or from the corresponding author on request.

Acknowledgements. The authors are grateful to the Departmental Special Assistance Scheme under the University Grants Commission, New Delhi (SAP-DRS-III, No. 540/12/DRS/2013) for financial support and to SAIF, NEHU for elemental analysis and NMR studies. We also thankfully acknowledge the Department of Biotechnology, N. B. U for the antibacterial analyses. One of the authors (D. B) is also thankful to UGC, India for granting him UGC BSR Research Fellowship in Science [Ref. No: 4-1/2008 (BSR)].

И З В О Д

СИНТЕЗА, КАРАКТЕРИЗАЦИЈА И АНТИБАКТЕРИЈСКА АКТИВНОСТ КОМПЛЕКСА Zn(II) И Cd(II) СА ШИФОВОМ БАЗОМ 3-АМИНО-2-ФЕНИЛХИНАЗОЛИН-4(3*H*)-ОНА

DHIRAJ BRAHMAN и BISWAJIT SINHA

Department of Chemistry, University of North Bengal, Darjeeling-734013, India

Описана је синтеза Zn(II) и Cd(II) комплекса са Шифовом базом 3-амино-2-хиназолин-4(3*H*)-она и 2-(2-формилфенокси)-сирћетне киселине као лигандом. Комплекси су окарактерисани помоћу елементалне микроанализе и различитих спектроскопских метода (IR, UV–Vis и NMR). На основу елементалне микроанализе претпостављено је да комплекси имају општу формулу: $[ML(AcO)]\cdot H_2O$, где је M Zn(II) или Cd(II), а L представља Шифову базу као лиганд. На основу кондуктометријских мерења закључено је да изоловани комплекси представљају неутралне комплексне врсте. Применом турбидиметријских метода испитивана је антимикробна активност изолованих комплекса.

(Примљено 30. јануара, ревидирано 18 јуна, прихваћено 11. септембра 2014)

REFERENCES

1. K. Arora, K. P. Sharma, *Synth. React. Inorg. Met-Org. Chem.* **32** (2002) 913
2. P. A. Vigato, S. Tamburini, *Coord. Chem. Rev.* **248** (2004) 1717
3. T. Katsuki, *Coord. Chem. Rev.* **140** (1995) 189
4. A. K. Sengupta, A. A. Gupta, *J. Antibact. Antifungal Agentc, Jpn.* **8** (1980) 7
5. G. Daidon, D. Raffa, S. Plescia, L. Mantione, *Eur. J. Med. Chem.* **36** (2001) 737
6. R. A. Sheldon, K. J. Kochi, *Metal Catalyzed Oxidation of Organic Compounds*, Academic Press, New York, 1981, p. 35
7. D. Liu, K. Kwasniewska, *Polyhedron* **15 (**1996) 1263
8. P. R. Ortiz de Montellano, *Cytochrome (P-450), Structure, Mechanism and Biochemistry*, Plenum Press, New York, 1986, p. 556
9. B. Halliwell, J. M. C. Gutteridge, *Free Radicals in Biology and Medicine*, 2nd ed., Clarendon Press, Oxford, 1988, p. 543
10. E. B. Hansen, Jr., K. L. Dooley, Jr., H. C. Thompson, *J. Chromatogr., B* **670** (1995) 259
11. H. R. Held, S. Landi, *J. Pharm. Sci.* **69** (1980) 1284
12. N. M. Raghavendra, M. S. Niranjan, P. Venkatesh, B. R. P. Kumar, N. B. Gowda, M. S. Sripathi, *Asian J. Chem.* **17** (2005) 57
13. V. Alagarsamy, R. Giridhar, H. R. Yadav, R. Revathi, K. Rukmani, *Indian J. Pham. Sci.* **68** (2005) 532
14. A. K. Nanda, S. Ganguli, R. Chakraborty, *Molecules* **12** (2007) 2413

15. K. S. Kumar, S. Ganguli, R. Veerasamy, E. D. Clercq, *Eur. J. Med. Chem.* **45** (2010) 5474
16. M. F. Abdel-Megeed, M. M. Azaam, G. A. El-Hiti, *J. Saudi Chem. Soc.* **18** (2014) 1022
17. S. K. Krishnan, S. Ganguli, R. Veerasamy, B. Jan, *Eur. Rev. Med. Pharm. Sci.* **15** (2011) 673
18. S. Ganguli, M. K. Panigrahi, P. Singh, P. K. Shukla, *Int. J. Pharm. Pharm. Sci.* **4** (2012) 434
19. S. Ganguli, M. Firdous, T. S. Maity, R. K. Bera, M. Panigrahi, *Int. J. Pharm. Pharm. Sci.* **4** (2012) 175
20. B. S. Furniss, A. J. Hamnnaford, R. Rogers, P. W. G. Smith, A. R. Tatchell, *Vogel's Textbook of Practical Organic Chemistry*, 4th ed., Longman Group Ltd., London, 1978, p. 923
21. V. Alagarsamy, V. R. Salomon, G. Vanikavitha, V. Paluchamy, M. R. Chandran, A. A. Sajin, A. Thangathiruppathy, S. Amuthalakshmi, R. Revathi, *Biol. Pharm. Bull.* **25** (2002) 1432
22. F. Hueso-Urena, N. A. Illan-Cabeza, M. N. Moreno-Carretero, A. L. Penans-Chamorro, *Acta. Chum. Slov.* **47** (2000) 481
23. K. K. Narang, A. Aggarwal, *Inorg. Chim. Acta* **9 (**1974) 137
24. T. F. Zafiropoulos, J. C. Plakaouras, S. P. Perlepes, *Polyhedron* **10 (**1991) 2405
25. M. Thomas, M. K. M. Nair, R. K. Radhakrishan, *Synth. React. Inorg. Met.-Org. Chem.* **25 (**1995) 471
26. K. Nakamoto, *Infrared and Raman Spectra of Inorganic and Coordination compounds*, 2nd ed., Wiley, New York, 1970, p. 156.

Journal of the Serbian Chemical Society
JSCS@tmf.bg.ac.rs • www.shd.org.rs/JSCS
J. Serb. Chem. Soc. 79 (12) S173–S174 (2014) *Supplementary material*

SUPPLEMENTARY MATERIAL TO

Synthesis, characterization and antibacterial activities of Zn(II) and Cd(II) complexes of a 3-amino-2-phenylquinazolin-4(3*H*)--one Schiff base

DHIRAJ BRAHMAN and BISWAJIT SINHA*

Department of Chemistry, University of North Bengal, Darjeeling-734013, India

J. Serb. Chem. Soc. 79 (12) (2014) 1505–1513

PHYSICAL, ANALYTICAL AND SPECTRAL DATA FOR THE LIGAND AND ITS Zn AND Cd COMPLEXES

*2-{2-[((4-oxo-2-phenyl-3(4*H*)-quinazolinyl)imino)methyl]phenoxy}acetic acid*. Yield: 74 %; white solid; m.p.: 174–178 °C, Anal. Calcd. for $C_{23}H_{17}N_3O_4$: C, 69.17; H, 4.29; N, 10.52 %. Found: C, 69.03; H, 4.33; N, 9.88 %; IR (KBr, cm^{-1}): 3230–3294 (–N–H stretching), 3084 (–O–H stretching, hydrogen bonded), 1734.6 (–C=O stretching –COOH group), 1653.8–1654.8 (–C=O stretching of $–CONH_2$ group) 1667 (–C=O, free), 1623 (–C=O, hydrogen bonded), 1602.7 (–C=N), 1215.1 ((>C–O–C< stretching), 930 (–N–N, stretching); ^{1}H-NMR (400 MHz, DMSO-d_6, δ / ppm): 4.79 (2H, *s*, O–CH_2), 6.99–8.56 (11H, *m*, Ar-H), 8.87 (1H, *s*, HC=N), 11.99–12.24 (1H, *s*, OH, hydrogen bonded with –N= group); ^{13}C-NMR (100 MHz, DMSO-d_6, δ / ppm): 169.94, 164.95, 164.51, 156.38, 144.61, 139.22, 134.26 132.56, 132.1, 131.68, 128.89, 128.59, 126.96, 125.82, 123.07, 122.29, 121.25, 120.88, 120.21, 112.61, 64.76; MS (*m*/*z*, (relative abundance, %)): 400.8 (M+1, 25).

[ZnL(AcO)]·H_2O. Yield 70 %; white solid; m.p.: >300 °C, Anal. Calcd. for $C_{25}H_{19}N_3O_6Zn$: C, 55.52; H, 3.91; N, 7.77. Found: C, 55.52; H, 3.43; N, 8.41; IR (KBr, cm^{-1}): 3435 (H_2O of crystallization), 3165 (–N–H stretching), 1684––1690 (–C=O stretching of –COOH group), 1653.8–1654.8 (–C=O stretching of $–CONH_2$ group), 1667 (–C=O, free), 1630 (–C=O stretching), 1590–1597.9 (–C=N stretching), 1232–1256 (>C–O–C< stretching), 963–960 (–N–N, stretching), 592.1 (M–N stretching frequency); Λ_M (DMF, S cm^2 mol^{-1}): 4.07.

[CdL(AcO)]·H_2O: Yield: 68 %, white solid, m.p.: >300 °C, Anal. Calcd. for $C_{25}H_{19}N_3O_6Cd$: C, 51.08; H, 3.60; N, 7.15 %. Found: C, 50.55; H, 3.03; N, 7.69 %; IR (KBr, cm^{-1}) 3420 (H_2O of crystallization), 3165 (–N–H stretching), 1684–

* Corresponding author. E-mail: biswachem@gmail.com

–1690 (–C=O stretching of –COOH group), 1653.8–1654.8 (C=O stretching of $–CONH_2$ group), 1667 (–C=O, free), 1630 (–C=O stretching), 1590–1595.9 (–C=N stretching), 1232–1256 (>C–O–C< stretching), 963–960 (N–N, stretching), 594.1 (M–N stretching frequency); ^{1}H-NMR (400 MHz, DMSO-d_6, δ / ppm): 4.53 (2H, *s*, $O–CH_2$), 6.20–8.71 (11H, *m*, Ar-H), 8.73 (1H, *s*, HC=N); ^{13}C-NMR (100 MHz, DMSO-d_6, δ / ppm): 170.72, 169.79, 164.95, 155.33, 151.65, 139.26, 135.69, 133.11, 131.84, 131.30, 130.39, 129.93, 128.77, 127.33, 123.78, 122.41, 121.73, 121.41, 119.16, 113.11, 67.24; Λ_M (DMF, S cm^2 mol^{-1}): 5.64.

Journal of the Serbian Chemical Society
JSCS-info@shd.org.rs • www.shd.org.rs/JSCS
J. Serb. Chem. Soc. 79 (12) 1515–1521 (2014)
JSCS–4684
UDC 547.53+549.746+549.328.3:
544.131:515.12
Original scientific paper

Topological properties of altan-benzenoid hydrocarbons

IVAN GUTMAN*#

Faculty of Science, University of Kragujevac, P. O. Box 60, 34000 Kragujevac, Serbia and State University of Novi Pazar, Novi Pazar, Serbia

(Received 19 June, revised 19 July 2014, accepted 21 July 2014)

Abstract: The main topological characteristics of altan-benzenoids were established. In particular, it was shown that the perimeter of Kekuléan altan-benzenoids is of size $4k$, having a destablizing (anti-aromatic) energy effect, similar to ($4k$)-annulenes.

Keywords: altan-benzenoid hydrocarbon; benzenoid hydrocarbon; annulene; molecular graph; cyclic conjugation.

INTRODUCTION

Altan derivatives of polycyclic conjugated molecules recently came into the focus of attention of theoretical organic chemists.[1–4] The name "altan" is an abbreviated form of "alternating annulene", which is a fragment encircling the parent conjugated system.

The altan derivative of a conjugated hydrocarbon is constructed so that each hydrogen atom is replaced by a vinyl group, and each two adjacent vinyl groups are condensed into a new cycle. The construction of altan-phenanthrene is shown in Fig. 1.

Altan conjugated systems are interesting for two reasons. If all the cycles surrounding the parent hydrocarbon are 5- and/or 6-memberd, then the altan molecule is non-planar, bowl shaped,[1,2] thus being a distant relative of fullerenes and nanotubes. The annulene system surrounding the parent hydrocarbon[5] may contain $4k$ cyclically delocalized π-electrons.

According to the Hückel ($4k$+2)-rule,[6–9] it thus contributes to anti-aromaticity and possesses a paratropic ring currect.[1–4,10,11]

The graph representation of an altan derivative of a conjugated molecule is shown in Fig. 2.

* E-mail: gutman@kg.ac.rs
# Serbian Chemical Society member.
doi: 10.2298/JSC140619080G

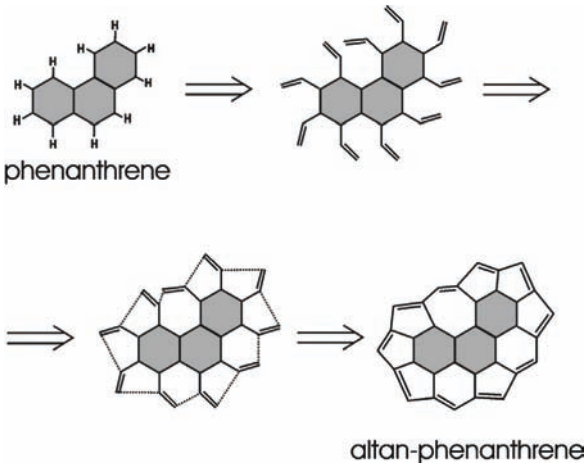

Fig. 1. Construction of altan-phenanthrene from phenanthrene. Note that the perimeter of altan-phenanthrene is a [20]annulene, encircling the phenanthrene subunit.

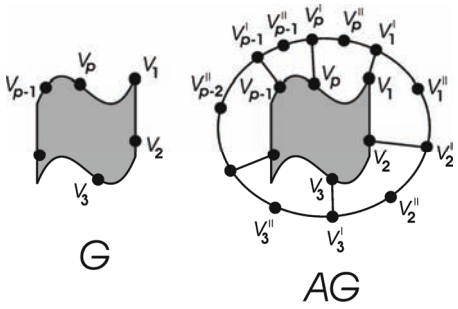

Fig. 2. The molecular graph *AG* of an altan, the molecular graph *G* of its parent hydrocarbon, and the labeling of some of their vertices; for details see text.

The molecular (Hückel) graph[12] of a polycyclic conjugated hydrocarbon is denoted by *G*, and is assumed to contain no $=CH_2$ groups. This graph has *n* vertices, all of which are of degree 2 and 3. There are *p* vertices of degree two, and in the diagram *G* in Fig. 2, these are indicated and labeled by $v_1, v_2, \ldots, v_n$ (the *n*–*p* vertices of degree three are not indicated). These degree-two vertices represent carbon atoms to which hydrogen atoms are attached. Thus, the formula of the conjugated hydrocarbon represented by the graph *G* is C_nH_n.

The altan graph, *AG*, corresponding to the parent molecular graph *G* (see Fig. 2), consists of a central fragment identical to *G*, and a cycle of size 2*p*, in which the vertex v_i' is connected with the vertex v_i of *G*, $i = 1,2,\ldots,p$. Therefore, if *G* has *n* vertices and *m* edges, then *AG* has $n + 2p$ vertices and $m + 4p$ edges.

If the distance between the vertices and of *G* is equal to *d*, then the cycle of *AG* embracing the vertices $v_i, v_{i+1}, v_i', v_{i+1}'$ is of size $d + 4$.

The parent conjugated system from which the altan derivative is constructed needs not be a benzenoid hydrocarbon,[1–4] but altan-benzenoids are certainly the most interesting (and also the most realistic) members of this class. In that which

follows, the considerations will be restricted to benzenoid altans, and their main topological properties established.

STRUCTURAL FEATURES OF ALTAN-BENZENOIDS

Details on the structural characteristics of benzenoid hydrocarbons can be found in the book[13] and the recent papers.[14–18] In particular, on the perimeter of a benzenoid system, one distinguishes features called fissures, bays, coves, and fjords,[13,14,19,20] *cf.* Fig. 3. The numbers of fissures, bays, coves, and fjords will be denoted by $b1$, $b2$, $b3$ and $b4$, respectively. The frequently used "bay number" of a benzenoid system[13] is then $b = b_2 + 2b_3 + 3b_4$.

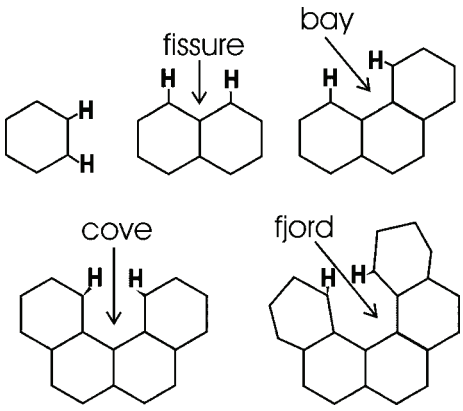

Fig. 3. The five different constellations of two nearest-lying hydrogen atoms on the perimeter of a benzenoid hydrocarbon. In order that all the rings of the altan-benzenoid be of size 5 and 6, bays, coves and fjords cannot be present. Note that in an earlier work,[21] the hydrogen atoms attached to a fissure, bay, cove, and fjord were labeled by *H*-α, *H*-α3, *H*-α4, and *H*-α5, respectively.

In view of the above-described construction of altan derivatives, the sizes of the newly formed rings depend on the mutual constellation of the nearest-lying hydrogen atoms of the parent benzenoid system. The following regularities are immediately established.

*Rule 1***.** a) Two nearest-lying hydrogen atoms attached to neighboring carbon atoms of the parent benzenoid system give rise to the formation of a 5-membered ring in the corresponding altan. b) Two nearest-lying hydrogen atoms separated by a fissure on the perimeter of the parent benzenoid system (see Fig. 3) give rise to the formation of a new 6-membered ring in the corresponding altan. c) Two nearest-lying hydrogen atoms separated by a bay or cove or fjord on the perimeter of the parent benzenoid system (see Fig. 3) give rise to the formation of a ring in the corresponding altan of size greater than 6.

A benzenoid systems is said to be convex[14,19,20] if there are no bays, coves or fjords on its perimeter, *i.e.*, if $b = 0$. From Rule 1, the condition under which an altan derivative consists of only 5- and 6-membered rings is evident:

*Rule 2***.** In order that all rings of an altan-benzenoid be of sizes 5 and 6, the parent benzenoid system must be convex.

The number m_{22} of edges of a benzenoid system connecting two vertices of degree two satisfies the relation:[13] $m_{22} = 6 + b$. Therefore, from Rule 1a, it could be concluded that the corresponding altan has $6 + b$ pentagons.

*Rule 3***.** The number of 5-membered rings of an altan-benzenoid is 6 if and only if the parent benzenoid is convex.

*Rule 4***.** a) If the parent benzenoid system has h hexagons, then the corresponding altan-benzenoid has $h + b_1$ hexagons. b) The numbers of 7- , 8-, and 9-membered rings in an altan are equal to b_2, b_3 and b_4, respectively.

Note that all altan derivatives considered until now were derivatives of convex (benzenoid or non-benzenoid) conjugated molecules, for which $b_2 = b_3 = = b_4 = 0$. This is understandable, since the 7- and higher-membered rings in altan derivatives of non-convex (benzenoid or non-benzenoid) π-electron systems would cause in them high steric strain and drastic deviation from planarity (*cf.* Fig. 3).

Let G be the molecular graph of a benzenoid system with h hexagons and n_i inner vertices.[13] Then the number of its vertices is equal to:[13]

$$n = 4h + 2 - n_i \tag{1}$$

The number of vertices of degree three in G is:[13]

$$n_3 = 2h - 2 \tag{2}$$

In addition:

$$n = n_3 + p \tag{3}$$

Combining Eqs. (1)–(3), one obtains $p = 2h + 4 - n_i$. Therefore, the size r of the annulene ring (*i.e.*, the perimeter) of the corresponding altan AG is equal to:

$$r = 4h + 8 - 2n \tag{4}$$

In order that a benzenoid system be Kekuléan (*i.e.*, to possess Kekulé structures),[13] the number n of the vertices must be even. Then, by Eq. (1), n_i must also be even. Bearing this in mind, Eq. (4) implies the following important result:

*Rule 5***.** The size of the annulene ring (*i.e.*, the perimeter) of an altan derivative of a Kekuléan benzenoid hydrocarbon is divisible by 4, *i.e.*, it contains $4k$ cyclically delocalized π-electrons.

The property stated here as Rule 5 was certainly known to earlier investigators of altans,[1–4] and might have been the chief motivation for the study of this class of conjugated π-electron systems. Yet, a demonstration of the general validity of this rule seems to be offered here for the first time.

π-ELECTRON PROPERTIES OF ALTAN-BENZENOIDS

The alternating double bonds in the annulene ring of an altan can be arranged in two different ways, which causes a duplication of the Kekulé structures of the parent benzenoid system. An illustrative example is given in Fig. 4,

where the pairs k_i, k_i'; i = 1,2,3 should be compared. Therefore, any altan-benzenoid has at least two times as many Kekulé structures as the parent benzenoid hydrocarbon, *i.e.*, $K(AG) \geq 2K(G)$. Now, it will be proven that in all cases, the equality $K(AG) = 2K(G)$ holds.

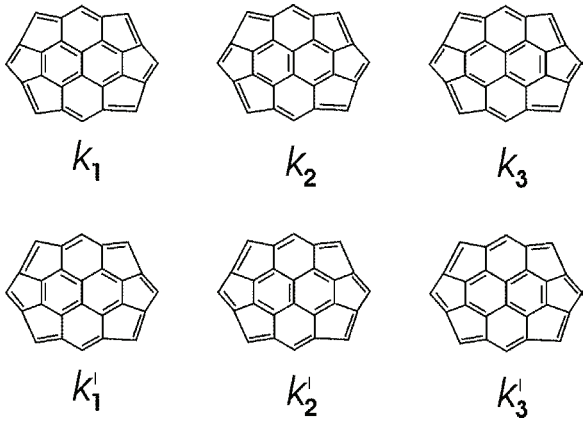

Fig. 4. Kekulé structures of altan-naphthalene.

*Rule 6***.** The Kekulé structure count of an altan-benzenoid is exactly twice the Kekulé structure count of the parent benzenoid hydrocarbon.

In order to verify Rule 6, the altan *AG* in Fig. 2 is considered and the indicated labeling of its vertices is referred to. It is necessary to show that in all Kekulé structures of *AG*, the bonds v_iv_i', i = 1,2,…,p are single.

Suppose the opposite, namely that there is a Kekulé structure of *AG* in which the bond v_1v_1' is double, see Fig. 2. Then also the bond $v_1''v_2'$ must also be double, and, continuing the same argument, all the bonds v_{i+1}', i = 1,2,…,p–1, must be double. Then, however, the vertex v_p'' remains isolated, which contradicts the existence of a Kekulé structure. Therefore, the bond v_1v_1' cannot be double.

If all bonds v_iv_i', i = 1,2,…,p, of *AG* are single in all its Kekulé structures, then the total number of Kekulé structures of *AG* is equal to the product of $K(G)$ and the number of Kekulé structures of the annulene ring, equal to two. This implies Rule 6.

In the terminology of Monaco and Zanasi,[10] it could be stated that Rule 6 proves "K-factorization" of the parent benzenoid system and its enveloping annulene. It is possible to show that such a "K-factorization" (*i.e.*, Rule 6) holds for all altan-species (both benzenoid and non-benzenoid).

From Rule 6, it can be see that the π-electron conjugation in the annulene ring of an altan-benzenoid is only weakly influenced by the conjugation modes of the parent benzenoid system. As a direct consequence of this, some π-electron

properties of annulenes[6,22–24] are preserved also in altan-benzenoids. From Rule 5, it is known that these annulenes are of size 4*k*. Of their properties, the most important may be that cyclic conjugation has a significant destabilizing energy effect. Some characteristic examples are presented in Table I. The energy effects of the perimeters have been computed by means of a standard procedure, the details of which were described elsewhere.[15,25–27]

TABLE I. Energy effects (in units of the HMO resonance integral β) of the perimeters of some altan-benzenoids and their parent hydrocarbons. According to the Hückel (4*k*+2)-rule, cycles of size 10, 14, 18,… have a positive (stabilizing) effect, whereas cycles of size 16, 20, 24,… have negative (destabilizing) energy effects. The destabilizing energy effects of the annulene-type perimeters of altan-benzenoid hydrocarbons are remarkably strong, and (except in the case of altan-naphthalene) exceed the stabilizing energy effect of the parent benzenoid system

Compound	Altan-benzenoid		Parent hydrocarbon	
	Size of perimeter	Energy effect	Size of perimeter	Energy effect
Naphthalene	16	–0.0565	10	+0.0709
Anthracene	20	–0.0694	14	+0.0279
Phenanthrene	20	–0.0295	14	+0.0198
Pyrene	20	–0.0196	14	+0.0128
Coronene	24	–0.0082	18	+0.0039

Another characteristic feature of the π-electron configuration of (4*k*)-annulenes is the existence of a pair of non-bonding molecular orbitals (NBMOs).[6,7,12] This property is also (partially) preserved in the case of altan-benzenoids. Namely, the following regularity holds.

*Rule 7***.** Altan-benzenoid hydrocarbons have NBMOs. Kekuléan altan-benzenoids have a unique NBMO.

The form of the single NBMO of Kekuléan altan-benzenoids should be evident from the examples depicted in Fig. 5.

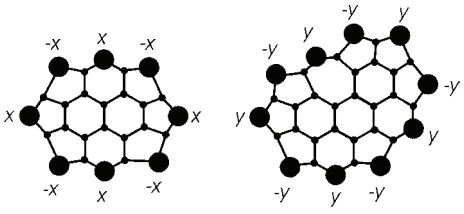

Fig. 5. The unique NBMO of altan-naphthalene ($x = 1/\sqrt{8}$) and altan-phenanthrene ($y = 1/\sqrt{10}$). The coefficients of the NBMOs on all other carbon atoms are equal to zero.

И З В О Д

ТОПОЛОШКА СВОЈСТВА АЛТАН-БЕНЗЕНОИДНИХ УГЉОВОДОНИКА

ИВАН ГУТМАН

Природно–математички факултет Универзитета у Крагујевцу, Крагујевац и Државни универзитет у Новом Пазару, Нови Пазар

Одређене су важније тополошке каратеристике алтан-бензеноидних угљоводоника. Између осталог, показано је да периметар Кекулеовских алтан-бензеноидних систем има величину $4k$, и да има дестаблизујући (антиароматични) енергетски ефекат, сличан $(4k)$-ануленима.

(Примљено 19. јуна, ревидирано 19. јула, прихваћено 21. јула 2014)

REFERENCES

1. G. Monaco, R. Zanasi, *J. Phys. Chem., A* **116** (2012) 9020
2. G. Monaco, M. Memoli, R. Zanasi, *J. Phys. Org. Chem*. **26** (2013) 109
3. T. K. Dickens, R. B. Mallion, *J. Phys. Chem., A* **118** (2014) 933
4. T. K. Dickens, R. B. Mallion, *J. Phys. Chem., A* **118** (2014) 3688
5. E. L. Spitler, C. A. Johnson, M. M. Haley, *Chem. Rev*. **106** (2006) 5344
6. G. M. Badger, *Aromatic Character and Aromaticity*, Cambridge Univ. Press, Cambridge, 1969
7. A. Graovac, I. Gutman, N. Trinajstić, *Topological Approach to the Theory of Conjugated Molecules*, Springer, Berlin, 1977
8. M. Randić, *Chem. Rev*. **103** (2003) 3449
9. M. K. Cirański, *Chem. Rev*. **105** (1005) 3773
10. G. Monaco, R. Zanasi, *J. Chem. Phys.* **131** (2009) 044126
11. J. A. N. F. Gomes, R. B. Mallion, *Chem. Rev.* **101** (2001) 1349
12. I. Gutman, O. E. Polansky, *Mathematical Concepts in Organic Chemistry*, Springer, Berlin, 1986
13. I. Gutman, S. J. Cyvin, *Introduction to the Theory of Benzenoid Hydrocarbons*, Springer, Berlin, 1989
14. R. Cruz, I. Gutman, J. Rada, *J. Serb. Chem. Soc.* **78** (2013) 1351
15. I. Gutman, S. Radenković, M. Antić, J. Đurđević, *J. Serb. Chem. Soc*. **78** (2013) 1539
16. J. Kovič, T. Pisanski, A. T. Balaban, P. W. Fowler, *MATCH Commun. Math. Comput. Chem.* **72** (2014) 3
17. J. Kovič, *MATCH Commun. Math. Comput. Chem.* **72** (2014) 27
18. C. P. Chou, H. A. Witek, *MATCH Commun. Math. Comput. Chem.* **72** (2014) 75
19. R. Cruz, I. Gutman, J. Rada, *MATCH Commun. Math. Comput. Chem*. **68** (2012) 97
20. J. Rada, R. Cruz, I. Gutman *MATCH Commun. Math. Comput. Chem*. **72** (2014) 125
21. R. H. Martin, *Tetrahedron* **20** (1964) 897
22. I. Gutman, M. Milun, N. Trinajstić, *Croat. Chem. Acta* **44** (1972) 207
23. N. Mizoguchi, *J. Mol. Struct*. **181** (1988) 245
24. T. K. Dickens, R. B. Mallion, *Croat. Chem. Acta* **86** (2013) 387
25. I. Gutman, *Monatsh. Chem.* **136** (2005) 1055
26. M. Marković, J. Đurđević, I. Gutman, *J. Serb. Chem. Soc.* **77** (2012) 751
27. I. Gutman J. Đurđević, Z. Matović, M. Marković, *J. Serb. Chem. Soc*. **77** (2012) 1401.

Journal of the Serbian Chemical Society
JSCS-info@shd.org.rs • www.shd.org.rs/JSCS
J. Serb. Chem. Soc. 79 (12) 1523–1536 (2014)
JSCS–4685
UDC 547.821–035.67:66.099.72+
541.135:66.087
Original scientific paper

Optimization of electrochemical decolorization of certain arylazo pyridone dyes

JELENA M. MIRKOVIĆ[#], NEVENA Ž. PRLAINOVIĆ[#], GORDANA S. UŠĆUMLIĆ[#], BRANIMIR N. GRGUR and DUŠAN Ž. MIJIN*[#]

Faculty of Technology and Metallurgy, University of Belgrade, Karnegijeva 4, 11020 Belgrade, Serbia

(Received 9 April, revised 30 May 2014, accepted 18 June 2014)

Abstract: Electrocatalytic decolorization of arylazo pyridone dyes was investigated in the presence of sodium chloride using a DSA Ti/PtO_x electrode in dilute sodium hydroxide. The decolorization could be attributed to the indirect oxidation of the investigated dyes by electrogenerated hypochlorite formed from the chloride oxidation. The electrochemical decolorization was investigated for the different sodium hydroxide concentrations in the range from 40 mg dm^{-3} to 4 g dm^{-3}, sodium chloride concentrations in the range from 15 to 40 g dm^{-3}, currents in the range of 100 to 250 mA and dye concentrations from 5 to 20 mg dm^{-3}. The optimum electrolysis conditions are suggested. The effect of substituents on the reaction rate was also studied.

Keywords: pyridone; electrolysis; hypochlorite; UV–Vis spectroscopy; donor––acceptor effects.

INTRODUCTION

Arylazo pyridone dyes have become important in the last several decades due to their high molar extinction coefficients and medium to high light and wash fastness properties.[1] These dyes generally find application as disperse dyes and are used for the dyeing of hydrophobic fibers (polyesters and nylons as the main synthetic fibers). Furthermore, disperse dyes have been employed in the inks for the heat-transfer printing of polyesters.[2]

Synthetic azo dyes are pollutants that represent a significant source of environmental contamination. Due to the presence of an azo group, they are not easily degradable. Most of the physico-chemical methods, such as chemical precipitation and separation of pollutants, coagulation, elimination by adsorption, *etc*.,

* Corresponding author. E-mail: kavur@tmf.bg.ac.rs
[#] Serbian Chemical Society member.
doi: 10.2298/JSC140409063M

do not degrade dye molecules but only transfer the contamination from one phase to another, causing a new kind of pollution.[3–5]

Photodegradation, ozonation, alkalinization, and electrochemical methods are some of the methods that could be used for the decolorization or the degradation of the dyes.[5,6] Indirect oxidation, based on the homogeneous reaction between anodically generated oxidizing species and dyes, is the most favorable of the electrochemical methods. The addition of an electrolyte is necessary in order to obtain better fixation and exhaustion during the dyeing process with reactive and direct or substantive dyes. An amount of 50–80 g dm^{-3} of a salt is generally added as an electrolyte, most commonly sodium chloride or sodium sulfate.[7] Since it is not necessary to add any salt during the dyeing process when disperse dyes are used, some salt should be introduced into the wastewater before the electrochemical treatment. Sodium chloride is one of the best solutions. During the electrolysis, depending on the conditions, strong oxidizing species – chlorine, hypochlorous acid or hypochlorite, are formed on the anode. At higher pH, *e.g.*, pH > 6, hypochlorous acid can dissociate to form hypochlorite and H^+. At pH lower than 3.5, hypochlorous acid yields Cl_2. Mixtures of these species are usually named "active chlorine".[7,8]

During electrolytic hypochlorite production, the oxidation of the chloride to solvated chlorine occurs first at the anode surface:

$$2Cl^- = Cl_2(aq) + 2e^- \quad (1)$$

followed by the secondary solution phase reactions:[7,8]

$$Cl_2(aq) + H_2O = HClO + Cl^- + H^+,\ K_1 = 5.1\times10^{-4}\ mol^2\ dm^{-6} \quad (2)$$

$$HClO = ClO^- + H^+,\ pK_a = 7.54 \quad (3)$$

Arylazo pyridone dyes were already subjected to photolysis and photocatalysis. The photofading kinetics of 3-(*p*- and *o*-substituted arylazo)-5-cyano-2-hydroxy-4-methyl-6-pyridone dyes in amide solvents (*N*,*N*-dimethylformamide, formamide, and *N*,*N*-dimethylacetamide) and *n*-hexane were previously studied. It was established that the photofading rate increases with increasing solvation of the dyes, as well as in the presence of two electron-withdrawing substituents (NO_2 and Cl) on the benzene ring.[9] The same authors also studied the photostability of 3-(mono- and di-substituted arylazo)-5-cyano-2-hydroxy-4-methyl-6--pyridones in *N*,*N*-dimethylformamide under 254 nm light. It was found that the simultaneous presence of two electron-withdrawing substituents in the diazo component of the dyes caused an increase in the fading rate, while the introduction of an hydroxyalkyl group to the coupling component resulted in a decrease in the fading rate.[10] In addition, the arylazo pyridone dyes were applied to polyester fabrics and the effects of substituents on the photofading on polyester substrates was studied.[11,12] Electron-withdrawing substituents on aniline inc-

reased the photostability and improved the sublimation fastness of azo dyes on polyesters, while the *β*-hydroxyethyl group increased the fading rate. Besides direct photodegradation, photocatalytic degradation of 5-(4-sulphophenylazo)-3--cyano-6-hydroxy-4-methyl-2-pyridone in the presence of commercial TiO_2 was studied in aqueous solution under simulated sunlight. Optimal conditions were established and the dye was successfully degraded.[13,14] Arylazo pyridone dyes (Fig. 1) have not been previously solely subjected to the electrochemical treatment except as a component of a wastewater.[15]

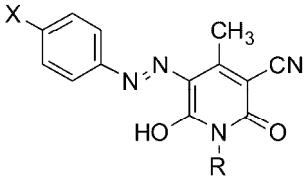

Fig. 1. Structure of the 5-arylazo-3-cyano-6-hydroxy-4-methyl-2-pyridones (R = CH_2CH_2OH, X = OCH_3 (**1**), OH (**2**), NO_2 (**3**), H (**4**), $COCH_3$ (**5**), CH_3 (**6**), COOH (**7**), Cl (**8**), Br (**9**), CN (**10**)); R = H, X = OCH_3 (**11**); R = CH_2CH_3, X = OCH_3 (**12**)).

The aim of the present study was to investigate the electrocatalytic decolorization of arylazo pyridone dyes in water by indirect electrochemical oxidation. The effects of different operating factors, such as agitation speed, concentration of supporting electrolyte, applied current density, initial dye concentration and solution pH, on the dye decolorization were analyzed in order to optimize the conditions of electrochemical treatment. The effect of the dye structure on the reaction rate was also studied.

EXPERIMENTAL

Materials and methods

All starting materials were obtained from Aldrich and Fluka, and were used without further purification. Sodium chloride was p.a. grade (Merck). Deionized water was obtained from a Milipore Waters Milli-Q purification unit. The IR spectra were determined using a Bomem Fourier transform-infrared (FT-IR) spectrophotometer, MB-Series in the form of KBr pellets. The ^{1}H- and ^{13}C-NMR spectral measurements were performed on a Varian Gemini 2000 (200 MHz). The spectra were recorded at room temperature in deuterated dimethyl sulfoxide (DMSO-d_6). The chemical shifts are expressed in ppm values referenced to TMS. The ultraviolet–visible (UV–Vis) absorption spectra were recorded on a Schimadzu 1700 spectrophotometer in the region 200–700 nm. All melting points were determined using a Stuart SMP30 apparatus and are given in degree Celsius. Elemental analyses were performed using a Vario EL III elemental analyzer.

Preparation of arylazo pyridone dyes

The investigated arylazo pyridone dyes were synthesized from the corresponding diazonium salts and substituted 2-pyridones using classical reaction for the synthesis of the azo compounds.[16] 3-Cyano-4-methyl-6-hydroxy-2-pyridone, 1-ethyl-3-cyano-6-hydroxy-4--methyl-2-pyridone and 3-cyano-6-hydroxy-1-(2-hydroxyethyl)-4-methyl-2-pyridone were prepared from cyanoacetamide or substituted cyanoacetamide and ethyl acetylacetate.[13,17] Substituted cyanoacetamides were prepared from corresponding amine and ethyl cyanoacetate.[18] Dyes **3**, **4**, **6**, **8**, **11** and **12** are described in literature.[10-12,19-22] The physical, analytic

and spectral data for the synthesized dyes are given in the Supplementary material to this paper.

Electrochemical decolorization

Electrochemical decolorization process was investigated in a cylindrical glass electrochemical cell with an electrolyte volume of 500 cm^3. The electrolyte was prepared from distilled water, NaCl and the required dye. A 5 cm^2 Ti/PtO_x electrode, obtained by thermal decomposition of H_2PtCl_6 in 2-propanol with 1 mg cm^{-2} of platinum loading, was used as the anode, while the cathode was a 10 cm^2 plate made from austenite 18Cr/8Ni stainless steel series 304. The electrodes with a gap of 3 mm were immersed at the top of the electrolyte. For the electrolysis of solution, the galvanostatic mode of a PAR M273 potentiostat/galvanostat was used. Mixing of the electrolyte was accomplished by a magnetic stirrer with controlled agitation speed. During the electrolysis, at certain times, 3 cm^3 of solution was removed with a micropipette and its UV–Vis spectrum was instantly recorded on a Shimadzu model 1700 spectrophotometer. This enabled the concentration of the dye to be followed during the course of its degradation.

RESULTS AND DISCUSSION

Reaction kinetics and UV–Vis spectra

Arylazo pyridone dyes, as mentioned before, are the disperse dyes characterized by low aqueous solubility. In order to study the reaction kinetics of the decolorization, an aqueous solution of the arylazo pyridone dye should be prepared first. Since these dyes are more soluble in the basic media, the influence of

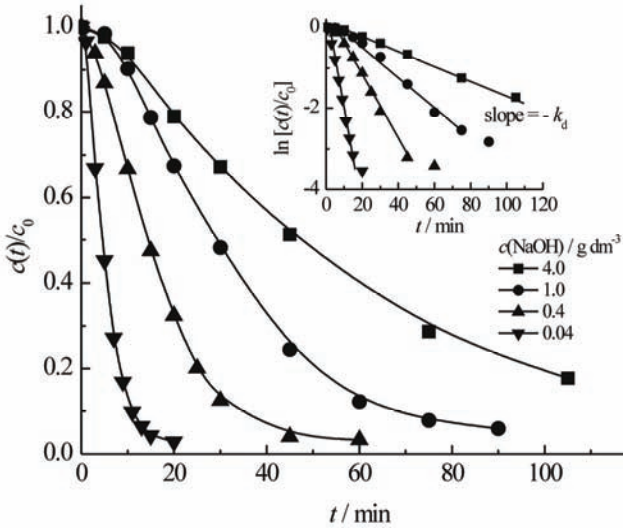

Fig. 2. Dependence of the relative dye **1** concentration over time for different sodium hydroxide concentration (marked in the figure). Insert: the logarithmic plot of the relative concentration of dye *vs*. electrolysis time for different sodium hydroxide concentrations. Conditions: *c*(dye **1**) = 10 mg dm^{-3} (30.4 μM), *c*(NaCl) = 20 g dm^{-3}, ω = 250 rpm, *I* = 200 mA.

sodium hydroxide concentration was studied and the results are given in Fig. 2. To increase solubility, dyes from 3-cyano-6-hydroxy-1-(2-hydroxyethyl)-4--methyl-2-pyridone were synthesized and dye **1** was used as a model compound to study the effect of the sodium hydroxide concentration on the reaction rate of the decolorization. The sodium hydroxide concentration was varied between 4 g dm^{-3} (0.1 M) to 40 mg dm^{-3} (1 mM). The initial sodium chloride concentration and the applied current value were taken according to the results in a previous paper.[23] During the electrochemical treatment, at certain times, 3 cm^3 of reaction solution was taken for instant UV–Vis analysis.

The reaction rate of dye **1** decolorization could be given by the kinetic expression:

$$r = -\frac{\mathrm{d}c_\mathrm{d}(\text{dye 1})}{\mathrm{d}t} = k\,c(\text{dye 1})^m c(\mathrm{Cl}_{2,\text{active}})^n c(\mathrm{Cl}^-)^p \quad (4)$$

where k is the rate constant, and m, n and p represent partial reaction orders. By testing the different kinetic models for pseudo-m orders, the best consent was obtained for pseudo-first order.

The apparent decolorization pseudo first-order rate constants for different sodium hydroxide concentrations were determined from the slope of the logarithmic plot of the relative concentration of the dye **1** *vs*. the electrolysis time, as shown in the insert of Fig. 2, in accordance with the kinetic equation:

$$\ln\frac{c(t)}{c_0} = -k_\mathrm{d}\,t \quad (5)$$

where k_d is the apparent pseudo first-order decolorization rate constant expressed in min^{-1}. For all sodium hydroxide concentrations after 20 min of electrolysis the color removal (*CR*), defined as:

$$CR = \frac{\left(\frac{c(t)}{c_0}\right)_{t=0} - \left(\frac{c(t)}{c_0}\right)_{t=20\text{min}}}{\left(\frac{c(t)}{c_0}\right)_{t=0}} \times 100 \quad (6)$$

depends on the sodium hydroxide concentration between 21 to 97 %. The values of k_d with the corresponding regression coefficients, and *CR* are given in Table I.

TABLE I. The influence of the sodium hydroxide concentration on the values of k_d with the corresponding regression coefficients and color removal (*CR*)

c(NaOH) / g dm^{-3}	k_d / min^{-1}	R^2	*CR* / %
0.04	0.221	0.9938	97
0.4	0.0740	0.9871	67
1.0	0.0366	0.9843	33
4.0	0.0171	0.9958	21

As can be seen from Fig. 2 and Table I, an increase in the sodium hydroxide concentration (solution pH) decreased the reaction rate. The changes in the absorption spectra of the dye **1** solution (sodium hydroxide concentration = 1 mM) during the electrochemical decolorization are presented in Fig. 3. Under the basic conditions, dye **1** exhibited a main band with a maximum absorption at 389 nm. The decrease of absorption peak actually indicates a rapid decolorization of the dye over time. After 20 min, almost complete decolorization was observed. The absorption peak observed at 292 nm is attributed to hypochlorite.[24]

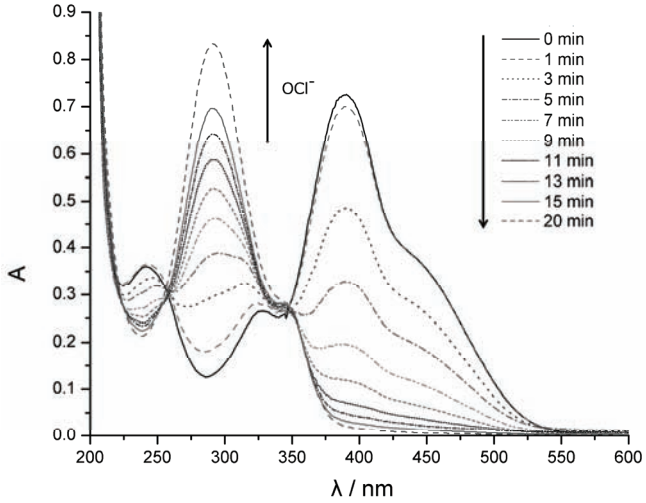

Fig. 3. Changes in the UV–Vis spectrum of dye **1** in water solution (c(NaOH) = 1 mM) during electrochemical decolorization. Conditions: c(dye **1**) = 10 mg dm^{-3} (30.4 μM), c(NaCl) = 20 g dm^{-3}, ω = 250 rpm, I = 200 mA.

The effect of the agitation speed is presented in Fig. 4. The obtained results show a practically negligible effect of the agitation speed on the decolorization of dye **1**. Since the diffusion rate and heterogeneous or homogenous oxidation rate are highly dependent on the hydrodynamic conditions, the only explanation is that the rate determining step is activation controlled (charge transfer) reaction. The only activation controlled reaction could be the oxidation of the chlorides to chlorine given by Eq. (1), followed by fast chlorine dispropotionation to HOCl and their dissociation to OCl^-. In order to resolve which species were active ones, the following experiment was performed: 450 ml of 10 g NaCl was electrolyzed 5 min with 200 mA, and after that a solution of the dye **1** (5 mg in 50 ml of water with 20 mg NaOH) was added. The decolorization occurred practically with an identical rate as during the electrolysis, as can be seen from the inset of Fig. 4. Since pH of the solution was almost constant with a value of ≈10, it could be concluded that hypochlorites were the active species.

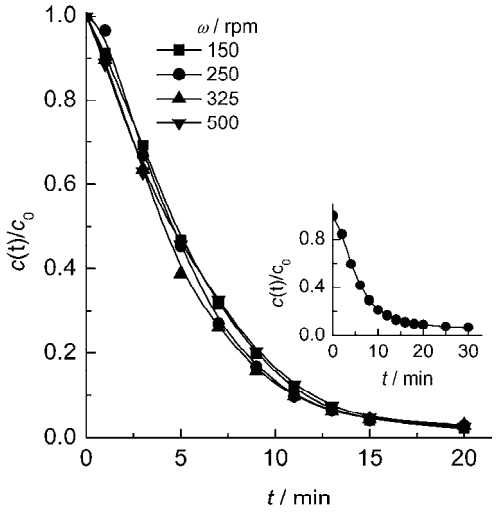

Fig. 4. Dependence of the relative concentration of dye **1** over time for different agitation speeds (marked in the figure). Inset: change of the normalized concentration with time when the dye was added to a hypochlorite solution (ω = 325 rpm).

Effect of the initial sodium chloride concentration

The influence of the sodium chloride concentration on the reaction rate of the decolorization was studied in the range from 15 to 40 g dm^{-3} in solution containing 10 mg dm^{-3} of dye **1.** The sodium hydroxide concentration was 1 mM and applied current 200 mA. As it can be seen, the rate constant increased with increasing salt concentration up to 30 g dm^{-3} (Fig. 5). At higher concentration, namely at 40 g dm^{-3}, a small decrease in the reaction rate was observed.

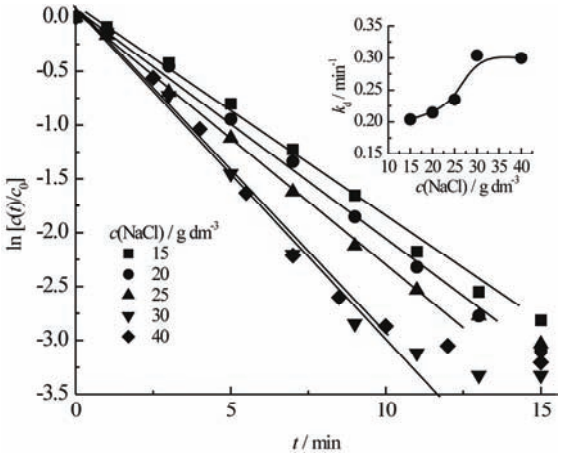

Fig. 5. Dependence of the relative dye **1** concentration over time for different sodium chloride concentrations (marked in the figure). Insert: the reaction rate constant of dye decolorization *vs.* electrolysis time for the different sodium chloride concentrations. Conditions: *c*(dye **1**) = 10 mg dm^{-3} (30.4 μM), ω = 325 rpm, *c*(NaOH) = 1 mM, *I* = 200 mA.

According to the Faraday Law, the amount of the produced hypochlorite should be proportional to the current and the rate should remain constant, *i.e.*, by applying the same current to different solutions, the same amount of hypochlorite should be produced and the rate should be independent (constant) of the elec-

trolyte concentration. One possible explanation is that the production of hypochlorite (Eqs. (1)–(3)) occurs in competition with the production of oxygen:

$$4OH^- = O_2 + 2H_2O + 4e^- \quad (7)$$

If this hypothesis is correct, then higher chloride concentrations will increase the percentage proportion of the reaction *via* hypochlorite and decrease the relative production of oxygen.[25] This is connected with current efficiency of the hypochlorite production. Namely, as determined by Kraft *et al.*,[8] in the concentration range of NaCl from 1 to 20 g dm^{-3}, the current efficiency of hypochlorite production on a Ti/PtO_x electrode linearly increase from ≈10 to 70 %. Hence, in a solution with a smaller concentration of NaCl, *e.g.*, 15–25 g dm^{-3}, the oxygen evolution reaction occurs at the high rate. In a solution with a higher concentration of NaCl, the steady state conditions of current efficiency are reached and the amount of the hypochlorite production becomes constant. Based on this data, the optimum concentration of NaCl would be ≈30 g dm^{-3}. However, due to economic and environmental reasons, a sodium chloride concentration of 20 g dm^{-3} was used for the further experiments.

Effect of the initial dye concentration

The next step in this study was to investigate the influence of the initial dye concentration (dye **1**) on the decolorization reaction rate. This investigation was realized using a sodium chloride concentration of 20 g dm^{-3}, an applied current of 200 mA and an agitation speed of 325 rpm. The effect of different initial dye concentrations (5–20 mg dm^{-3}) on the decolorization rate of dye **1** is displayed in Fig. 6. As can be seen from Fig. 6, and from the inset of Fig. 6, increasing the dye concentration decreased the reaction rate, while above a concentration of 20 mg dm^{-3}, there was a small decrease in the electrocatalytic rate of the decolorization.

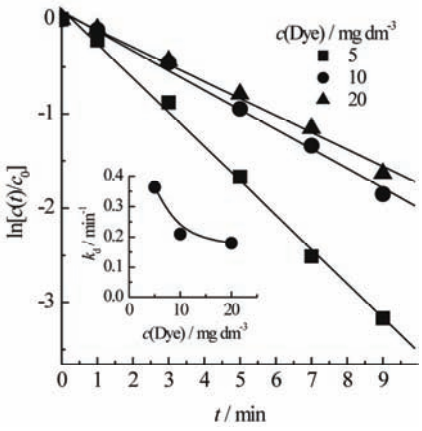

Fig. 6. Dependence of the relative concentration of dye **1** over time for the different dye concentrations (marked in the figure). Insert: the reaction rate constant of dye decolorization *vs.* electrolysis time for the different dye concentrations. Conditions: c(NaCl) = 20 g dm^{-3}, ω = 325 rpm, 1 mM NaOH, I = 200 mA.

Effect of applied current and pH

Applied current is an important variable in electrochemical engineering. Different current values (100, 120, 200 and 250 mA) were applied to the cell in order to investigate the influence of applied current on the electrochemical decolorization of dye **1** a sodium chloride concentration of 20 g dm^{-3} and a dye concentration of 10 mg dm^{-3}. Figure 7 shows the dependence of the relative dye **1** concentration over time and the decolorization kinetic rate constants for different values of applied current are shown in Fig. 7. As can be seen, the rate constant, ≈0.21 min^{-1}, was partially independent of the applied current in the range from 100 to 200 mA. Above 200 mA, the rate constant deviated from the linearity, probably due to direct oxidation of the dye on the electrode surface.[26] Therefore, the current for the further electrochemical studies was fixed at 200 mA.

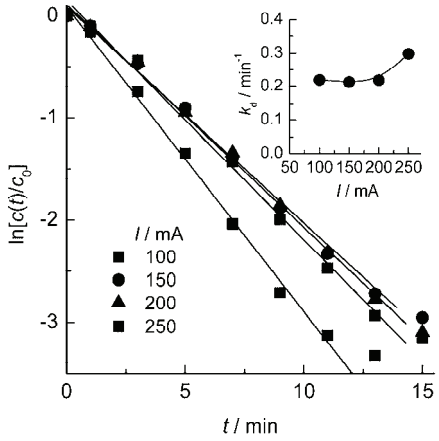

Fig. 7. Dependence of the relative concentration of dye **1** over time for the different values of the applied current (marked in the figure). Inset: the reaction rate constant of dye decolorization *vs.* electrolysis time for different values of the applied current. Conditions: *c*(dye **1**) = 10 mg dm^{-3} (30.4 μM), *c*(NaCl) = 20 g dm^{-3}, ω = 325 rpm, 1 mM NaOH.

In addition, the pH value of the reaction mixture was measured during the electrolysis of dye **1**. As mentioned before, due to the low solubility of arylazo pyridone dyes, the reactions were performed under basic conditions. It was shown earlier that an increase of pH is evident during electrochemical decolorization.[23] The increase in the solution pH decreases the reaction rate, which could be connected with the dissociation of hypochlorous acid to hypochlorite. Here, the initial pH was 10.3 and there was almost no change in the pH value during the reaction. The increase in the hypochlorite concentration is evident from UV–Vis spectra, as shown in Fig. 3.

Influence of the dye structure

It is well known that arylazo pyridone dyes exhibit azo–hydrazone tautomerism, which is presented in Fig. 8.[27,28] Structure (1) presents the azo tautomer, while structure (4) presents the hydrazone tautomer. Under the basic conditions, they form the azo (2) and hydrazone anion (3), which are resonance hybrids.

Generally, arylazo pyridone dyes exist in the hydrazone form in the solid state, while in solvents, depending on the dye structure and the solvent used, the azo––hydrazone equilibrium exists.[16,27] Under basic conditions, depending on the substituent in the aryl component of dye, the dye exists mainly as the azo or hydrazone anion. As it can be seen from Fig. 3, the main absorption peak for dye **1** was at 389 nm, which corresponds to the azo anion structure. The shoulder observed at ≈470 nm is ascribed to the hydrazone form. The same pattern was observed for other dyes (Fig. 9), except for dye **2**, which exhibited a distinguished peak for the hydrazone form at 460 nm.

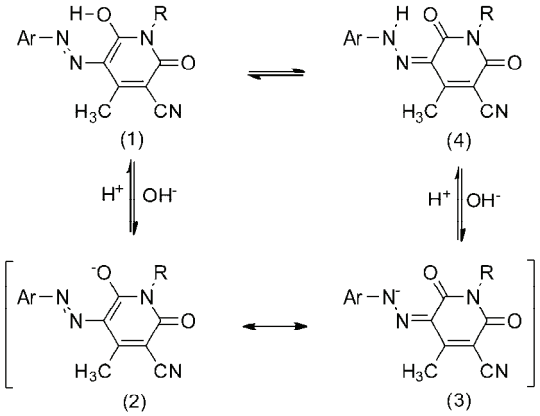

Fig. 8. Azo–hydrazone tautomerism in the arylazo pyridone dyes (azo tautomer (1), azo anion (2), hydrazone anion (3) and hydrazone tautomer (4)).

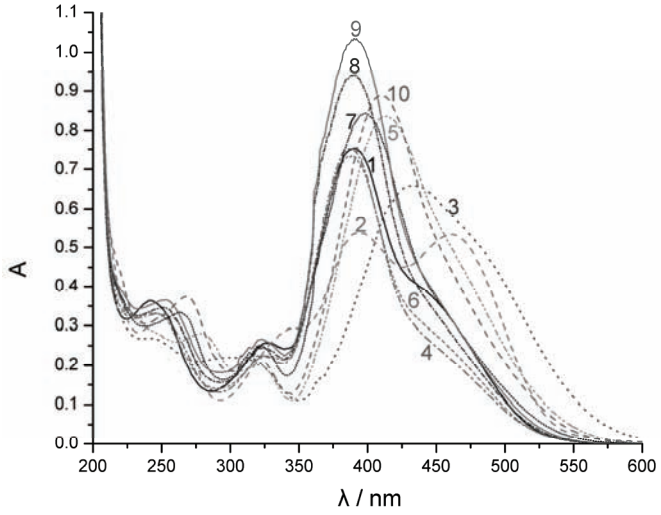

Fig. 9. UV–Vis spectra of the dyes (5-(4-substituted-phenylazo)-3-cyano-1-(2-hydroxyethyl)--6-hydroxy-4-methyl-2-pyridones (**1**–**10**) in water solutions (1 mM NaOH).

In order to obtain more information on the reaction mechanism, a series of 5-(4-substituted-phenylazo)-3-cyano-1-(2-hydroxyethyl)-6-hydroxy-4-methyl-2-pyridones (**1**–**10**) were subjected to electrochemical decolorization under the following conditions: dye concentration = 30.4 μM, sodium chloride concentration = 20 g dm^{-3}, agitation speed = 325 rpm, sodium hydroxide concentration = 1 mM and current = 200 mA. A lower sodium chloride concentration was selected in order to obtain slower reactions, which made the experimental work (UV–Vis handling) easier. The obtained results are presented in Table II.

The effects of the substituents in the investigated compounds were interpreted by correlation of the reaction rate constants with the Hammett substituent constants σ_p/σ_{p-} where σ_p/σ_{p-} measures the electronic effect of the substituent in the *para* position.[31,32]

TABLE II. Substituent effect on the electrochemical decolorization of 5-(4-substituted-phenylazo)-3-cyano-1-(2-hydroxyethyl)-6-hydroxy-4-methyl-2-pyridones (**1**–**10**)

Dye	X	λ_{max} / nm	k_{app} / min^{-1}	σ_p/σ_{p-}
1	OCH_3	389	0.221	–0.28[31]
2	O^-	460	0.3557	–2.30[32]
3	NO_2	434	0.1233	1.27[31]
4	H	388	0.21	0.00[31]
5	CH_3CO	412	0.171	0.47[31]
6	CH_3	389	0.234	–0.14[31]
7	COO^-	398	0.3463	0.31[32]
8	Cl	390	0.2724	0.24[31]
9	Br	390	0.2847	0.26[31]
10	CN	411	0.158	1.00[31]

A better correlation of the reaction rate constants was obtained with the σ_{p-} constants for electron-accepting substituents, than with the σ_p constants (excluding Cl, Br and COO^- groups as substituents with negative inductive and positive resonance effects), which indicates extensive delocalization of the negative charge on the reaction center. The correlation presented in Fig. 10 is interpreted as the existence of the hydrazone anion in the transition state of this reaction. Electron-accepting substituents inhibit the reaction, while electron-donating substituents promote the reaction.

In addition, dye **11** was decolorized under the same conditions as given in Table II, in order to determine the effect of a substituent in position 1 of the 2-pyridone ring. Dye **12** was partially soluble in the aqueous sodium hydroxide water at a concentration of 1 mM and so only the reaction with dye **11** was achieved. The obtained results are given in Fig. 11, indicating that group in position 1 of the pyridone ring has negligible influence on the reaction rate. This indicates that the substituents on the phenyl ring have more influence on the reaction center during the electrochemical decolorization of the dyes.

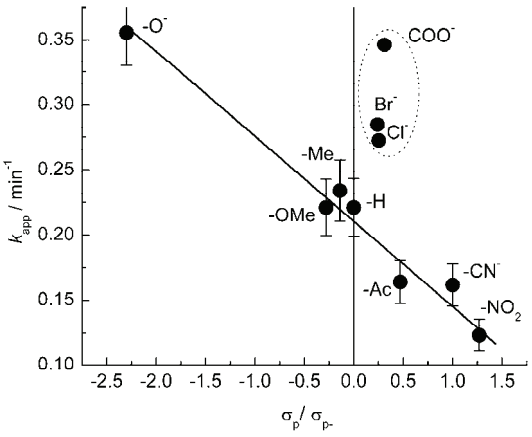

Fig. 10. Relationship between k_{app} and σ_p/σ_{p-} for arylazo pyridone dyes **1**–**10**.

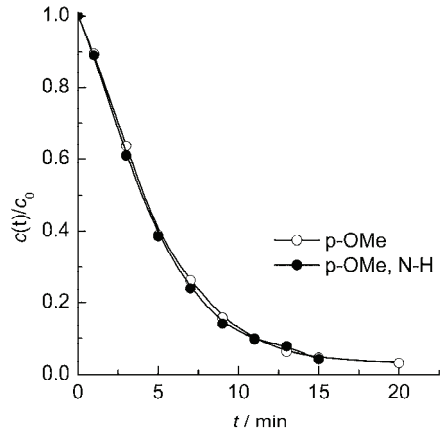

Fig. 11. Dependence of the relative dye concentration over time for dyes **1** and **11**. Conditions: c(dye) = 10 mg dm^{-3} (30.4 μM), c(NaCl) = 20 g dm^{-3}, ω = 325 rpm, 1 mM NaOH, I = 200 mA.

According to Kanazawa and Onami, the conversion of the hydrazone tautomer (here anion) to hydrazone chloride (N(Cl)–N=) is considered to be the rate determining step of the reaction.[33] Moreover, Omura suggested that the electrophilic attack of the chloronium ion (Cl^+) on the nitrogen atom in the hydrazone tautomer of azo dyes is a rate-determining step and because of that the degradation rate of the azo dyes depends on the first power of the dye concentration.[34] Thus, the hydrazone anion would be attacked by chloronium ion. Then OCl^- attacks the imino group of hydrazone chloride giving a single bond between two nitrogens and thus producing the decolorization of an azo dye. Since it was suggested that the rate-determining step is the electrophilic attack of the chloronium ion on the nitrogen atom of the hydrazone anion, it is clear why electron-accepting substituents retard the reaction, while electron-donating substituents promote the reaction. The electron-donating substituents promote the

reaction by increasing the electron density on the nitrogen atom of the hydrazone anion, thus lowering the energy barrier for the electrophilic attack.

CONCLUSIONS

Based on the presented data, the following could be evaluated. The agitation speed between 150 and 500 rpm had a negligible effect of on the decolorization rate. The rate constant increased with increasing salt concentration up to 30 g dm^{-3}. At a higher concentration, namely at 40 g dm^{-3}, a small decrease in the reaction rate was observed. Increasing the dye concentration decreased the reaction rate, up to concentration of 10 mg dm^{-3}, above which there was a small, almost negligible decrease in the electrocatalytic rate of decolorization. Above 200 mA, the rate constant deviated from linearity, probably due to the direct oxidation of the dye on the electrode surface. The optimum electrolyte should contain ≈30 g dm^{-3} NaCl, and the current should be 200 mA (400 mA dm^{-2}). It could also be concluded that electron-accepting substituents inhibited the reaction, while electron-donating substituents promoted the reaction. Electron-donating substituents promoted the reaction by increasing the electron density on the nitrogen atom of the hydrazone anion thus lowering the energy barrier for the electrophilic attack by chloronium ion.

SUPPLEMENTARY MATERIAL

Physical, analytic and spectral data for the synthesized dyes are available electronically from http://www.shd.org.rs/JSCS/, or from the corresponding author on request.

Acknowledgement. The work was supported by the Ministry of Education, Science and Technological Development of the Republic of Serbia under the Research Projects Nos. OI172013 and OI172046.

ИЗВОД

ОПТИМИЗАЦИЈА ЕЛЕКТРОХЕМИЈСКОГ ОБЕЗБОЈАВАЊА ОДРЕЂЕНИХ АРИЛАЗО ПИРИДОНСКИХ БОЈА

ЈЕЛЕНА М. МИРКОВИЋ, НЕВЕНА Ж. ПРЛАИНОВИЋ, ГОРДАНА С. УШЋУМЛИЋ, БРАНИМИР Н. ГРГУР и ДУШАН Ж. МИЈИН

Технолошко–металуршки факултет, Универзитет у Београду, Карнегијева 4, 11020 Београд

Електрокаталитичко обезбојавање арилазо пиридонских боја испитивано је у присуству натријум-хлорида у разблаженом раствору натријум-хидроксида користећи DSA Ti/PtO_x електроду. Обезбојавање се може приписати индиректној оксидацији испитиваних боја помоћу хипохлорита насталог електрохемијском оксидацијом хлорида. Процес обезбојавања је испитиван варирањем концентрације натријум-хидроксида у опсегу од 40 mg dm^{-3} до 4 g dm^{-3}, концентрације натријум-хлорида од 15 до 40 g dm^{-3}, јачине струје од 100 до 250 mA и концентрације боје од 5 до 20 mg dm^{-3}. На основу добијених резултата утврђени су оптимални услови електролизе. Поред тога, испитиван је и утицај супституената на брзину електрохемијског обезбојавања арилазо пиридонских боја.

(Примљено 9. априла, ревидирано 30. маја, прихваћено 18. јуна 2014)

REFERENCES

1. H. Zollinger, *Colour Chemistry*, Wiley–VCH, Weinheim, 1987, p. 85
2. R. J. Chudgar, J. Oakes, in *Kirk-Othmer Encyclopedia of Chemical Technology*, Wiley, New York, 2003, doi: 10.1002/0471238961.01261503082104.a01.pub2
3. E. Foracs, T. Cserhati, G. Oros, *Environ. Int.* **30** (2004) 953
4. I. K. Konstantinou, T. A. Albanis, *Appl. Cat., B* **49** (2004) 1
5. Y. M. Slokar, A. M. Le Marechal, *Dyes Pigm.* **37** (1998) 335
6. A. H. Konsowa, *Desalination* **158** (2003) 233
7. C. A. Martinez-Huitle, E. Brillas, *Appl. Cat., B* **87** (2009) 105
8. A. Kraft, M. Stadelmann, M. Blaschke, D. Kreysig, B. Sandt, F. Schroéder, J. Rennau, *J. Appl. Electrochem.* **29** (1999) 861
9. I. J. Wang, P. Y. Wang, *Text. Res. J.* **60** (1990) 297
10. P. Y. Wang, I. J. Wang, *Text. Res. J.* **60** (1990) 519
11. P. Y. Wang, I. J. Wang, *Text. Res. J.* **61** (1991) 162
12. P. Y. Wang, I. J. Wang, *Text. Res. J.* **62** (1992) 15
13. J. M. Dostanić, D. R. Lončarević, P. T. Banković, O. G. Cvetković, D. M. Jovanović, D. Ž. Mijin, *J. Environ. Sci. Heal., A* **46** (2011) 70
14. J. M. Dostanić, D. R. Lončarević, Lj. S. Rozić, S. P. Petrović, D. Ž. Mijin, D. M. Jovanović, *Desalin. Water Treat.* **51** (2013) 2802
15. L. Szpyrkowicz, C. Juzzolino, S. N. Kaul, *Water Res.* **35** (2001) 2129
16. N. Ertan, P. Gurkan, *Dyes Pigm.* **33** (1997) 137
17. J. M. Bobbit, D. A. Scola, *J. Org. Chem.* **25** (1960) 560
18. D. Ž. Mijin, B. D. Milić, M. M. Mišić-Vuković, *Indian J. Chem., B* **45** (2006) 993
19. C. C. Chen, I. J. Wang, *Dyes Pigm.* **15** (1991) 69
20. Q. Peng, M. Li, K. Gao, L. Cheng, *Dyes Pigm.* **18** (1992) 271
21. J. Dostanić, N. Valentić, G. Uščumlić, D. Mijin, *J. Serb. Chem. Soc.* **76** (2011) 499
22. J. Mirković, J. Rogan, D. Poleti, V. Vitnik, Ž. Vitnik, G. Uščumlić, D. Mijin, *Dyes Pigm.* **104** (2014) 160
23. D. Ž. Mijin, M. L. Avramov Ivić, A. E. Onjia, B. N. Grgur, *Chem. Eng. J.* **204**–**206** (2012) 151
24. L. C. Adam, I. Fábián, K. Suzuki, G. Gordon, *Inorg. Chem.* **31** (1992) 3534
25. J. P. Lorimer, T. J. Mason, M. Plattes, S. S. Phull, D. J. Walton, *Pure Appl. Chem.* **73** (2001) 1957
26. H. S. Awad, N. Abo Galwa, *Chemosphere* **61** (2005) 1327
27. G. S. Uščumlić, D. Ž. Mijin, V. V. Vajs, B. M. Sušić, *Chem. Phys. Lett.* **397** (2004) 148
28. A. Alimmari, D. Mijin, R. Vukićević, B. Božić, N. Valentić, V. Vitnik, Ž. Vitnik, G. Uščumlić, *Chem. Cent. J.* **6** (2012) 1
29. M. B. Smith, J. March, *March's Advanced Organic Chemistry - Reactions, Mechanisms, and Structure*, Wiley, Hoboken, NJ, 2007, p. 404
30. H. Corwin, A. Leo, R. W. Taft, *Chem. Rev.* **97** (1991) 165
31. L. P. Hammett, *J. Am. Chem. Soc.* **59** (1937) 96
32. M. Charton, *Prog. Phys. Org. Chem.* **13** (1981) 119
33. H. Kanazawa, T. Onami, *Color. Technol.* **117** (2001) 323
34. T. Omura, *Dyes Pigm.* **26** (1994) 33.

Journal of the Serbian Chemical Society
JSCS@tmf.bg.ac.rs • www.shd.org.rs/JSCS
J. Serb. Chem. Soc. 79 (12) S175–S179 (2014) *Supplementary material*

SUPPLEMENTARY MATERIAL TO

Optimization of electrochemical decolorization of certain arylazo pyridone dyes

JELENA M. MIRKOVIĆ[#], NEVENA Ž. PRLAINOVIĆ[#], GORDANA S. UŠĆUMLIĆ[#], BRANIMIR N. GRGUR and DUŠAN Ž. MIJIN*[#]

Faculty of Technology and Metallurgy, University of Belgrade, Karnegijeva 4, 11020 Belgrade, Serbia

J. Serb. Chem. Soc. 79 (12) (2014) 1523–1536

PHYSICAL, ANALYTIC AND SPECTRAL DATA FOR THE SYNTHESIZED DYES

*6-Hydroxy-1-(2-hydroxyethyl)-5-((4-methoxyphenyl)diazenyl)-4-methyl-2-oxo--1,2-dihydropyridine-3-carbonitrile (**1**).* Yield: 38 %; red orange powder; m.p.: 232.8–233.3 °C; Anal. Calcd. for $C_{16}H_{16}N_4O_4$: C, 58.53; H, 4.91; N, 17.06 %. Found: C, 58.35; H, 5.01; N, 16.95 %; IR (KBr, cm^{-1}): 3459 (N–H stretching of hydrazone unit), 2221 (–C≡N stretching of cyano group), 1667, 1630 (C=O stretching of carbonyl groups); ^{1}H-NMR (200 MHz, DMSO-d_6, δ / ppm): 2.50 (3H, *s*, CH_3), 3.54 (2H, *t*, *J* = 6.2 Hz, C**H**$_2$CH$_2$OH), 3.79 (3H, *s*, OCH_3), 3.94 (2H, *t*, *J* = 6.2 Hz, CH$_2$C**H**$_2$OH), 7.04 (2H, *d*, *J* = 9.0 Hz, Ar-H), 7.67 (2H, *d*, *J* = = 9.0 Hz, Ar-H), 14.75 (1H, *s*, NH hydrazone); ^{13}C-NMR (50 MHz, DMSO-d_6 δ / ppm): 160.9 (Py), 160.5 (Py), 159.1 (Py), 158.9 (Ar), 134.7 (Ar), 122.2 (Py), 119.4 (Ar), 115.6 (CN), 115.3 (Ar), 99.3 (Py), 57.6 (CH$_2$**C**H$_2$OH), 55.7 (OCH_3), 41.5 (**C**H$_2$CH$_2$OH), 16.4 (CH_3). UV–Vis (EtOH) (λ_{max} / nm (ε / L mol^{-1} cm^{-1})): 460.0 (26360), 273.5 (6400).

*6-Hydroxy-1-(2-hydroxyethyl)-5-((4-hydroxyphenyl)diazenyl)-4-methyl-2-oxo--1,2-dihydropyridine-3-carbonitrile (**2**).* Yield: 45 %; red powder; m.p.: 272.2––272.4 °C; Anal. Calcd. for $C_{15}H_{14}N_4O_4$: C, 57.32; H, 4.49; N, 17.83 %. Found: C, 57.46; H, 4.58; N, 17.71 %. IR (KBr, cm^{-1}): 3494 (O–H stretching of hydroxy group, substituent), 2221 (–C≡N stretching of cyano group), 1661, 1618 (C=O stretching of carbonyl groups); ^{1}H-NMR (200 MHz, DMSO-d_6, δ / ppm): 2.50 (3H, *s*, CH_3), 3.54 (2H, *t*, *J* = 6.2 Hz, C**H**$_2$CH$_2$OH), 3.95 (2H, *t*, *J* = 6.2 Hz, CH$_2$C**H**$_2$OH), 4.82 (1H, *bs*, CH$_2$CH$_2$O**H**), 6.87 (2H, *d*, *J* = 9.0 Hz, Ar-H), 7.57 (2H, *d*, *J* = 9.0 Hz, Ar-H), 9.99 (1H, *s*, OH substituent), 14.84 (1H, *s*, NH hydrazone); ^{13}C-NMR (50 MHz, DMSO-d_6, δ / ppm): 161.0 (Py), 160.5 (Py),

* Corresponding author. E-mail: kavur@tmf.bg.ac.rs

159.0 (Py), 157.7 (Ar), 133.4 (Ar), 121.9 (Py), 119.7 (Ar), 116.6 (Ar), 115.8 (CN), 98.7 (Py), 57.7 (CH_2**C**H_2OH), 41.5 (**C**H_2CH_2OH), 16.4 (CH_3). UV–Vis (EtOH) (λ_{max} / nm (ε / L mol^{-1} cm^{-1})): 466.5 (33280), 276.0 (8260).

*6-Hydroxy-1-(2-hydroxyethyl)-4-methyl-5-((4-nitrophenyl)diazenyl)-2-oxo-1,2--dihydropyridine-3-carbonitrile (**3**)*. Yield: 54 %; Yellow powder; m.p.: 279.6–280.4 °C; IR (KBr, cm^{-1}): 3467 (N–H stretching of hydrazone unit), 2227 (–C≡N stretching of cyano group), 1675, 1630 (C=O stretching of carbonyl groups); ^{1}H--NMR (200 MHz, DMSO-d_6, δ / ppm): 2.52 (3H, *s*, CH_3), 3.56 (2H, *t*, *J* = 6.2 Hz, C**H**$_2$$CH_2OH$), 3.94 (2H, *t*, *J* = 6.2 Hz, CH_2**CH**$_2$OH), 4.80 (1H, *bs*, CH_2CH_2O**H**), 7.90 (2H, *d*, *J* = 9.0 Hz, Ar-H), 8.29 (2H, *d*, *J* = 9.0 Hz, Ar-H), 14.32 (1H, *s*, NH hydrazone); ^{13}C-NMR (50 MHz, DMSO-d_6, δ / ppm): 160.5 (Py), 160.1 (Py), 159.3 (Py), 146.7 (Ar), 144.6 (Ar), 125.7 (Ar), 125.6 (Py), 117.8 (Ar), 114.8 (CN), 103.3 (Py), 57.5 (CH_2**C**H_2OH), 41.8 (**C**H_2CH_2OH), 16.6 (CH_3); UV–Vis (EtOH) (λ_{max} / nm (ε / L mol^{-1} cm^{-1})): 429.0 (27360), 315.5 (8940), 270.0 (5320).

*6-Hydroxy-1-(2-hydroxyethyl)-4-methyl-2-oxo-5-(phenyldiazenyl)-1,2-dihydropyridine-3-carbonitrile (**4**)*. Yield: 48 %; yellow orange powder; m.p.: 227.2–227.8 °C; IR (KBr, cm^{-1}): 3447 (N–H stretching of hydrazone unit), 2225 (–C≡N stretching of cyano group), 1671, 1626 (C=O stretching of carbonyl groups); ^{1}H-NMR (200 MHz, DMSO-d_6, δ / ppm): 2.51 (3H, *s*, CH_3), 3.55 (2H, *t*, *J* = 6.2 Hz, C**H**$_2$$CH_2OH$), 3.94 (2H, *t*, *J* = 6.2 Hz, CH_2C**H**$_2$OH), 4.29 (1H, *bs*, CH_2CH_2O**H**), 7.28 (1H, *t*, *J* = 7.6 Hz, Ar-H), 7.47 (2H, *t*, *J* = 7.6 Hz, Ar-H), 7.69 (2H, *d*, *J* = 7.6 Hz, Ar-H), 14.54 (1H, *s*, NH hydrazone); ^{13}C-NMR (50 MHz, DMSO-d_6, δ / ppm): 160.9 (Py), 160.3 (Py), 159.3 (Py), 141.3 (Ar), 130.0 (Ar), 127.2 (Ar), 123.1 (Py), 117.6 (Ar), 115.3 (CN), 100.7 (Py), 57.6 (CH_2**C**H_2OH), 41.6 (**C**H_2CH_2OH), 16.5 (CH_3); UV–Vis (EtOH) (λ_{max} / nm (ε / L mol^{-1} cm^{-1})): 428.5 (36340), 275.5 (7580).

*5-((4-Acetylphenyl)diazenyl)-6-hydroxy-1-(2-hydroxyethyl)-4-methyl-2-oxo--1,2-dihydropyridine-3-carbonitrile (**5**)*. Yield: 35 %; dark yellow powder; m.p.: 229.7–230.9 °C; Anal. Calcd. for $C_{17}H_{16}N_4O_4$: C, 59.99; H, 4.74; N, 16.46 %. Found: C, 59.84; H, 4.84; N, 16.57 %; IR (KBr, cm^{-1}): 3509 (N–H stretching of hydrazone unit), 2224 (–C≡N stretching of cyano group), 1679, 1636 (C=O stretching of carbonyl groups); ^{1}H-NMR (200 MHz, DMSO-d_6, δ / ppm): 2.51 (3H, *s*, CH_3 on heterocyclic), 2.56 (3H, *s*, $COCH_3$), 3.56 (2H, *t*, *J* = 6.0 Hz, C**H**$_2$$CH_2OH$), 3.94 (2H, *t*, *J* = 6.0 Hz, CH_2C**H**$_2$OH), 4.83 (1H, *bs*, CH_2CH_2O**H**), 7.78 (2H, *d*, *J* = 9.0 Hz, Ar-H), 8.02 (2H, *d*, *J* = 9.0 Hz, Ar-H), 14.41 (1H, *s*, NH hydrazone); ^{13}C-NMR (50 MHz, DMSO-d_6, δ / ppm): 196.8 ($COCH_3$), 160.6 (Py), 160.2 (Py), 159.3 (Py), 144.9 (Ar), 134.5 (Ar), 130.2 (Ar), 124.5 (Py), 117.3 (Ar), 115.0 (CN), 102.1 (Py), 57.6 (CH_2**C**H_2OH), 41.7 (**C**H_2CH_2OH), 26.8 ($COCH_3$), 16.6 (CH_3); UV–Vis (EtOH) (λ_{max} / nm (ε / L mol^{-1} cm^{-1})): 439.0 (35420), 281.5 (9380).

*6-Hydroxy-1-(2-hydroxyethyl)-4-methyl-2-oxo-5-(p-tolyldiazenyl)-1,2-dihydropyridine-3-carbonitrile (**6**)*. Yield: 52 %; orange powder; m.p.: 231.2––231.9 °C; IR (KBr, cm^{-1}): 3420 (N–H stretching of hydrazone unit), 2223 (–C≡N stretching of cyano group), 1676, 1627 (C=O stretching of carbonyl groups); ^{1}H-NMR (200 MHz, DMSO-d_6, δ / ppm): 2.31 (3H, *s*, CH_3 substituent), 2.48 (3H, *s*, CH_3 on heterocyclic), 3.54 (2H, *t*, *J* = 6.2 Hz, C**H**$_2$CH$_2$OH), 3.93 (2H, *t*, *J* = 6.2 Hz, CH$_2$C**H**$_2$OH), 4.83 (1H, *bs*, CH$_2$CH$_2$O**H**), 7.26 (2H, *d*, *J* = 8.6 Hz, Ar-H), 7.56 (2H, *d*, *J* = 8.6 Hz, Ar-H), 14.59 (1H, *s*, NH hydrazone); ^{13}C--NMR (50 MHz, DMSO-d_6, δ / ppm): 160.9 (Py), 160.4 (Py), 159.2 (Py), 139.0 (Ar), 137.2 (Ar), 130.5 (Ar), 122.7 (Py), 117.6 (Ar), 115.4 (CN), 100.1 (Py), 57.6 (CH$_2$**C**H$_2$OH), 41.6 (**C**H$_2$CH$_2$OH), 20.9 (CH_3 substituent), 16.6 (CH_3 on heterocyclic); UV–Vis (EtOH) (λ_{max} / nm (ε / L mol^{-1} cm^{-1})): 441.0 (37280), 277.5 (7960).

*4-((5-Cyano-2-hydroxy-1-(2-hydroxyethyl)-4-methyl-6-oxo-1,6-dihydropyridin--3-yl)diazenyl)benzoic acid (**7**)*. Yield: 41 %; yellow powder; m.p.: 289.8–290.9 °C. Anal. Calcd. for $C_{16}H_{14}N_4O_5$: C, 56.14; H, 4.12; N, 16.37 %. Found: C, 55.98; H, 4.23; N, 16.50 %; IR (KBr, cm^{-1}): 3410 (N–H stretching of hydrazone unit), 2227 (–C≡N stretching of cyano group), 1684, 1635 (C=O stretching of carbonyl groups); ^{1}H-NMR (200 MHz, DMSO-d_6, δ / ppm): 2.50 (3H, *s*, CH_3), 3.56 (2H, *t*, *J* = 6.2 Hz, C**H**$_2$CH$_2$OH), 3.94 (2H, *t*, *J* = 6.2 Hz, CH$_2$C**H**$_2$OH), 4.46 (1H, *bs*, CH$_2$CH$_2$O**H**), 7.72 (2H, *d*, *J* = 8.6 Hz, Ar-H), 7.96 (2H, *d*, *J* = 8.6 Hz, Ar-H), 12.90 (1H, *bs*, COOH), 14.39 (1H, *s*, NH hydrazone); ^{13}C-NMR (50 MHz, DMSO-d_6, δ / ppm): 166.8 (COOH), 160.7 (Py), 160.2 (Py), 159.3 (Py), 144.7 (Ar), 131.2 (Ar), 128.4 (Ar), 124.3 (Py), 117.3 (Ar), 115.1 (CN), 102.0 (Py), 57.6 (CH$_2$**C**H$_2$OH), 41.7 (**C**H$_2$CH$_2$OH), 16.6 (CH_3); UV–Vis (EtOH) (λ_{max} / nm (ε / L mol^{-1} cm^{-1})): 433.0 (34940), 270.0 (8040).

*5-((4-Chlorophenyl)diazenyl)-6-hydroxy-1-(2-hydroxyethyl)-4-methyl-2-oxo--1,2-dihydropyridine-3-carbonitrile (**8**)*. Yield: 55 %; orange powder; m.p.: 246.8–247.2 °C; IR (KBr, cm^{-1}): 3447 (N–H stretching of hydrazone unit), 2227 (–C≡N stretching of cyano group), 1677, 1626 (C=O stretching of carbonyl groups); ^{1}H-NMR (200 MHz, DMSO-d_6, δ / ppm): 2.49 (3H, *s*, CH_3), 3.53 (2H, *t*, *J* = 6.4 Hz, C**H**$_2$CH$_2$OH), 3.94 (2H, *t*, *J* = 6.4 Hz, CH$_2$C**H**$_2$OH), 4.80 (1H, *bs*, CH$_2$CH$_2$O**H**), 7.49 (2H, *d*, *J* = 9.0 Hz, Ar-H), 7.68 (2H, *d*, *J* = 9.0 Hz, Ar-H), 14.43 (1H, *s*, NH hydrazone); ^{13}C-NMR (50 MHz, DMSO-d_6, δ / ppm): 160.7 (Py), 160.3 (Py), 158.7 (Py), 142.2 (Ar), 131.1 (Ar), 129.7 (Ar), 123.7 (Py), 119.9 (Ar), 116.1 (CN), 100.2 (Py), 57.8 (CH$_2$**C**H$_2$OH), 41.5 (**C**H$_2$CH$_2$OH), 16.7 (CH_3); UV–Vis (EtOH) (λ_{max} / nm (ε / L mol^{-1} cm^{-1})): 430.5 (27700), 264.0 (6540).

*5-((4-Bromophenyl)diazenyl)-6-hydroxy-1-(2-hydroxyethyl)-4-methyl-2-oxo--1,2-dihydropyridine-3-carbonitrile (**9**)*. Yield: 52 %; yellow powder; m.p.: 258.0–258.6 °C; Anal. Calcd. for $C_{15}H_{13}BrN_4O_3$: C, 47.76; H, 3.47; N, 14.85 %.

Found: C, 47.88; H, 3.59; N, 14.98 %; IR (KBr, cm^{-1}): 3491 (N–H stretching of hydrazone unit), 2227 (–C≡N stretching of cyano group), 1679, 1633 (C=O stretching of carbonyl groups); ^{1}H-NMR (200 MHz, DMSO-d_6, δ / ppm): 2.50 (3H, *s*, CH_3), 3.55 (2H, *t*, *J* = 6.2 Hz, C**H**$_2$CH$_2$OH), 3.94 (2H, *t*, *J* = 6.2 Hz, CH$_2$C**H**$_2$OH), 4.60 (1H, *bs*, CH$_2$CH$_2$O**H**), 7.55–7.74 (4H, *m*, Ar-H), 14.41 (1H, *s*, NH hydrazone); ^{13}C-NMR (50 MHz, DMSO-d_6, δ / ppm): 160.7 (Py), 160.3 (Py), 159.3 (Py), 140.8 (Ar), 132.8 (Ar), 123.6 (Py), 119.6 (Ar), 119.4 (Ar), 115.2 (CN), 101.3 (Py), 57.6 (CH$_2$**C**H$_2$OH), 41.6 (**C**H$_2$CH$_2$OH), 16.6 (CH_3); UV–Vis (EtOH) (λ_{max} / nm (ε / L mol^{-1} cm^{-1})): 435.5 (39840), 275.0 (9240).

*5-((4-Cyanophenyl)diazenyl)-6-hydroxy-1-(2-hydroxyethyl)-4-methyl-2-oxo--1,2-dihydropyridine-3-carbonitrile (**10**)*. Yield: 44 %; yellow powder; m.p.: 279.1–280.9 °C. Anal. Calcd. for $C_{16}H_{13}N_5O_3$: C, 59.44; H, 4.05; N, 21.66 %. Found: C, 59.61; H, 4.16; N, 21.77 %; IR (KBr, cm^{-1}): 3423 (N–H stretching of hydrazone unit), 2230, 2219 (–C≡N stretching of cyano groups), 1683, 1641 (C=O stretching of carbonyl groups); ^{1}H-NMR (200 MHz, DMSO-d_6, δ / ppm): 2.51 (3H, *s*, CH_3), 3.56 (2H, *t*, *J* = 6.2 Hz, C**H**$_2$CH$_2$OH), 3.94 (2H, *t*, *J* = 6.2 Hz, CH$_2$C**H**$_2$OH), 4.82 (1H, *bs*, CH$_2$CH$_2$O**H**), 7.83 (2H, *d*, *J* = 9.0 Hz, Ar-H), 7.90 (2H, *d*, *J* = 9.0 Hz, Ar-H), 14.28 (1H, *s*, NH hydrazone); ^{13}C-NMR (50 MHz, DMSO-d_6, δ / ppm): 160.5 (Py), 160.1 (Py), 159.2 (Py), 145.0 (Ar), 134.1 (Ar), 124.9 (Py), 118.9 (Ar), 118.0 (Ar), 114.9 (CN on heterocyclic), 108.2 (CN substituent), 102.8 (Py), 57.6 (CH$_2$**C**H$_2$OH), 41.8 (**C**H$_2$CH$_2$OH), 16.6 (CH_3); UV–Vis (EtOH) (λ_{max} / nm (ε / L mol^{-1} cm^{-1})): 42.0 (30120), 268.0 (7080).

*6-Hydroxy-5-((4-methoxyphenyl)diazenyl)-4-methyl-2-oxo-1,2-dihydropyridine-3-carbonitrile (**11**)*. Yield: 53 %; red powder; m.p. 271.8–272.5 °C. IR (KBr, cm^{-1}): 3433 (N–H stretching of hydrazone unit), 3121 (N–H stretching on heterocyclic ring), 2221 (–C≡N stretching of cyano group), 1655, 1603 (C=O stretching of carbonyl groups); ^{1}H-NMR (200 MHz, DMSO-d_6, δ / ppm): 2.50 (3H, *s*, CH_3), 3.80 (3H, *s*, OCH_3), 7.06 (2H, *d*, J = 8.4 Hz, Ar-H), 7.65 (2H, *d*, *J* = 8.4 Hz, Ar-H), 11.96 (1H, *s*, NH heterocyclic), 14.75 (1H, *s*, NH hydrazone); ^{13}C-NMR (50 MHz, DMSO-d_6, δ / ppm): 161.7 (Py), 161.1 (Py), 160.5 (Py), 158.8 (Ar), 134.7 (Ar), 122.8 (Py), 119.2 (Ar), 115.5 (CN), 115.3 (Ar), 99.5 (Py), 55.7 (OCH_3), 16.6 (CH_3). UV–Vis (EtOH) (λ_{max} / nm (ε / L mol^{-1} cm^{-1})): 457.0 (13740), 273.5 (3780).

*1-Ethyl-6-hydroxy-5-((4-methoxyphenyl)diazenyl)-4-methyl-2-oxo-1,2-dihydropyridine-3-carbonitrile (**12**)*. Yield: 73 %; red powder; m.p.: 215.6–217.2 °C; IR (KBr, cm^{-1}): 3433 (N–H stretching of hydrazone unit), 2221 (C≡N stretching of cyano group), 1672, 1627 (C=O stretching of carbonyl groups); ^{1}H-NMR (200 MHz, DMSO-d_6, δ / ppm): 1.13 (3H, *t*, *J* = 7.0 Hz, C**H**$_3$CH$_2$), 2.50 (3H, *s*, CH_3), 3.80 (3H, *s*, OCH_3), 3.89 (2H, *q*, *J* = 7.0 Hz, CH$_3$C**H**$_2$), 7.06 (2H, *d*, *J* = 9.0 Hz, Ar-H), 7.71 (2H, *d*, *J* = 9.0 Hz, Ar-H), 14.81 (1H, *s*, NH hydrazone); ^{13}C-NMR (50 MHz, DMSO-d_6, δ / ppm): 161.8 (Py), 161.2 (Py), 160.6 (Py), 158.9 (Ar),

134.8 (Ar), 122.9 (Py), 119.5 (Ar), 115.4 (Ar), 115.3 (CN), 99.6 (Py), 55.8 (OCH_3), 34.5 (**C**H_3CH_2), 16.6 (CH_3), 12.9 (**C**H_3CH_2); UV–Vis (EtOH) (λ_{max} / / nm (ε / L mol^{-1} cm^{-1})): 460.0 (15380), 273.5 (4180).

Journal of the Serbian Chemical Society
JSCS-info@shd.org.rs • www.shd.org.rs/JSCS
J. Serb. Chem. Soc. 79 (12) 1537–1543 (2014)
JSCS–4686
UDC 663.551.5:634.22+543.51+543.544–14:547.576
Short communication

SHORT COMMUNICATION

Development and validation of an LC–MS/MS method with a multiple reactions monitoring mode for the quantification of vanillin and syringaldehyde in plum brandies

VELE TEŠEVIĆ[1]*, IVANA ALJANČIĆ[2], VLATKA VAJS[1,2], MARIJANA ŽIVKOVIĆ[2], NINOSLAV NIKIĆEVIĆ[3], IVAN UROŠEVIĆ[3] and LJUBODRAG VUJISIĆ[1]

[1]*Faculty of Chemistry, University of Belgrade, Studentski trg 16, 11058 Belgrade, Serbia,* [2]*Institute of Chemistry, Technology and Metallurgy, University of Belgrade, Njegoševa 12, 11001 Belgrade, Serbia and* [3]*Faculty of Agriculture, University of Belgrade, Nemanjina 6, 11080 Zemun, Serbia*

(Received 25 February, revised 21 July, accepted 22 July 2014)

Abstract: An ultra-performance liquid chromatographic–triple quadrupole mass spectrometric (UPLC–QqQ–MS/MS) method with a multiple reactions monitoring mode (MRM) was developed and validated for the quantification of vanillin and syringaldehyde in plum brandy. The method showed good linearity (0.05 to 10 mg L^{-1}) and low limits of detection and quantification (the *LOD* and *LOQ* values were 11.6 and 38.2 μg L^{-1} for vanillin, and 12.7 and 42.0 μg L^{-1} for syringaldehyde, respectively). The overall intra-day and inter-day variations were less than 4.21 % and the overall recovery was over 93.0 %. The correlation coefficients (R^2) of the calibration curves were higher than 0.9999. In order to evaluate whether the method was suitable for use as a routine analytical tool, vanillin and syringaldehyde were determined in 31 samples of Serbian plum brandy.

Keywords: vanillin; syringaldehyde; plum brandy; LC–MS/MS.

INTRODUCTION

Plum tree (*Prunus domestica* L.) is a traditional plant in Serbian village households. Serbian plum brandy (Serbian Slivovitz) is the most popular Serbian alcoholic beverage obtained by distilling fermented fruit pulp. The production of aged brandy consists of: *i*) preparation of the raw material and fermentation, *ii*) distillation and *iii*) aging in oak wood casks when the organoleptic qualities of the distillate develop to produce the mature brandy.[1]

* Corresponding author. E-mail: vtesevic@chem.bg.ac.rs
doi: 10.2298/JSC140225079T

Plum brandy, as well as other spirits, is aged in oak barrels for a period that can last for several years. Aging is the stage of the production process important for the extraction of phenolic compounds that enhance the sensory qualities, and the antioxidant capacity of a brandy, which may have health benefit if consumed in moderation.

The aromatic phenolic aldehydes, among others vanillin and syringaldehyde, formed by degradation of lignin from the oak barrels during coopering are extracted into spirit.[2] In a simulated experiment with four oak wood samples, the content of syringaldehyde was more than double the vanillin content.[3] Previous studies performed with several spirits showed ratio of syringaldehyde to vanillin was 1.4 to 2.5 when these aldehydes were produced by ageing of the spirit in oak barrels over a long period.[4] Thus, their concentrations could indicate the time of aging in oak casks. Since vanillin is an aldehyde that contributes the most to the aroma of alcoholic beverages and is easily obtained industrially, producers may be encouraged to add it to brandies, thereby simulating an aged character.[5] The syringaldehyde/vanillin ratio seems to be one of the characteristics of the original composition of a brandy, and may be considered as a marker to distinguish counterfeit alcoholic beverages from genuine ones.[4]

The undeniable appeal of oak aging makes the caution of the industry to change a tradition that is fundamental to the finished product understandable.[6] The analytical methods reported in the literature to quantify aromatic aldehydes in alcoholic beverages are HPLC with UV detection,[7,8] gas chromatography coupled with mass spectrometry (GC/MS),[9] derivative spectrophotometry[10] and high performance capillary electrophoresis with UV detection.[2]

The aim of the present study was to develop and validate a fast method for the quantification of vanillin and syringaldehyde in mature plum brandies of different origin using ultra-performance liquid chromatography (UPLC) combined with a triple quadrupole tandem mass spectrometry (QqQ–MS/MS) system operated in the multiple reaction-monitoring (MRM) mode. The advantage of UPCL over HPLC is higher resolution and speed of analysis owing to small particle sizes (2 μm compared to 5 μm), large surface areas, and application of high pressure to the solvent flow. UPLC is just a special variant of HPLC that affords better separation and very fast analysis.[11] The analytical procedure was tested on specimens of authentic Serbian plum brandy obtained directly from the producers.

EXPERIMENTAL

Chemicals and materials

Ultra high-purified water, acetonitrile HPLC grade, and formic acid (Merck Darmstadt, Germany) were used as solvents for the chromatography. Vanillin and syringaldehyde used as external standards were purchased from Sigma–Aldrich (St. Louis, MO, USA).

Samples

Specimens of Serbian plum brandy produced from single or mixed plum varieties of the genus *Prunus* L. that were aged in oak wood casks (29 samples) and mulberry wood casks (2 samples), were filtered through 0.45μm pore size membrane filteres and injected directly without preliminary treatment such as concentration, extraction, *etc*.

UPLC Analysis

The development and validation of chromatographic method and analysis of plum brandy samples was performed on a Waters Acquity UPLC system, equipped with a binary solvent manager, an autosampler, a column heater, a PDA detector, and interfaced to a tandem quadrupole detector. The separation column was an ACQUITY UPLC BEH C18 column (2.1 mm i.d.×50 mm, 1.7 μm particle size). The column heater was set at 30 °C and the mobile phase flow rate was maintained at 0.5 mL min^{-1}. The gradient (solvent A, 100 % acetonitrile, solvent B water/formic acid 99.8:0.2, *V*/*V*) was 0–3.0 min (16.0 % A), 3.0–8.0 min (98.0 % A). The injection volume was 1 μL. The DAD detector range was 190–600 nm.

QqQ–MS/MS–MRM

Identification of vanillin and syringaldehyde was performed by comparing the retention times and UV and mass spectra with those of the reference standards. Quantification of the identified compounds was performed using the external standard method. Calibration curves were established for vanillin and syringaldehyde. MS detection performed using a Waters TQD tandem quadrupole detector interfaced with an Acquity UPLC system *via* an ESI probe. The ESI source was operated in the positive ionization mode at 150 °C, with a desolvation temperature of 450 °C, a 700 L h^{-1} desolvation gas flow rate, and the capillary voltage was set at 3.5 kV. Argon was used as the collision gas at a flow rate of 0.10 mL min^{-1}. The collision energy used for vanillin was 16 eV and for syringaldehyde 10 eV. Based on the full-scan mass spectra of the aldehydes, the most abundant ions were selected and the mass spectrometer was set to monitor the transitions of the precursors to the product ions as *m*/*z* 153/93 for vanillin and *m*/*z* 183/155 for syringaldehyde. Data acquisition, peak integration and calibration were performed with Mass Lynx 4.0 software.

RESULTS AND DISCUSSION

UPLC method validation

The proposed method was validated for linearity, accuracy, precision and limits of detection and quantification.

Linearity. Calibration graphs were plotted based on linear regression analysis of the integrated peak areas *vs*. concentration (mg L^{-1}) in the standard solution at four different concentrations. The correlation coefficients obtained from the standard curves were for vanillin (0.99997) and syringaldehyde (0.99992). There was a strong linear correlation of the concentrations of the compounds with the peak areas.

Precision. Three different concentrations of vanillin and syringaldehyde (0.05, 0.5 and 1.0 mg L^{-1}) were analyzed in six independent series in triplicate during the same day (intraday precision) and over 3 consecutive days (interday precision). The relative standard deviation (*RSD*) was taken as a measure of

precision, and the results are given in Table I. The method showed a high degree of precision for both of the analyzed compounds.

TABLE I. Regression equations, linearity ranges, correlation coefficients, limits of detection (*LOD*), limits of quantification (*LOQ*), recoveries and relative standard deviations (*RSD*) for vanillin and syringaldehyde determination

Cmpd.	Regression equation	Linearity range mg L^{-1}	R^2	*LOD* µg L^{-1}	*LOQ* µg L^{-1}	Recovery %	Intra-day *RSD* / % (*n* = 6)	Inter-day *RSD* / % (*n* = 3)
Vanillin	$y = 6921900x + 184.24$	0.05–10	0.99997	11.6	38.2	99.0–103.2	0.59	1.23
Syringaldehyde	$y = 5254820x + 83.07$	0.05-10	0.99992	12.7	42.0	93.0–106.8	1.93	4.21

Limits of detection and quantification. The limit of detection (*LOD*) and limit of quantification (*LOQ*) were estimated from the signal-to-noise ratio. The *LOD* is defined as the lowest concentration resulting in a peak area of three times the baseline noise. The *LOQ* is defined as the lowest concentration that provides a signal-to-noise ratio higher than 10. The limits of detection and quantification observed for vanillin and syringaldehyde are listed in Table I.

Accuracy. The recovery (*R*) was used to evaluate the accuracy of the method. A known amount (*G*) of the considered compound (0.05, 0.5 and 1.0 mg L^{-1}) was added into a hydroalcoholic (40 vol. %) solution and the samples were injected under identical conditions in six replicate determinations (each concentration in triplicate). The values were calculated using the following equation:

$$R\ (\%) = \frac{G_{\text{determined}}}{G_{\text{added}}} \times 100$$

The proposed method afforded a recovery of 96.8–103.2 % for vanillin and 93.0–106.8 % for syringaldehyde (Table I). The accuracy was expressed as the percentage recovery.

Determination of vanillin and syringaldehyde in Serbian plum brandies

In order to evaluate whether the method is suitable for use as a routine analytical tool, vanillin and syringaldehyde were determined in 31 Serbian plum brandy samples and the results are given in Table II. The analyses were performed in triplicate and data are presented as mean ±*SD*. The concentrations of aldehydes were calculated by reference to the peak areas of the external standards. Checking for matrix effect was performed by addition of reference standards in the same concentration as obtained for brandy samples from the calibration curve. No matrix effect was found.[12] The chromatogram of plum brandy sample

5 is shown in Fig. 1, together with the extracted MRM chromatograms of vanillin and syringaldehyde.

TABLE II. Description of plum brandy analyzed and its quantification of vanillin (V) and syringaldehyde (S); hm. – homemade; in. – industrial, o.n.y.p. – old, no year of production

Plum variety	Type of barrel	Type / year of production	Age y	EtOH vol. %	V±*SD* mg L^{-1}	S±*SD* mg L^{-1}	S/V
Požegača + Crvena ranka	Oak	hm. / 1979	34	38.96	5.11±0.18	6.76±0.09	1.32
Požegača	Oak	hm. / 1983	30	37.62	5.10±0.08	6.25±0.13	1.23
Mixed varieties	Oak	in. / 1997	16	42.88	0.69±0.06	1.05±0.11	1.52
Mixed varieties	Oak	in. /1992	21	38.64	3.02±0.13	3.89±0.42	1.29
Mixed varieties	Oak	in. / 1995	16	44.60	2.68±0.06	2.71±0.04	1.01
Mixed varieties	Oak	hm. / o.n.y.p.	–	43.80	2.41±0.11	1.94±0.07	0.80
Požegača + Trnovača	Oak	hm. / 1991	22	45.56	1.23±0.04	1.46±0.13	1.19
Mixed varieties	Oak	hm. / 1992	21	43.17	1.37±0.09	2.03±0.14	1.48
Mixed varieties	Oak	in. / o.n.y.p.	–	43.74	0.12±0.003	0.07±0.01	0.57
Mixed varieties	Oak	in. / 1998	15	41.45	0.65±0.03	0.25±0.02	0.38
Mixed varieties	Oak	hm. / 1992	21	38.50	1.92±0.08	1.02±0.05	0.53
Požegača	Oak	hm. / 1951	62	40.92	3.46±0.03	5.21±0.34	1.51
Mixed varieties	Oak	hm. / 1998	15	38.59	1.65±0.05	0.66±0.03	0.40
Požegača	Oak	hm. / 1991	22	41.17	1.33±0.07	1.35±0.31	1.01
Mixed varieties	Mulberry	hm. / o.n.y.p.	–	45.44	0.82±0.08	0.95±0.04	1.16
Mixed varieties	Oak	hm. / 2003	10	41.20	0.36±0.01	0.34±0.01	0.94
Požegača	Oak	hm. / o.n.y.p.	–	42.08	1.04±0.02	1.17±0.04	1.13
Mixed varieties	Oak	hm. / 1990	23	43.10	3.16±0.30	2.86±0.06	0.91
Požegača	Oak	hm. / 1978	35	42.67	4.23±0.15	5.32±0.12	1.26
Mixed varieties	Oak	in. / 1992	21	44.47	0.23±0.007	0.25±0.003	1.08
Požegača	Oak	hm. / 1998	15	44.95	0.83±0.02	1.05±0.01	1.26
Požegača + Crvena ranka	Oak	hm. / 2003	10	52.3	0.67±0.07	0.58±0.06	0.87
Požegača + Crvena ranka	Oak	hm. / 1993	20	52.3	3.05±0.25	5.11±0.34	1.67
Požegača + Crvena ranka + Čačanska rodna + Stenli	Oak	hm. / 1994	19	50.7	4.23±0.28	10.61±0.67	2.51
Mixed varieties	Oak	hm. / 1999	14	49.7	1.76±0.23	4.06±0.52	2.31
Požegača	Oak	hm. / 1997	16	56.3	2.44±0.31	4.01±0.43	1.64
Požegača + Crvena ranka	Oak	hm. / 2003	10	44.6	0.30±0.02	0.66±0.03	2.18
Mixed varieties	Oak	hm. / 2006	7	53.3	4.27±0.21	8.89±0.32	2.08
Požegača + Crvena ranka + Čačanska rodna + Stenli	Oak	hm. / 1998	15	50.7	2.26±0.17	3.03±0.27	1.34
Mixed varieties	Oak	hm. / 1996	17	39.5	2.74±0.22	5.77±0.35	2.11
Mixed varieties	Oak	hm. / 2002	11	53.3	2.36±0.29	5.37±0.36	2.27

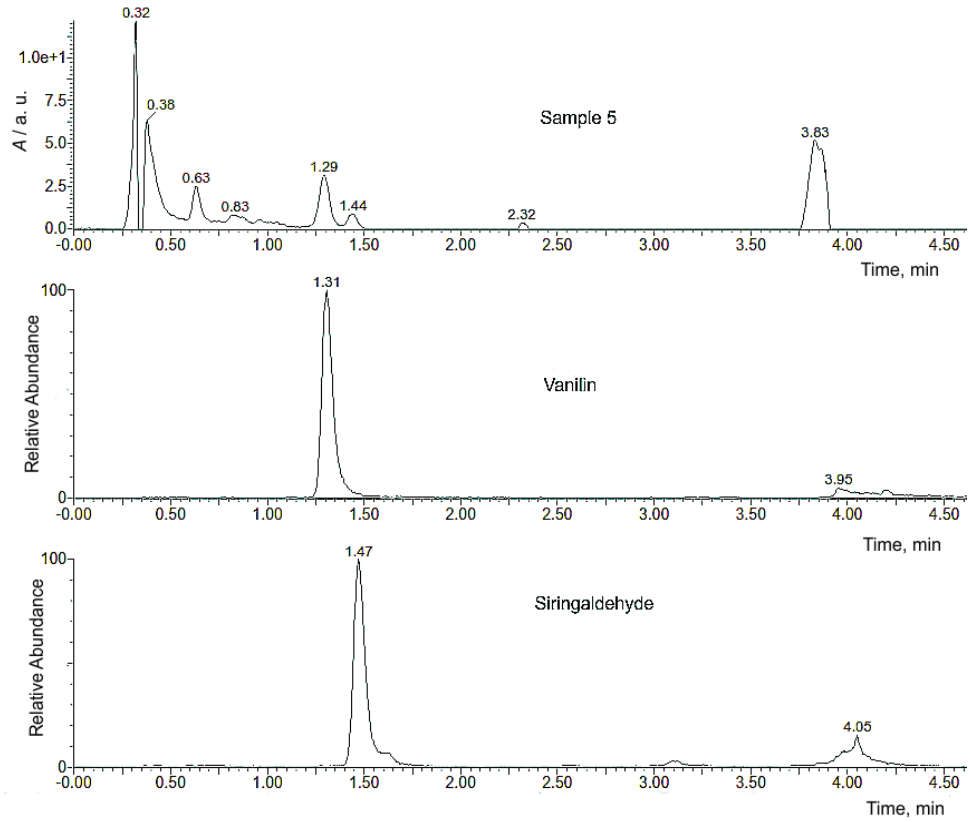

Fig. 1. DAD chromatogram of a plum brandy and extracted MRM chromatograms of vanillin and syringaldehyde, a) HPLC–UV–DAD chromatogram of plum brandy (Sample 5), b and c) extracted MRM chromatograms of vanillin and syringaldehyde in the ES+ mode, respectively.

CONCLUSIONS

This novel UPLC–QqQ–MS/MS–MRM method is proposed for the simple and reproducible detection and quantification of vanillin and syringaldehyde in one rapid chromatographic analysis. The short analytical run time (about five min per run) allows the use of a low amount of solvent and hence, the small amount of waste generation makes the method well suited for routine analysis. The method is useful for the identification of counterfeit brandy, which is easy to recognize by the ratios of syringaldehyde to vanillin.

Acknowledgement. The authors acknowledge their gratitude to the Ministry of Education, Science and Technological Development for financial support (Project No. 172053).

ИЗВОД

РАЗВОЈ И ВАЛИДАЦИЈА LC–MS/MS МЕТОДЕ У MRM РЕЖИМУ ЗА КВАНТИФИКАЦИЈУ ВАНИЛИНА И СИРИНГАЛДЕХИДА У РАКИЈАМА ШЉИВОВИЦАМА

ВЕЛЕ ТЕШЕВИЋ[1], ИВАНА АЉАНЧИЋ[2], ВЛАТКА ВАЈС[1,2], МАРИЈАНА ЖИВКОВИЋ[2], НИНОСЛАВ НИКИЋЕВИЋ[3], ИВАН УРОШЕВИЋ[3] и ЉУБОДРАГ ВУЈИСИЋ[1]

[1]Хемијски факултет, Универзитет у Београду, Студентски трг 16, 11058 Београд, [2]Институт за хемију, технологију и металургију, Универзитет у Београду, Његошева 12, 11001 Београд и [3]Пољопривредни факултет, Универзитет у Београду, Немањина 6, 11080 Земун

Развијена је и валидована UPLC–QqQ–MS/MS метода у MRM режиму за квантификацију ванилина и сирингалдехида у ракији шљивовици. Метода показује добру линеарност (0,05–10 mg L^{-1}) и низак лимит детекције и квантификације (*LOD* и *LOQ* за ванилин су 11,6 и 38,2 μg L^{-1}, а за сирингалдехид 12,7 и 42,0 μg L^{-1}). Варијације резултата у току једног и више дана су мање од 4,21 %, а *Recovery* преко 93,0 %. Корелациони коефицијент (R^2) калибрационих кривих је већи од 0,9999. У циљу процене погодности коришћења методе као рутинске, одређен је садржај ванилина и сирнгалдехида у тридесет и једном узорку српске шљивовице.

(Примљено 25. фебруара, ревидирано 21. јула, прихваћено 22. јула 2014)

REFERENCES

1. T. Varavut, L. Vichai, M. Samart, V. Kanit, *Thai J. Biotechnol.* **8** (2007) 14
2. A. Panossian, G. Mamikonyan, M. Torosyan, E. Gabrielyan, S. Mkhitaryan, *Anal. Chem.***73** (2001) 4379
3. E. Garcia-Romero, M. S. Perez-Coello, J. Sanz, M. D. Cabezudo, *Analysis* **26** (1998) 33
4. J. L. Puech, C. Jouret, *Ann. Falsif. Expert Chim.* **75** (1982) 81
5. R. Giménez, M. Villalón, H. López, M. Navarro, C. Cabrera, M. Olalla, J. J. Quesada, M. C. López, *Cienc. Tecnol. Aliment.* **3** (2000) 13
6. J. R. Mosedale, J,-L. Puech, *Trends Food Sci. Tech.* **9** (1998) 95
7. S. Canas, M. C. Leandro, M. I. Spranger, A. P. Belchior, *J. Agric. Food Chem*. **47** (1999) 5023
8. J. J. Mangas, R. Rodríguez, J. Moreno, J. Blanco, *Agric. Food Chem.* **44** (1996) 268
9. V. N. Vlassov, D. S Maruzhenkov, *Analysis* **27** (1999) 663
10. F. Garcia Sanchez, C. Carnero Ruiz, J. C. Marquez Gomez, M. Hernandez Lopez, A. Heredia Bayona, *Analyst* **115** (1990) 1121
11. M. Gumustas, S. Kurbanoglu, B. Uslu, S. A. Ozkan, *Chromatographia* **76** (2013) 1365
12. M. Schwarz, M. C. Rodríguez, D. A. Guillén, C. G. Barroso, *J. Sep. Sci.* **32** (2009) 1782.

Journal of the Serbian Chemical Society
JSCS-info@shd.org.rs • www.shd.org.rs/JSCS

J. Serb. Chem. Soc. 79 (12) 1545–1559 (2014)
JSCS–4687

UDC 546.47'221+539.12+546.141:
519.877+544.112
Original scientific paper

Molecular modelling of zinc sulphide nanoparticles stabilized by cetyltrimethylammonium bromide

PETR KOVÁŘ[1], PETR PRAUS[2,3]*, MIROSLAV POSPÍŠIL[1] and RICHARD DVORSKÝ[4,5]

[1]*Charles University in Prague, Faculty of Mathematics and Physics, Ke Karlovu 3, 12116 Prague 2, Czech Republic,* [2]*Institute of Environmental Technology, VŠB-Technical University of Ostrava, 17. Listopadu 15, 708 33 Ostrava-Poruba, Czech Republic,* [3]*Department of Chemistry, VŠB-Technical University of Ostrava, 17. Listopadu 15, 708 33 Ostrava-Poruba, Czech Republic,* [4]*Institute of Physics, VŠB-Technical University of Ostrava, 17. Listopadu 15, 708 33 Ostrava-Poruba, Czech Republic and* [5]*Regional Materials Science and Technology Centre, VŠB-Technical University of Ostrava, 17. Listopadu 15, 708 33 Ostrava-Poruba, Czech Republic*

(Received 15 November 2013, revised 28 February 2014, accepted 10 May 2014)

Abstract: ZnS nanoparticles stabilized by cetyltrimethylammonium bromide (CTAB) were modelled in the Materials Studio environment. Four types of models with different distances between the ZnS nanoparticles and different amounts of cetyltrimethylammonium (CTA) cations without water and in a water environment were built and characterized by calculation of sublimation energies. The results of the molecular modelling without water showed that the most favourable model consisted of two ZnS nanoparticles with a distance of 8–9 nm separated without immersion of CTAs. On the contrary, the most favourable model in a water environment was composed of ZnS nanoparticles that nearly touched each other. CTA cations exhibited a tendency to be located on the ZnS surface forming sparse covers. The size distributions of the ZnS nanoparticles obtained by transmission electron microscopy (TEM) measurements agreed well with the molecular modelling results.

Keywords: molecular modelling; ZnS nanoparticles; cetyltrimethylammonium bromide; interactions.

INTRODUCTION

Semiconductor nanoparticles, such as metal oxides or metal sulphides, are well known for their outstanding electrochemical properties, which make them utilizable in photo-optics, opto-electronics, photocatalysis, *etc*.[1] One of the most important factors related to nanomaterials is the dependence of physical and chemical properties on their particle sizes. Decreasing particle size of a semicon-

* Corresponding author. E-mail: petr.praus@vsb.cz
doi: 10.2298/JSC131115050K

ductor leads to an increase of its specific surface area and gap energy, which is known as the quantum size effect or quantum confinement.[2,3]

Zinc sulphide is a semiconductor with a wide direct band gap energy of about 3.7 eV. ZnS nanoparticles have been synthesized by precipitation of zinc ions with sulphides forming ZnS in the sphalerite (solubility product, K_S = = 1.6×10^{-4}) and wurtzite structure (K_S = 2.5×10^{-22}). Freshly prepared ZnS nanoparticles, as well as other nanoparticles, tend to agglomerate and, therefore, are mostly stabilized by macromolecules or surfactants.[4–6]

Stabilization mechanisms of nanoparticles cannot be directly observed by laboratory experimental methods but can be simulated by molecular modelling based on empirical force fields. The analysis of some the characteristics of the interaction energy can provide information on the stability of systems, mutual interactions of their parts and probability estimation for some processes.

The aim of this work was to model the interactions between ZnS nanoparticles and CTAB by molecular simulations. From the simulation point of view, some authors published papers dealing with structure of ZnS nanoparticles and their characteristics, *e.g.*, structural changes of the ZnS nanostructure depending on its size and on the species surrounding the nanoparticles.[7–10] Although interactions between CTAB and some nanoparticles were modelled by several authors,[11,12] mutual interactions of ZnS nanoparticles stabilized by CTAB were simulated for the first time in this study. In previous papers,[4,5] only the structure of CTAB layers formed on the ZnS nanoparticles surface were modelled. Along with molecular modelling, colloid dispersions of ZnS nanoparticles and CTAB were examined by transmission electron microscopy, and the growth of the ZnS nanoparticles was studied to confirm the modelling results.

EXPERIMENTAL

Material and chemicals

The used chemicals were of analytical reagent grade: zinc acetate, sodium sulphide, (all from Lachema, Czech Republic), cetyltrimethylammonium bromide (Sigma, USA). Water deionised by reverse osmosis (Aqua Osmotic, Czech Republic) was used for the preparation of all solutions.

Precipitation of ZnS nanoparticles

ZnS nanoparticles were precipitated by adding zinc acetate to sodium sulphide.[6] The precipitation was performed in the micellar dispersion of CTAB with the concentration of 3 mmol L^{-1}. The S^{2-}:Zn^{2+} mole ratio was kept at 1.5:1.

Transmission electron microscopy

Transmission electron microscopy was performed on a JEM 1230 (Jeol, Japan) microscope operated at 80 kV. The freshly prepared samples of the ZnS nanoparticles stabilized by CTAB were placed on a copper grid (400 mesh) coated by a film of 1.5–3 % of poly(vinyl formaldehyde) in chloroform and dried by blotting paper. The contrast of the micrographs was improved by the addition of a 1 % solution of ammonium molybdate to the samples.

Molecular modelling

The data for the wurtzite structure were used for building the ZnS nanoparticles.[6] Crystallographic data for wurtzite are the following: space group $P6_3mc$, $a = b = 0.382$ nm, $c = = 0.626$ nm.[13] According to experimental data, nanoclusters in the shape of a sphere with radii of 2.0 nm were created in a nanostructure builder module and two ZnS nanoparticles were used in the simulations. Molecular modelling was performed in the Materials Studio modelling environment.[14]

Since the CTAB molecule dissociates in water to form a CTA cation and a bromide anion, interactions of ZnS nanoparticles and CTA cations were modelled. The ZnS nanoparticle with adsorbed CTA cations was denoted as ZnS–CTA in this manuscript. The interactions and structure of two ZnS–CTA nanoparticles can be subsequently generalized for interactions and behaviour of a larger amount of ZnS–CTA ones. The number of CTA cations surrounding each ZnS nanoparticle was 30, 50, 70 and 90 and the following four models were built:

1. ZnS nanoparticles were nearly touching each other; the distance between ZnS nanoparticle centres was about 4.0 nm.

2. One ZnS–CTA nanoparticle shared CTA cations with other ZnS–CTA nanoparticle so that CTA cations were immersed in one another. The distance between the centres of the ZnS nanoparticles was about 6.0 nm.

3. ZnS–CTA nanoparticles were connected together *via* CTA chains. Models were used with various amounts of CTA (12–25), which formed chains of various distances between ZnS nanoparticle centres, ranging from 8.0 to 10.0 nm.

4. ZnS–CTA nanoparticles were separated without immersing CTA cations and without chain connection. The distance between ZnS centres ranged from 8.0 to 9.0 nm.

For each type of presented structure model, a set of initial models was created and the models were optimized without water and in a water environment. The models optimized without water contained two ZnS nanoparticles and CTA cations. Each model optimized in a water environment contained an additional 5760 water molecules together with compensating bromide anions randomly surrounding the ZnS nanoparticles. As found recently,[4,5] the ZnS––CTA structure exhibited a bilayer arrangement of CTA cations around the ZnS nanoparticles, *i.e.*, half of CTA cations were oriented with their polar headgroup towards the outer space and the half with their polar headgroup towards the ZnS nanoparticle surface. In case of model 1, due to the close arrangement of ZnS nanoparticles, some of the CTA exhibited a bilayer arrangement and some was randomly distributed around the ZnS nanoparticles and among the CTA cations in the bilayer arrangement. The geometry optimization was realised in the Universal force field[15] in the Materials Studio modelling environment. The advantage of this force field is a high speed of convergence, especially in case of large systems like those presented in this paper. On the other hand, the parameters in this force field can be used for a wide class of structure, which leads to less precise results, *e.g.*, infrared spectra. Nevertheless, this force field was employed in previous papers[4,5] dealing with one ZnS–CTA nanoparticle and the results were in a good agreement with the experimental data. Therefore, this force field was used for the simulation of two ZnS–CTA particles. The geometry optimization was performed with all variable atomic positions and with the following convergence criteria: $E = 1\times10^{-4}$ kcal mol^{-1}*, force = 0.05 kcal mol^{-1} nm^{-1} and atomic displacement of 5×10^{-6} nm. The electrostatic and van der Waals energy were calculated by cubic spline with a cut-off distance of 1.55 nm. The charges of ZnS nanoparticles were calculated by the QEq method (charge equilibrium

* 1 kcal = 4.184 kJ

approach)[16] and the partial charges of water molecules and CTA cations were assigned by the Compass force field.[17]

After geometry optimization, the models with the lowest energy were chosen for quench dynamics. The quench molecular dynamics simulations were performed in an NVT statistical ensemble (constant number of particles, constant volume and constant temperature) at a temperature of 298 K. One step of the simulation was 0.5 fs and 500–1000 ps were performed. The time interval between two quenches was 50000 steps (25 ps) of the simulation. The atomic positions of the ZnS nanoparticles were fixed and the other atomic positions were variable during the simulations. After quench dynamics, the optimized models with minimum energy were selected and they were subsequently minimized with the requested convergence criteria mentioned above and with all atomic positions variable to obtain the final structure of the models.

RESULTS AND DISCUSSION

Models of ZnS nanoparticles without water

Although real ZnS nanoparticles were dispersed in water, mutual interactions of two ZnS–CTA nanoparticles without water were calculated for comparison and the results are summarized in Table I. This table shows the dependence of the total sublimation energy E_{total}, which is the sum of van der Waals E_{vdw} and electrostatic E_{elst} interaction energies between ZnS–CTA nanoparticles, on the number of CTA cations for all the tested models. The interactions were calculated as interactions between rigid bodies. A rigid body is defined as a part

TABLE I. Total sublimation energies for various types of models and CTA concentrations without water

No. of CTA cations	E_{total} / kcal mol^{-1}	E_{vdw} / kcal mol^{-1}	E_{elst} / kcal mol^{-1}
	Model 1		
30	–81	–8	–73
50	–59	–10	–49
70	–37	–13	–24
90	–27	–16	–11
	Model 2		
30	–96	–10	–86
50	–74	–11	–63
70	–37	–1	–36
90	–40	–15	–25
	Model 3		
30	–94	–8	–86
50	–70	–9	–61
70	–54	–11	–43
90	–41	–14	–27
	Model 4		
30	–99	–10	–89
50	–79	–10	–69
70	–58	–13	–45
90	–45	–14	–31

of a system where all the interactions (bonded and non-bonded) between atoms within this part are neglected. To investigate the stability and probability of the occurrence of various models, the total sublimation energy (Table I) was divided into several energy contributions: *i*) interactions between CTA cations and ZnS nanoparticles, *ii*) interactions between CTA cations and *iii*) interactions between ZnS nanoparticles.

The interactions between CTAs and ZnS nanoparticles were the main energy contribution to the E_{total} sublimation energy. The average CTA and ZnS interactions of all amounts of CTA for models 1 and 3 exhibited higher energy values (–64 kcal mol^{-1}) than for models 2 and 4 (–71 kcal mol^{-1}). This could be explained by the fact that in models 2 and 4, all the CTA cations interacted with the ZnS nanoparticle surface *via* attractive interactions while some of the CTA cations in models 1 and 3 interacted only with one another *via* repulsive interactions. Moreover, the CTA–ZnS interaction energies increased with increasing amounts of CTA from an average value of –86 kcal mol^{-1} for 30 CTA cations to –54 kcal mol^{-1} for 90 CTA cations. The increase in the CTA–ZnS interactions could be explained by changes in the arrangement of CTA on the ZnS nanoparticles in dependence on the amount of CTA.

The arrangement of CTA with respect to the ZnS nanoparticle can be characterized by a tilted angle. This is defined as the angle between the tangent plane of a ZnS nanoparticle at the point of the perpendicular projection of nitrogen or the last carbon atom of CTA to the ZnS surface and the CTA chain. In the case of the perpendicular orientation of CTA, the value of the tilted angle is of 90°, while in the case of the parallel arrangement, it is 0°. The tilted angle distribution is shown in Fig. 1 for model 4 and in Figs. S-1–S-3 of the Supplementary material to this paper. Another suitable characteristic of the CTA arrangement is the distribution of nitrogen with respect to the ZnS surface. This is characterized by the distances of the nitrogen of the CTA cations from the ZnS surface and can give us information about a width of the CTA bilayer structure. The distribution is shown in Fig. 2.

In case of 30 CTAs, 14–25 % of CTAs adopted a nearly parallel arrangement with respect to the ZnS surface and more than 60 % of CTAs exhibited an angle lower than 40° with an average of 28°. On the other hand, in case of 90 CTAs, a larger part of the ZnS surface was occupied by CTA cations that tended to adopt an orientation with a higher tilted angle. In this case, less than 10 % of CTAs on average adopted parallel orientation and more than 50 % of CTAs on average exhibited the tilted angle larger than 40°. If the distributions of CTA nitrogen atoms in Fig. 2 are compared, it can see that in case of 30 CTAs, the distance of nitrogen atoms of CTA oriented with their polar headgroups towards to the ZnS surface is about 0.3 nm with a relatively low deviation. In the case of 90 CTAs, the distance and its deviation is higher due to repulsive CTA–CTA inter-

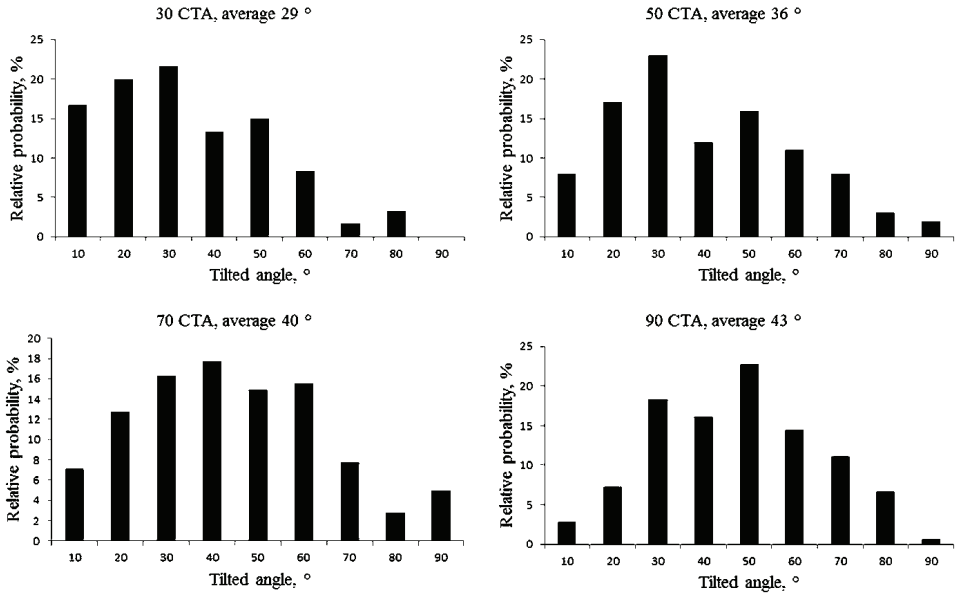

Fig. 1. Angle distribution of the CTAs in model 4 without water.

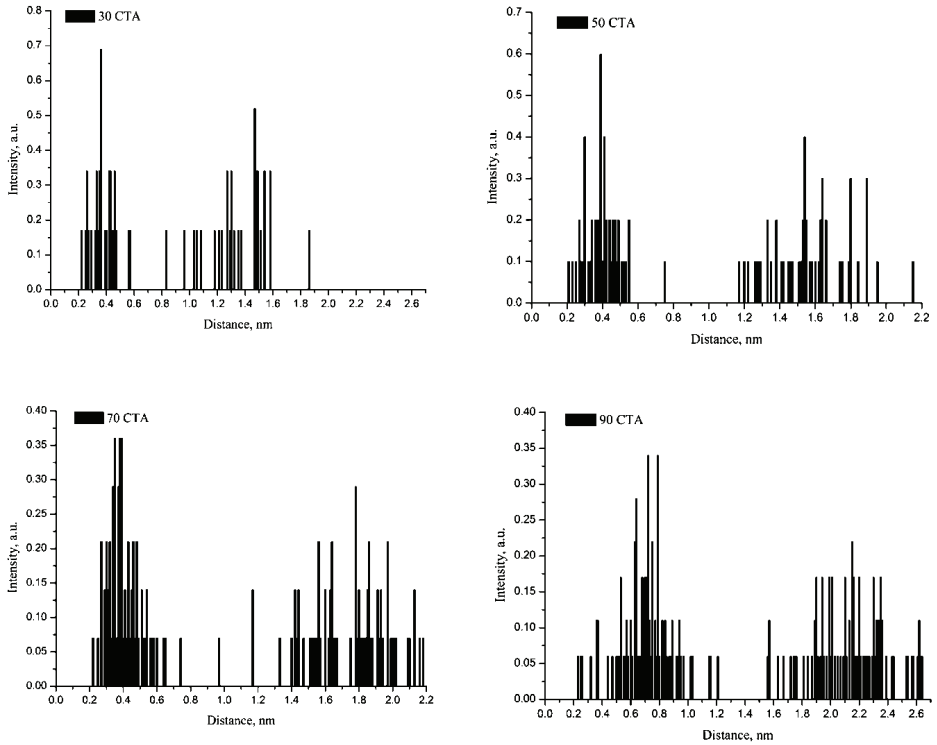

Fig. 2. Distribution of the CTA nitrogen atoms in model 4 without water.

actions leading to a partial expelling of CTA from the ZnS surface, which caused weaker CTA–ZnS interactions.

The mutual interactions between CTA cations depended on the amount of CTA. The van der Waals energy decreased as follows: –5 kcal mol^{-1} on average for 30 CTAs and –12 kcal mol^{-1} on average for 90 CTAs. The electrostatic interactions rapidly increasing amount of CTA from < 1 kcal mol^{-1} on average for 30 CTAs to 29 kcal mol^{-1} on average for 90 CTAs. The resulting value of mutual CTA interactions was negative in case of 30 CTAs. For 50 CTAs, models 1 and 2 exhibited repulsive CTA–CTA interactions (6 kcal mol^{-1} on average).

Models 3 and 4 exhibited attractive CTA–CTA interactions (–3 kcal mol^{-1} on average) due to the lower electrostatic interactions in comparison to the absolute value of the van der Waals energy. In case of higher amounts of CTA the interactions between CTAs were repulsive: 12 kcal mol^{-1} for 70 CTAs and 17 kcal mol^{-1} for 90 CTAs. Model 4 for 30 CTAs is shown in Fig. 3. Model 4 had the lowest total sublimation energy and, therefore, was the most probable.

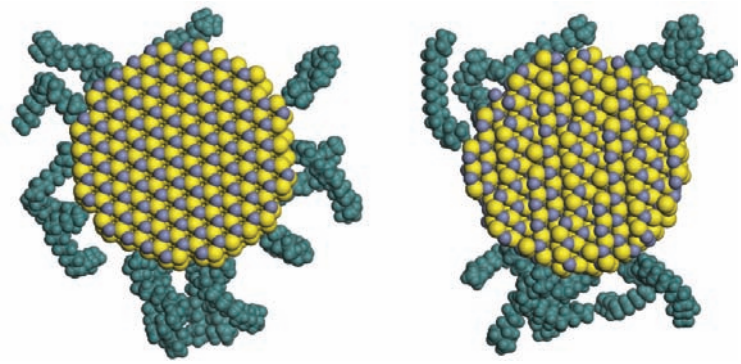

Fig. 3. Cross section of model 4 for 30 CTAs without water. Green chains represent CTA cations.

The interactions between ZnS nanoparticles represented the least energy contribution in the total sublimation energy, *i.e.*, 15 % of the maximum total sublimation energy for model 1. For example, the total sublimation energy in case of 90 CTAs was –2452 kcal mol^{-1} and the value of ZnS–ZnS interactions was –378 kcal mol^{-1}. The interactions between ZnS nanoparticles were calculated only for model 1. For the other models, they were neglected due to the large distance between the nanoparticles. The complete information on the mutual interactions in the systems can be found in Table S-I of the Supplementary material.

Models of ZnS nanoparticles in water environment

In the next modelling calculations, ZnS–CTA particles were simulated in water environment together with bromide anions to be similar to real laboratory

conditions. Total sublimation energies and their components E_{vdw} and E_{elst} were also calculated for different numbers of CTA cations related to each ZnS nanoparticle (30, 50, 70 and 90 CTAs). The non-bonded interactions E representing E_{elst}, E_{vdw} and their sum E_{total} were calculated as follows:

$$E = \frac{E_{(ZnS–CTA)+Br+H_2O} - E_{H_2O} - E_{(ZnS+H_2O)}}{n} \quad (1)$$

where $E_{(ZnS–CTA)+Br+H_2O}$ is the non-bonded interaction energy within all parts of the systems, E_{H_2O} represents the interaction energy within the bulk of the water surrounding the ZnS nanoparticles, $E_{(ZnS+H_2O)}$ represents the interaction between the ZnS nanoparticles and the surrounding water molecules and n represents the number of CTA cations related to each ZnS nanoparticle. The values of the interactions used in Eq. (1) can be found in Table S-II of the Supplementary material. As in the models without water, the total sublimation energies can be divided into these components: *i*) interactions between CTA cations and water molecules, *ii*) interactions between bromide anions and water molecules, *iii*) interactions between CTA cations and bromide anions and *iv*) interactions between ZnS nanoparticles and water molecules.

First, the interactions between different parts of the system were compared, *i.e.*, the interactions were calculated without mutual repulsive interactions between atoms or molecules in the same part of the system (Br–Br and CTA–CTA interactions). The most significant energy contributions were CTA–H_2O interactions (the interaction energy was calculated only between the bulk of CTA cations and the bulk of water molecules). The average value of these interactions was –440 kcal mol^{-1}. The CTA–Br interactions decreased linearly with increasing amount of CTA, *e.g.*, from –136 kcal mol^{-1} for 30 CTAs to –232 kcal mol^{-1} for 90 CTAs. The Br–H_2O interactions decreased linearly with decreasing amount of bromide, *e.g.*, from –352 kcal mol^{-1} for 30 CTAs to –330 kcal mol^{-1} for 90 CTAs. The interaction energy between one ZnS nanoparticle and water was –19400 kcal mol^{-1} on average. The absolute values of the interactions between CTA cations and ZnS nanoparticles were very low, *i.e.*, 32 kcal mol^{-1} on average. In comparison with the models optimized without water, the absolute values of the CTA–ZnS interactions was about 50 % lower due to strong interactions with water and bromide anions causing a change in the geometry and positions of CTAs with respect to the ZnS nanoparticles. ZnS–ZnS interactions were similar to those calculated for the systems without water and were hundreds of kcal mol^{-1} at the maximum. The absolute value of these interactions was at least two times lower in comparison with total CTA–ZnS interactions (see Table S-I of the Supplementary material). The indicates the ability of CTAs to separate the ZnS–CTA nanoparticles.

Secondly, the average repulsive CTA–CTA and Br–Br interactions increased with increasing amount of CTA cations: 55 kcal mol^{-1} for 30 CTAs and 109 kcal mol^{-1} for 90 CTAs. Moreover, the repulsive CTA–CTA interactions in the models with water significantly differed from those without water. As an illustration, the average interaction energy for the systems without water was 7 kcal mol^{-1} and for the systems in a water environment, it was 33 kcal mol^{-1}. This change was ascribed to CTA–H_2O interactions and CTA–Br interactions, the absolute values of which were much higher in comparison to the CTA–CTA interactions without water. The CTA–H_2O and CTA–Br interactions caused geometry changes of CTA leading to the increase in the CTA–CTA interactions.

The total sublimation energies related to the number of CTAs corresponding to each ZnS nanoparticle are presented in Table II, from which it can see that the total sublimation energies were nearly independent of the number of CTAs. Therefore, CTA cations exhibited a similar probability of being located on the ZnS surface. Due to the lowest interaction energies between different parts in model 1, this model had the lowest total sublimation energy in comparison with the others. Therefore, model 1 was the most probable one and it is presented in Fig. 4 together with models 2, 3 and 4.

TABLE II. Total sublimation energies for the various types of models in a water environment

No. of CTA cations	E_{total} / kcal mol^{-1}	E_{vdw} / kcal mol^{-1}	E_{elst} / kcal mol^{-1}
	Model 1		
30	–973	–15	–958
50	–996	–3	–993
70	–957	–7	–950
90	–956	–13	–943
	Model 2		
30	–845	–20	–825
50	–895	–3	–892
70	–864	–1	–863
90	–906	7	–913
	Model 3		
30	–935	–4	–931
50	–916	–11	–905
70	–892	–12	–880
90	–861	–22	–839
	Model 4		
30	–894	–5	–889
50	–845	–10	–835
70	–872	–10	–862
90	–931	–17	–914

The coverage of the surface depended on the CTA concentration and it could be estimated by calculating the surface area of the ZnS nanoparticle occupied by

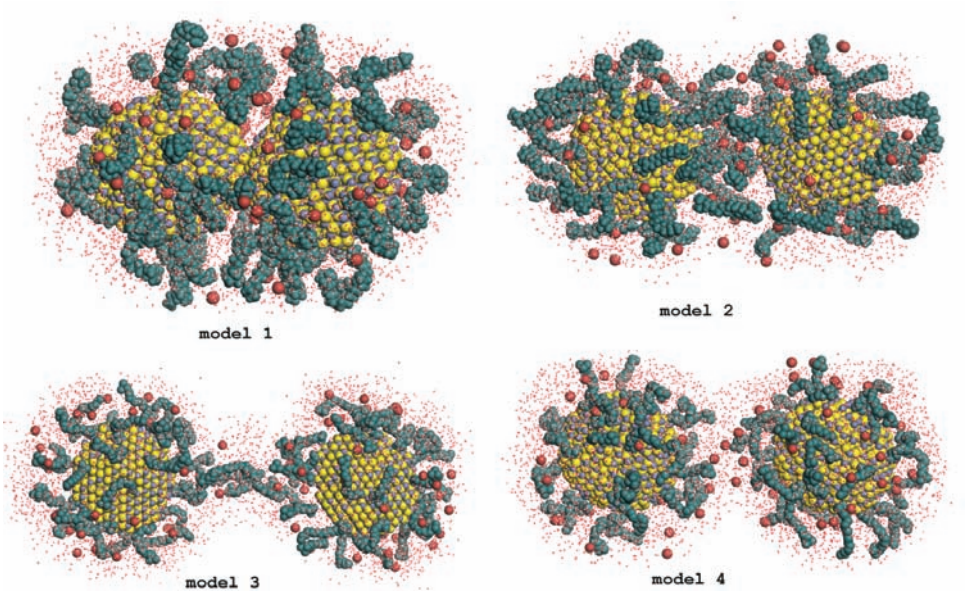

Fig. 4. ZnS nanoparticles of models 1–4 with water surrounded by 30 CTA cations and compensating bromide anions. The green chains represent CTA cations and the brown balls represent bromide anions.

headgroups and by the ends of CTA chains using van der Waals radii. One polar headgroup occupies 0.27 nm^2 and 0.04 nm^2 is occupied by one end of CTA. The coverage of the ZnS nanoparticle surface with a radius of 2 nm is of 9, 15, 22 and 28 % in case of 30, 50, 70 and 90 CTAs, respectively. If the fact that the orientation of CTA is tilted with respect to the ZnS nanoparticle is taken into account, a higher coverage of the surface could be expected. Nevertheless, the ZnS nanoparticles are not "hermetically" isolated by CTA from the surrounding water environment (see Fig. S-4 in the Supplementary material) and the CTA cations tend to form sparse covers around the nanoparticles. This indicates that these nanoparticles should grow in time, which was verified by a study of the growth kinetics. A final radius of 2.46 nm after 24 h was determined and no coagulation was observed. In addition, the recently evidenced photocatalytic activity of ZnS–CTA nanoparticles in the decomposition of phenol[18] confirms that various chemical compounds can move to the surface of such nanoparticles to react with photogenerated hydroxyl radicals.

As for the models without water, the CTA arrangement on the ZnS surface can be described by the angle distribution, as shown in Fig. 5 for model 1. The angle distributions for models 2, 3 and 4 are given in the Supplementary material (Figs. S-5–S-7). In case of the lower concentrations of CTA, the average angle values in the models with water were about 10 higher than those without water,

while at higher CTA concentrations, the average angle values were comparable to those without water. The average angle values ranged in the interval of 35–49°. In case of model 1, the angle values range in the interval of 40–45°.

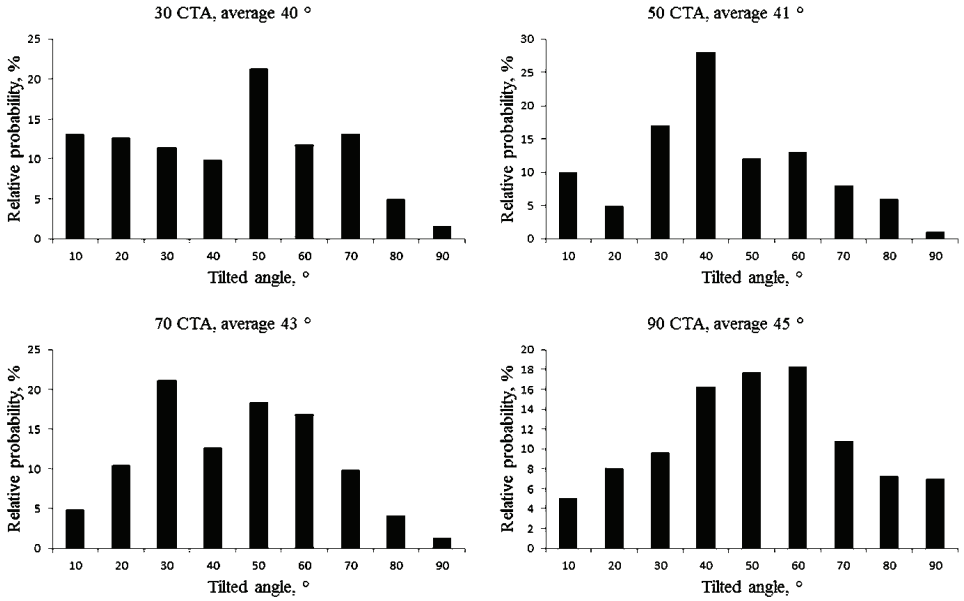

Fig. 5. Angle distribution of CTAs in model 1 with water.

The TEM micrograph presented in Fig. 6 shows the agglomeration of ZnS–CTA nanoparticles into flocs (flakes of precipitate that come out of solution during flocculation) of different sizes. The size histogram is included in Fig. 6 as

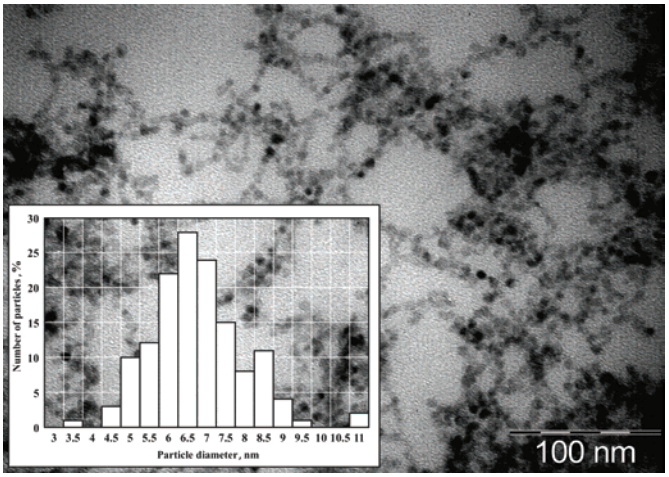

Fig. 6. TEM micrograph of ZnS–CTA dispersion.

well. The mean radius was determined to be about 3.25 nm. This value covers the radii of ZnS nanoparticles and the thickness of the CTA cover around it. The radii of single ZnS nanoparticles increased from 2.07 to 2.39 nm within a time interval of 0.05–3 h at room temperature. At longer times up to 24 h the radii increased up to 2.46 nm. These radii were calculated based on band-gap energies estimated from UV spectra of ZnS colloid dispersions as described, *e.g.*, in our earlier papers.[4,6] The TEM micrograph was obtained during the early stage of the ZnS nanoparticles growth, that is, at 3 min when the calculated ZnS nanoparticles radius was about 2 nm. Sizes of these flocs in a range of 9–122 nm with a modus of 16 nm were found by the dynamic light scattering method.[5]

The results of TEM compared with models 1–4 showed that ZnS nanoparticles tended to adopt the mutual arrangement close to that presented in model 1. The flocs with the size of 9 nm likely correspond to the case when they are consisted of two ZnS nanoparticles touching each other as it is shown in Figure 4. Total sublimation energy values of model 1 were about 9 % lower on average in comparison with other types of models. It indicates that one can expect the occurrence of these models with lower probability. Figure 6 shows that some ZnS nanoparticles are isolated by CTA or joined together by CTA chains (see Fig. 4). The histogram of diameters of nanoparticles (Fig. 6) represents the sum of ZnS nanoparticle diameter and the thickness of the bilayer that can be characterized by distances of outer nitrogen atoms of CTA and ZnS nanoparticle surface. All types of models exhibited similar distributions of nitrogen atoms and they are demonstrated for model 1. The results of modelling showed a weak dependence of total sublimation energy on the number of CTAs surrounding ZnS nanoparticles and we can suppose that CTA of all studied concentrations have similar probability to be located on ZnS nanoparticle surface.

Figure 7 shows a combination of distributions of nitrogen atoms for all studied concentrations in model 1 fitted by a polynomial of 9^{th} order to obtain the best fit. We can observe three maxima. The first maximum at the distance of 0.3 nm corresponds to the nitrogen atoms of CTAs with their polar headgroups oriented towards the surface of the ZnS nanoparticle. The distance between the nitrogen atom and the hydrogen atom of the polar headgroup is 0.15 nm and, if one take into account the van der Waals radius of hydrogen atom, *i.e.*, 0.06 nm, it could be stated that the polar headgroups nearly touch the surface of the ZnS nanoparticle. The other maxima at 1.5 and about 2.2 nm represent the positions of outer CTA nitrogen atoms. If a ZnS nanoparticle radius of 2 nm is considered and the length of CTA cation represented by the maximum at 1.5 nm, a total diameter of 7 nm is obtained, which is close to the maximum at 6.5 nm obtained from TEM measurements. The maximum at the distance of 2.2 nm (8.4 nm in diameter) is in agreement with the measured distance of 8.5 nm. It shows good agreement between the experimental and calculated results.

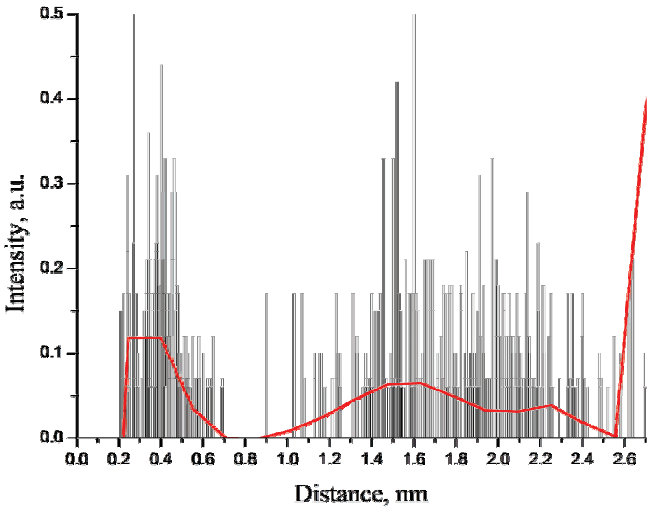

Fig. 7. Distribution of CTA nitrogen atoms in model 1 with water.

CONCLUSION

ZnS nanoparticles stabilized by CTAB were modelled in the Materials Studio environment. The nanoparticle geometry was optimised in the Universal force field and charges of ZnS nanoparticles were calculated by the QEq method. The partial charges of water molecules and CTA cations were assigned by the Compass force field. ZnS nanoparticles with radii of 2.0 nm surrounded with various amounts of CTA cations were modelled without water and in a water environment. Four models with different distances between the ZnS nanoparticles and the arrangement of the CTA cations were built and characterized by calculated sublimation energies.

Based on the molecular modelling results without water, it could be concluded that the most favourable model consisted of two ZnS nanoparticles at a distance of 8–9 nm separated without immersing CTAs. In a water environment, the energies of the ZnS–CTA interactions were significantly higher than in vacuum. The most favourable model was composed of two ZnS nanoparticles that nearly touched each other. The CTA cations acted as a sparse cover around the ZnS nanoparticles and exhibited a tilted orientation with respect to ZnS nanoparticle surface with tilted angle values ranging from 26 to 43° in the models without water and from 35 to 49° in the models with water. Size histogram of ZnS–CTA particles measured by TEM was compared with the models using the distribution of outer nitrogen atoms and good agreement between the experiment and calculated results was obtained.

SUPPLEMENTARY MATERIAL

Figures S-1–S-7 and Tables S-I and S-II are available electronically from http://www.shd.org.rs/JSCS/ or from the corresponding author on request.

Acknowledgements. This work was supported by the Czech Science Foundation (P107/11/1918), by the Ministry of Education, Youth and Sports of the Czech Republic in the "National Feasibility Program I" (project LO1208 "TEWEP"), by the Regional Materials Science and Technology Centre (CZ.1.05/2.1.00/01.0040) in Ostrava and by VŠB-Technical University of Ostrava (SP 2014/55), Czech Republic.

И З В О Д

МОЛЕКУЛСКО МОДЕЛОВАЊЕ ПОЛОЖАЈА ЦИНК-СУЛФИДНИХ НАНОЧЕСТИЦА СТАБИЛИСАНИХ ЦЕТИЛТРИМЕТИЛАМОНИЈУМ-БРОМИДОМ

PETR KOVÁŘ[1], PETR PRAUS[2,3], MIROSLAV POSPÍŠIL[1] и RICHARD DVORSKÝ[4]

[1]Charles University in Prague, Faculty of Mathematics and Physics, Ke Karlovu 3, 12116 Prague 2, Czech Republic, [2]Regional Materials Science and Technology Centre, VŠB-Technical University of Ostrava, 17. Listopadu 15, 708 33 Ostrava-Poruba, Czech Republic, [3]Department of Chemistry, VŠB-Technical University of Ostrava, 17. Listopadu 15, 708 33 Ostrava-Poruba, Czech Republic и [4]Institute of Physics, VŠB-Technical University of Ostrava, 17. Listopadu 15, 708 33 Ostrava-Poruba, Czech Republic

Положај ZnS наночестица стабилисаних цетилтриметиламонијум-бромидом (CTAB) моделована је у *Materials Studio* програмском окружењу. Постављена су четири модела са различитим растојањима између ZnS наночестица и различитом количином CTAB у неводеној и воденој средини и окарактерисана помоћу израчунатих енергија сублимације. Резултати у неводеној средини без CTAB су показали да се најповољнији модел састоји од две ZnS наночестице на растојању од 8 до 9 nm. С друге стране, у воденој средини најповољнији модел предвиђа да се наночестице готово додирују. CTAB показује тенденцију смештања са ретким паковањем на површину наночестица. Расподела ZnS–CTA честица по величини која је добијена трансмисионом електронском микроскопијом добро се слагала са резултатима добијеним молекулском моделовањем.

(Примљено 15. новембра 2013, ревидирано 28. фебруара, прихваћено 10. маја 2014)

REFERENCES

1. D. Schroder, *Semiconductor Material and Device Characterization*, Wiley, New York, 2006
2. Z. Wang, N. Herron, *J. Phys. Chem.* **95** (1991) 525
3. L. E. Brus, *J. Chem. Phys.* **80** (1984) 4403
4. P. Praus, R. Dvorský, P. Horínková, M. Pospíšil, P. Kovář, *J. Colloid Interf. Sci.* **377** (2012) 58
5. P. Praus, R. Dvorský, P. Kovář, J. Trojková, *Acta Chim. Slov.* **59** (2012) 784
6. O. Kozák, P. Praus, K. Kočí, M. Klementová, *J. Colloid Interf. Sci.* **352** (2010) 244
7. S. Hamad, S. M. Woodley, C. R. Catlow, *Mol. Simul.* **35** (2009) 1015
8. H. Zhang, B. Chen, Y. Ren, G. A. Waychuans, J. F. Banfield, *Phys. Rev., B* **81** (2010) 125444.
9. F. Huang, B. Gilbert, H. Zhang, J. F. Banfield, *Phys. Rev. Lett.* **92** (2004) 155501-1
10. B. Gilbert, H. Zhang, F. Huang, J. F. Banfield, *J. Chem. Phys.* **120** (2004**)** 11785
11. C. J. Yang, X. Chen, Z. M. Sui, L. Y. Wang, *Colloids Surfaces, A* **274** (2006) 219
12. J. Yue, X. C. Jiang, Q. H. Zeng, A. B. Yu, *Solid State Sci.* **123** (2011) 1152

13. J. W. Anthony, R. A. Bideaux, K. W. Bladh, M. C. Nichols, *Handbook of Mineralogy*. Mineralogical Society of America, Chantilly, USA, http://www.handbookofmineralogy.org (accessed on 25th October 2013)
14. *Materials Studio Modeling Environment*, Release 4.3 Documentation, Accelrys Software Inc., San Diego, CA, 2003
15. A. K. Rappe, C. J. Casewit, K. S. Colwell, W. A. Goddard, W. M. Skiff, *J. Am. Chem. Soc*. **114** (1992) 10024
16. A. K. Rappe, W. A. Goddard, *J. Phys. Chem.* **95** (1991) 3358
17. H. Sun, D. Rigby, *Spectrochim. Acta, A* **53** (1997) 1301
18. P. Praus, J. Matys, O. Kozák, *J. Braz. Chem. Soc.* **23** (2012) 1900.

Journal of the Serbian Chemical Society
JSCS@tmf.bg.ac.rs • www.shd.org.rs/JSCS
J. Serb. Chem. Soc. 79 (12) S180–S185 (2014) *Supplementary material*

SUPPLEMENTARY MATERIAL TO

Molecular modelling of zinc sulphide nanoparticles stabilized by cetyltrimethylammonium bromide

PETR KOVÁŘ[1], PETR PRAUS[2,3*], MIROSLAV POSPÍŠIL[1] and RICHARD DVORSKÝ[4]

[1]Charles University in Prague, Faculty of Mathematics and Physics, Ke Karlovu 3, 12116 Prague 2, Czech Republic, [2]Regional Materials Science and Technology Centre, VŠB-Technical University of Ostrava, 17. Listopadu 15, 708 33 Ostrava-Poruba, Czech Republic, [3]Department of Chemistry, VŠB-Technical University of Ostrava, 17. Listopadu 15, 708 33 Ostrava-Poruba, Czech Republic and [4]Institute of Physics, VŠB-Technical University of Ostrava, 17. Listopadu 15, 708 33 Ostrava-Poruba, Czech Republic

J. Serb. Chem. Soc. 79 (12) (2014) 1545–1559

ADDITIONAL FIGURES AND TABLES

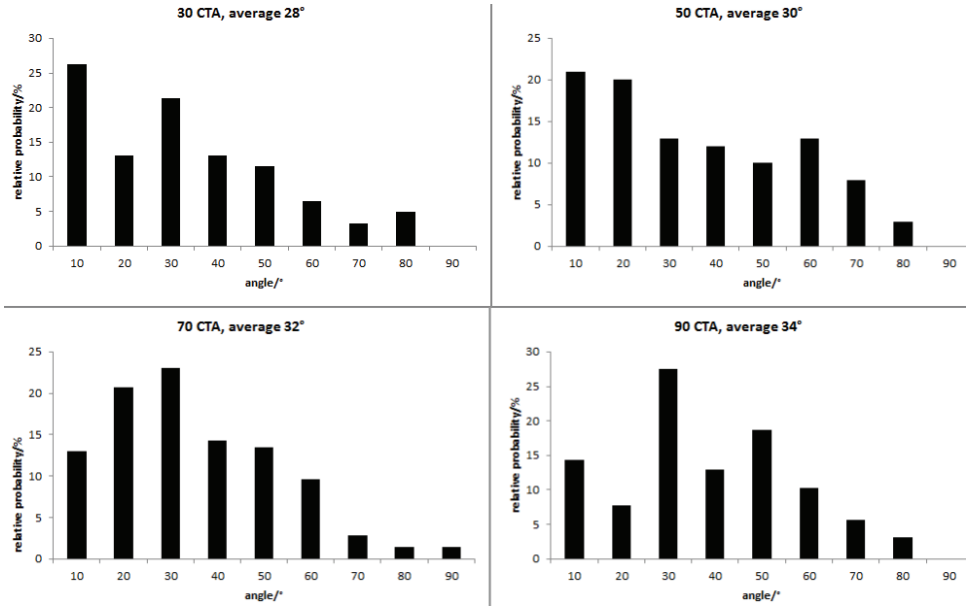

Fig. S-1. Angle distribution of the CTAs in model 1 without water.

* Corresponding author. E-mail: petr.praus@vsb.cz

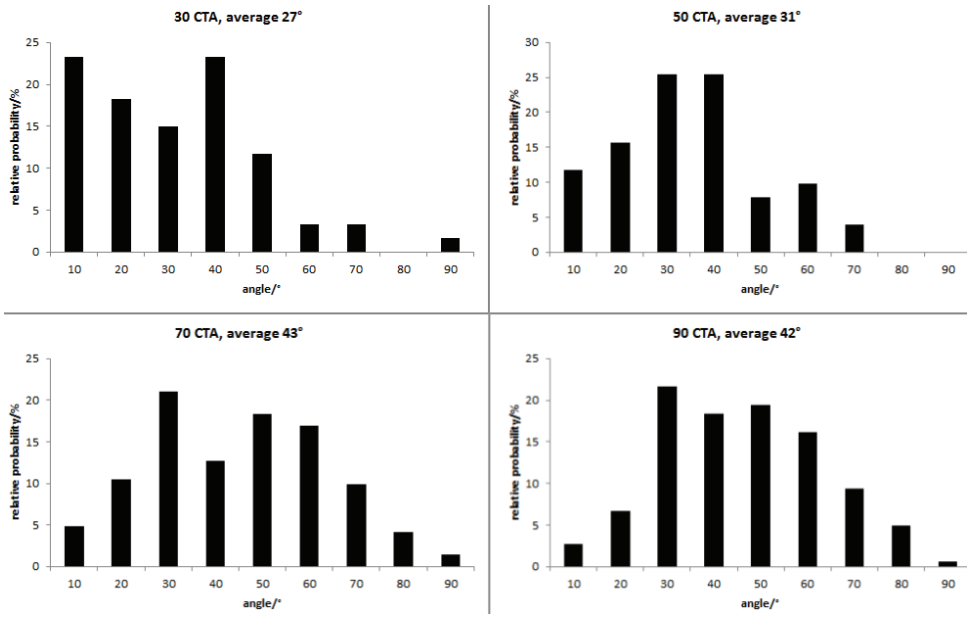

Fig. S-2. Angle distribution of CTAs in model 2 without water.

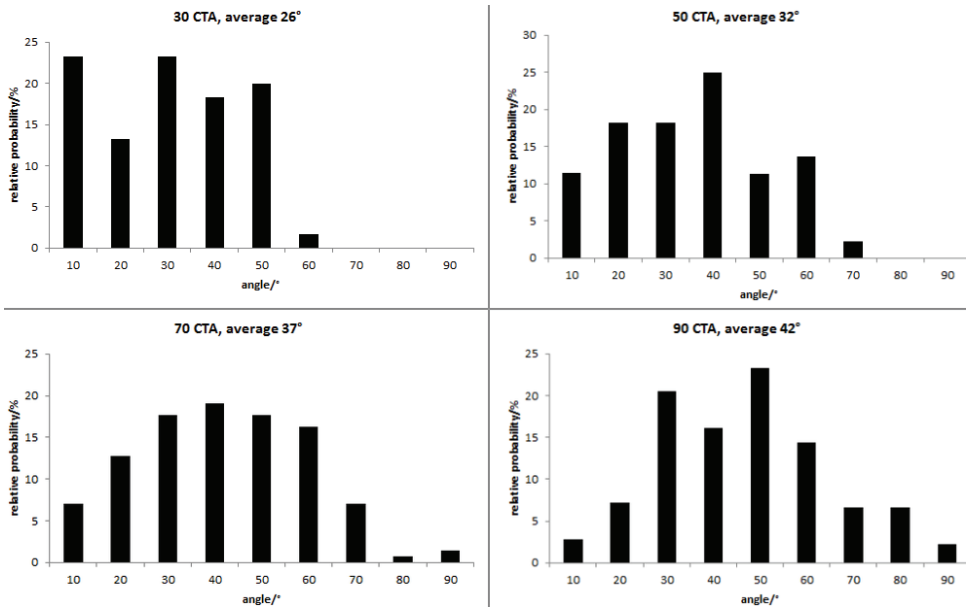

Fig. S-3. Angle distribution of CTAs in model 3 without water.

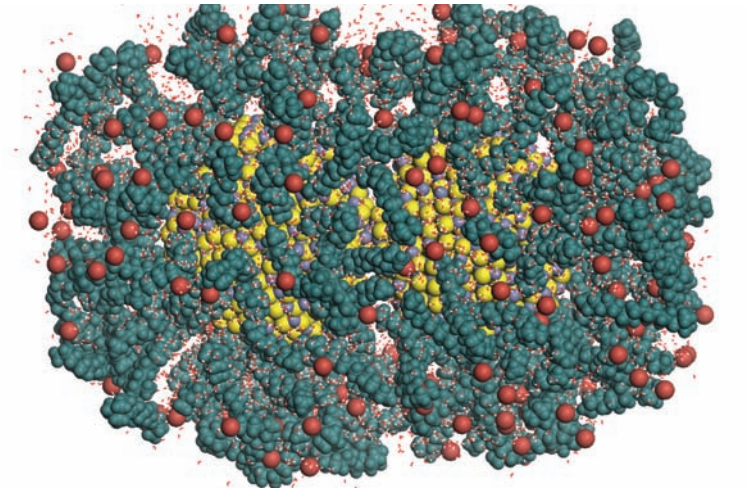

Fig. S-4. A ZnS nanoparticle covered with 90 CTAs, simulated according to Model 1. The green chains represent CTA cations and the brown balls represent bromide anions.

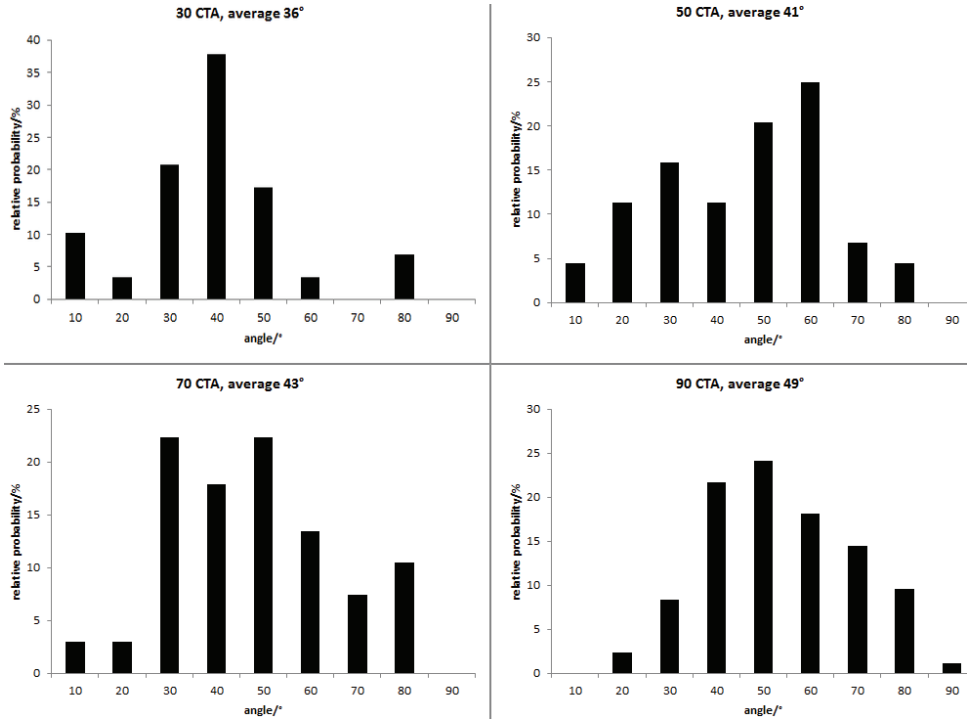

Fig. S-5. Angle distribution of the CTAs in model 2 with water.

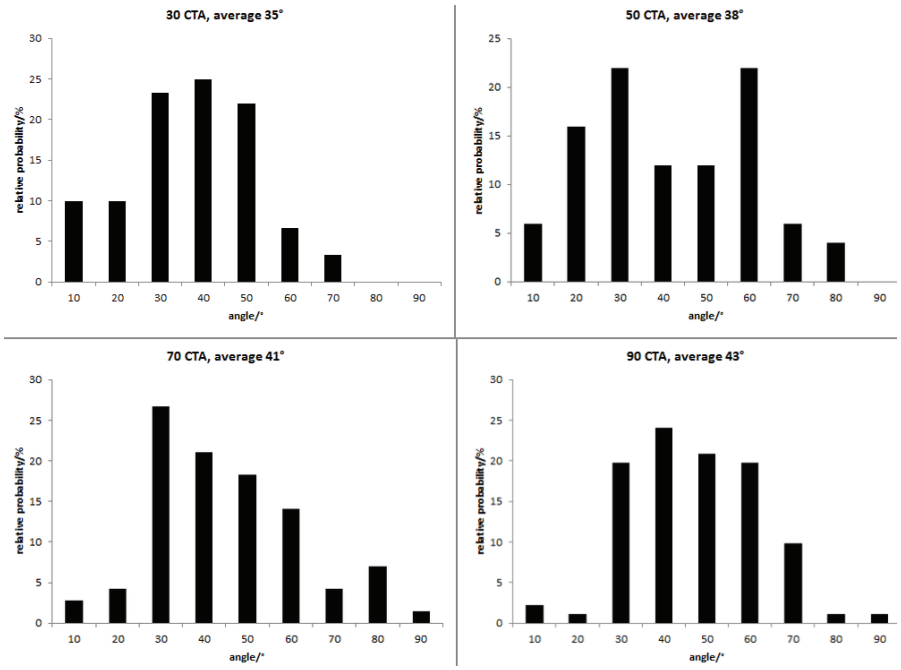

Fig. S-6. Angle distribution of the CTAs in model 3 with water.

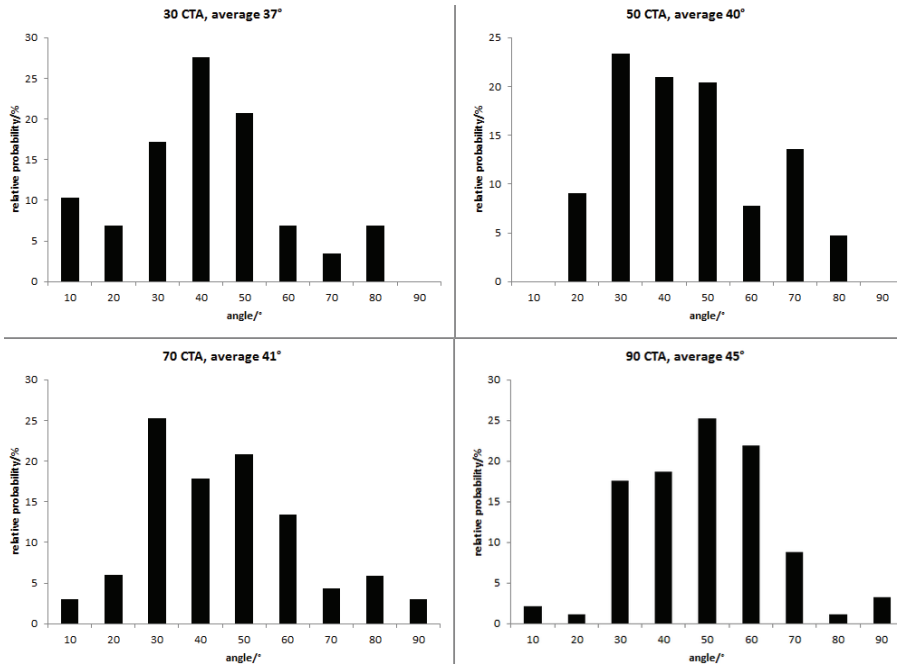

Fig. S-7. Angle distribution of the CTAs in model 4 with water.

TABLE S-1. Nonbonded interactions and their components for the models without water

Model type	CTA amount	Interaction	E_{total} / kcal* mol^{-1}	E_{vdw} / kcal mol^{-1}	E_{elst} / kcal mol^{-1}
1	30	Total	–2431	–252	–2179
		CTA–CTA	–99	–140	41
		ZnS–CTA	–2116	–106	–2010
		ZnS–ZnS	–215	–5	–210
2		Total	–2894	–308	–2586
		CTA–CTA	–147	–148	1
		ZnS–CTA	–2747	–159	–2588
3		Total	–2820	–248	–2572
		CTA–CTA	–97	–107	10
		ZnS–CTA	–2723	–141	–2582
4		Total	–2992	–284	–2708
		CTA–CTA	–231	–171	–60
		ZnS–CTA	–2761	–114	–2647
1	50	Total	–2935	–523	–2412
		CTA–CTA	266	–365	631
		ZnS–CTA	–3107	–148	–2959
		ZnS–ZnS	–94	–9	–85
2		Total	–3683	–556	–3127
		CTA–CTA	308	–334	642
		ZnS–CTA	–3991	–222	–3769
3		Total	–3479	–426	–3053
		CTA–CTA	–81	–257	176
		ZnS–CTA	–3398	–169	–3229
4		Total	–3930	–473	–3457
		CTA–CTA	–177	–247	70
		ZnS–CTA	–3753	–225	–3528
1	70	Total	–2597	–909	–1688
		CTA–CTA	1336	–753	2089
		ZnS–CTA	–3802	–146	–3656
		ZnS–ZnS	–131	–9	–122
2		Total	–2601	–54	–2547
		CTA–CTA	1205	–740	1945
		ZnS–CTA	–3806	686	–4492
3		Total	–3803	–790	–3013
		CTA–CTA	535	–599	1134
		ZnS–CTA	–4338	–190	–4148
4		total	–4026	–902	–3124
		CTA–CTA	393	–705	1098
		ZnS–CTA	–4419	–197	–4222
1	90	total	–2452	–1401	–1051
		CTA–CTA	2168	–1196	3364
		ZnS–CTA	–4242	–198	–4044
		ZnS–ZnS	–378	–7	–371

* 1 kcal = 4.184 kJ

TABLE S-1. Continued

Model type	CTA amount	Interaction	E_{total} / kcal mol^{-1}	E_{vdw} / kcal mol^{-1}	E_{elst} / kcal mol^{-1}
2		total	–3562	–1311	–2251
		CTA–CTA	1719	–1074	2793
		ZnS–CTA	–5281	–237	–5044
3		total	–3716	–1216	–2500
		CTA–CTA	1189	–967	2156
		ZnS–CTA	–4905	–248	–4657
4		total	–4022	–1249	–2773
		CTA–CTA	1116	–1011	2127
		ZnS–CTA	–5138	–239	–4899

TABLE S-II. Nonbonded interactions obtained by the simulations for the models with water

Number of CTA	$E_{(ZnS-CTA)+Br+H_2O}$ / kcal mol^{-1}	E_{H_2O} / kcal mol^{-1}	E_{ZnS+H_2O} / kcal mol^{-1}
	Model 1		
30	–488140	–439046	–19900
50	–503913	–433381	–20729
70	–513910	–427110	–19813
90	–529874	–422786	–21034
	Model 2		
30	–483663	–438661	–19649
50	–470433	–406874	–18787
70	–487375	–409768	–17120
90	–521702	–420507	–19629
	Model 3		
30	–454654	–407826	–18770
50	–468993	–403851	–19358
70	–479255	–396095	–20699
90	–490624	–393556	–19594
	Model 4		
30	–459347	–412522	–20010
50	–444415	–383126	–19019
70	–467141	–388087	–18024
90	–500200	–397597	–18827

Journal of the Serbian Chemical Society
JSCS-info@shd.org.rs • www.shd.org.rs/JSCS
J. Serb. Chem. Soc. *79* (12) 1561–1570 (2014)
JSCS–4688
UDC 54.001.5+37:303.71:001.818
Extended abstract

EXTENDED ABSTRACT

How to present and publish research results≠

ALEKSANDAR DEKANSKI*#

ICTM – Department of Electrochemistry, University of Belgrade
Njegoševa 12, Belgrade, Serbia

(Received 10 June, accepted 25 June 2014)

Abstract: The end of each research is the presentation of its results to the public, especially to those who are engaged in similar research. This is particularly true for scientific research. A scientific paper is a written report that contains a presentation of the results of original scientific research. Its format is defined by centuries-old tradition of writing, the editorial practices of the publishers, scientific ethics, accepted standards and requirements of modern printing and publishing. Unfortunately, the experience of publishers and editors of scientific books and journals show that a large number of submitted contributions do not meet the minimum requirements to be even considered for publication. This article indicates the most important principles that one should bear in mind during the creation of a full text paper or presentation of scientific results.

Keywords: scientific paper; instructions for authors; creating tables; creating illustrations; article submission.

INTRODUCTION

It is noticeable that the real explosion of scientific research worldwide and the vast number of papers submitted each year flood the publishers with poorly written and poorly prepared articles. It is obvious that many authors, especially younger ones, have not acquired knowledge about how to write and to prepare technically a manuscript. This is confirmed by the increasing number of articles and texts which are devoted to this problem.[1–8] Before the decision to publish the results of a scientific research is made, two things must be kept in mind: first, there must be a clear and logical message to the readers, and second, the manuscript must be prepared in the required form. The first is, of course, much

* E-mail: dekanski@ihtm.bg.ac.rs
# Serbian Chemical Society member.
doi: 10.2298/JSC140610066D
≠ Presented as an Invited Lecture on the 2nd Conference of the Young Chemists of Serbia, Niš, June 7, 2014.

more important. No matter how carefully and well results are processed, if there is nothing important and significant to say, the work may be rejected. So, before writing or preparing a presentation, the results should be discussed with others dealing in the same or similar area of research, either in ones immediate environment or beyond.

Creation of scientific manuscripts

Any scientific paper, as a rule, should contain the following: title, abstract, introduction, experimental part (materials and methods), results (and) discussion and conclusions. Some journals do not require the existence of all these parts, or require some other with a similar name, but when creating manuscript, it is advisable to adhere to this structure. Each of these parts has its own characteristics and each of them will be discussed below. Before that, a few general remarks:

Firstly, the Instructions for authors and Artwork instructions (instructions for creating illustrations), must always be read and then the writer should proceed in accordance with these instructions.

It is recommended that a paper undergo editing before submission, either by someone who is conversant in the language in which the paper is written, or by a professional editor, especially if the writer does not know the language very well. Nevertheless, it is advisable that the manuscript be read by someone who is able to check the language. Of course, the final version of the manuscript should "pass" through the Spelling checker.

It is best to avoid jargon terms and acronyms (if it is necessary to use them, with the first mention in the text they must to be precisely defined, no matter how well-known they are)

Paying attention to the style of writing is strongly advised, some journals require writing in active (we are investigating...) not in passive (the investigation was carried out...).

Title

Title should be as short as possible and without unnecessary words such as study, research, analysis and so on. Indexing and database searches use words from the title and thus, the more accurate the title, the more successful is a search. If the article subject is a concrete material, chemical, species, area, region,..., it is beneficial to have their names appear in the title.

Keywords

Nearly always, the keywords in papers include parts of the title, which is completely wrong. Keywords are entered into the system for indexing (Indexing and abstracting services), as well as the title, so keywords should include some others words that will best indicate the content of the paper. This increases the likelihood that the paper reaches the targeted readers.

Abstract

Abstract is a concise and comprehensive view of the whole paper. When writing the author should be guided by the aim: title and abstract must clearly describe the contents of the whole paper, it could be published independently of the paper (as, for example, in Chemical Abstracts or Current Contents). The abstract should not repeat the information clear from the title; any literature citations, tables, illustrations, acronyms, descriptions of methods or experimental procedures should be omitted. Abstracts should simply introduce the subject and the aims of the research, as well as the conclusions. Journals often limit the number of words in the abstract, but if such limit is 200 words, and all matters may be indicated by 100 words, there is no need to burden the abstract. The reader is most likely based on reading the abstract to decide whether to read the whole article or not!

Introduction

In general, the introduction has a dual role: to introduce the reader to a review the literature related to the subject of the research and to present clearly the reasons and aims of the research presented in the paper.

Very often, the review of the literature is reduced to arid listing of relevant papers, without mentioning the main findings presented in them. Bearing in mind that this is the place where the reader first meets the essence of the research, the introduction should be easy to read, and the sentence should not be interrupted by citing the names of the authors and redundant phrases. It is best to cite the literature at the end of a sentence or phrase, whether by the names of the authors or a number from the list of references. The introduction must clearly show the need, the reason and the purpose of the research. The reader must have a clear idea of what kind and how significant are the contributions of the presented results.

Experimental (materials and methods)

The aim of this part of the paper is to show all the procedures and describe all materials used in the research, in a way that the reader is able to repeat them in full. The scientific method of working means that the results are reproducible, so the reader has to get identical results if the details presented in this section are followed.

The employed equipment must be described in detail, including the model and the name of the manufacturer. The material should also be described in detail. For example, if the quality of a used chemical is affected by its origin, it is necessary to specify the name of the manufacturer. Modification or construction of equipment must be described in detail, as well as the methods of preparation of reagents or chemicals and methods used (unless it involves a well-known standard procedure, when it is sufficient to specify the relevant literature).

Whenever possible, experiments and measurements should be listed in chronological order, in order to avoid confusion of the readers. The best way to check the clarity and precision is to ask a person who is engaged in a similar area of research but had not participated in the study to read this section. When asked if they would be able to repeat the measurements based on what was written, the answer must be affirmative.

Results (and) discussion

Results and discussion can be presented in one or in two separate chapters. Some journals insist on either of the options, but the choice is usually left to the authors. The decision depends on personal preferences, but also on the content of the presented. Sometimes one way is more appropriate, sometimes the other way. In any case, it is desirable to follow some recommendations:

This section presents the obtained research results; figures and tables are the basis of this part of the manuscript. Data should be presented very concisely, stating the basic description of the most important trends and results. Since these results mean new information, *i.e*., the contribution of the paper to the world, it is important to present them simply and clearly. In order to convey as much information to the readers, authors often burden this chapter with unnecessary details and lots of irrelevant information. Identical or similar information, which lead to the same conclusion, should not be displayed in both tables and figures; one or the other is enough. However, the presentation of the results should not be too concise; the reader cannot be expected to be able to draw conclusions from the text or to identify trends without your help. Hence, the text, images and tables have to be combined to highlight the most important findings and the most important data. When creating tables and figures, it is recommended to follow the Instructions for authors or Artwork instructions of the chosen journal. Otherwise, there is a possibility that the manuscript will be rejected for technical reasons, regardless of the value of the content.

The text should be easy to read, arid enumeration of facts and data makes the text incomprehensible and repugnant. Established and cumbersome phrases such as “Figure 1 clearly shows that the yield increases with reaction temperature” is better replaced with the sentence: “A greater yield was achieved with increasing reaction temperature (Fig. 1).”

Discussions need to show which general principles were established or confirmed by the research, which general conclusions could be drawn from it, and how findings have come to agree with expectations and the findings of other authors. Finally, the discussion should show the practical and theoretical contributions of the presented information.

It is crucial that the discussion directly refers to the evidence presented in the results. A clear reference to the results should be the basis for the discussion.

Conclusions should not go beyond that shown by the results. It is acceptable to make assumptions concerning the significance of the results on a global scale, but not to be the basis of this part of the manuscript. The discussion must be in accordance with the aims and objectives of the research set out in the introduction and the significance of the results should be clearly explained. After reading this chapter, the reader must not think, "Well, and what then."

Conclusions

It is not necessary that the conclusions exist as a separate chapter; it can be a logical completion of the discussions. Nevertheless, it should summarize the most important inferences set forth in the discussion and briefly explain the importance of the research. What and how it was investigated should be clear from the conclusions, together with the Abstract, as well as what new knowledge was revealed.

Nomenclature, physical quantities, units and measures

The chemical nomenclature recommended by the IUPAC (International Union of Pure and Applied Chemistry) must be respected.[9–14]

Units of physical quantities must be in accordance with the International System of Units (SI). The official site of the International Bureau of Weights and Measures (Bureau International des Poids et Mesures), which is responsible for the system of units, is the best place for the elimination of all concerns regarding the choice of units.[15]

In accordance with the recommendations of IUPAC and SI, the appointment of physical quantities and their units can be twofold:

The designation of physical quantities must be in italic throughout the text (including figures, tables and equations), whereas the units and indexes (except for indexes having the meaning of physical quantities) are in upright letters. A slash should be used to separate the designation of a physical quantity from the unit, for example: p / kPa, t / °C, T / K, τ / h. When it comes to complex units, and contain the fractional line, this unit must be placed in brackets, for example, units of concentration can be written as: mg dm^{-3} or as (mg/dm^3).

If the full name of a physical quantity is unavoidable, it should be given in upright letters and separated from the unit by a comma (example: Pressure, kPa; Temperature, K; Current density, mA cm^{-1}…).

Creating tables

When creating tables the following should be born in mind:

The names and titles of tables, as well as rows and columns in it, must ensure that the table is completely clear, without reading the text of the manuscript.

The data presented in the text should not appear in the tables, and *vice versa*. It is wrong to repeat same data in tables and figures (charts or graphs).

A table that is not referred to in the text should not be used.

A table that can be explained simply with a sentence or two in the text is unnecessary and preferably avoided. In other words, a table with one column or one row is usually not required.

Quantities and units in the tables should be displayed with the smallest number of digits or letters.

Tables with the same value in the columns (rows) or with many empty cells, as well as large tables with lots of data should be avoided. This information is much better shown by graphs or diagrams

Highlighting important data in the tables in a footnote or in the titles of the table is advised.

Long titles of columns or rows should be replaced with abbreviations that are explained in a footnote to the table.

Except when necessary, it is best to avoid vertical lines between columns.

The instructions and requirements of publishers (if any) specified in the Instructions for Authors, must always be followed.

Creating illustrations

Caption must exist for every illustration. As a rule, it should be located below the illustration. It is recommended that a legend in the illustration be kept to a minimum, all the explanations, if needed, should be stated in the caption.

General recommendations for creating illustrations are as follows:

Each axis on the charts and graphs must be named, including units.

The length of the axis should be adjusted to the extent of the data presented. For example, if the maximum value shown in the diagram is 105, the axis should not extend above a value of 110.

Displaying images that are not cited in the text or that can be replaced with a few sentences is not advised.

Adherence to recommendations of IUPAC and SI is required.

The decision of whether to present an illustration in color or not depends on several factors: Printing color images in the paper editions of a journal is expensive and often has to be paid for by the authors (this information is usually found in the Instructions for Authors). However, in the electronic version of a paper, color illustrations are published without charge. In this case, two versions of the image can be prepared (in color and in black and white), if the publisher offers this option. For electronic journals (which are issued only in electronic form on the Internet), the choice of whether to prepare color or black and white illustration depends on the authors. In all other cases, it is advisable to prepare black and white illustration, unless it is necessary to be in color.

The size and format of illustrations must be in accordance with the requirements of the publisher. Some formats are unsuitable for printing on paper, and depending on the publisher, the allowed formats are limited. For graphics and diagrams (line-art), TIF, EPS, AI and PDF formats are usually allowed, while for photos and halftone image, JPG format is also allowed. Concerning combined images (line-art and halftone), JPG format is usually not allowed.

More and more publishers are allowing the inclusion of multimedia content in the electronic versions of works – videos, animations, sound recordings. As there are a number of multimedia formats, it is necessary to enquire about the possibilities offered by different publishers. Elsevier, one of the leading and largest publishers in the world, has very detailed instructions for preparing illustrations on its Web site.[16] Bearing in mind that many other publishers draw on the experience of Elsevier, it is a good idea to visit this site to gain knowledge of current opportunities, requirements and standards.

References

For any data taken from literature, the source must be specified, immediately afterwards. The way in which references appear in the text, as well as in the reference list, differ from journal to journal, but they are always explained in detail in the Instructions for authors[17,18]. The authors are required to comply with these instructions!

If the entire part of the text is taken from the literature, it must be placed in quotation marks, while the list of literature must state the page number(s) from which the quotation was taken.

Publications that are not cited in the text must not be mentioned in the list of references. If the stated literature is written in a language different to that used in the paper, it must be indicated in the list, next to the reference.

Additional material

Additional material can be joined to the article (Appendix or Supplementary material). It usually contains detailed information regarding the content presented in the text of the paper, which is primarily for a close group of readers who are engaged in a narrow area close to the subject of the article.

The existence of additional material must be indicated at the appropriate locations within the article. Spectra, measurement data, large tables, multimedia, *etc*., are the most common contents of an Appendix. Frequently, the additional material is published exclusively in electronic form. The printed version of the article only mentions its existence and gives the Internet address where the additional material is located.

Format, technical processing and submission of the paper

Each publisher provides guidance for application and submission of manuscripts – Instructions for Authors, or Guide(lines) for Authors. The guidance describes how to write and to prepare technically a paper, how to create illustrations, charts or other specific contents. Very often, there are special instructions for the preparation of the graphical material – figures, diagrams, graphics, photos, *etc*. – called Artwork Instructions.

Before writing, one must ALWAYS read the directions and prepare the article according to the Instructions for Authors. Moreover, before sending, it is advisable to check once again whether the manuscript was prepared in accordance with these instructions. This not only saves the Editor's time and accelerates the process of manuscript evaluation, but also, more importantly, helps to avoid the possibility that the submitted paper be rejected for "technical" reasons. If the article used materials that are protected by copyright of the publisher (organization or individual), along with the submitted manuscript, the agreement of the rights holder that copyrighted material can be used, should also be submitted.

A supporting letter (Cover letter) must always be submitted in addition to the article. It must contain a statement that the research paper is original, not published or submitted for publication to another publisher and that does not contain copyrighted material (or if it does, refer to the attached agreement that these materials can be used).

After paper submission

After the article is submitted, it is likely that the author will obtain feedback that the paper arrived at the editorial office and a reference number will be assigned to the contribution. If there is no response after a few weeks, it is recommended to contact the editorial office with a brief e-mail in which the confirmation that the paper came to the office and the reference number of the manuscript is requested. The message should be addressed to the name of the editor to whom the manuscript was sent (especially if the journal has multiple editors).

After the reviews, the editor, or someone on behalf of the editors, will send a letter with the decision on the fate of the paper, usually along with reports of the reviewers. If the work requires revision, the comments should be read and each one should be answered, whether or not the author accepts or rejects them. No remarks should be ignored. In case a remark is not understandable, the editor should be contacted with a request to explain and/or clarify the instruction. Even asking for advice on how to revise the manuscript is appreciated, in this case.

In preparing the text of a manuscript text and the presentation of results, it may be useful to read the article by Bornman *et al*.,[19] which analyzes the process of the peer review of scientific papers and the contents of reviewers' reports.

If paper is rejected, before deciding what to do next, the Editor's report should be discussed with co-authors and colleagues. It is crucial to consider all comments of the reviewers and editors seriously. After additional measurements are performed and the manuscript is refined, it is ready to be re-submitted to the same, or if decided, some another journal. In the case that there are no valid reason for the rejection of the manuscript (rejection based on misinterpretation or misunderstanding of the content by the editor or reviewer), submitting an appeal to the Editor is welcomed.

If the manuscript is accepted for publication, information on copyright and reprints should be requested from the editorial office immediately, as well as any possible additional conditions of publications, if they are unknown. If the journal is charges for author's copies, it is often still possible to obtain a few free copies, but only if requested in due time. Finally, one should not forget to inform all of the co-authors that the paper will be published, and in which Journal.

И З В О Д

КАКО ПРЕЗЕНТОВАТИ И ПУБЛИКОВАТИ РЕЗУЛТАТЕ НАУЧНИХ ИСТРАЖИВАЊА

АЛЕКСАНДАР ДЕКАНСКИ

ИХТМ – Центар за електрохемију, Универзитет у Београду, Његошева 12, Београд

На крају сваког истраживања, посебно научног, потребно је добијене резултате представити јавности, посебно оном делу научне јавности који се бави сличним темама. То се најчешће чини кроз научни рад, писани извештај који садржи приказ резултата оригиналног научног истраживања. Његов формат је дефинисан вековима старом традицијом писања научних радова, уређивачком праксом издавача научних публикација, научном етиком, прихваћеним стандардима и захтевима савременог издаваштва и штампања. Нажалост, искуства издавача и уредника научних књига и часописа показују да велики број достављених прилога не испуњава минималне услове чак ни да се узму у разматрање. Овај чланак указује на најважније принципе које треба имати у виду при презентацији научних резултата писањем оригиналног нучног рада.

(Примљено 10. јуна. прихваћено 23. јуна 2014)

REFERENCES

1. L. C. Perelman, E. Barrett, J. Paradis, *Mayfield Electronic Handbook of Technical & Scientific Writing*, McGraw-Hill Education, Columbus, OH, www.mhhe.com/mayfieldpub/tsw/home.htm (accessed October 2013)
2. J. C. Boyd, N. Rifai, T. M. Annesley, *Clin. Chem.* **55** (2009) 1259
3. School of Chemistry and Biochemistry, Georgia Institute of Technology, The Sherrill Group, http://vergil.chemistry.gatech.edu/resources/writing-papers.pdf (accessed November 2013)
4. M. A. Kliewer, *Am. J. Roentgenol.* **185** (2005) 591
5. G. H. Guyatt, R. Brian Haynes, *J. Clin. Epidemiol.* **59** (2006) 900
6. K. Sand-Jensen, *Oikos* **116** (2007) 723
7. V. Chernick, *Paediatr. Respir. Rev.* **13** (2012) 130
8. G. M. Liumbruno, C. Velati, P. Pasqualetti, M. Franchini, *Blood Transfus.* **11** (2013) 217

9. G. J. Leigh, H. A. Favre, W. V. Metanomski, in *Principles of Chemical Nomenclature, A Guide to IUPAC Recommendations*, G. J. Leigh, Ed., Blackwell Science, Oxford, 1998, http://old.iupac.org/publications/books/principles/principles_of_nomenclature.pdf (accessed in November 2013)
10. A. D. McNaught, A. Wilkinson, *Compendium of Chemical Terminology, The Gold Book*, Blackwell Science, Oxford, 1997
11. E. R. Cohen, T. Cvitaš, J. G. Frey, B. Holmström, K. Kuchitsu, R. Marquardt, I. Mills, F. Pavese, M. Quack, J. Stohner, H. L. Strauss, M. Takami and A. J. Thor, *Quantities, Units and Symbols in Physical Chemistry – The Green Book*, RSC Publishing, Cambridge, 2007
12. *Nomenclature of Inorganic Chemistry, IUPAC Recommendations 2005*, N. G. Connelly, T. Damhus, R. M. Hartshorn, A. T. Hutton, Eds., The Royal Society of Chemistry, Cambridge, 2005
13. R. Panico, W. H. Powell, J.-C. Richer, *A Guide to IUPAC Nomenclature of Organic Compounds*, Blackwell Science, Oxford, 1993
14. H. A. Favre, K.-H. Hellwich, G. P. Moss, W. H. Powell, J. G. Traynham, *Pure Appl. Chem.* **71** (199) 1327
15. Bureau International des Poids et Measures, SI Brochure, http://www.bipm.org/en/si/ (accessed November 2013)
16. Elsevier, Artwork & media instructions, http://www.elsevier.com/wps/find/ /authors.authors/authorartworkinstructions (accessed November 2013)
17. H. B. Michaelson, *Tech. Commun.***28** (1981) 20
18. E. Garfield, *Library Q.* **66** (1996) 449
19. L. Bornmann, H. Herich, H. Joos, H.-D. Daniel, *Scientometrics* **93** (2012) 915.

Journal of the Serbian Chemical Society
JSCS-info@shd.org.rs • www.shd.org.rs/JSCS
J. Serb. Chem. Soc. 79 (12) 1571–1574 (2014) UDC 556.551+546.3:544.362:579.68(497.11)
JSCS–4689 *Letter to the Editor*

LETTER TO THE EDITOR

Commentary on the article entitled "Investigation of the microbial diversity of an extremely acidic, metal-rich water body (Lake Robule, Bor, Serbia)" by Srđan Stanković, Ivana Morić, Aleksandar Pavić, Branka Vasiljević, D. Barrie Johnson and Vladica Cvetković, published in the *Journal of the Serbian Chemical Society*, Volume 79, Issue 6, Pages: 729–741 (available online 27 June 2013)

VLADIMIR P. BEŠKOSKI* and MIROSLAV M. VRVIĆ

Faculty of Chemistry, University of Belgrade, 11158 Belgrade, Studentski trg 16, P. O. Box 51, Serbia and Department of Chemistry, Institute of Chemistry, Technology and Metallurgy, 11001 Belgrade, Njegoševa 12, P. O. Box 473, Serbia

(Received 28 December 2013, accepted 17 October 2014)

This letter and comments within refer to the article by Srđan Stanković, Ivana Morić, Aleksandar Pavić, Branka Vasiljević, D. Barrie Johnson and Vladica Cvetković, "Investigation of the microbial diversity of an extremely acidic, metal-rich water body (Lake Robule, Bor, Serbia)" (hereinafter: **Paper**) published in the *Journal of the Serbian Chemical Society*, 2014, Volume 79, Issue 6, Pages: 729–741.

This communication highlights only the most relevant comments, while the Addendum part (given as Supplementary material to this letter) comprises all the essential and technical issues and also shortcomings of the review of this **Paper**, listed one by one, issues that could attract the attention of colleagues dealing with biogeochemical cycles, especially in extreme environments.

The results of an investigation of the microbial diversity in the said habitat are published in the **Paper** for which the authors used culture-dependant and culture-independent (T-RFLP) methods. T-RFLP analysis revealed that the dominant bacteria in the lake water samples were the obligate heterotroph *Acidiphilium cryptum* (≈50 % of the total bacteria) and the iron-oxidizing autotroph *Leptospirillum ferrooxidans* (≈40 %).

* Corresponding author. E-mail: vbeskoski@chem.bg.ac.rs
doi: 10.2298/JSC131228100B

The authors of the **Paper** compared their results with those of another paper: V. P. Beškoski, P. Papić, V. Dragišić, V. Matić, M. M. Vrvić, *Long term studies of the impact of thionic bacteria on the global pollution of waters with toxic ion*s, published in Advanced Materials Research, *Proceedings of the 18th International Biohydrometallurgy Symposium 2009*, Bariloche-Argentina, 105 (2009) p. 71.[1] In this study, on selective media, sulphur- and iron-oxidizing microorganisms were monitored (primarily *Acidithiobacillus ferrooxidans*), which produce sulphuric acid and Fe^{3+} and it is these which, as potent oxidants in an acid environment, contribute to the release of heavy metals into the environment. However, there is not a single reference to microbial communities or biodiversity in the cited paper, since these were not the focus of that investigation; rather, the cited study presents the results of multi-year monitoring of the impacts of thionic bacteria on water polluted by toxic metals.

The claim that the authors of the **Paper** grew *At. ferrooxidans* on solid medium is inexplicably contrasted with their inability to identify it by the use of T-RFLP method (without any reference to statistical data). This leads to the only possible conclusion, that some methodological and/or conceptual errors may have been made in this **Paper,** both during the sampling procedure and the analysis of the results, and which would normally be addressed during the scientific review process. Such misunderstandings can be seen in numerous sections of the **Paper**. The result that the obligate heterotroph *A. cryptum* comprised approximately 50 % of the total bacterial population in a habitat where the concentration of dissolved organic substance is low is particularly dubious. The result that *L. ferrooxidans* makes up about 40 % of the total bacterial population of the lake water also seems highly unlikely to be correct.[2] If the native preparation of sampled water was examined microscopically by the authors of the **Paper**, it would be clear to them that this bacterial species was sporadic.[2,3]

It is inappropriate for a reputable journal to publish, and for the reviewers to allow the publication of, statements which are notoriously false, and which is found in the 3rd paragraph of page 6: “Redox potential of the lake water was measured by calomel electrode (personal correspondence with author).” Any competent chemistry technician is aware that redox potential cannot be measured by using only a reference electrode.

Additional confusion is contributed by the fact that the **Paper** draws conclusions based on speculation. For example, the authors extrapolated meaning outside the framework of the data presented (in the context of timeframe), and made an ill-founded comparison to data in other studies (they compared their estimates of bacterial percentages in water sample(s) to bacterial most probable number (*MPN*) counts).

Among the flaws in the **Paper**, we highlight the analysis of water samples (probably more than 50 mL should have been taken), and that this analysis

should have been more complete and conducted at multiple times (the current analysis, as published in the **Paper**, appears to be lacking basic chemical data and is described as being "point-like", since water samples were taken only once). Scientific doubts about the obligate heterotrophy of the habitat would, in this case, have been removed. Furthermore, talking about the presence of organic substance in the lake based only on the determined microorganisms and without conducting any basic analysis, such as determination of the chemical oxygen demand (*COD*), biological oxygen demand (*BOD*) and total organic carbon (*TOC*), should be unacceptable.

Readers are left with the impression that the speed with which this **Paper** was reviewed and accepted contributed to such flaws.

The main aim of publishing scientific work in peer-reviewed journals is to ensure quality standards are maintained in science. Good peer-review also serves to improve studies in the natural sciences, and must necessarily encompass these points: 1) Does the work express a clear aim which has been achieved?; 2) Are the methods and materials used suitable for purpose?; 3) Is the work able to be repeated by other experts in the field, and is enough detail given in the Experimental to allow this without hindrance?; 4) Have quantifiable results been collected impartially in a suitable manner?; 5) Are data analysis methods correctly applied to all the data?; 6) Is the data analysis valid and are the datasets of an appropriate size?; 7) Does the work fairly and correctly represent and discuss the relevant work of other experts in the field, and other findings?; 8) Does the work compare the results obtained with those of other studies in a suitable manner?; 9) Are the conclusions based on the results presented and the discussion?; 10) Are there any novel findings in the work, or does the work contribute to the body of knowledge? The review of this **Paper** seems to be lacking in several of these fundamental areas.

The authors believe that the publication of these well-meaning comments will be of benefit not only to the authors of the **Paper**, but also to all who work or intend to work in this complex and difficult multidisciplinary scientific field, which requires a substantial understanding of all aspects of biogeochemical cycles.

SUPPLEMENTARY MATERIAL

Adendum to this Commentary is available electronically from http://www.shd.org.rs/JSCS/ or from the corresponding author on request.

И З В О Д

КОМЕНТАРИ НА РАД ПОД НАСЛОВОМ „ИСТРАЖИВАЊЕ МИКРОБИОЛОШКОГ ДИВЕРЗИТЕТА ЕКСТРЕМНО КИСЕЛЕ ВЕШТАЧКЕ АКУМУЛАЦИЈЕ ВОДЕ СА ВИСОКИМ САДРЖАЈЕМ МЕТАЛА (ЈЕЗЕРО РОБУЛЕ, БОР, РЕПУБЛИКА СРБИЈА), АУТОРА СРЂАН СТАНКОВИЋ, ИВАНА МОРИЋ, АЛЕКСАНДАР ПАВИЋ, БРАНКА ВАСИЉЕВИЋ, D. BARRIE JOHNSON И ВЛАДИЦА ЦВЕТКОВИЋ, ОБЈАВЉЕНОГ У *JOURNAL OF THE SERBIAN CHEMICAL SOCIETY*, VOLUME 79, ISSUE 6, PAGES: 729–741 (ЕЛЕКТРОНСКИ ОБЈАВЉЕНОГ 27. ЈУНА 2013)

ВЛАДИМИР П. БЕШКОСКИ и МИРОСЛАВ М. ВРВИЋ

Хемијски факултет, Универзитет у Београду, Студентски трг 16, п. пр. 51, 11158 Београд и Центар за хемију, Институт за хемију, технологију и металургију, Његошева 12, п. пр. 473, 11001 Београд

Ова кратка комуникација са припадајућим коментарима се односи на рад објављен у *Journal of the Serbian Chemical Society*, а који је био објављен електронски 27. јуна 2013 године, под насловом „Истраживање микробиолошког диверзитета екстремно киселе вештачке акумулације воде са високим садржајем метала (језеро Робуле, Бор, Србија) чији су аутори Срђан Станковић, Ивана Морић, Александар Павић, Бранка Васиљевић, D. Barrie Johnson и Владица Цветковић, doi: 10.2298/JSC130605071S. Комуникација и припадајући додатак истичу најрелевантније коментаре, суштинска и техничка питања, а такође и недостатке процеса рецензије овог рада, питања која би могла привући пажњу колега који се баве биогеохемијским циклусима, посебно у екстремним условима. Аутори ове комуникације верују да ће објављивање ових добронамерних коментара бити од користи не само ауторима предметног рада, већ и свима који се баве или намеравају да раде у овој комплексној и тешкој мултидисциплинарној научној области, која изискује суштинско разумевање свих аспеката биогеохемијских циклуса.

(Примљено 28. децембра 2013, прихваћено 17. октобра 2014)

REFERENCES

1. V. P. Beškoski, P. Papić, V. Dragišić, V. Matić, M. M. Vrvić, in *Proceedings of the 18th International Biohydrometallurgy Symposium 2009*, Bariloche, Argentina, 2009, *Adv. Mater. Res.* **105** (2009) 71
2. M. M. Vrvić, *PhD Thesis*, Faculty of Chemistry, University of Belgrade, Belgrade, 1991, pp. 319–360 (in Serbian)
3. M. M. Vrvic, in *Proceedings of UNEP International Seminar on Dump and Underground Bacterial Leaching of Metals from Ores*, G. I. Karavaiko, G. Rossi, Z. A. Avakyan, Eds., Centre for International Projects, USSR State Committee for Environment Protection, Moscow, 1990, pp. 59–73.

Journal of the Serbian Chemical Society
JSCS@tmf.bg.ac.rs • www.shd.org.rs/JSCS
J. Serb. Chem. Soc. 79 (12) S186–S190 (2014) *Supplementary material*

SUPPLEMENTARY MATERIAL TO

Commentary on the article titled "Investigation of the microbial diversity of an extremely acidic, metal-rich water body (Lake Robule, Bor, Serbia)" by Srđan Stanković, Ivana Morić, Aleksandar Pavić, Branka Vasiljević, D. Barrie Johnson and Vladica Cvetković, published in the *Journal of the Serbian Chemical Society*, Volume 79, Issue 6, Pages: 729–741 (available online 27 June 2013)

VLADIMIR P. BEŠKOSKI* and MIROSLAV M. VRVIĆ

Faculty of Chemistry, University of Belgrade, 11158 Belgrade, Studentski trg 16, P. O. Box 51, Serbia and Department of Chemistry, Institute of Chemistry, Technology and Metallurgy, 11001 Belgrade, Njegoševa 12, P. O. Box 473, Serbia

J. Serb. Chem. Soc. 79 (12) (2014) 1571–1574

ADDENDUM

Page 731, paragraph 2. "Lake water samples were collected in 50 mL sterile plastic containers on July 26th, 2012. Water temperature, pH, and conductivity were measured on site using a Hanna Instruments HI98311 mobile instrument." The location or the site from which the samples were taken is not specified (the former cementation plant; at the foot of Visoki planir; at the centre of the lake; at the exit point; from the lake bottom; in the vicinity of communal wastewater, *etc*.). The authors should provide the GPS coordinates of the sampling sites. Authors also say "water samples", without specifying how many different water samples were actually taken on this day.

Page 731, paragraph 2. "The redox potential of the water was measured using a combined Pt–Ag/AgCl electrode." In the experimental section, it is not clear whether the oxidation/reduction potential (ORP) was measured in the field or not, so this data should be included. Furthermore, the authors do not specify the temperature conditions under which the samples were later transported to the laboratory. Finally, there are no data concerning the timeframe after sampling, and within which the microbiological analyses were commenced/finished.

Page 731. The authors do not mention whether microscopy methods were used to aid in the identification of the microorganisms (MOs). It is presumed they

* Corresponding author. E-mail: vbeskoski@chem.bg.ac.rs

did use microscopy, as this is such a fundamental method for identification of MOs.

Page 731. The authors also do not specify whether biochemical characterization of any of the isolated MOs grown on solid media was conducted, or, indeed, any other standard microbiological characterization.

Page 731. MOs were isolated on a solid medium, but they were not counted, so the authors do not mention the number of MO per mL (or at least the order of magnitude) obtained by the methods of classical microbiology. Later on, they specify the prevalence of the MOs in percentages by T-RFLP methods. Unfortunately, their presence was confirmed only by this method (and this involved making a comparison with a database that is available only to the authors, but is not publically available to the scientific community).

Page 732, paragraph 2. "PCR products were analyzed by gel electrophoresis on 0.7 % agarose gel." The authors studied the 16S rRNA gene of colonies grown on a solid medium. However, they do not specify whether the identity of these MOs was confirmed by the sequencing of this gene, which is a standard method of identifying microorganisms, including environmental isolates, and is the best confirmation that the isolated MO is really the one that is being presumed.

Page 732, paragraph 3. "Approximately 400 mL of lake water was filtered through a 0.2 μm (pore size) sterile membrane filter." The authors should specify what type of membrane was used.

Page 734, paragraph 1. "The approximate relative abundance of bacteria in the lake water was calculated from the peak areas of each terminal restriction fragment as a percentage of the total peak area." The authors give the approximate relative presence based on the T-RFLP results, without the specification of any statistics. Data on the use of statistics should be included.

Page 734, paragraph 1. "The most abundant colonies were colonies of *A. cryptum*, followed by those of *L. ferrooxidans*; colonies of *At. ferrooxidans* were the least abundant." The authors must state clearly whether there were also other types of colonies on the solid medium. The authors should provide complete colony descriptions for all three species growing on their solid medium at a specified temperature, under a specified atmosphere and for a specified time in order to allow other researchers to replicate the methods of the study. The authors provide results in a descriptive manner, without specific numbers and the study would be enhanced if actual numbers were provided.

Page 735, paragraph 2. "After three weeks of bioleaching experiment, the pH value of the solution was 2.20 and redox potential was +820 mV. The concentration of total iron was (815±1.633) mg L^{-1} and the concentration of the total copper was (808.97±5.735) mg L^{-1}. Concentrations of total iron and copper are mean values of three measurements." and page 8, paragraph 1. "The concen-

tration of copper determined in bioleaching solution was greater than this, 808.97 mg L^{-1}." Such over-precision and mixing of the number of decimal places is seen throughout the **Paper.**

Page 736, paragraph 1. "The redox potential of the lake water was measured by a calomel electrode (personal correspondence with the author)." In the personal correspondence with the authors of the cited paper, it has been stated that the ORP was determined using a setup consisting of a calomel reference electrode and a platinum electrode, which the authors of the **Paper** wrongly quote, stating only that the reference electrode was used for the measurement. This does unfortunately cast doubt on knowledge of the authors' of the **Paper** of analytical chemistry. We would also like to mention that authors of the **Paper** were not granted authorization for publishing the personal correspondence.

Page 737, paragraph 1. The authors mention the presence of *Acidisphaera rubrifaciens* based on T-RFLP and confirmed the negligible presence of *At. ferrooxidans* regardless of biogeochemical indicators which show otherwise. Discussion about these extremely interesting results is missing and some discussion on this point should have been included.

Page 737, paragraph 1. "Interestingly, *At. ferrooxidans*, previously reported as the dominant bacterial species in Lake Robule, was not detected in the lake water by T-RFLP analysis, though was isolated on solid medium (FeSo plates), along with *A. cryptum* and *L. ferrooxidans*." The authors should have explained this.

Page 737, paragraph 2. "Earlier studies suggested that microbial communities in acidic environments were dominated by *At. ferrooxidans*, but it appears this was an artefact of the methods, particularly enrichment culture and most probably number (MPN) counts. Media for cultivation of acidophilic bacteria that have been widely used, and sometimes still are, such 9K, contain very high concentrations of Fe^{2+} iron (9 g L^{-1} in 9K) and favour the growth of *At. ferrooxidans*." The authors suggest that 9K is a selective media that favours the growth of *At. ferrooxidans.* Of course, this cannot be disputed, since in the cited investigation, it was of interest to determine, as accurately as possible, the count of *At. ferrooxidans* in the environment which was very heavily burdened with iron. We chose to do so using the MPN technique, which is a very common and well-accepted standard technique for estimating bacterial numbers in liquid samples (http://www.fda.gov/Food/FoodScienceResearch/LaboratoryMethods/ /ucm109656.htm). In fact, the medium, 9K reflects, in an excellent manner, the natural conditions under which *At. ferrooxidans* live, it is a widely-accepted and the most suitable medium with which to obtain MPN counts of this MO from these types of water samples. The authors should note that the use of any medium, including their solid medium, is selective, as is the choice of the incubation atmosphere, time and temperature. For any given sample (*e.g.*, food,

water, soil, biological tissue, *etc*.), the choice of medium, atmosphere and time/ /temperature combination affects the ability of individual microorganisms contained within that sample to form colonies (and thus be noticed and "counted" under the chosen conditions). Thus, in any given sample, the "total bacterial population" or "total bacterial count" only ever encompasses those bacteria able to thrive under the given conditions on the given medium, while those which cannot do so are not included. Therefore, to selectively count a given microorganism in any given sample, the medium, atmosphere, time and temperature are all adjusted to suit the organism of interest, and to allow/promote its growth. The authors should have explained that it is not possible to compare the estimates of bacterial percentage prevalences obtained in the **Paper** with bacterial MPN counts obtained in the cited study.

Page 737. We note that polymerase chain reaction (PCR) is also selective and that it will multiply only those fragments for which primers have been added. It is only with repetition using different primer sets that the probability of finding all 16S rRNA present in a PCR-tube is increased.

Page 737, paragraph 3. "Reports on the composition of the microbial community in the lake published by Beškoski *et al*. (2009) that differ significantly from the results presented in this paper are..." In the quoted paper of Beškoski *et al*. (2009), the microbial community was not studied and is not mentioned, so this appears to be a misinterpretation of results obtained by us, and therefore, compares things that cannot be compared at all. Neither the total community nor the biodiversity were analysed in our study, but instead, *At. ferrooxidans* and other thionic bacteria were the main targeted MOs. The authors of the **Paper** speculate about a historical bacterial population, which is difficult to justify, as, to the best of our knowledge, no published record of the microbial community in this lake exists, and there is no evidence of its change, or lack thereof, over time.

Page 738, paragraph 1. "The obligatory acidophilic heterotroph *A. cryptum*, the most abundant bacterium in the lake water as determined by T-RFLP analysis and isolation on solid medium". Since the solid medium was prepared with the addition of *A. cryptum*, the issue of contamination cannot be excluded. The authors should have provided information about the steps they took to prevent such contamination, and their proof that the solid medium could not have been contaminated with supplemented *A. cryptum*.

Page 738, paragraph 2. "One potential source of organic matter in the lake is a municipal waste dump, which is in close proximity to the lake, while other potential sources could be acidophilic algae." and *page 9, paragraph 1*. "The most abundant microorganism in lake is the heterotrophic bacterium *A. cryptum*. This finding suggests that the lake water has a constant supply of organic matter. A possible source of organic matter could be municipal waste dump that is very close to the lake. Another source of organic matter in the lake is probably acido-

philic algae that populate the microbial mat at the bottom of the lake." The authors state that the organic substance from the municipal waste dump (or the acidophilic algae) is the reason for the presence of organic substance which stimulates the growth of *A. cryptum* and *Acidisphaera rubrifaciens*. However, they have not confirmed the presence and the quantity of the organic substance using basic analysis (*COD*, *BOD*, *TOC*, *etc*.).

Page 739, paragraph 1. "The most abundant microorganism in the lake is heterotrophic bacterium *A. cryptum*." The authors reach this conclusion based on one point-like sampling and the use of the solid medium on which this MO was used anyway to remove organic compounds. One (or even several) water sample(s) taken on one day would not seem to be representative of the entire lake. The authors should have replaced the word "lake" in this sentence with "the water samples".

Page 739, paragraph 1. "Those conditions are less suitable for the growth of *At. ferrooxidans*, which was not detected by T-RFLP analysis, but was isolated directly from lake water on overlay solid medium." This result, which indicates that this MO was present in sufficient numbers that its colonies appeared on the solid medium, but it was not present in sufficient numbers to enable isolation of metagenomic DNA, is very interesting and it is surprising that the authors did not attempt to explore it further. This is an important scientific point which must be developed, as it has wider scientific repercussions than just for the current **Paper**.

Page 739, paragraph 2. "Physical and chemical properties of the lake display both seasonal and long-term variations." This cannot be concluded for Lake Robule from the results of the authors of the **Paper**, since the results of the **Paper** are based on one sampling time. Nor can the results regarding microorganisms be compared directly with the results of others, as explained above.

Page 740, paragraph 1. "Такође, испитивана је способност нативних бактерија из језера да врше луженье бакра из узорка минералног концентрата." The term "indigenous bacteria" is translated into non-standard terminology by the authors as "нативне бактерије".

Page 733, Table I. No data are available about the concentration of dissolved O_2, or the content of organic substance.

Pages 733 and 736, Figures 1 and 2. Figure 2 has been produced based on the data taken from Figure 1. The authors should have specified what fragment of T-RF (*HaeIII, AluI* or *CfoI*) was used for this quantification and provide statistics.

Page 734, Figure 2. The quality of the black and white photograph is not satisfactory, so that readers cannot see what the authors refer to in the **Paper**.

Journal of the Serbian Chemical Society
JSCS-info@shd.org.rs • www.shd.org.rs/JSCS
J. Serb. Chem. Soc. 79 (12) 1575–1578 (2014) UDC 556.551+546.3:544.362:579.68(497.11)
JSCS–4690 *Letter to the Editor*

LETTER TO THE EDITOR

Reply on the Commentary on paper "Investigation of microbial diversity of an extremely acidic metal-rich water body Lake Robule (Bor, Serbia) published in *Journal of the Serbian Chemical Society*, Volume 79, Issue 6, Pages: 729–741

SRĐAN STANKOVIĆ[1]*, BRANKA VASILJEVIĆ[2] and VLADICA CVETKOVIĆ[1]

[1]*University of Belgrade, Faculty of Mining and Geology, Đušina 7, 11000 Belgrade, Serbia and* [2]*University of Belgrade, Institute of Molecular Genetics and Genetic Engineering, Vojvode Stepe 444a, 11000 Belgrade, Serbia*

(Received 5 November, accepted 11 November 2014)

This is a reply to the Commentary (hereafter: **Commentary**) by V. Beškoski and M. Vrvić on the article entitled "Investigation of the microbial diversity of an extremely acidic, metal-rich water body (Lake Robule, Bor, Serbia)" by Srđan Stanković, Ivana Morić, Aleksandar Pavić, Branka Vasiljević, D. Barrie Johnson and Vladica Cvetković, published in the *Journal of the Serbian Chemical Society*, Volume 79, Issue 6, Pages: 729–741.

We welcome the **Commentary** and thank the authors for showing interest in our research. In this reply, we only address the most important remarks of the **Commentary**, and provide additional arguments for the conclusions originally presented in the paper. We, therefore, put the strongest emphasis on the comments related to the major scientific results of our paper, leaving aside all technical remarks of the Commentary as well as those comments focused on improving the editorial handling of the *Journal of the Serbian Chemical Society*.

The aim of our work was to study the microbial diversity of Lake Robule using the molecular fingerprinting method (Terminal Restriction Fragment Length Polymorphism – T-RFLP) and cultivation of bacteria on selective solid media. In the last twenty years or so, new molecular methods were introduced into microbiology, allowing more comprehensive detection of bacterial diversity in environmental samples in comparison to traditional cultivation-based approaches.[1] It is estimated that traditional cultivation based methods can isolate only 0.1 to 1 % of total bacterial species present in the analyzed samples.[2]

* Corresponding author. E-mail: srdjan.stankovic@gmail.com
doi: 10.2298/JSC141105111S

At the time of sampling (July 2012), the most abundant bacteria in the analyzed samples of the water collected at several locations from Lake Robule were *Acidiphilium cryptum* and *Leptospirillum ferrooxidans,* with a relatively smaller number of *Acidithiobacillus ferrooxidans.* We clearly showed that the diversity and relative abundance of bacteria grown on selective solid media reflects the relative abundance and diversity of bacteria determined by T-RFLP analysis. Of course, both methods have their drawbacks and for this reason, we combined these two approaches.

The authors of the **Commentary** ignore strong evidence presented in the paper and suggest that microscopic examination of the samples would be enough to prove that our findings were wrong. We performed microscopic examination of the samples and saw numerous small spirilli and larger bacilli. It is all documented in microscopic images that can be presented on the Editor's request.

The authors of the **Commentary** based their conclusion that "some methodological and/or conceptual errors may have been made in this paper" on the fact that *At. ferrooxidans* was not detected in the T-RFLP profile, but it was detected on the selective solid media. In order to remove confusion and to solve this dispute, we need to explain in more detail some basic concepts of the T-RFLP analysis.

The T-RFLP analysis of the bacterial community structure is a technique based on Polymerase Chain Reaction (PCR) amplification of the bacterial 16S rRNA genes, enzymatic digestions of the amplified genes, and detection of the size of each of the individual resulting terminal restriction fragments.[3] PCR reaction in T-RFLP analysis requires the use of a primer labeled with a fluorescent dye at its 5′ end. The primers used for 16S rRNA gene amplification (fluorescently labeled 27F and unlabeled 1387R) are designed to bind to a highly conserved region in bacterial DNA. These primers are regularly used to amplify successfully 16S rRNA genes of all known species of acidophilic bacteria, and many other bacterial species. After PCR amplification, the amplified fragments were digested by endonucleases, producing restriction fragments of different lengths. Capillary electrophoresis instrument (DNA sequencer) detects restriction fragments labeled with a fluorescent dye; the so-called terminal restriction fragments (T-RFs), and determines their length. The most abundant T-RFs produce the most intensive fluorescent signals, identified as peaks in the electropherogram, while T-RFs with low abundance produce low intensity peaks, which are undetectable, or masked, by more intensive signals. It is not uncommon to isolate bacterial species on solid media, but not to detect it by T-RFLP analysis since, at least theoretically, a single bacterial cell is enough to produce a colony on selective solid media. On the other hand, T-RFLP analysis can reveal the presence of bacteria that were unable to grow on selective solid media. The best approach to estimate microbial diversity of environmental samples is to use both molecular-

and cultivation-based methods.[4–7] The T-RFLP analysis was performed in the laboratory of Bangor Acidophile Research Team (BART), Bangor University, UK under supervision of Professor D. Barrie Johnson, one of the most influential authors in this area of microbiology. Professor Johnson kindly provided BART's comprehensive database of the T-RFs of acidophilic bacteria, since this information is not available in public T-RF databases.

Chunbo *et al*. (2010) reported *A. cryptum* as the dominant bacteria in an extremely acidic open pit lake in China. The physicochemical properties of the lake at the time of sampling were very similar to those of Lake Robule.[8] The physical and chemical conditions in both lakes at the time of sampling were nearly optimal for the growth of *A. cryptum*.[10] This fact could be one of the reasons for the dominance of this bacterial species in the analyzed water samples.

Again, it must be stressed that our results reflect only the structure of the bacterial community at the moment of sampling. Summer of 2012 was one of the hottest and driest summers ever recorded in Serbia, and it certainly affected the structure of the bacterial community of the Lake. The physical and chemical properties of Lake Robule express significant seasonal variations.[11] In the conclusion of the paper, we suggested tracking seasonal changes in physicochemical properties and microbial diversity of the Lake in order to provide a more detailed insight into the dynamics of the bacterial population of the Lake.

In conclusion, we truly hope that this reply clarifies the major scientific results of our paper on the microbial diversity in Lake Robule.

Acknowledgements. On behalf of all authors, this response was written by the first and corresponding author, Srdjan Stanković, and the principal investigators, Vladica Cvetković and Branka Vasiljević, of Project Nos. 176016 and 173048, supported by the Ministry of Education, Science and Technological Development of the Republic of Serbia.

И З В О Д

ОДГОВОР НА КОМЕНТАР НАУЧНОГ РАДА "INVESTIGATION OF MICROBIAL DIVERSITY OF AN EXTREMELY ACIDIC METAL-RICH WATER BODY LAKE ROBULE (BOR, SERBIA)" ОБЈАВЉЕНОГ У *JOURNAL OF THE SERBIAN CHEMICAL SOCIETY* (2014), *VOLUME* 79, *ISSUE* 6, PP. 729–741

СРЂАН СТАНКОВИЋ[1], БРАНКА ВАСИЉЕВИЋ[2] и ВЛАДИЦА ЦВЕТКОВИЋ[1]

[1]Универзитет у Београду, Рударско–геолошки факултет, Ђушина 7, 11000 Београд и [2]Универзитет у Београду, Институт за молекуларну генетику и генетички инжењеринг, Војводе Степе 444а, 11000 Београд

Колеге В. Бешкоски и М. Врвић са Хемијског факултета Универзитета у Београду су у свом коментару изразили сумњу у резултате објављене у студији "*Investigation of the microbial diversity of an extremely acidic metal-rich water body lake Robule (Bor, Serbia)*" објављеној у *Journal of the Serbian Chemical Society* (2014), *Volume* 79, *Issue* 6, pp. 729–741. Аутори коментара су изнели тврдњу да су објављени резултати последица методолошких или концептуалних грешака у научно–истраживачком раду описаном у овој публикацији. Као одговор на ове тврдње, изнели смо додатне доказе који поткрепљују резултате

изнете у овом научном раду, као и додатна појашњења примењених метода идентификације микроорганизама, која ће отклонити недоумице у вези са валидношћу приказаних резултата.

(Примљено 5. новембра, прихваћено 11. новембра 2014)

REFERENCES

1. M. E. Guazzaroni, P. N. Golyshin, M. Ferrer in *Metagenomics: Theory, Methods and Application*, D. Marco, Ed., Caister Academic Press, Norfolk, 2010, p. 55
2. V. Torsvik, L. Øvreås, *Curr. Opin. Microbiol.* **5** (2002) 240
3. W. Liu, T. L. Marsh, H. Cheng, L. J. Forney, *Appl. Environ. Microb.* **63** (1997) 4516
4. E. Gonzalez-Toril, E. Llobet-Brossa, E. O. Casamayor, R. Amann, R. Amils, *Appl. Environ. Microb.* **69** (2003) 4853
5. O. F. Rowe, H. Sanchez-Espana, K. H. Hallberg, D. B. Johnson, *Environ. Microb.* **9** (2007) 1761
6. D. B. Johnson, *FEMS Microbiol. Ecol.* **81** (2012) 2
7. C. Falagan, J. Sanchez-Espana, D. B. Johnson, *FEMS Microbiol. Ecol.* **87** (2014) 231
8. H. Chunbo, W. Lihua, G. Yanan, Z. Lina, D. Hailiang, *Extremophiles* **14** (2010) 465
9. M. Korać, Ž. Kamberović, *Metall. Mater. Eng.* **13** (2007) 41
10. B. J. Baker, J. F. Banfield *FEMS Microbiol. Ecol.* **44** (2003) 139
11. Z. Stevanović, Lj. Obradović, R. Marković, R. Jonović, Lj. Avramović, M. Bugarin, J. Stevanović, in *Waste Water – Treatment Technologies and Recent Analytical Developments*, F. S. G. Einschlag, L. Carlos, Eds., InTech, Rijeka, 2013, Ch. 2.

Journal of the Serbian Chemical Society
JSCS@tmf.bg.ac.rs • www.shd.org.rs/JSCS
J. Serb. Chem. Soc. 79 (12) 1579–1589 (2014)

Contents of Volume 79

NUMBER 1

NUMBER 2

NUMBER 3

NUMBER 4

NUMBER 5

NUMBER 11

NUMBER 12

Journal of the Serbian Chemical Society
JSCS-info@shd.org.rs • www.shd.org.rs/JSCS
J. Serb. Chem. Soc. 79 (12) 1591–1597 (2014)

Author Index

Subject Index of Vol. **79** and List of Referees in 2014 are given in the electronic form at the Internet address of the Journal of the Serbian Chemical Society: http://www.shd.org.rs/JSCS/Vol79/No12.html

End of Volume 79.

Journal of the Serbian Chemical Society
JSCS-info@shd.org.rs • www.shd.org.rs/JSCS
Volume *79* (2014)

Subject index

Journal of the Serbian Chemical Society
JSCS-info@shd.org.rs • www.shd.org.rs/JSCS
Volume *79* (2014)

2014 List of Referees

Editorial Board of the Journal is grateful to the following referees for reviewing the manuscripts during 2014:

Habib Abbasipour, *Dep. Of Plant Protection, Faculty of Agricultural Sciences, Shahed University, Tehran, Iran*
Biljana Abramović, *Faculty of Science, University of Novi Sad, Serbia*
Sahar M. Abou-Seri, *Pharmaceutical Chemistry Department, Faculty of Pharmacy, Cairo University, Egypt*
Borivoj Adnađević, *Faculty of Physical Chemistry University of Belgrade, Serbia*
Miroljub Adžić, *Faculty of Mechanical Engineering, University of Belgrade,Serbia*
Antreas Afantitis, *Department of Chemoinformatics, NovaMechanics Ltd, Nicosia, Cyprus*
Sarwar Alam, *Department of Chemistry, Faculty of Science, Hamdard University, New Delhi, India*
Mara Aleksić, *Faculty of Pharmacy, University of Belgrade, Serbia*
Mira Aničić Urošević, *Institute of Physics, University of Belgrade, Serbia*
Vesna Antić, *Faculty of Agriculture, University of Belgrade, Serbia*
Mališa Antić, *Faculty of Agriculture, University of Belgrade, Serbia*
Mihail Atanasov, *Institute for General and Inorganic Chemistry, Bulgarian Academy of Sciences, Sofia, Bulgaria*
Milka Avramov Ivić, *Institute of Chemistry, Technology and Metallurgy, University of Belgrade, Serbia*
Biljana Babić, *Institute of Nuclear Sciences Vinča, Belgrade, Serbia*
Wojciech Bal, *Institute of Biochemistry and Biophysics, Polish Academy of Sciences, Warsaw, Poland*
Adam Bald, *Department of Physical Chemistry, University of Łódź, Poland*
Jiri Barek, *Charles University, Prague, Czech Republic*
Zorica Basić, *Institute of Hygiene, Military Medical Academy, Belgrade, Serbia*
Ivana N. Beara, *Department of Chemistry, Biochemistry and Environmental Protection, Faculty of Sciences University of Novi Sad, Serbia*
Svetlana Begel, *Department of Chemistry and Pharmacy, University of Erlangen-Nürnberg, Erlangen, Germany*
Shanmugasundaram Bhagavathy, *Shasun Research Centre, Tamil Nadu, India*
Y.S. Bhat, *Chemistry Research Laboratory, Bangalore Institute of Technology, Bangalore, India*

Milos I. Đuran, *Department of Chemistry, Faculty of Science, University of Kragujevac, Serbia*
Enis Džunuzović, *Faculty of Technology and Metallurgy, University of Belgrade, Serbia*
Mohammed I. El-Gamal, *Department of Medicinal Chemistry, Faculty of Pharmacy, University of Mansoura, Egypt*
Nagwa Thabet Abo El-Maali, *Department of Chemistry, Faculty of Science, Assiut University, Assiut, Egypt*
Hala Bakr El-Nassan, *Pharmaceutical Organic Chemistry Department, Faculty of Pharmacy, Cairo University, Egypt*
Tarik El-Sayed Ali, *Department of Chemistry, Faculty of Education, Ain Shams University, Cairo, Egypt*
Christopher M. Fellows, *School of Science and Technology, The University of New England, Australia*
Zorana Ferjančić, *Faculty of Chemistry, University of Belgrade, Serbia*
Antonio Frontera, *Departament de Química, Universitat de les Illes Balears, Palma de Mallorca (Balears), Spain*
Baoquan Fu, *Lanzhou Veterinary Research Institute, Chinese Academy of Agricultural Sciences, Lanzhou, China*
Boris Furtula, *Department of Chemistry, Faculty of Science, University of Kragujevac, Serbia*
Hans-Joachim Gabius, *Tierärztliche Fakultät der Ludwig-Maximilians-Universität, Munich, Germany*
Hariprasad Gali, *College of Pharmacy, The University of Oklahoma Health Sciences Center, Oklahoma City, OK, USA*
Achilleas Garoufis, *Department of Chemistry, University of Ioannina, Greece*
Biljana Dj. Glišić, *Department of Chemistry, Faculty of Science, University of Kragujevac, Serbia*
Snežana Gojković, *Faculty of Technology and Metallurgy, University of Belgrade, Serbia*
Aleksandar Golubović, *Institute of Physics, Center for Solid State Physics and New Materials, Belgrade, Serbia*
Maria Angeles Gomez Morales, *Istituto Superiore di Sanità, European Union Reference Laboratory for Parasites, Rome, Italy*
Encarna Gomez Plaza, *University of Murcia, Faculty of Veterinary, Spain*
Gustavo González-Neves, *Facultad de Agronomía. Universidad de la República. Uruguay*
Kristina Gopčević, *School of Medicine, University of Belgrade, Serbia*
Marija Gorjanc, *Faculty of Natural Sciences and Engineering, University of Ljubljana, Slovenia*
Paola Grammatico, *Medical Genetics, Experimental Medicine and Pathology Department, University "La Sapienza, Rome, Italy*
Branimir Grgur, *Faculty of Technology and Metallurgy, University of Belgrade, Serbia*
Alisa Gruden-Movsesijan, *Institute for the application of nuclear energy-INEP, Belgrade, Serbia*
Shaohui Guo, *China University of Petroelum, Beijing, PR China*
Ivan Gutman, *Department of Chemistry, Faculty of Science, University of Kragujevac, Serbia*
Hiroki Hamada, *Department of Life Science, Faculty of Science, Okayama University of Science, Okayama, Japan*
Radmila Hercigonja, *Faculty of Physical Chemistry, University of Belgrade. Serbia*

Konstantinos E. Litinas, *Department of Chemistry, Aristotle University of Thessaloniki, Greece*
Anica Lancuški, *Faculty of Mechanical Engineering, Technion University of Technology, Haifa, Israel*
Carlos Lupiañez, *CIRCE Foundation, University of Zaragoza, Spain*
Sridhar Madabhushi, *Fluoroorganics Division, Indian Institute of Chemical Technology, Hyderabad, India*
Zoran Maksimović, *Faculty of Pharmacy, University of Belgrade, Serbia*
Danijela Maksin, *Vinča Institute of Nuclear Sciences, University of Belgrade, Serbia*
Dragan Manojlović, *Faculty of Chemistry, University of Belgrade, Serbia*
Smilja Marković, *Institute of Technical Sciences of the Serbian Academy of Sciences and Arts, Belgrade, Serbia*
Svetlana Marković, *Department of Chemistry, Faculty of Science, University of Kragujevac, Serbia*
Fleming Martinez, *Departamento de Farmacia, Facultad de Ciencias, Universidad Nacional de Colombia, Columbia*
Radomir Matović, *Institute of Chemistry, Technology and Metallurgy, University of Belgrade, Serbia*
Zoran Matović, *Department of Chemistry, Faculty of Science, University of Kragujevac, Serbia*
Dragan Manojlović, *Faculty of Chemistry, University of Belgrade, Serbia*
Slavko Mentus, *Faculty of Physical Chemistry, University of Belgrade, Serbia*
Michel Meyer, *Chargé de Recherche CNRS, Institut de Chimie Moléculaire de l'Université de Bourgogne (ICMUB), DIJON Cedex, France*
Dušan Mijin, *Faculty of Technology and Metallurgy, University of Belgrade, Serbia*
Jelena Miladinović, *Faculty of Technology and Metallurgy, University of Belgrade, Serbia*
Maja Milojević-Rakić, *Faculty of Physical Chemistry, University of Belgrade, Serbia*
Slobodan Milonjić, *Vinča Institute of Nuclear Sciences, University of Belgrade, Serbia*
Ubavka Mioč, *Faculty of Physical Chemistry Unoveristy of Belgrade, Serbia*
Milan Momčilović, *Vinča Institute of Nuclear Sciences, Belgrade, Serbia*
Nirup B. Mondal, *Indian Institute of Chemical Biology, Councilof Scientific & Industrial Research, Jadavpur, Kolkata, India*
Vladimir S. Moshkin, *Department of Chemistry, Ural Federal University, Ekaterinburg, Russia*
Malose J. Mphahlele, *College of Science, Engineering and Technology, University of South Africa, Pretoria, South Africa*
Samik Nanda, *Department of Chemistry, Indian Institute of Technology, Kharagpur, India*
Mahendra Nath, *Department of Chemistry, University of Delhi, Delhi, India*
Bojana Nedić Vasiljević, *Faculty of Physical Chemistry, University of Belgrade, Serbia*
Olgica Nedić, *Institute for the Application of Nuclear Energy, University of Belgrade, Serbia*
Jovan Nedeljković, *Institute of Nuclear Sciences Vinča, Belgrade, Serbia*
Stevan Nemoda, *Institute of Nuclear Sciences Vinča, Belgrade, Serbia*
Aleksandra Nešić, *Faculty of Technology and Metallurgy, University of Belgrade, Serbia*
Jasmina Nikodinović-Runić, *Institute of Molecular Genetics and Genetic Engineering, University of Belgrade, Serbia*
Branislav Ž Nikolić, *Serbian Chemical Society, Belgrade, Serbia*
Irena Nikolić, *Faculty of Metallurgy and Technology, University of Podgorica, Montenegro*

Vladislav Rac, *Faculty of Agriculture, University of Belgrade, Zemun, Serbia*
Bojan Radak, *Vinča Institute of Nuclear Sciences, University of Belgrade, Serbia*
Serbia
Maja Radetic, *Faculty of Technology and Metallurgy, University of Belgrade, Serbia*
Velimir Radmilović, *Faculty of Technology and Metallurgy, University of Belgrade, Serbia*
Ana Radosavljević Mihajlović, *Vinča Institute of Nuclear Sciences, University of Belgrade, Serbia*
Tatjana Radosavljević, *School of Medicine, University of Belgrade, Serbia*
Aleksandar Radu, *Keele University, UK*
Ljubinka Rajaković, *Faculty of Technology and Metallurgy, University of Belgrade, Serbia*
Vladana Rajaković-Ognjanović, *Faculty of Civil Engineering, University of Belgrade, Serbia*
Vesna Rakić, *Faculty of Agriculture, University of Belgrade, Serbia*
Eugenia Rapoport, *The Shemyakin-Ovchinnikov Institute of Bioorganic Chemistry of the Russian Academy of Sciences, Moscow, Russia*
Slavica Ražić, *Faculty of Pharmacy University of Belgrade, Serbia*
Mathias Ricking, *Free University of Berlin, Germany*
Encarnacion Rodríguez-Gonzalo, *Department of Analytical Chemistry, Nutrition and Food Sciences, University of Salamanca, Spain*
Nebojša Romčević, *Institute of Physics, Belgrade, Serbia*
Jasmina Savić, *Vinča Institute of Nuclear Sciences, University of Belgrade, Serbia*
Reinhard Schomäcker, *Department of Chemistry, Technische Universität Berlin, Germany*
Jan Schwarzbauer, *RWTH Aachen University, Institute of Geology and Geochemistry of Petroleum and Coal, Aachen, Germany*
Antonio Scopa, *School of Agricultural, Forestry, Food and Environmental Sciences – University of Basilicata, Italy*
Pradeep K. Sengupta, *Saha Institute of Nuclear Physics, Kolkata, India*
Ruofeng Shang, *Ministry of Agriculture, Lanzhou Institute of Husbandry and Pharmaceutical Sciences of CAAS, Lanzhou, PR China*
Farhad Shirini, *Department of Chemistry, College of Science, University of Guilan, Rasht, Iran*
Marjana Simonič, *University of Maribor, Slovenia*
Marc Since, *Aix-Marseille Univ, UMR CNRS 7273, Faculté de Pharmacie, Marseille Cedex 5, France*
Modjtaba Shamsipur, *Department of Chemistry, Razi University, Tehran, Iran*
Shu Shan Du, *Protection and Utilization of Traditional Chinese Medicine of Beijing Area Major Laboratory, Beijing Normal University, China*
Hamid Reza Shaterian, *Faculty of Sciences, University of Sistan and Baluchestan, Zahedan, Iran*
Vilim Simanek, *Palacky University in Olomouc, Czech Republic*
Dejan Skala, *Faculty of Technology and Metallurgy, University of Belgrade, Serbia*
Helen Skaltsa, *School of Pharmacy, University of Athens, Greece*
Dušan Sladić, *Faculty of Chemistry, University of Belgrade, Serbia*
Maxim N. Sokolov, *Nikolaev Institute of Inorganic Chemistry SB RAS, Novosibirsk, Russia*
Olivier Sparagano, *Faculty of Health and Life Sciences, Northumbria University, Newcastle upon Tyne, UK*
Ivan Spasojević, *Institute for Multidisciplinary Research, University of Belgrade, Serbia*
Vojislav Spasojević, *Vinča Institute of Nuclear Sciences, Belgrade, Serbia*

Nenad Vuković, *Department of Chemistry, Faculty of Science, University of Kragujevac, Serbia*
Jelena Vuksanović, *Faculty of Technology and Metallurgy, University of Belgrade, Serbia*
Eng-Chi Wang, *Department of Medicinal and Applied Chemistry, Kaohsiung Medical University, Kaohsiung City, Taiwan*
Barbara Wionczyk, *Institute of Leather Industry, Łódź, Poland*
Hui Wu, *Key Laboratory of Biotechnology on Medical Plant of Jiangsu Province, Xuzhou, PR China*
Cui-Lian Xu, *College of Sciences, Henan Agricultural University, Zhengzhou P. R. China*
Zhiwei Yin, *Chemistry Department, Hunter College, New York, NY, USA*
Joanna Zakrzewska, *Institute of General and Physical Chemistry, University of Belgrade, Serbia*
Snežana Zarić, *Faculty of Chemistry, University of Belgrade, Serbia*
Slavica Zec, *Vinča Institute of Nuclear Sciences, Belgrade, Serbia*
Gordana Zdunić, *Institute for Medicinal Plants Research "Dr Josif Pančić", Belgrade, Serbia*
Junwu Zhu, *Laboratory of Soft Chemistry and Functional Materials, Nanjing University of Science and Technology. P.R. China*
Matija Zlatar, *Institute of Chemistry, Technology and Metallurgy, University of Belgrade, Serbia*
Mario Zlatović, *Faculty of Chemistry, University of Belgrade, Serbia*
Branka Žarković, *Faculty of Agriculture, University of Belgrade, Serbia*
Emila Živković, *Faculty of Technology and Metallurgy, University of Belgrade, Serbia*
Ljiljana Živković, *Vinča Institute of Nuclear Sciences, Belgrade, Serbia*
Dragana Živojinović, *Faculty of Technology and Metallurgy, University of Belgrade, Serbia*
Irena Žižović, *Faculty of Technology and Metallurgy, University of Belgrade, Serbia*